SPECTRAL AND STATISTICAL CHARACTERISTICS OF SHOALING WAVES OFF ALLEPPEY - WEST COAST OF INDIA

THESIS SUBMITTED TO THE

COCHIN UNIVERSITY OF SCIENCE AND TECHNOLOGY

FOR THE DEGREE OF

DOCTOR OF PHILOSOPHY

IN

PHYSICAL OCEANOGRAPHY

UNDER THE FACULTY OF MARINE SCIENCES

by

T. S. SHAHUL HAMEED
CENTRE FOR EARTH SCIENCE STUDIES
COCHIN - 682 018

MARCH 1989

DECLARATION

I do hereby declare that this Thesis contains results of research carried out by me under the guidance of Dr. M.Baba, Head, Centre for Earth Science Studies, Regional Centre, Cochin, and has not previously formed the basis of the award of any degree, diploma, associateship, fellowship or other similar title of recognition.

Ernakulam,

27.3.1989.

T.S. SHAHUL HAMEED
Regional Centre
Centre for Earth Science Studies
Cochin - 682 018

CERTIFICATE

This is to certify that this Thesis is an authentic record of research work carried out by Mr. T.S.Shahul Hameed under my supervision and guidance in the Centre for Earth Science Studies for Ph.D. Degree of the Cochin University of Science and Technology and no part of it has previously formed the basis for the award of any other degree in any University.

Ernakulam,
27.3.1989.

Dr. M. BABA
(Research Guide)
Head,
Regional Centre
Centre for Earth Science Studies
Cochin - 682 018

ACKNOWLEDGEMENTS

CONTENTS

PREFACE

Waves in the oceans generated by the continuous interaction of the winds and the ocean surface, fascinated man's curiosity since time immemorial. The numerous hazards due to the ocean waves, which at times attain heights of a few tens of metres, were of concern to navigators and harbour engineers. There is an increasing awareness in recent times about the importance of the study of ocean waves, because of the tremendous force exerted by waves on offshore, harbour and coastal structures, their influence on defence, commercial and industrial operations and their importance in weather prediction, remote sensing and other scientific applications. Among the useful aspects of ocean waves are their capability to provide electric power, to enhance sediment deposition/removal as desired, to enhance breeding of fish under controlled conditions, etc. Considerable efforts are being put now-a-days by oceanographers and engineers to understand the ocean waves right from their generation to their dissipation.

As most of the ocean-related developmental activities are confined to the coastal waters the study of waves in shoaling waters is of vital importance. Unlike deep water waves, those in shallow waters exhibit complex characteristics due to non-linearities caused by various processes like shoaling, frictional attenuation, refraction, diffraction, wave-wave interaction, etc., observed during the propagation of the waves to the shore.

The random waves in the ocean are not amenable to simple mathematical explanation due to the large number of parameters involved and their complex nature. Hence these waves are often described in terms of their spectral and statistical characteristics. Among the above two, the spectral characteristics stand first, as the spectrum provides information on the energy contained in the component frequencies. It also reveals the existence of different wave systems. This information is required for studies such as harbour resonance, wave forces on structures, wave power generation, and many others. The spectral function is important not only due to its own information content, but also because of the fact that various statistical measures of the ocean surface wave field are expressed either in terms of or as quantities derived from the spectrum. The statistical parameters depict the randomness of surface wave field. Among the various statistical measures the probability

i

density functions of the surface elevation, period and their joint distribution are the basic ones. The parameters to represent the random sea state are derived on the basis of the distribution of the probability densities.

Some investigations on the spectral and statistical characteristics of deep water waves are available for Indian waters. But practically no systematic investigation on the shallow water wave spectral and probabilistic characteristics is made for any part of the Indian coast except for a few restricted studies. Hence a comprehensive study of the shallow water wave climate and their spectral and statistical characteristics for a location (Alleppey) along the southwest coast of India is undertaken based on recorded data. The results of the investigation are presented in this thesis.

The thesis comprises of seven chapters. In the introductory Chapter, the status of the problem and the aim and objectives of the investigation are given. In the second Chapter, a review of the relevant literature is carried out. The third Chapter deals with the methods of data collection and analysis. The characteristics of the observed spectra are presented in Chapter 4. Comparisons of the observed spectra with the shallow water spectral models are made in the 5th Chapter. Based on the results of the comparison, recommendations are given for the choice of spectral models for shallow water conditions. Chapter 6 deals with the statistical characteristics of shallow water waves. The observed distributions of individual wave heights, periods and their joint distributions are compared with the theoretical models. The last chapter projects the summary of the present investigation and recommendations for future research.

The fitness of the different height and period distributions and the X^2 values obtained for the different joint distribution models are provided at the end of the thesis as appendices.

The following research papers are published based on the work reported in this thesis:

1. Wave height distribution in shallow water. Ocean Engng., Vol.12, No.4, pp.309-319, 1985. (T.S.Shahul Hameed and M.Baba)

2. A spectral form for shoaling waves. Proc. 3rd Indian Conf. on Ocean Engng., IIT, Bombay, Vol.1, pp.A1-A6, 1986. (M.Baba and T.S. Shahul Hameed)

3. High energy waves off the southwest coast of India.
    Proc. Symp. Short-term Variability of Physical
    Oceanogr. Features in the Indian Waters, NPOL, Cochin,
    pp.191-195, 1987.(T.S. Shahul Hameed and M.Baba)

4. Wave climatology and littoral processes at Alleppey.
    In: Ocean Waves and Beach Processes (Ed. M.Baba and
    N.P.Kurian), Centre for Earth Science Studies,
    Trivandrum, pp.67-90, 1988. (T.S. Shahul Hameed)

5. Shallow water wave spectral and probabilistic
    characteristics. In: Ocean Waves and Beach Processes
    (Ed. M.Baba and N.P.Kurian), Centre for Earth Science
    Studies, Trivandrum, pp.141-164, 1988 (M. Baba, T.S.
    Shahul Hameed and C.M. Harish)

A list of research papers/reports published by the
author in the related fields are given at the end.

iii

LIST OF SYMBOLS

a	:	Wave amplitude
A,B	:	Coefficients of the Scott-Weigel spectrum
C	:	Phase velocity of the wave
C_p	:	Phase Velocity corresponding to the peak frequency
E	:	Energy of the wave
f	:	Frequency in Hz
f_a	:	Average frequency
f_m	:	frequency corresponding to maximum spectral density
g	:	Acceleration due to gravity
h	:	Water depth
H	:	Wave height
$\bar{H}$	:	Average wave height
H_0	:	Deepwater wave height
H_0'	:	Deep water equivalant wave height
H_b	:	Breaker wave height
H_{max}	:	Maximum wave height
H_p	:	Raw wave height obtained from pressure record
H_s	:	Significant wave height
H_{ss}	:	H_s derived from the spectrum
H_{st}	:	H_s derived from Tucker-Draper analysis
H_{sw}	:	H_s derived from wave-by-wave analysis
H_*	:	H normalised with water depth
I_0	:	Zero order modified Bessel function of first kind

iv

k : Wave number

k_p : Wave number corresponding to peak frequency

K_r : Refraction coefficient

K_s : Shoaling coefficient

L_0 : Deep water wave length

L_m : Wave length corresponding to peak frequency

m_n : nth moment of the spectrum

n : Instrument factor

$p(x)$: Probability density of x

$P(x)$: Probability distribution of x

$R(\tau)$: Autocorrelation function

s : Surface tension

$S(f)$: Spectral density at frequency f

$S(f_m)$: Peak spectral density

$S_p(f)$: Pressure spectrum

SS : Significant slope of the wave field

t : Instantaneous time

T : Wave period

$\bar{T}$: Average wave period

T_c : Average crest period

T_p : Period corresponding to maximum spectral density

T_s : Average period of the highest one-third of the waves

T_z : Average zero-crossing wave period

u_* : Wind friction velocity

U_r : Ursell number

α : Phillips' constant

α_J : Scale parameter of the JONSWAP spectrum

α_V : Spectral scale parameter defined by Vincent (1984)

β : Scale parameter of the Wallops spectrum

γ : Peak enhancement factor of the JONSWAP spectrum

Γ : Gamma function

δ : Parameter defining the width of the JONSWAP spectrum

ϵ_s : Spectral width parameter derived from the spectrum

ϵ_w : Spectral width parameter from wave-by-wave analysis

η : Instananeous surface elevation with respect to still water level

θ : Phase angle

ν, ν_1 : Parameters measuring the spectral width (narrowness)

ρ : Density of water

σ_x : Standard deviation of x

τ : Lag of a stationary ergodic process

$\mathfrak{D}(_h)$: Shallow water dispersion parameter after Kitaigorodskii et al. (1962)·

ω : Angular frequency in radians

ABBREVIATIONS

Ch.	:	Chapter
d.f.	:	degrees of freedom
DI	:	Deviation Index
DI_{LC}	:	DI corresponding to lower confidence limit spectrum
Eq.	:	equation
Fig.	:	Figure
hrs	:	duration in hours
Hrs	:	time (I.S.T.)
Hz	:	hertz
m	:	metre
pdf	:	probability density function
s	:	second
%	:	Percentage

CHAPTER I

INTRODUCTION

The knowledge of surface wave conditions in the seas and oceans is important in coastal and offshore engineering, defence, navigation, fishing, ocean mining, pollution control, and above all, in planning coastal development programmes. In addition, attempts are being made in different parts of the world including India to extract electrical energy from the ocean waves. There is little surprise, therefore, that considerable work has been done and is being done on various aspects of ocean waves.

The wind generated ocean waves are a direct manifestation of the complex physical processes in the oceans involving interaction of the sea with the atmosphere. Wind waves are always random as a result of the action of the generating forces as well as the consequence of the dynamic processes in wave evolution which induce different kinds of instabilities. As these complex phenomena are difficult, if not impossible, to be described correctly in mathematical terms, they are often described in terms of their statistical and spectral characteristics. Thus a detailed knowledge of the statistical and spectral

1

characteristics of ocean waves becomes important not only for the scientific understanding of the ocean wave phenomena, but also for the practical applications mentioned earlier. With the recent increase in the usage of active microwave remote sensing techniques, the importance of the knowledge of these characteristics increased. The qualitative results of the past cannot satisfy the need for precise interpretation of the radar signals for the present day applications.

Among the various statistical measures to represent the random sea state, the probability density functions of the surface elevation and the period are the most basic ones. The importance of the joint distribution of heights and periods is well known in the study of certain important phenomena like harbour resonance, irregular wave run-up, overtopping, wave forces on structures, etc. The spectral functional form, which provides the vital information on the energy carried by the component frequencies in a wave train, is another important information required for practical applications. The spectral function is important not only due to its own information content, but also because various other statistical characteristics of the surface wave field are expressed either in terms of or by quantities derived from the spectrum.

In practical applications the importance of the knowledge of these waves in finite water depths are at least equal, if not more, to that in deep water. Majority of the present-day activities in the oceans are confined to the shelf-break and inwards. Waves in waters of finite depth behave differently from those in the deep water. When the waves enter into regions where the water depth is less or equal to half the wave length, the waves feel the bottom. Shoaling, refraction, diffraction and other non-linear processes in the shallow waters make their characteristics more complex. Important changes are brought about in the wave profile, phase velocity and dispersive relationships.

Depending on the nearshore environmental parameters like bathymetry, bottom slope and geometry, sediment properties, presence of natural/man-made barriers/ structures, the properties of waves vary from location to location. This spatial variation restricts the applicability of nearshore wave data obtained from one location for another regardless of their proximity. As far as the west coast of India is concerned, detailed wave studies are limited to a few locations (Baba, 1985). The available literature reveals that there is considerable variation in the wave characteristics at different locations (Baba et al., 1987). Hence, in order to get a comprehensive picture

3

of the wave climate and wave characteristics for the entire coast, it may be necessary to establish a large number of observation stations, which will be very expensive. Kurian (1987) established that the bottom slope and sediment characteristics are the major factors influencing the shallow water wave climate. Based on this conclusion the coast of Kerala was divided into different catagories according to energy levels.

About half of the south-west coast of India comes under medium energy catagory, and Alleppey is a typical location in it. This coast is of recent origin, geologically, and hence is fragile. It is threatened by severe erosion during the south-west monsoon. Since it is thickly populated, the erosion brings about much damages to life and property. It is well known that the major causative factor for the coastal erosion is the ocean waves. Practically no systematic study on the wave climate or the spectral and probabilistic properties of the shallow water waves have been made at this or any neighbouring locations. Hence, a comprehensive study of the nearshore wave climate and their spectral and statistical characteristics at this location is undertaken. The present study is expected to provide this most vital information which is essential for many an application.

CHAPTER 2

SPECTRAL AND STATISTICAL CHARACTERISTICS

OF OCEAN WAVES - A REVIEW

Although the interest and study on ocean waves date back to antiquity, the first systematic research effort to study the characteristics of ocean waves were started during the World War II. Since then considerable attention has been paid to the study of spectral and statistical characteristics of wind generated waves. A review of the relevant literature is undertaken in the following sections.

2.1. WAVE SPECTRUM

The term 'wave energy spectrum' is derived from the concept that a random wave field is characterised by the superposition of a large number of linear progressive waves with different heights and periods. Generally the wave spectrum is presented as a plot of the component wave energies against wave frequencies.

The actual water surface profile of wind-generated ocean waves varies widely in time as well as in space, and hence the instantaneous surface elevation above the still water level, η, at position x and time t is expressed as

$$\eta(x,t) = \sum a_i \cos(k_i x - \omega_i t + \theta_i) \qquad \qquad \dots\dots(2.1)$$

5

where k and ω are the wave number and angular frequency respectively. Θ is the phase angle and is assumed to be uniformly distributed over the interval $(0, 2\pi)$.

Mathematically, the spectral density function is defined as the Fourier transform of the autocorrelation function and is given by

$$S(f) = \int_{-\infty}^{\infty} R(\tau) \exp[-i2\pi f\tau] \, d\tau \qquad \ldots \ldots (2.2)$$

where $R(\tau)$ is the autocorrelation function which is the average lagged product of the neighbouring values. For a stationary ergodic process with lag τ it is defined as

$$R(\tau) = E[x(t).x(t+\tau)]$$
$$= Lt_{T->\infty} (1/T) \int_{0}^{T} x(t)x(t+\tau) \, dt \qquad \ldots \ldots (2.3)$$

Since $S(f)$ and $R(\tau)$ form a Fourier Transform pair,

$$R(\tau) = \int_{-\infty}^{\infty} S(f) \exp[-i2\pi f\tau] \, df \qquad \ldots \ldots (2.4)$$

The $S(f)$ defined above is two-sided, but f can never be negative. Hence, physically realisable one-sided spectral density function, keeping the area under the spectrum the same, is obtained from

$$S(f) = 2\int_{-\infty}^{\infty} R(\tau) \exp[-i2\pi f\tau] \, d\tau \; ; \text{ for } 0 \le f \le \infty$$
$$= 0 \qquad\qquad\qquad ; \text{ for } f < 0 \quad \ldots \ldots (2.5)$$

6

S(f) can be determined directly as well as from the observed time series. From Eqs.(2.3-2.5) we obtain

$$R(0) = \text{Lt}_{T\to\infty} (1/T)\int_0^T x^2(t)\, dt = \int_0^\infty S(f)\, df \quad \ldots\ldots(2.6)$$

If x(t) is the instantaneous sea surface elevation with zero mean it follows that

$$R(0) = \sigma_x^2 \qquad\qquad \ldots\ldots(2.7)$$

is the variance of the sea surface elevation and is equal to the area under the spectral curve.

For a deterministic linear wave the total energy is given by

$$E = \rho g a^2/2 \qquad\qquad \ldots\ldots(2.8)$$

and hence the total energy of a random wave

$$E \propto (1/2) \sum a_i^2 \qquad\qquad \ldots\ldots(2.9)$$

Kinsman (1965) has shown that

$$\sum (1/2)a_i^2 \propto S(f_i)\Delta f \qquad\qquad \ldots\ldots(2.10)$$

That is, energy of irregular waves is proportional to the spectral density function. Hence, the total energy

$$E \propto \int_0^\infty S(f)\, df \qquad\qquad \ldots\ldots(2.11)$$

From Eqs.(2.6), (2.7) and (2.11) it follows that the area under the wave spectrum gives the variance of the surface elevations and the total energy of the irregular wave system. The integration of the wave spectrum with different powers of frequencies yield different height and period statistics. Also, it is possible to reconstitute the time series of the sea surface fluctuations from the spectrum and this method is usually adopted to generate random waves in the laboratory.

2.2. DEEP WATER WAVE SPECTRAL MODELS

It is impossible to model wave spectrum using the basic mathematical-physical laws owing to the complexity of the wind-wave generation processes. As a result, the void due to the lack of a spectral function has been filled in by various empirical or semi-empirical models.

2.2.1. Phillips Spectrum

Most of the recent spectral models can be traced back to the spectral function proposed by Phillips (1958). He used the dimensional analysis to derive the upper limit of the equilibrium or saturation range of the spectral form for the deep water conditions and established an f^{-5} dependence. The functional form is given by

$$S(f) = \alpha g^2 (2\pi)^{-4} f^{-5} \quad ; \quad f \geq f_m \qquad \ldots\ldots(2.12)$$

8

This form accounts for the frequencies higher than f_m only. For practical applications, rather than the high frequency range, the energy content of the spectrum is more important. However, this served as a stepping stone to the studies on the ocean wave spectrum.

2.2.2. Pierson-Moskowitz Spectrum

Based on Phillips' equilibrium theory and some additional similarity analysis by Kitaigorodskii (1962), Pierson and Moskowitz (1964) proposed a continuous functional form for fully developed sea spectrum. The spectral density is given by

$$S(f) = \alpha g^2 (2\pi)^{-4} f^{-5} \exp [-(5/4)(f/f_m)^{-4}] \qquad \ldots\ldots(2.13)$$

Although a large number of field and laboratory observations did provide data to support this model, there are still some difficulties in its practical application. This model simulates the high frequency range better than the portion near the spectral peak where the energy is concentrated (Huang et al., 1981). It is based on the physical conditions of equilibrium (saturated or fully developed sea state) which is an ideal condition rather than the actual in the field. As a result, the use of this model is limited in the real field conditions.

9

2.2.3. JONSWAP Spectrum

The efforts to arrive at a generalized spectral function for an unsaturated sea culminated in the Joint North Sea Wave Project experiments and Hasselmann et al. (1973,1976) proposed the now well known JONSWAP spectral model for the fetch-limited (unsaturated) sea conditions. The spectral density of this form is given by

$$S(f) = \alpha_J g^2 (2\pi)^{-4} f^{-5} \exp[-(5/4)(f/f_m)^{-4}] \gamma^q \quad \ldots (2.14)$$

$$\text{where,} \quad q = \exp[-(f-f_m)^2/2(\delta f_m)^2] \quad \ldots (2.15)$$

$$\text{and} \quad \delta = \begin{cases} \delta_a & ; \ f \leq f_m \\ \delta_b & ; \ f > f_m \end{cases} \quad \ldots (2.16)$$

This model is basically the P-M (Pierson-Moskowitz) model (Eq.2.13) with a peak enhancement factor, γ^q. γ is the ratio of the maximum spectral density to the corresponding maximum derived from the P-M spectrum. When $\gamma = 1$ Eq.(2.14) reduces to Eq.(2.13). The mean value of γ for all the JONSWAP data is around 3.3. The average values of δ_a and δ_b are given as 0.07 and 0.09 respectively.

In order to use Eq.(2.14) one will have to determine the five free parameters, all of which are given empirically as functions of the non-dimensional peak frequency which cannot be determined 'apriori'. Further, it is developed for

10

the fetch limited developing sea state cases only. As opined in Huang et al. (1981) whether it also fits in un-saturated decaying sea is questionable.

2.2.4. Neumann Spectrum

The above well known models involve a number of parameters which differ from model to model and are not known for all seas. For general applicability the theoretical spectrum must be expressed in terms of some common parameters which are readily available. Attempts were made in this direction and a few empirical/semi-empirical models were proposed. They are expressed mainly in terms of the total variance (m_0) and the frequency corresponding to the maximum spectral density (f_m). Working in the above direction Neumann (1953) proposed a spectral model with functional form:

$$S(f) = 24(m_0/f_m)(f/f_m)^{-6}(3/\pi)^{1/2} \exp [-3(f/f_m)^{-2}]$$

$$.....(2.17)$$

As this was the first analytically expressed spectral form, it was widely used till 1964. This model assumes an f^{-6} dependence in the high frequency region, unlike the subsequent models most of which assume an f^{-5} dependence in this part of the spectrum. However, some of the later studies (Hasselmann et al., 1973; Dattatri, 1978; Narasimhan and Deo, 1979a,b; Goda, 1983; Baba and Harish, 1986; etc.) show that higher values are possible in the deep water.

11

2.2.5. Darbyshire Spectrum

Based on the wind-wave data collected from the Atlantic Ocean, Darbyshire (1959) proposed an empirical spectral model, the functional form of which may be written as

$$S(f) = 23.9 \, m_0 \, \exp \left[-(f-f_m)^2 / [0.0085(f-f_m+0.042)]^{1/2} \right]$$

$$\dotsc (2.18)$$

This form was derived from the plot of energy densities of 64 wave records selected in such a way that the effect of extraneous swell was insignificant. In a later study, this was modified by Darbyshire (1963) to incorporate the effect of small fetch, by replacing $(f-f_m)$ with $y(f-f_m)$, where

$$y = (X^3+3X^2+65X)/(X^3+12X^2+260X+80) \qquad \dotsc (2.19)$$

X being the fetch in nautical miles. But, Burling (1963) observed that this modification is unnecessary since the spectral densities at high frequencies usually decrease with fetch.

2.2.6. Bretschneider Spectrum

Another model, as a modification of the Neumann spectrum was put forward by Bretschneider (1963). The spectral density of this model is given by

$$S(f) = 5(m_0/f_m)(f/f_m)^{-5} \exp [-1.25(f/f_m)^{-4}] \quad \dotsc (2.20)$$

12

In this form the frequency dependence is assumed to be analogous to Phillips' (1958) theory. This model is identical to the P-M spectrum when found from the measured values of m_0 and f_m.

2.2.7. Scott and Scott-Weigel Spectra

Based on the analysis of the wave data from a number of sources covering the Irish Sea and Atlantic Ocean, Scott (1965) modified the spectrum proposed by Darbyshire(1959) as

$$S(f) = 21.51 \ m_0 \ \exp \left[-[96.66(f-f_m)^2/(f-f_m+0.042)]^{1/2} \right]$$

$$\text{for} \quad -0.042 < (f-f_m) < 0.26 \quad \ldots\ldots(2.21)$$

Weigel (1980) points out that this is not the spectrum for purely locally generated waves as the data set used for the calibration of this model included swells also. Thus for application in other seas it is necessary to compare the model with the measured spectra and calibrate it.

From the studies of a large number of energy spectra available from wave measurements in the North Atlantic Ocean Wiegel (1980) concluded that the empirical constant in Scott's spectral model is not constant, but is a function of the variance, the value increasing with the increase in variance. With this modification the form is known as Scott-Weigel spectrum and the spectral density is given by

$$S(f) = A\ m_0\ \exp\left[-[(f-f_m)^2/(B(f-f_m+0.042))]^{1/2}\right]..(2.22)$$

When the normalized energy spectrum $(S(f)/H_s^2)$ is integrated with respect to $(f-f_m)$ the dimensionless number 1/16 will be obtained. Based on this, Weigel has given the values of A and B for a range of H_s values.

The studies on the above spectral models carried out at different places along the southwest coast of India show that the Scott and the Scott-Weigel models fit the observed spectra in a number of cases. Dattatri et al. (1977), Dattatri (1978), Deo (1979), Prasad (1985), Sunder (1986) and Kurian (1987) obtained the best fit with the Scott spectrum for their data. Saji (1987) concludes that both the forms represents the data fairly well. Bhat (1986) found that the high frequency part is well represented by the Scott spectrum but it over-estimated the spectral peak. Baba and Harish (1986) observed that the Scott's model simulated the spectral peak closely in the cases of low energy conditions and it over-estimated the high energy conditions. From the above studies it is seen that though the Scott and Scott-Weigel spectral forms are derived for wind waves of the deep water, it could explain the observed spectra in some shallow water cases also. Further studies are required to validate the range of validity of these models in shallow water conditions.

14

2.2.8. Toba's Model

In the studies on the balance in the air-sea boundary processes Toba (1973) observed that the high frequency part of the spectrum is f^{-4} dependent as against the f^{-5} dependence assumed in other models. Based on this observation a new model is proposed, the spectral density of which is given by

$$S(f) = (2\pi)^{-3} g_* C_1 u_* f^{-4} \qquad \qquad \ldots\ldots(2.23)$$

where $g_* = g(1+sk^2/\rho g)$ with s as surface tension. C_1 is a constant and u_* is the wind friction velocity at the sea surface. Later works by Goda (1974), Forristall (1981), Kahma (1981), Huang et al., (1983b), Kitaigorodskii (1983) and Battjes et al. (1987) give evidences for the existence of a negative 4th power dependence also, in the high frequency side of the spectrum.

Joseph et al.(1981) modified this model assuming a symmetrical form for the low frequency side and suggested the continuous form

$$S(f) = \begin{cases} (2\pi)^{-3} g \, C_1 u_* f^{-4} & ; \ f > f_m \\ (2\pi)^{-3} g \, C_1 u_* f_m^{-8} f^{-4} & ; \ f \leq f_m \end{cases} \qquad \ldots\ldots(2.24)$$

Toba (1973) suggested 0.062 for the constant C_1. Based on many subsequent works Joseph et al.(1981) recommended 0.096 for C_1. The value of this constant is not

15

known for all seas. Moreover, it is not an easy task to compute the wind friction velocity at the sea surface correctly since it depends on the drag coefficient, which again depends on the wind velocity at the sea surface, and is highly variable. In a comparison of the above model with the observed spectra from the southwest coast of India Baba and Harish (1986) found that this form does not fit to the data unless the value of C_1 and u_* are suitably adjusted.

2.3. SHALLOW WATER WAVE SPECTRAL MODELS

As against the deep water ones, the waves in the shallow water behave entirely differently. The factors that modify the wave characteristics in the shallow waters are many and are complex. The shoaling, refraction, breaking and other shallow water processes like percolation, friction, etc. play their roles and the spectral form is modified accordingly. In shallow waters the slope of the high frequency portion of the spectrum is found to be lower (Goda, 1974; Kitaigorodskii et al., 1975; Ou, 1977,1980; Thornton,1977,1979; Dattatri, 1978; Vincent, 1982a,b; Vincent et al., 1982; Baba and Harish, 1986; etc.) and values as low as 1.6 are reported. As the shallow water waves are almost always unrelated to the local wind conditions, the applicability of the deep water spectral models to the shallow waters becomes restricted. The usual

16

practice is to adopt a deep water model and another model to propagate the wave to the shallow waters. Following this approach a few spectral models are proposed for the shallow water conditions.

2.3.1. Kitaigorodskii et al. Spectrum

Kitaigorodskii et al. (1975) extended Phillips' (1958) argument to the shallow waters by applying a finite depth dispersion relationship. They proposed a spectral model which is a modification of the Phillips' spectrum (Eq.2.12), the functional form of which may be written as

$$S(f) = \alpha \ g^2 (2\pi)^{-4} f^{-5} \Phi(\omega_h) \qquad \ldots\ldots(2.25)$$

where Φ is a non-dimensional function of the quantity

$$\omega_h = 2\pi f (h/g)^{1/2} \qquad \ldots\ldots(2.26)$$

The function Φ varies monotonously from 1 in deep water to 0 in depth h = 0. When $\omega_h < 1$,

$$\Phi \cong (\omega_h)^2/2 \qquad \ldots\ldots(2.27)$$

Then for shallow waters Eq.(2.25) becomes,

$$S(f) = 0.5 \alpha \ gh(2\pi)^{-2} f^{-3} \qquad \ldots\ldots(2.28)$$

Observational evidence to this form has been reported by many researchers (Thornton, 1977; Ou, 1977,1980; Iwata,

17

1980; Vincent, 1982a,b; Vincent et al., 1982; Baba and Harish, 1986; Kurian, 1987; etc.). Although this model simulates the high frequency side of the shallow water wave spectrum it shows the same limitations in practical applications as seen in the case of the Phillips' spectrum. However, this model offers ample scope to serve as a base for the development of spectral models applicable to finite depths.

2.3.2. Thornton's Model

The functional form of Eq.(2.28) was later derived independently by Thornton (1977) based on quite different arguments. He started from the first principles and postulated reasonably that breaking occurs when particle velocity approaches the phase velocity of the wave. Consequently, the parameters controlling breaking should be the phase velocity (C) and the frequency (f). Then by dimensional analysis he obtained

$$S(f) = \alpha c^2 (2\pi)^{-2} f^{-3} \qquad \ldots\ldots(2.29)$$

By applying the shallow water approximation for the phase velocity, $c^2 = gh$, Eq.(2.29) becomes

$$S(f) = \alpha gh (2\pi)^{-2} f^{-3} \qquad \ldots\ldots(2.30)$$

Although this form is similar to that proposed by Kitaigorodskii et al. (Eq.2.28), the difference of a factor of 2 is by no means negligible.

2.3.3. Jensen's Modification

Considering the importance of the total spectrum in practical applications, Jensen (1984) modified Eq.(2.28) to account for the low frequency side of the spectrum also. The forward face (the low frequency side) is assumed to be represented by the relation

$$S(f) = 0.5 \; \alpha \; gh(2\pi)^{-2}(f_m)^{-3} \; \exp \; [1-(f/f_m)^{-4}] \; \ldots \; (2.31)$$

The study areas were restricted to semi-enclosed bodies of water and the model was tested using the data obtained from Saginaw Bay, Michigan. Agreement within ± 0.15 m significant wave height and ± 1.0 s peak period is reported (Jensen, 1984).

2.3.4. Shadrin's Model

Assuming the equilibrium range proposed by Phillips (1958) and the deviations from it in the shallow waters due to the effects of small depths Shadrin (1982) derived a spectral model for the shallow water waves. The spectral density is given by the equation

$$S(f) = \alpha g^2 (2\pi)^{-4} f^{-5} f_r \qquad \ldots \ldots (2.32)$$

19

where f_r is a dimensionless frequency. It may be noted that this form is similar to the relation obtained by Kitaigorodskii et al. (Eq.2.25) and the procedures are exactly similar. It is further assumed that in the coastal regime as the waves propagate over uniformly decreasing depths, from a certain time when the depths become comparable to the wave height, the wave crests undergo strong deformation. Hence for very small depths relative wave height (H/h) is considered as the most representative parameter. Based on the above argument and dimensional considerations f_r is derived as

$$f_r = (2 \pi f)^{C_2} (H/g)^{C_2/2} \qquad \qquad \dots\dots(2.33)$$

where $C_2 = br'/(1+C_3 r')$; $r' = H/h$ $\qquad \dots\dots(2.34)$

On the basis of the data from the coastal regions of the Black and Baltic Seas the values of b and C_3 are obtained as 20 and 4 respectively (Shadrin, 1982). Verification/calibration of this model elsewhere is not seen in the literature.

2.3.5. TMA Spectrum

The postulation of Kitaigorodskii et al. (1975) that the saturation level of wind wave energy spectrum in wave number space would be independent of water depth is extended to the entire spectrum (beyond the saturation range also) by

Bouws et al. (1985). By assuming a JONSWAP spectrum in deep water and the finite depth dispersion relation of Kitaigorodskii et al. to propagate it into shallow waters a new spectral model was formulated. The functional form of this model is given as

$$S(f) = S_J(f) \ \Phi(\omega_h) \qquad \qquad \dots\dots(2.35)$$

where $S_J(f)$ is the JONSWAP spectrum defined by Eq.(2.14) and $\Phi(\omega_h)$ is given by Eqs.(2.26 & 2.27).

The validity of the model was verified using the data collected from the so-called TEXEL storm in the North Sea and from the projects MARSEN and ARSLOE and hence named it 'TMA' spectrum.

On an evaluation of this model one may find that there are some difficulties in its use. As this is an extension of the JONSWAP spectrum the limitations of that model (disc-ussed elsewhere) will be transmitted to this new form also. Hence, this model may find limited applications. In a recent study, Vincent (1984) shows that the scale parameter is linked to the wave steepness and derived the relation

$$\alpha_v = 16 \ \pi^2 ss^2 \qquad \qquad \dots\dots(2.36)$$

where the parameter SS is given by

$$SS = (m_0)^{1/2}/L_m \qquad \qquad \dots\dots(2.37)$$

L_m is the wave length corresponding to the frequency at the spectral peak. Data collected from 2 average depths (17 m and 2 m) at CERC's Field Research Facility indicated excellent fit with TMA model at high steepness and some divergence at low steepness (Vincent, 1984).

2.3.6. Wallops Spectrum

Based on the assumption that the sea surface can be represented by a linear superposition of many countable, independent Stokean wave components, Huang et al.(1981) proposed a unified 2-parameter spectral model, which is termed as 'WALLOPS' spectrum, as an alternative to the many-parameter JONSWAP spectrum. The spectral density is given by

$$S(f) = (2\pi)^{-4}\beta\, g^2 (f_m)^{-5} (f_m/f)^m \exp\,[-(m/4)(f_m/f)^4]$$
$$\dots\dots(2.38)$$

where $\quad \beta = (2\pi SS)^{2m\,(m-1)/4}/[4^{(m-5)/4}\,\Gamma[(m-1)/4]]\dots\dots(2.39)$

and $\quad m = \left|\log(\sqrt{2}\,\pi SS)^2/\log\,2\right|\qquad\dots\dots(2.40)$

Γ is the gamma function and SS is the significant slope of the wave field defined by Eq.(2.37).

The justification for adopting the assumption of super-position of Stokean wave components in this model is the weakness of the non-linear wave-wave interaction proposed by many researchers (Phillips, 1977; Huang and Long, 1980; Huang et al., 1981, 1983b; etc.).

22

Basically this model is a generalization of the Phillips' saturation range concept by relaxing the fixed negative fifth power law of the high frequency portion of the spectrum. When the slope m equals 5, this model approaches to the P-M spectrum (Eq.2.13) allowing variability to the constant (α to β). Since the range of validity of the spectrum slope emphasized is from f_m to $2f_m$ this model could provide a better representation of the energy containing range than the high frequency range alone. Mc Clain et al. (1982) have reported excellent agreement in a comparison between their data and this model for developing seas.

For shallow waters Huang et al. (1983b) modified the Wallops spectrum (Eqs.2.38-2.41) and derived two cases based on the non-dimensional depth ($k_p h$) with k_p, the wave number corresponding to the peak energy:

(i) For $0.75 \leq k_p h < 3$, Stoke's shallow water wave theory was used. This lead to the following relations for m and in the Wallops spectrum

$$m = \left| \log \left[\sqrt{2} \, \pi SS \, \coth(k_p h) [1+3/(2 \, \sinh^2 k_p h)] \right] / \log \sqrt{2} \right|$$

.....(2.41)

$$\beta = (2 \pi SS)^2 m^{(m-1)/4} \tanh^2(k_p h) / \left[4^{(m-1)/5} \Gamma[(m-1)/4] \right]$$

.....(2.42)

23

(ii) For $k_p h < 0.75$, solitary wave theory was applied to yield,

$$m = \left| \log(\cosh \mu)/\log \sqrt{2} \right| \quad \quad \ldots\ldots(2.43)$$

$$\mu = \pi/(3U_r)^{1/2} \quad \quad \ldots\ldots(2.44)$$

where U_r is the Ursell number given by

$$U_r = 2\pi SS/(kh)^3 \quad \quad \ldots\ldots(2.45)$$

$$\beta = (2\pi SS)^2 m^{(m-1)/4} (C_p^2 k_p/g)^2/\left[4^{(m-5)/4} \ulcorner[(m-1)/4]\right] \quad \quad \ldots\ldots(2.46)$$

where C_p is the phase velocity corresponding to the peak frequency. Huang et al. (1983) recommended the use of the phase velocity of Stoke's wave, quoting Bona et al. (1981), to give a highly accurate answer for most studies. Then,

$$\beta = (2\pi SS)^2 m^{(m-1)/4} \tanh^2 k_p h/\left[4^{(m-5)/4} \ulcorner[(m-1)/4]\right] \quad \quad \ldots\ldots(2.47)$$

This is perhaps the first full representation of a shallow water wave spectrum developed by using Stoke's and solitary wave theories. Liu (1985) on a comparison with field data collected from the south eastern coast of Lake Erie at depths ranging from 1.4-3.8 m found that the semi-empirical Wallops model provides fair agreement with the observed data at the deeper stations but only marginal agreement in very shallow waters. In a later study Liu

24

(1987) found that the value of 0.75 for the non-dimensional depth ($k_p h$) as the division between solitary and Stoke's wave theories should be modified to 1.5 to give better results. That is, for $k_p h$ between 0.75 and 1.5 solitary wave theory fits the spectrum better than the Stoke's theory. However, it may be noted that the expressions for the spectral parameters and coefficients used in the study (Liu, 1987) differ from those suggested in the original.

As the Wallops model depend on the internal parameters it maintains a variable band width as a function of the significant slope which measures the non-linearity of the wave field. Also, it contains the exact total energy of the true spectrum since the total energy content is a built-in feature in the definition of the coefficient β .

2.3.7. GLERL Spectrum

In most of the spectral models, though the overall forms are basically similar, they consists of a number of empirical coefficients and exponents that vary from location to location, depending on the environmental conditions. This restricts the universal applicability of these models. With the aim to solve this problem, Liu (1983) proposed an empirical 'Generalized Spectrum' in a form similar to the Wallops spectral model. The spectral density is given by

$$S(f) = C_4 (m_0/f_m)(f/f_m)^{-C_5} \exp \left[-C_6 (f/f_m)^{-C_5/C_6}\right]$$

$$\ldots\ldots(2.48)$$

where $C_{i=4,5\&6}$ are dimensionless coefficients and exponents that are to be determined from the given spectral parameters. The following relations are provided to derive these coefficients iteratively

$$C_4 = \exp(C_6) S(f_m) f_m/m_0 \qquad\qquad \ldots\ldots(2.49)$$

$$m_0/S(f_m)f_m = \exp\left[C_6 + (1-C_6 + C_6/C_5)\ln C_6\right] \Gamma(C_6 - C_6/C_5)/C_5$$

$$\ldots\ldots(2.50)$$

$$C_5 = \exp\left[C_6 + (1-C_6 + 3C_6/C_5)\ln C_6\right] \Gamma(C_6 - 3C_6/C_5)/D$$

$$\ldots\ldots(2.51)$$

$$D = (f_a/f_m)^2 m_0/[S(f_m)f_m] \qquad\qquad \ldots\ldots(2.52)$$

$$f_a = (m_2/m_0)^{1/2} \qquad\qquad \ldots\ldots(2.53)$$

The practical application of this form require the parameters m_0, f_m, f_a and $S(f_m)$ to be known. In other words, the spectrum has to be fully defined for its shape and energy apriori. Usually, the total energy (m_0) and the peak frequency (f_m) are obtained from design wave information. $S(f_m)$ and f_a have to be obtained from the individual spectrum (this limits the generalization of the model) or from empirical relations. Liu (1983) derived the following empirical relations for deep water wave spectra when $S(f)$ is in $m^2 s$ and f in Hz:

$$f_a = 0.82 \ (f_m)^{0.74} \qquad\qquad \ldots\ldots(2.54)$$

$$S(f_m) = 17.0 \ (m_0)^{1.13} \qquad\qquad \ldots\ldots(2.55)$$

The applicability of Eqs.(2.54 and 2.55) has been further corroborated in Liu (1984). In the subsequent works Liu (1985,1987) shows that this form applies equally well in shallow water and deep water. Though water depth is not a parameter in this model it seems that the effect of depth is included through the exponents and coefficients. This model requires validation for different environmental conditions.

2.4. STATISTICAL CHARACTERISTICS

The deterministic approach, which incorporates wave theories derived from the equations of classical hydrodynamics, rarely represent the observed ocean wave characteristics. Each wave theory assumes the wave as regular, ie., having a fixed profile that repeats exactly after a certain time (wave period) and then gives fixed solutions. The wind-generated ocean waves are usually irregular and hence the solutions based on the wave theories are approximate and inadequate to describe the actual complex phenomena. A meaningful description of the irregular wave field can be obtained from the various statistical methods.

The statistical analysis of waves is mainly aimed at deriving the probability distributions of wave heights and periods. The magnitude of the different parameters like significant, average, root-mean-square wave heights and periods, zero-crossing period, etc., having a specified recurrence can be derived easily if the probability distributions of heights and periods are known.

The probability distribution of a random variable is the probability that the given random variable will be less than or equal to a specified value. If x_n denotes a specified value of the random variable x, then the probability distribution is given by

$$P(x_n) = \text{Prob } (x \leq x_n) \qquad \qquad \ldots\ldots(2.56)$$

Hence, by convention, $P(-\infty) = 0$ and $P(\infty) = 1$ $\ldots\ldots(2.57)$

The probability density function (pdf) is basically the probability that the random variable lies in a given range. From Eq.(2.56) it follows that

$$P(x_n < x \leq x_n + \Delta x) = \text{Prob } (x \leq x_n + \Delta x) - \text{Prob } (x \leq x_n)$$
$$= P(x_n + \Delta x) - P(x_n)$$
$$= \Delta P(x_n) \qquad \qquad \ldots\ldots(2.58)$$

At the limit $x \rightarrow 0$, this is the probability density at $x = x_n$ and is given by

$$p(x) \Big|_{x=x_n} = \underset{x \rightarrow 0}{\text{Lt}} \; P(x_n)/\Delta x = d[P(x_n)]/dx \ldots(2.59)$$

28

Generalizing for all the x_n values, the probability density function is given by

$$p(x) = d[P(x)]/dx \qquad \dots \dots (2.60)$$

Similarly the probability distribution is given by

$$P(x) = \int p(x)dx \qquad \dots \dots (2.61)$$

The concepts of the statistical height and period parameters of ocean waves were made more meaningful by the studies of many researchers (Seiwell, 1948; Weigel, 1949; Rudnick, 1951; Munk and Arthur, 1951; Darbyshire, 1952; Putz, 1952; Pierson and Marks, 1952; Watters, 1953; Yoshida et al.,1953; Darlington, 1954; etc.) on the distribution of wave heights and periods about their mean values.

2.5. DISTRIBUTION OF INDIVIDUAL WAVE HEIGHTS

The distribution of individual wave heights, especially in the shallow waters, has attracted the attention of many researchers (Longuet-Higgins, 1952; Putz, 1952; Gluhovskii, 1968; Goda, 1975; Lee and Black, 1978; Tayfun, 1980, 1981, 1983a,b; Huang et al., 1983a; Tang et al., 1985; etc.) and different mathematical/empirical models are put forward for the probability densities. The important ones are discussed in the following sections.

2.5.1. Rayleigh Distribution

Based on the works of Rice (1944, 1945) it was shown by Longuet-Higgins (1952) that the distribution of individual wave heights are Gaussian and follow the distribution function suggested by Rayleigh (1880). Similar conclusions are drawn by Putz (1952) also. The pdf is given by

$$p(H) = (H/4\sigma^2) \exp [-H^2/8\sigma^2] \qquad \ldots\ldots(2.62)$$

where H is the individual wave height and σ^2, the veriance. In terms of the significant wave height (H_s) this can be written as

$$p(H) = (4H/H_s^2) \exp [-2(H/H_s)^2] \qquad \ldots\ldots(2.63)$$

and in terms of the average height ($\bar{H}$), this becomes

$$p(H) = (\pi H/2\bar{H}^2) \exp [-(\pi/4)(H/\bar{H})^2] \qquad \ldots\ldots(2.64)$$

The assumptions made in deriving the above relations are

(i) the wave spectrum contains a single narrow band of frequencies, and

(ii) the wave energy is being received from a large number of different sources whose phases are random.

This model is tested worldover by many researchers and evidences are provided for the applicability of this to

30

waves with broad-band spectra also under the condition of individual waves being defined by zero-crossing method (Bretschneider, 1959; Chakraborti and Snider, 1974; Longuet-Higgins, 1975; Tayfun, 1977; Dattatri et al., 1979; Goda, 1979; Huang and Long, 1980;etc.). The use of this distribution is sometimes extended to the shallow waters also. Good agreement of the shallow water data with the Rayleigh distribution is reported in some studies (Goodknight and Russel,1963; Koele and Bruyn, 1964; Harris, 1972; Manohar et al., 1974; Ou and Tang, 1974; Thornton and Guza, 1983;etc.). However, from detailed studies, many authors (Thompson, 1974; Dattatri, 1973; Goda, 1974; Black, 1978; Deo, 1979; Deo and Narasimhan, 1979; Baba, 1983; Baba and Harish, 1985;etc.) have reported that the waves higher than H_s depart from the Rayleigh distribution in many cases to an alarming extent. Kuo and Kuo (1975) suggested that this is due to

(i)   the non-linear effects of wave interactions yielding more larger waves,

(ii) the effect of bottom friction yielding reduction in the low frequency components, and

(iii) the effect of wave breaking which would truncate the distribution and transfer some of the kinetic energy to the high frequency components.

31

From an experimental study of the surface elevation probability distribution of wind waves in the laboratory Huang and Long (1980) derived a form for highly non-Gaussian conditions, based on Gram-Charlier expansion and a 4-term relation was suggested as a good approximation. This 4-term expansion is closely similar to the one given by Longuet-Higgins (1963). As a viable alternative to the computation of the pdf by the Gram-Charlier approximation, Huang et al. (1983a) derived equation for the probability density function of non-linear random wave field based on Stokes expansion to the 3rd order. For finite waters an additional parameter, the non-dimensional depth, is incorporated. This model is strictly for narrow band cases and is therefore more restrictive as far as the band width is concerned.

The Rayleigh distribution has a strong mathematical base and it has been widely used for quite some time in predicting the crest-to-trough heights of sea waves with apparent success (Huang and Long, 1980; Tayfun, 1983a; etc.). In spite of the deviation of the higher waves in shallow waters from this model, it is being used as a first approximation in view of its simplicity as a single-parameter model.

2.5.2. Gluhovskii's Distribution

Considering the fact that waves experience transformation in accordance with the water depth, once they enter shallow waters, Gluhovskii (1968) after analysing a large number of wave records from different coasts suggested a semi-empirical function for the distribution of wave heights by incorporating the relative water depth as a controlling parameter. The probability density function is given by

$$p(H) = (\pi/2\bar{H})[(1+H_*/(2\pi)^{1/2})(1-H_*)]^{-1}(H/\bar{H})^{(1+H_*)/(1-H_*)}$$
$$\exp\left[[-\pi/4(1+H_*/(2\pi)^{1/2}](H/\bar{H})^{2/(1-H_*)}\right] \quad \ldots\ldots(2.65)$$

where $H_* = \bar{H}/h$ $\qquad\qquad \ldots\ldots(2.66)$

This model is a modification of the Rayleigh distribution with the introduction of a relative depth parameter. In the deep water conditions where $\bar{H} \ll h$ this model assumes the form of Rayleigh (Eq.2.64). This form was verified for different bottom slopes (0.1-0.001) and bottom sediments (sand and gravel) and it is claimed that this can be applied to any region from the deep water to the breaker zone (Gluhovskii, 1968). Some observational evidence to the applicability of this model to the shallow water waves are available from the southwest coast of India (Baba, 1983; Baba and Harish, 1985; Rachel, 1987; Saji, 1987; etc.).

33

2.5.3. Ibrageemov's Distribution

In an analysis of Gluhovskii's function (Eq.2.65) and field data, Ibrageemov (1973) found that the distribution of wave heights in and near the breaker zone is controlled not only by depth, but also by the periods of the individual waves. In addition to the depth, the wave period is introduced as a controlling parameter and an empirical function is suggested for the distribution of wave heights, the pdf of which is given by

$$p(H) = (\pi/2\bar{H}\,\psi)(H/\bar{H})^{(2-\psi)/\psi}\exp\left[(-\pi/4)(H/\bar{H})^{2/\psi}\right]$$

$$\ldots(2.67)$$

where $\psi = 1-0.56\exp(-4.6h/\bar{T}^2)$ $\ldots\ldots(2.68)$

In deep water conditions, when $h \gg \bar{T}$, this model also assumes the form of Rayleigh distribution (Eq.2.48). That is, though the dependence of the wave period was established for the surf zone conditions it is capable of predicting the deep water wave height distribution also. Based on this observation, it is argued that this model can be applied to all regions ranging from deep water to the breaker zone. In the shallow waters the depth is small and the empirical parameter assumes definite values. The validity of this factor in the shallow water conditions is yet to be verified.

2.5.4. Truncated Rayleigh Distributions

The wave attenuation due to irregular breaking was studied by Goda (1975) and a theory was formulated. Based on this theory the Rayliegh distribution was modified to explain the distribution of breaking and broken components in area of water depth shallower than about 2.5 times the equivalent deep water significant wave height. The probability density of this truncated Rayleigh distribution (Goda,1975) is given by

$$p(x) = \mu \, 2\lambda^2 x \, \exp \, [-\lambda^2 \, x^2] \qquad \qquad \ldots\ldots(2.69)$$

where

$$1/\mu = 1-[1+\lambda^2 x_1(x_1-x_2)] \, \exp \, [-(\lambda x_1)^2] \qquad \ldots\ldots(2.70)$$

$x = H/H_0'$, the non-dimensional wave height,

$H_0' = K_r H_0$, the deep water equivalent wave height, and

$\lambda = 1.416/K_s$

in which K_r and K_s are the refraction and shoaling coefficients. x_1 and x_2 are the ranges of breaker heights which can be calculated using Goda's breaker index

$$x_b = C_7(L_0/H_0') \left[1-\exp \, [-1.5(\pi h/H_0')(H_0'/L_0)(1+K\tan^n \phi)]\right]$$

$$\ldots\ldots(2.71)$$

ϕ is the angle of inclination of sea bed. For a best fit of the index curves Goda recommended the values

35

$$K = 15$$

$$n = 4/3$$

$$C_7 = \begin{cases} 0.18 & \text{for } x_1 \\ 0.12 & \text{for } x_2 \end{cases}$$

$$\dots\dots(2.72)$$

This model assumes the constancy of wave number and mean wave period. For deep water conditions, $x \leq x_2$, this assumes the form of Rayleigh distribution. The simultaneous wave observations carried out at depths of about 20, 14 and 10 m at the Port of Sakata supported Goda's theory of decrease of wave heights due to irregular breaking in very shallow waters (Irie, 1975).

In a study to investigate the effect of breaking on wave statistics, Kuo and Kuo (1975) also observed that the probability density function of wave heights with a certain intensity of breaking waves could be explained by a truncated Rayleigh distribution. In extreme cases for very shallow waters they used the limiting height of solitary wave to predict the breaking wave heights. A similar form of truncated Rayleigh distribution is recommended by Battjes (1974) for the shallow water wave heights. In a comparison with the field data collected from the Ala Moana Beach (Hawai) Black (1978) obtained excellent fit with the truncated Rayleigh distribution in the breaker zone, but poor fit in both offshore and shoreward of this region.

2.5.5. Weibull Distribution

In search for a general distribution which fits for all positions in a reef Lee and Black (1978) suggested the Weibull distribution, the pdf of which is given by

$$p(H) = C_8 C_9 H^{C_9 - 1} \exp [-C_8 H^{C_9}] \qquad \ldots (2.73)$$

The peakedness coefficient, C_9, for a Weibull distribution is given by

$$C_9 = 4 \int_0^\infty H \, p(H)^2 \, dH \qquad \ldots (2.74)$$

The approximate value of C_9 for data divided into bins of width ΔH can be computed from the relation

$$C_9 = (4/N^2 \Delta H) \sum_{i=1}^{NBINS} H_i (m_i)^2 \qquad \ldots (2.75)$$

where N is the total number of waves, NBINS is the number of bins and H_i and m_i are the heights and number of occurrences respectively in the 'i'th bin. Since the squared probability density term in the distribution width function tends to magnify small deviations from the theoretical distribution and C_9 is sensitive to the choice of the number of bins, it should be selected such that NBINS < N/10.

The Weibull coefficient, C_8, may be determined using the relation

$$C_8 = [\Gamma(1+1/C_9)/\bar{H}]^{C_9} \qquad \ldots (2.76)$$

It should be noted that Rayleigh is a special case of the Weibull distribution with $C_9 = 2$ and $C_8 = 1/(H_{rms})^2$. Where Rayleigh distribution is a function of the veriance, the Weibull distribution is a function of the higher moments about the mean.

In a comparison of the probability densities predicted by this model with the measured ones, Lee and Black (1978) obtained correlation coefficients greater than 0.98, which is unity for a perfect fit. Forristall (1978) also recommended the use of Weibull distribution for wave heights from the analysis of hurricane-generated waves in the Gulf of Mexico. As reported in Lee and Black (1978), Arhan and Ezraty (1975) also used Weibull distribution successfully to fit their wave data in the shallow waters.

2.5.6. Tayfun's Distribution

From the studies on the consequences of the fact that the crest and trough of the wave do not occur at the same time, Tayfun (1981) developed an envelope approach to explain the distribution of crest-to-trough wave heights. The equation of Rice (1945) for the joint distribution for the amplitudes of two points on the envelope separated by time T is integrated to give the distribution of zero crossing wave heights. The probability density is given by

$$p(H') = 2 \int_{-1/\nu}^{\nu\nu} \hat{p}(T) \int_{0}^{2H'} p(A',2H'-A';\bar{T}/2)dA'dT, \quad \text{for } H' \geq 0$$

$$\ldots\ldots(2.77)$$

where $\hat{p}(T)$ represents the probability density of normalised zero-up- crossing periods such as that given by Longuet-Higgins (1975) and $H' = H/\bar{H}$ is the normalised wave height.

$$p(A',A'';T/2) = (\pi^2/4)[A'A''/(1-r^2)] \; I_0[\pi r A'A''/2(1-r^2)]$$

$$\exp [-(\pi/4)[A'^2+A''^2]/(1-r^2)]\ldots\ldots(2.78)$$

in which A' and A" are the normalized trough and crest heights given by

$$A' = A(t)/\bar{A} \qquad = 2A(t)/\bar{H} \qquad\qquad \ldots\ldots(2.79)$$

$$A'' = A(t+T/2)/\bar{A} = 2A(t+T/2)/\bar{H} \qquad \ldots\ldots(2.80)$$

I_0 denotes the zero-order modified Bessel function of the first kind, and

$$r(T/2) = (F_1{}^2+F_2{}^2)^{1/2} \qquad\qquad \ldots\ldots(2.81)$$

$$F_1(T/2) = (m_0)^{-1}\int_{0}^{\infty} S(\omega)\cos(\omega - \bar{\omega})(T/2)d\omega \qquad \ldots\ldots(2.82)$$

$$F_2(T/2) = -(m_0)^{-1}\int_{c}^{\infty} S(\omega)\sin(\omega - \bar{\omega})(T/2)d\omega \qquad \ldots\ldots(2.83)$$

Under narrow band conditions, as $\nu^2 \to 0$, $S(\omega)$ and $\hat{p}(T)$ tend to behave as pseudo-delta functions centered at $\omega = \bar{\omega}$ and $T = \bar{T}$ respectively. With $T = \bar{T}$ being fixed, the trigonometric terms in Eqs.(2.82 and 2.83) when expanded in Taylor series to second-order in $(\omega - \bar{\omega})$ gives

39

$$F_2(\bar{T}/2) \simeq 0 \text{ and } r(\bar{T}/2) \simeq F_1(\bar{T}/2) = 1-[(\pi\nu)^2/2]\ldots(2.84)$$

On this basis Eq.(2.77) reduces to

$$p(H') = 2\int_o^{2H'} p(A',2H'-A';\bar{T}/2)dA' \qquad \ldots(2.85)$$

Tayfun (1983) has shown that as $\nu^2 \rightarrow 0$, the approximation improves considerably and, for $\nu^2 \leq 0.04$ the error is less than 2% relative to the exact solution for values of H' in the range 0.25-3.50, which represents at least 98% of the total probability mass in all cases.

If the spectrum is not narrow, the envelope will change during half-wave period and if the wave is high, so that the crest is near the extreme on the envelope, it is likely that the associated trough will have a small amplitude, and the wave height will be less than twice the value of the envelope at the crest. Thus different amplitudes are considered for the envelope at the time of the crest and trough. This approach seems to give a good representation of the effect of spectral width on the wave height distribution. A case study given by Tayfun (1981) showed very favourable results supporting the concepts developed in the study. Forristall (1984) compared this distribution to simulated waves with different spectral shapes as well as to field observations from the Gulf of Mexico and reports excellent agreement.

2.6. JOINT DISTRIBUTION OF WAVE HEIGHTS AND PERIODS

Studies on probability density function of period, height and wave lengths have been conducted over the last 2-3 decades. However, studies on the joint distribution of heights and periods of sea waves are not as extensive as that on the distribution of heights. Knowledge of the joint distribution of heights and periods of ocean waves is essential for any ocean/coastal engineering application. The majority of the studies reported have been mainly concerned with theoretical or deep water aspects of the problem. The few theories available in the literature are discussed here.

2.6.1. Rayleigh Distribution

On the basis of wave data from various deep and shallow water locations Krilov (1956) and later based on field and laboratory data Bretschneider (1959) recommended the use of Rayleigh distribution for the square of wave periods. The probability density of the distribution function is given by

$$p(T) = exp \ [-0.675 \ (T/\bar{T})^4] \qquad \qquad .....(2.86)$$

Different authors opined differently regarding the suitability of this in modelling the distribution of wave periods. Chakraborti and Snider (1974) observed that the Rayleigh's form shows poor fit with the height data and better fit with T^2. According to Goda (1979) this semi-

empirical proposal of the Rayleigh distribution for T^2 provides a fair approximation to the wind waves although the formulation of a joint distribution in a closed form is lacking. Studies conducted with field data collected from different parts of the Indian coasts show that this model is incapable of simulating the period distributions (Narasimhan and Deo, 1979a; Dattatri et al., 1979).

Assuming that the marginal pdfs of wave heights and square of periods to be Rayleigh distributed, Bretschneider (1959) examined its joint distribution for the extreme cases of correlation (0 and +1). For the cases of total independence (zero correlation) the pdf is given by

$$p(H',T') = 1.35H' \exp [-\pi H'^2/4]T'^3 \exp [-0.675T'^4]$$

$$.....(2.87)$$

where $\qquad$ $T' = T/\bar{T}$ and $H' = H/\bar{H}$ $\qquad$ .....(2.88)

For the case of total dependence (correlation coefficient equals to 1) all data points on a plot of joint Rayleigh pdfs fall on a 45 degree straight line through the origin.

2.6.2. Gluhovskii's Distribution

Following the assumption of total independence between the wave height and period distribution Gluhovskii (1968)

42

suggested a depth controlled relation for the joint distribution of heights and periods of sea waves. The probability density is given by

$$p(H,T) = (0.4165 \pi^2/[(1+0.4H_*)(1-H_*)\bar{H}](T^3/\bar{T}^4)(H')^{p-1}$$
$$\exp\,[-(\pi/4)[1/(1+0.4H_*)(H')^p+0.833(T/\bar{T})^4]]$$
$$\dots\dots(2.89)$$

where $p = 2/(1-H_*)$. H_* and H' are given by Eqs.(2.66 & 2.88).

Although the theoretical models developed by Bretscheneider and Gluhovskii (Eqs.2.87 and 2.89) are based on the primary condition that the two variables (height and period) are mutually independent, observational evidence show considerable correlation (Chakraborti and Cooley, 1977; Goda, 1978,1979; Thornton and Schaeffer, 1978; Dattatri et al., 1979; Baba and Harish, 1985; Harish and Baba, 1986; etc.). Baba and Harish (1985) obtained correlation coefficients ranging up to 0.69. Dattatri et al. (1979) observed still higher correlation between the individual heights and periods for the monsoon data collected off Mangalore. Houmb and Overik (1976) have shown that the assumption of independency between the height and period leads to an overestimation of the heights of breaking waves lower than H_s. This deviation leads to the failure of these models in predicting the joint distribution of heights and periods as observed in the field.

43

2.6.3. Longuet-Higgins' Distributions

The theory of the joint distribution of wave heights and periods in a closed form was provided by Longuet-Higgins (1975) under the assumption of a narrow band spectrum. It is actually a recapitulation of a previous· work of the author (Longuet-Higgins, 1957) on the statistical properties of random moving surface. The joint probability density is given by

$$p(H',T') = (\pi H'^2/4\nu) \exp [-(\pi/4)H'^2[1+(T'-1)^2/\nu^2]]$$

$$\dots\dots(2.90)$$

where $\nu = (m_0 m_2/m_1^2 - 1)^{1/2}$ $\qquad$ $\dots\dots(2.91)$

and H' and T' are given by Eq.(2.88).

The joint distribution given by Eq.(2.90) has its axis of symmetry at T' = 1 (or T = $\bar{T}$) and yields no correlation between wave heights and periods. Generally, ocean waves exhibit a distinctly positive correlation (as seen before) especially for the low waves, which sometimes amounts to more than 0.7 among sea waves (Goda, 1978). The results obtained from the analysis of 89 wave records from the Japanese coast (Goda, 1978) and data from the 1961 storm in the North Atlantic (Chakraborti and Cooley, 1977) it is seen that this theory could explain the characteristics of the

44

joint distribution in its upper portion with high waves if the spectral width parameter is selected in such a way that it would fit the marginal distribution of wave periods. But the theory disagrees with the observed joint distribution in its lower portion with low waves. Disagreement of the theory with the observed are reported by others also (Houmb and Overik, 1976; Ezraty et al., 1977; Tayfun, 1981,1983a,b; etc.). Lee and Black (1978) explained the poor fit of the data with the model as mainly due to the positive skewness observed in the actual shallow water distribution of periods. However, Shum and Melville (1984) observed good agreement with their data from both calm and hurricane sea states, when an integral transform method was used to obtain continuous time series of wave amplitude and period from ocean wave measurements.

More recently Longuet-Higgins (1983) remodelled his earlier equations to incorporate the effects of non-linearities and finite band width. The modified function is derived by considering the statistics of the wave envelope and in particular the joint distribution of envelope amplitude and the time derivative of the envelope phase. By relating the frequency to the period and assuming that the phase envelope is an increasing function of time, the following distribution function is derived:

$$p(H",T") = C_{LH}(H"/T")^2 \exp \left[-(H"^2/8)[1+\nu^{-2}(1-1/T")^2]\right]$$

$$\ldots\ldots(2.92)$$

where $\quad C_{LH} = (1/8)(2\pi)^{-1/2}\nu^{-1}/[1+(1+\nu^2)^{-1/2}]\ldots\ldots(2.93)$

$$H" = H/(m_0)^{1/2} \text{ and } T" = T/(m_0/m_4) \quad\ldots\ldots(2.94)$$

It can be seen that this distribution depends only on the spectral width parameter ν. Shum and Melville (1984) obtained good agreement of this model with their data based on wave envelope analysis (rather than waves themselves). Srokosz and Challenor (1987) report that this model did not fit their broad band data, but gave good fit with zero-crossing height and period distribution for $\nu < 0.4$, rather than $\nu \leq 0.6$ as suggested by Longuet-Higgins (1983). In a subsequent study Srokosz (1988) reports that for spectra narrower than those examined in the earlier study, while the overall shape of the predicted distribution is similar to the observed, the mode is incorrectly placed by this model.

2.6.4. CNEXO Distribution

The asymmetric pattern of the joint distribution of wave heights and periods is incorporated in the theory developed by the group of CNEXO (Ezraty et al., 1977) which is basically for the joint distribution of the amplitudes and periods of positive maxima. The time interval between successive positive maxima is estimated by extending the

46

theory of Cartwright and Longuet-Higgins (1956). They further presumed that it could be applicable to the joint distribution of heights and periods of zero-up-crossing waves by replacing the amplitude of positive maximum with one-half wave height and the quasi-period of positive maximum with zero-crossing wave period. The probability density of this joint distribution has the following form:

$$p(H'', T_1) = e'^3 H''^2 / [4(2\pi)^{1/2} \epsilon_s (1-\epsilon_s^2) T_1^5] \times$$
$$\exp[(H''^2/8\epsilon_s^2 T_1^4)[(T_1^2 - e'^2)^2 + e'^4 e''^2]]$$

$$\ldots\ldots(2.95)$$

where
$$T_1 = \bar{T}_1 T/\bar{T} ;$$
$$e' = [1+(1-\epsilon_s^2)^{1/2}]/2 ;$$
$$e'' = \epsilon_s/(1-\epsilon_s^2)^{1/2} ;$$
$$\epsilon_s = (1-m_2^2/m_0 m_4)^{1/2} \qquad \ldots\ldots(2.96)$$

and H" is defined in Eq.(2.94). The mean value of the non-dimensional wave period, $\bar{T}_1$, can be obtained by numerically integrating the marginal distribution of wave period of the following form

$$p(T_1) = e'^3 e''^2 T_1 / [(T_1^2 - e'^2)^2 + e'^4 e''^2]^{3/2} \ldots\ldots(2.97)$$

Goda (1978) found that the value of $\bar{T}_1$, obtained by numerical integration of Eq.(2.97), remained close to 1 for the range of $0 < \epsilon_s < 0.95$. When this theory was applied for ocean waves by the group of CNEXO, the spectral width

47

parameter was estimated by the formula given in Eq.3.3. In an analysis of the governing parameters of the joint distribution Goda (1978) observed that the apparent spectral width parameter is less influential and the correlation coefficient between individual wave heights and periods could be the governing parameter. The correlation coefficient is defined as:

$$r(H,T) = 1/\sigma_H \ \sigma_T \ N_Z \ \sum_{i=1}^{N_Z} (H_i - \bar{H})(T_i - \bar{T}) \qquad \ldots\ldots(2.98)$$

where σ_H and σ_T denotes the standard deviations of wave heights and periods respectively and N_Z is the number of zero-crossing waves.

Battjes (1977) pointed out that the theory of CNEXO is theoretically inconsistent, especially in its approximation of the mean zero-up-crossing wave period with the mean interval of positive maxima. However, Goda (1978,1979) and Harish and Baba (1986) observed that it could provide a good approximation to the joint distribution. Goda (1978) points out that as the correlation coefficient r(H,T) increases, especially when r(H,T) $\geq$ 0.4 the asymmetry of joint distribution becomes conspicuous, which is in accordance with the theory of CNEXO.

A shortcoming of this theory is that the asymmetry of the joint distribution with respect to the wave period

48

becomes too pronounced with the increase of the spectral width parameter (Goda, 1979; Harish and Baba, 1986) and the theory predicts the probability of long periods much higher than that observed (Goda, 1979). Further, Goda (1978) found that the observed density followed the theory of CNEXO only when H' < 0.4 and the rest followed closely the theory of Longuet-Higgins. That is, the portion of high waves in the joint distribution retains the symmetry around their mean value of periods irrespective of the value of spectral width parameter.

2.6.5. Tayfun's Distribution

Another theoretical expression for the joint distribution of crest-to-trough wave height and zero-up-crossing periods is developed by Tayfun (1983b) from a modified extension of presently available results relevant to wave envelopes and periods under narrow band conditions. The wave profile is viewed in time as a slowly modulated carrier wave considering the narrow band approximation. The joint probability density of this model is given by

$$p(H',T_2) = 2 \hat{p}(T_2) \int_0^{2H'} p[A',2H'-A';(\bar{T}/2)(1+\mathcal{V} T_2)]dA'$$
$$\text{for } H' \geq 0 \text{ and } T_2 \leq \mathcal{V}^{-1} \quad \ldots\ldots(2.99)$$

in which H' and $\mathcal{V}$ are given in Eqs.(2.88 & 2.91) and

$$T_2 = (T-\bar{T})/\nu \bar{T}$$

$$\hat{p}(T_2) = (1+\nu^2)^{1/2}/2(1+T_2^2)^{3/2} \quad \text{for} \quad |T_2| \le \nu^{-1}$$

$$\ldots\ldots(2.100)$$

The other parameters are same as given in section 2.5.6. As in the case of height distribution Tayfun (1983) has shown that for $\nu^2 \le 0.04$, this displays an error of less than 5% relative to the exact solution.

2.7. SUMMARY

From the literature it is seen that a generalized spectral form is very much lacking. Different models are proposed for different environmental conditions like deep water, shallow water, fully developed seas, developing sea state, etc. The parameters and coefficients vary from researcher to researcher. For instance, in the deep water conditions the high frequency face of the spectrum was first intuitively set by Neumann (1953) to be proportional to f^{-6}. Later Phillips (1958) deduced from dimensional considerations that it should be f^{-5} and this has been substantiated by many field and laboratory experiments. More recently some workers found that it is f^{-4} instead. Further, in the shallow water conditions observational evidences are abundant for a negative power of 3 and less.

Most of the spectral models are described by one, two or more independent wave parameters. However, a large number of these models are based on two commonly used design wave parameters, the total energy and the peak frequency. In an analysis of these spectral forms it can be seen that most of these models unify into one form with varying coefficients. Chakraborti (1986) has reported such a form in a comparison of a few two-parameter models.

The models derived for deep water conditions are found to fail in simulating the shallow water wave spectra satisfactorily. However, the empirical Scott's model and its modified form (Scott-Weigel spectrum) are found to fit the observed shallow water spectra in some cases. Most of the shallow water wave spectral models are the modification of one or other of the deep water models with a finite depth dispersion relationship. Extensive field calibration under a wide range of wave conditions is required for any model to be used for a particular location, until a generalized model with universal applicability is developed.

Most of the models to predict the distribution of individual heights of sea waves are based on the theoretically sound Rayleigh distribution derived for the deep water conditions. Owing to the simplicity as a single parameter model, the Rayleigh distribution is extensively used as a

first approximation, even in the shallow waters. Observations at different environmental conditions reveal that though the Rayleigh form is valid beyond the narrow band cases, the distribution of heights in the shallow waters are non-Gaussian. The depth-controlled forms appear to be promising for the future. The envelope approach to describe the height distribution offers scope for the future studies as this new concept seems to be more realistic. Most of the shallow water models lack sufficient field verifications.

Studies on the distribution of wave periods and its joint distribution with heights are not extensive. Most of the studies are based on the assumption that the height and period distributions are mutually independent. Recently, dependency of heights and periods are reported by many researchers and correlation coefficients of the order of 0.7 are reported. Asymmetry of the joint distribution is revealed in the recent studies and this concept seems to throw more light into the study of the joint distribution. The models developed on the basis of this concept also require sufficient field verification.

CHAPTER 3

WAVE RECORDING AND ANALYSIS

The study essentially involved the long-term recording of waves at a shallow water location. A brief description of the location and its coastal environment are given first, followed by a description of the instrumentation and mode of wave recording, in this chapter. The criteria for selection of wave records for analyses, the different types of analyses performed and some preliminary results on wave climate are also dealt with in detail.

3.1. LOCATION

Alleppey (lat.$9^\circ 29' 30'' N$, long.$76^\circ 19' 10'' E$) is a small coastal town at the southwest coast of India (Fig.3.1). The coastline is almost straight with a 350° North orientation. The shelf is gently sloping and the isobaths are more or less parallel to the shoreline. The sediment up to a distance of about 80 m from the Mean Water Line (MWL) consists mainly of fine sand, and further offshore - predominantly of clay. The tide here is semi-diurnal and the maximum range is only about 1 m.

A 300 m long pier present at this location provides a convenient platform for carrying out the studies even during the rough monsoon season when the sea is otherwise inaccessible due to high breakers.

53
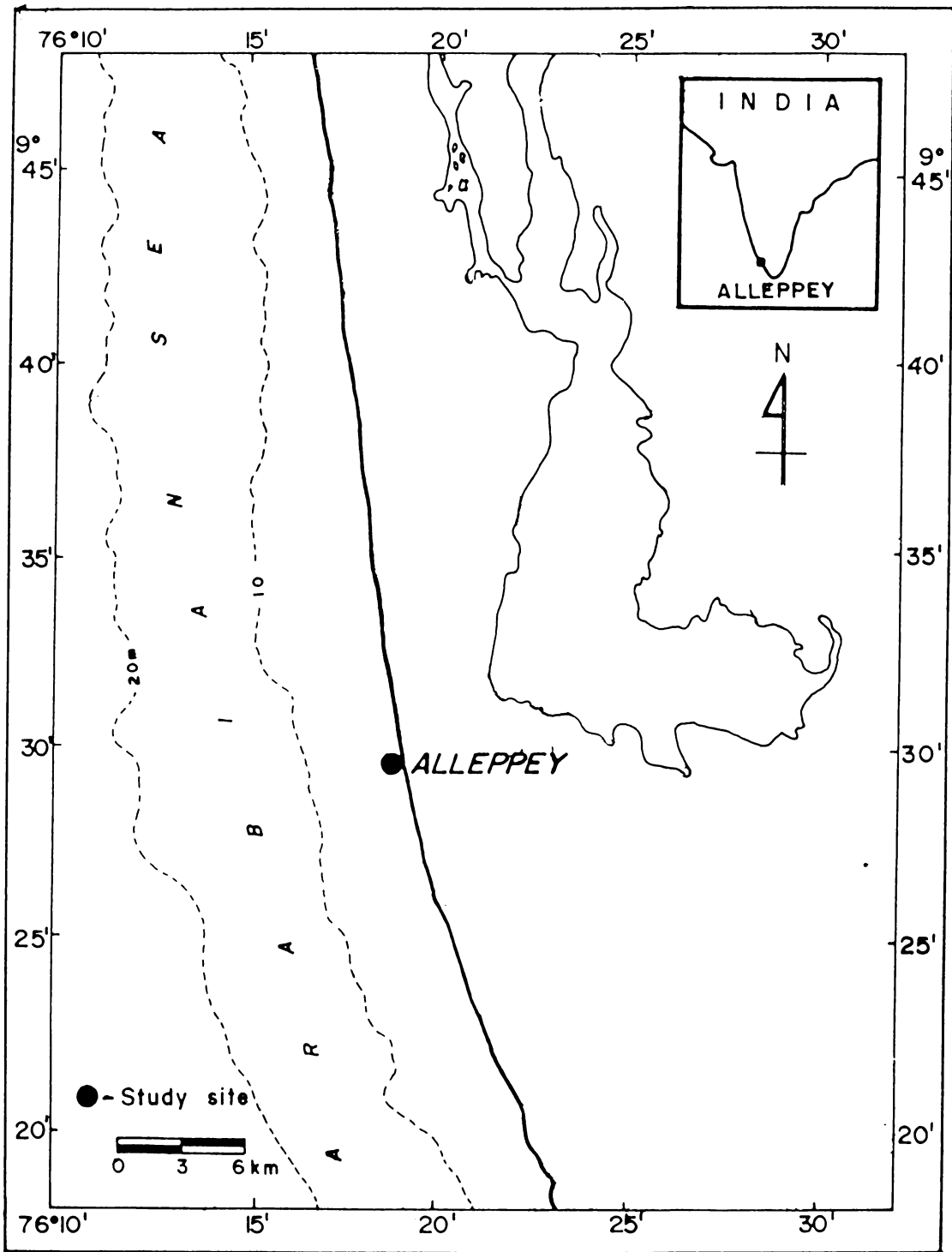
Fig.3.1 Location map.

3.2. WAVE RECORDING SYSTEM

Devices ranging from human eye to sophisticated electronic instruments are used in measuring the ocean surface waves, depending upon the accuracy required. When visual observations are sufficient for the determination of average period or velocity of propagation, instrumental recordings are necessary for the determination of various characteristics of these complex random waves. Obtaining a true measurement of the ocean surface conditions depend on many factors like selection and location of the measuring device, its installation, data control and recording, processing, maintenance of the system, etc.

The three types of wave measuring devices that are commonly employed for the measurement of ocean waves are those measuring (i) from above the sea surface - mainly remote sensing techniques, (ii) at the sea surface and (iii) from below the sea surface.

3.2.1. Selection of Recording System

In general, remote sensing techniques are very expensive and the methods of processing and analysis are yet to be standardized. Surface measuring instruments, especially the accelerometer type buoys give a better representation of the actual sea surface. These are very useful

for the studies like wave growth processes where the energy in the higher frequencies are critical. These are expensive, though not as high as remote sensing, and chances of damage and loss are high. Resistance/capacitance wave staffs and pressure recorders are comparatively cheaper, but require a supporting structure (except for bottom mounted pressure gauges). The wave staffs are more susceptible to wave impacts, leakage, corrosion, fouling and other hazards and require continuous inspection and servicing. Subsurface pressure recorders are suitable particularly for shallow waters since they are almost sheltered from excessive water particle velocities and breaking waves. Also, they are less susceptible to damages by ships, fishing activities, floating debris and corrosion, since no surface penetrating or floating parts are required. They are not affected by tidal variations or storm surges, and on the other hand provide information on mean water level and do not require frequent maintenance. The main disadvantages are that they require signal correction, have restricted frequency response (higher frequencies are filtered out) and are subjected to fouling.

3.2.2. The Recording System Used

In the study of the wave energy spectrum, more attention is paid generally to the energy containing

portion. In the height and period distribution studies the high frequency-filtered data is more appropriate since shorter period waves superimposed near the zero-crossings may lead to erroneous period and height values in the wave-by-wave analysis (usually a filter is applied to eliminate this error). In the present study the wave energy in the higher frequencies are considered insignificant. Hence, a sub-surface pressure recorder is selected to measure the shallow water waves.

The pressure type recorder used consists of a Wave and Tide Telemetering System (Sivadas, 1981), a standard strip chart recorder, a timer and power supply and control units (Fig.3.2). The Wave and Tide Telemetering System comprises of an air-filled stainless steel bellow-type pressure transducer connected by a two-core cable to the shore-based receiving and processing unit which in turn is connected to the strip chart recorder (Fig.3.3). The transducer functions on the principle of proportional variation of electrical inductance. A plunger core is connected to the bellow. With the passage of waves the core moves up and down freely through the centre of an activated coil, in accordance with the movements of the bellow, inducing voltage in the coil proportional to the movements. The bellow and coil are kept inside a protection casing. The signals transmitted by the coil through the 2-core cable is

56
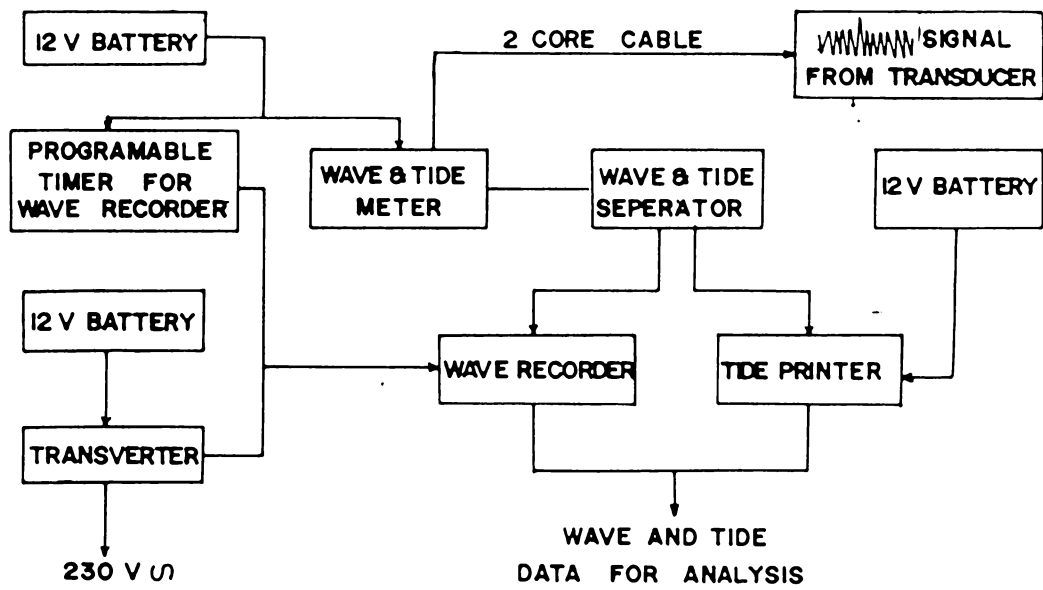
Fig.3.2 Schematic diagram of the wave recording system.
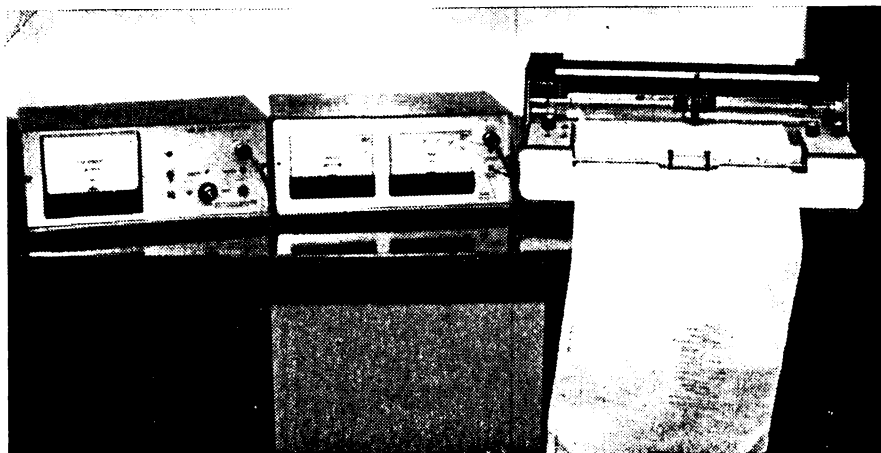
Fig.3.3 View of the wave recording system used.

received in the wave and tide telemeter which processes the signal and transmits to the wave and tide separator. This unit separates the tide and wave components using a low-pass filter. The wave output, in millivolts, is recorded on strip charts. The timer which can be programmed for the starting time and duration of recording, in fact, controls the AC power supply to the recorder. This facilitates the collection of wave records at fixed intervals for the required duration. A unique facility available in the system separates the waves undistorted, unlike some similar systems in which waves are reshaped to its nearest sinusoidal form.

3.2.3. Transducer Installation

The transducer is installed on a pile at the end of the pier at a depth of 5.5 m (Fig.3.4 & 3.5). The transducer projects 1.5 m seaward of the pile (Fig.3.5) to eliminate the possible effects of the piles on the waves being recorded. The attenuation of pressure due to waves increases with the depth of installation of the transducer. Hence it would be better if the transducer can be as close as possible to the water surface, depending upon the lowest tide and maximum depth of wave trough at the location. Taking into consideration of the low tidal range here (about 1 m only) and the maximum depression during the highest wave

Fig.3.4 Site of wave recording and
the pier at Alleppey.
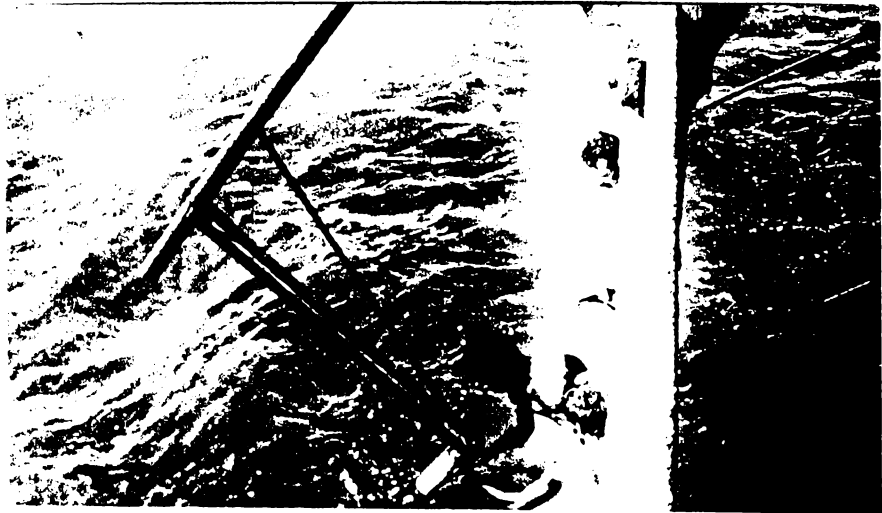
Fig.3.5 Installation of pressure transducer.

possible, the depth of installation is chosen to be 3.5 m below the Mean Sea Level. Thus the transducer is very close to the sea surface and at the same time will never get exposed. The transducer is protected against deposition of mud, marine fouling and corrosion by covering its open end with a flexible neoprine rubber hose filled with silicon oil (Fig.3.5). The cable is fastened to the installation mount and taken out through the GI pipe fixed to the pile of the pier, to shield it from the wave forces and vagaries of the marine environment.

3.2.4. Calibration

The system is calibrated in such a way that the output is linear and is 20 mv per meter of wave height. This signal is fed to the chart recorder running at 5 cm/min to give 5 cm deflection per meter of wave height. The calibration was checked periodically at site and in the laboratory. The site checking is done by noting the crest and trough heights against the calibrated pipe to which the transducer is attached and by comparing the wave heights with the ones recorded simultaneously (after applying the corrections towards attenuation of pressure, which will be explained later in this chapter).

The frequency response of the system has been checked for a wide range of height and period conditions (Fig.3.6).

58
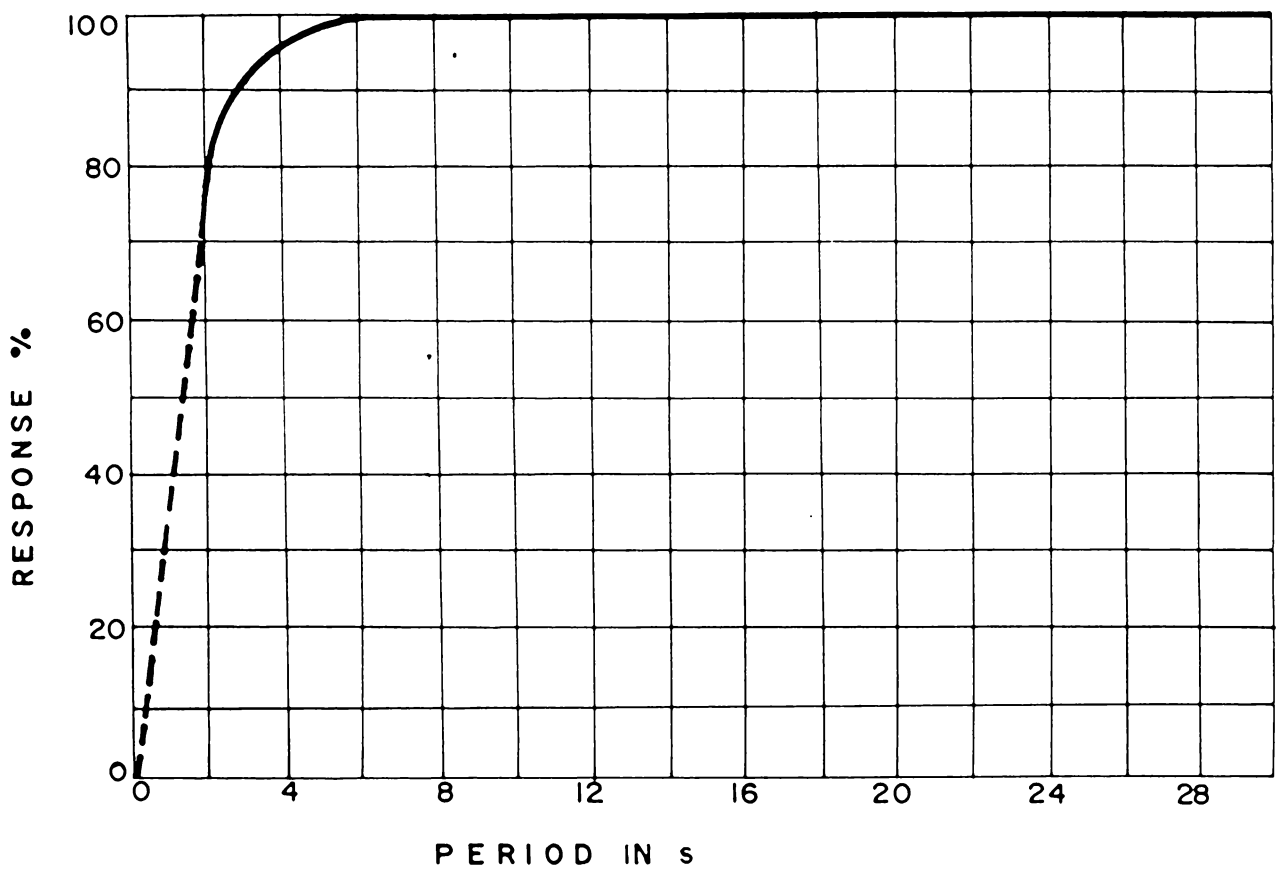
Fig.3.6 Frequency response diagram of the wave recorder.

It is found that the response is more than 95% for waves of period greater than 3 seconds and it is nearly 100% for waves of period 5 seconds and more.

3.3. RECORDING PROCEDURE AND SCREENING OF RECORDS

The recordings were carried out for 30 min. at every 3 hrs except during the periods of interruptions due to power failure, instrumental problems or servicing of the system. The predominant wave direction at the recording point was also noted at the site using a Brunton Compass.

From the available records, those with the following defects or limitations are discarded:

- a drift in the mean zero-line due to instrumental problems;
- breaks in the records due to power failure, cable fault, instrumental problems, etc.;
- noise due to power fluctuations, vibration of the transducer due to slackening of the installation; and
- near-straight-line records during very calm seas, particularly during the periods of mud banks.

All other records are considered for analysis.

3.4. PRELIMINARY ANALYSIS (TUCKER-DRAPER METHOD)

A reliable estimate of wave climate statistics can be obtained from the analysis of wave records collected

systematically over a sufficiently long period with a sample of one observation per day (Thompson and Harris, 1972; Baba, 1983; etc.). The records collected during a four year period (1980-1984), sampled at one record per day, is selected for a preliminary analysis. This analysis is carried out using the Tucker-Draper method (Draper, 1967; Silvester, 1974), which is regarded as the simplest of all.

In this method a portion of the record having a length of 720 s without any disturbance is selected for the analysis. The Mean Water Line (MWL) is drawn by fixing it with the eye. The heights of the highest and the second highest crests, A and B respectively, are measured from the MWL. Similarly the depths of the lowest and the second lowest troughs C and D are measured. The number of zero-crossings (N_z) and the number of crests (N_c) are also counted. From these values the different statistical parameters are estimated as detailed below.

The root mean square ~~wave~~ amplitude height (a_{rms}) can be computed from the following equations:

$$2a_{rms}/H_1 = 1/(2lnN_z)^{1/2} [1+(0.289/lnN_z)-(0.247/lnN_z^2)]$$

$$\ldots\ldots(3.1)$$

$$2a_{rms}/H_2 = 1/(2lnN_z)^{1/2} [1-(0.211/lnN_z)-(0.103/lnN_z^2)]$$

$$\ldots\ldots(3.2)$$

60

where H_1 = A+C and H_2 = B+D. As per theory, the results from H_1 and H_2 should be essentially the same. The statistical errors involved in this procedure are of the same order as averaging the highest 1/3 waves in the record for significant wave height, H_s (Silvester, 1974). In this study a_{rms} is determined using Eq.3.1. The spectral width parameter (e_w) is computed from

$$e_w^2 = 1 - (N_z/N_c)^2 \qquad \ldots\ldots(3.3)$$

This parameter helps to assess a more accurate proportion of $H_{1/10}$, H_s and $\bar{H}$. The ratio of these parameters to a_{rms} are given in the form of tables and nomograms in Silvester (1974).

The average zero-crossing period ($\bar{T}_z$) is given by

$$\bar{T}_z = 720/N_z \text{ s} \qquad \ldots\ldots(3.4)$$

In order to compensate for the attenuation of pressure with depth, correction is applied to the height parameters derived from this analysis using the following relation:

$$H = nH_p\cosh(2\pi h/L)/\cosh[(2\pi h/L)(1-z/h)] \qquad \ldots\ldots(3.5)$$

where H and H_p are the corrected and un-corrected heights and n is the instrument factor, L is the wave length corresponding to T_z, h is the water depth and z is the depth at which the transducer is installed.

61

Values ranging from 1.0 to 1.5 have been assigned to the instrument factor by various researchers (Homma et al., 1966; Bergan et al., 1968; Cizlak and Kowalzki, 1969; Kurian and Baba, 1986; etc.). The value of 1.25 suggested by Dattatri (1973) is used in the present analysis.

3.5. WAVE CLIMATE AT ALLEPPEY

The wave climate at this location is influenced by the southwest monsoon as is the case at any other location along the west coast of India. Following the suggestions of Thomas and Baba (1983) the data is grouped into two seasons - 'rough season' from May to October and 'fair season' from November to April.

3.5.1. Wave Height

The percentage exceedance of H_{st} and H_{max} for the two seasons are presented in Fig.3.7a. From the different percentages of exceedance it is seen that the wave intensity during the rough season is double of that during the other season. When 25, 50 and 75 percent of H_{st} exceed 1.40, 0.95 and 0.62 m respectively during the rough season, it exceed only 0.70, 0.52 and 0.42 m respectively during the fair season. Similar trend is shown by H_{max} also. During the rough season the above percentages of H_{max} exceed 1.90, 1.35 and 0.85 m respectively and during the fair season they

exceed 0.95, 0.72 and 0.58 m. The maximum wave height obser-
ved during the rough season is 3.8 m and that during the
fair season is 2.0 m. Similarly, the maximum value of H_{st}
during the rough and fair seasons are 3.0 and 1.4 m respec-
tively. Eventhough the wave activity is maximum during the
month of June, the formation of the mud-bank brings in a
few-weeks-long calm sea towards the end of the month.

3.5.2. Zero-Crossing Period

The zero-crossing periods ranged from 6 to 21 s with
the prominent periods falling in the range 7-15 s. The
frequency, in percentage, for the two seasons are presented
in Fig.3.7b. During the rough season the waves are better
sorted and are of comparatively shorter periods, the most
frequent being 8-9 s, which contribute to 31%. During the
other season waves with periods 9-11 s dominate and this
contribute to 46% of the distribution.

3.5.3. Wave Direction

Though the wave direction range from 200-320° with
respect to north, the majority of waves were confined to a
small range of 230-265°. The percentage occurrence of dire-
ction of wave approach is presented in Fig.3.7c. The waves
are more parallel to the coastline during the rough season.
The dominant direction during this season is 245-250° and
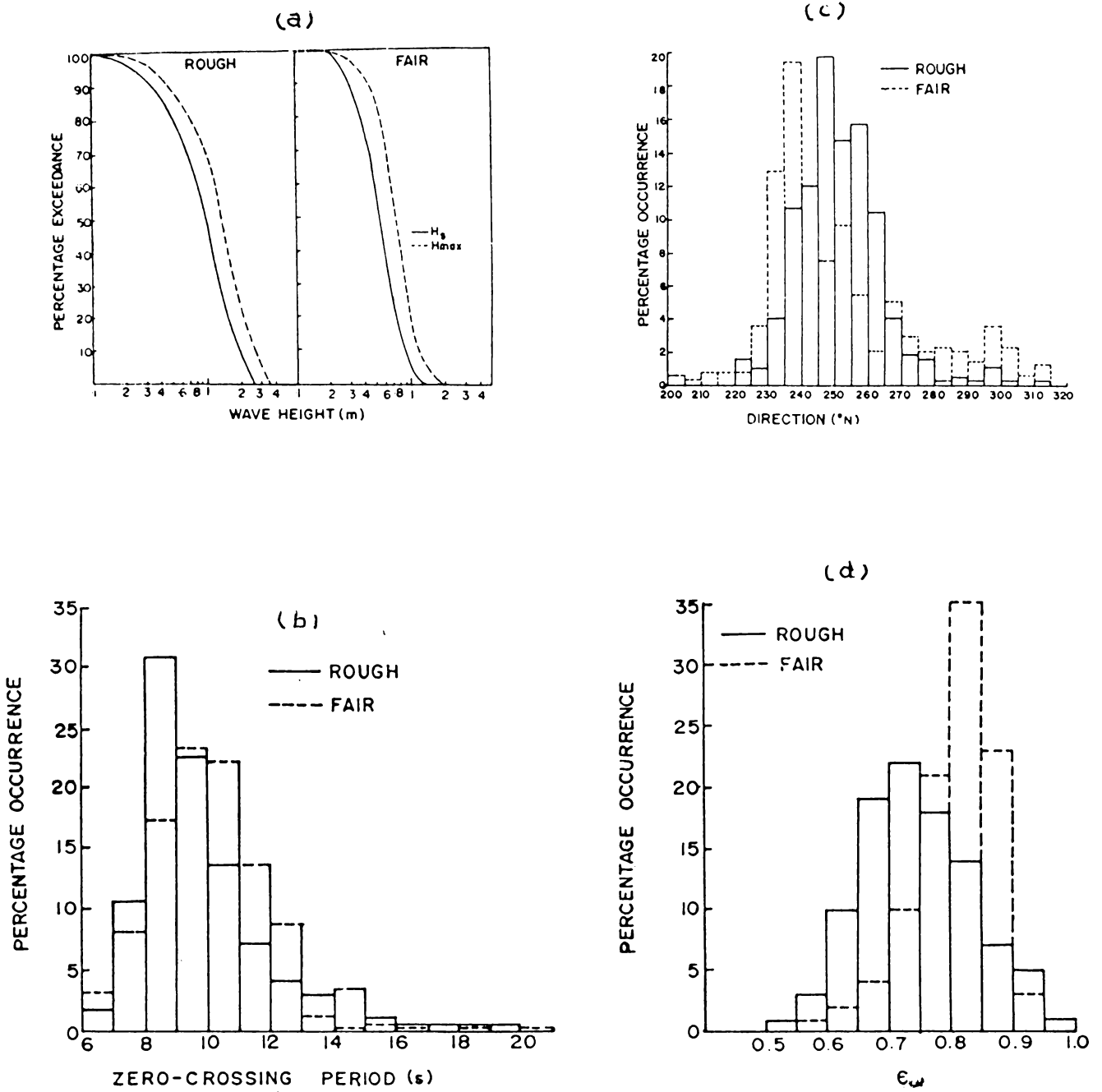
Fig.3.7 Wave climate at Alleppey during fair and rough season:
percentage exceedance of wave heights, H_{st} and H_{max} (a)
and frequency distribution of zero-crossing period (b);
direction (c) and spectral width parameter (d).

this contribute to about one-fifth of the total of the season. During this season 50% waves arrive from the direction 245-260° and 83% from 235-265°. During the fair season the waves are more southerly and about one-fifth of them arrive from the direction 235-240°. Waves from 230-245° contribute to 44% and that from 230-255° contribute to 61% during this season.

3.5.4. The Spectral Width

The spectral width parameter (ε_w) for both the seasons are presented in Fig.4.7.d as percentage occurrence. The values range from 0.5 to 1.0 during both the seasons. However, the average value is less during the rough season. During this season 70% of the values fall in the range 0.6-0.8 and 90% in the range 0.6-0.9. During the fair season about 60% of the values are in the range 0.8-0.9 and 90% in the range 0.7-0.9.

3.5.5. Persistence of Waves and Calm

Persistence diagrams serve as a ready reference to determine the number of times a range of wave conditions (at or above in the case of 'persistence of waves' and at or below in the case of 'persistence of calm') persist for at least for a given length of time. The significant wave heights computed for three-hourly intervals during 1981 are

selected for the preparation of these diagrams. At times of break in the data the wave condition prior to the interruption is assumed for the elapsed time. This appears to be justifiable since the nearshore wave characteristics show near-stationary conditions for durations of the order of a day (Thompson and Harris, 1972; Kurian et al., 1985a, etc.). Persistence of waves and calm are presented for height intervals of 0.25 m (Fig.3.8a-b). From the diagrams it can be seen that high wave conditions persist for very short durations and low wave conditions persist for long durations at this coast. For example, wave heights (H_{st}) at or above 2 m persisting for a day occurred on less than 20 occasions only during a year. It can be inferred easily from these diagrams that if a study requires a minimum wave height of 2.5 m persisting for 100 hrs, it cannot be conducted at this location. Similarly, if wave heights (H_{st}) not more than 1 m prevailing for a minimum of 60 hrs is required for a particular study, 95 such occasions are available during a year.

3.5.6. DISCUSSION ON THE WAVE CLIMATE

On an assessment of the distribution of the above parameters it can be seen that the waves during the rough season exhibit certain characteristic features. They are well sorted and arrive from the same generating area, as evidenced from the distribution of periods, directions and
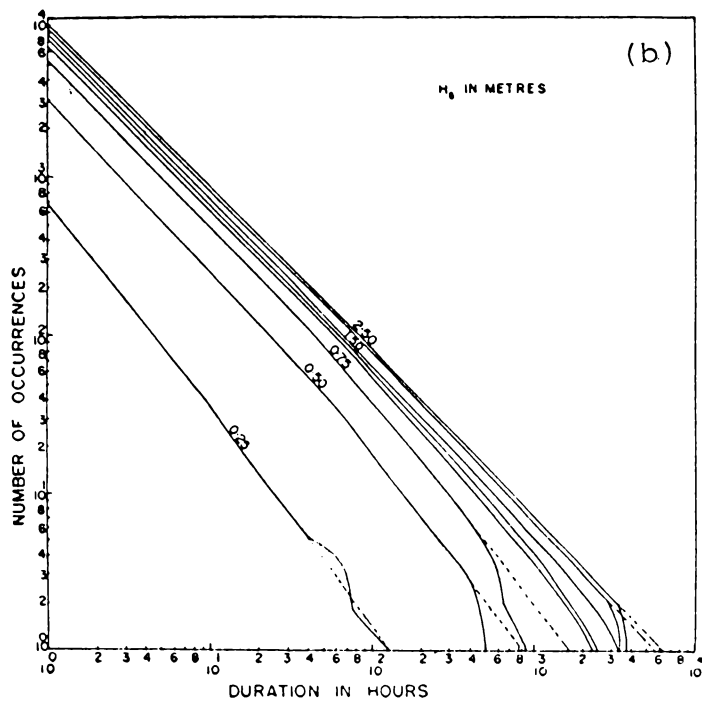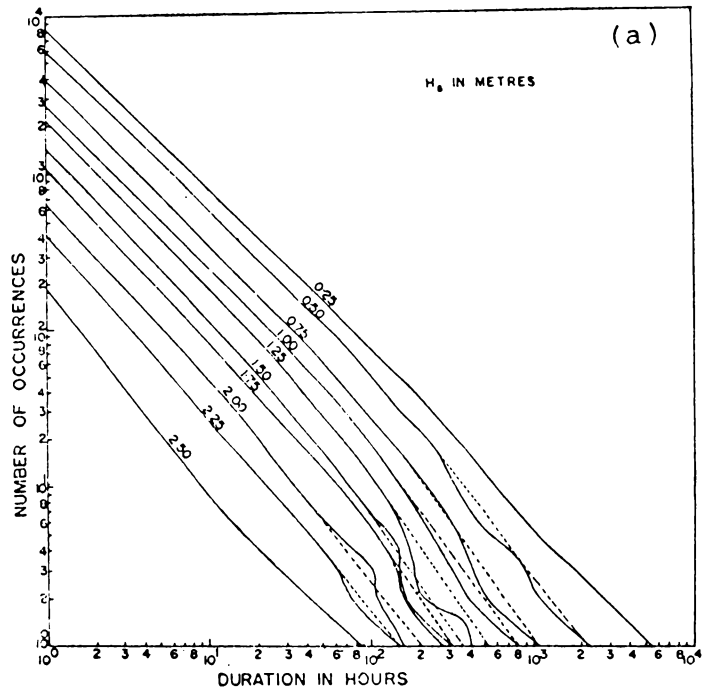
Fig.3.8. Persistence of (a) waves and
(b) calm at Alleppey.

spectral width. The lower periods are indicative of a not-far-away origin of these waves. Evidently these are generated under the influence of the south-west monsoon winds. From the monthly wind speed summary for the Arabian Sea and Northwest Indian Ocean (Boisvert, 1966) it is seen that from May the winds get intensified, the dominant direction being south-west. The intensification continues through June, July and August and the entire Arabian Sea and the North-western Indian Ocean become the wave generating area. Wind speeds of the order of 28 knots and more are reported all over this region. These winds prevail till September and the direction is reversed to northeast by November and continues till March, April and October being the transition periods. During the fair season the waves are poorly sorted as waves generated at different areas arrive at this coast. The larger period waves during this season associated with smaller heights and lesser frequencies of occurrence indicate that these waves are generated at great distances and have undergone different transformation processes like wave-wave and wave-current interactions, shoaling, refraction, diffraction, etc. Incidently, the prevailing wind in the Arabian Sea and the North-eastern Indian Ocean during this season has low velocities and north-easterly direction, leading to the generation of waves which also contribute to the wave climate.

3.6. DETAILED ANALYSIS

3.6.1. Selection of Records

The wave climate characteristics are found to vary only slightly from year to year during the examined 4 year period. Hence, the wave records collected during a one year period is selected for the detailed analysis of spectral and probabilistic characteristics. Records collected during 1981 are selected, as maximum number of records, with lesser number of disruptions, are available during this year. Thus 287 records, at the rate of one record per day (corresponding to 1200 Hrs), are used for the detailed analysis.

Since the coastal erosion is during the southwest monsoon, a more intensive study of the wave characteristics during this season is also warranted. Hence, an additional 30 three-hourly records collected for one month from mid-May are also utilised for this study.

3.6.2. Spectral Analysis

Two procedures are generally used to estimate the wave spectrum. One is using the data to estimate the covariance function first and then to compute the cosine Fourier transform of the covariance function numerically, in turn to compute the raw spectrum (Blackman and Tukey, 1958). The other uses the Fast Fourier Transform (FFT) computer

algorithm (Cooley and Tukey, 1965) to get the raw spectrum directly from the data. The basic principle of FFT lies in splitting the given time series into two half-series, which is performed many times during the process of computing the fourier transform. This involves lesser number of arithmetic operations compared to the covariance method, thereby leading to a large reduction in computation time. Both the procedures give the same results except that the covariance method applies an intrinsic smoothing to the spectrum. From the viewpoint of simplicity, computational speed and preservation of information, the FFT method is preferable. The FFT method is applied here to compute the wave spectrum.

The stability and accuracy of the spectral estimates depend on many parameters such as the record length, sampling interval, spectral window used, high/low frequency cut off, etc. (Goda, 1974; Harris, 1974; Baba et al., 1986; Kurian, 1987; etc.).

3.6.2.1. Digitization and processing

The records are digitized manually at 1 s interval, for accuracy and simplicity in digitization, since each cm of the chart paper, on which the waves were recorded, is divided into 6 divisions and the recordings were done on the chart running at a speed of 5 cm/s. In a few cases the

digitization is done at 1.2 s interval, since each cm of the chart paper is divided into 5 divisions in those cases. For the computation of spectral densities, 512 data points each are utilized. This is sufficient to obtain a reasonably stable spectrum (Baba et al., 1986).

Usually the time series digitized at equal time interval is subjected to a trend removal procedure before the spectral analysis. Even in the absence of any trend of significance, as the recording system used in the present study removes the trends, the raw data is subjected to a linear trend removal, which makes the arithmetic mean of the process zero.

3.6.2.2. Spectral window

In order to minimize the distortions in any desired aspect of the spectrum, spectral windows are applied. Eventhough the spectral windows are many, the most commonly used ones are the 'hanning' and the 'hamming' windows. Though the highest side lobe for the hamming spectral window is about one-third of the height of the highest side lobe for the hanning window, the heights of the side lobes for the latter fall off more rapidly than for the former (Wilson et al., 1974). The hanning window is selected in the present study. The hanning window function for a digitized time series of N points is defined as:

69

$$W_i = 0.5 [1+\cos 2\pi/N (i-(N+1)/2)] \qquad \ldots\ldots(3.6)$$

As a consequence of the application of this window all the spectral estimates have to be scaled by the constant factor $8\pi/0.375$ and this is incorporated in the computer programme.

3.6.2.3. Pressure attenuation

The pressure spectrum thus computed is subjected to pressure attenuation correction to obtain the surface spectrum using the standard relation (Harris, 1972; Black, 1978; etc.), which is given as

$$S(f) = [\cosh (2\pi h/L)/\cosh [(2\pi h/L)(1-z/h)]]^2 S_p(f) \ldots\ldots(3.7)$$

Grace (1978) modified this relation by incorporating an empirical correlation factor, $n(f)$, based on wave tank measurements. Since the use of this factor is not yet firmly substantiated and may introduce some uncertainty in the spectral data, as observed by Knowles (1982), it is not included in the present analysis.

3.6.2.4. Spectral parameters

In accordance with the frequency response of the recorder and the maximum wave period possible in this region, the low and high frequency cut off are fixed at 0.04 and 0.33 Hz respectively in the computation of moments and

70

other spectral parameters. The different spectral parameters computed are:

(i) nth moment of the spectrum

$$m_n = \int f^n S(f) df \qquad \qquad \ldots\ldots(3.8)$$

(ii) significant wave height

$$H_{ss} = 4(m_0)^{1/2} \qquad \qquad \ldots\ldots(3.9)$$

(iii) zero-crossing period

$$T_{m0,2} = (m_0/m_2)^{1/2} \qquad \qquad \ldots\ldots(3.10)$$

(iv) mean wave period

$$T_{m0,1} = m_0/m_1 \qquad \qquad \ldots\ldots(3.11)$$

(v) mean crest period

$$T_{m2,4} = (m_2/m_4)^{1/2} \qquad \qquad \ldots\ldots(3.12)$$

(vi) spectral band width parameters

$$\epsilon_s = (1 - m_2^2/m_0 m_4)^{1/2} \qquad \qquad \ldots\ldots(3.13)$$

$$\nu = (m_0 m_2/m_1^2 - 1)^{1/2} \qquad \qquad \ldots\ldots(3.14)$$

$$\nu_1 = (1 - m_1^2/m_0 m_2)^{1/2} \qquad \qquad \ldots\ldots(3.15)$$

(vii) spectral peakedness parameter

$$Q_p = 2/m_0^2 \int f S^2(f) df \qquad \qquad \ldots\ldots(3.16)$$

and (viii) slope of the high frequency side of the spectrum

$$S(f) \propto f^{-m} \quad ; \quad f_m < f < 1.8 f_m \qquad \qquad \ldots\ldots(3.17)$$

3.6.2.5. Smoothing

The wave spectrum obtained from the FFT method of analysis exhibits details much more than that required for

applications like graphical presentation and comparison with theories. The irrelevant details are usually suppressed by applying a smoothing function. The smoothing depends on the type of smoothing applied and the number of spectral lines used. In the comparison of the observed spectrum with theoretical ones a well-smoothed spectrum would be much useful since the theories are developed for single-peaked spectrum only. However, in the present case the prominent peaks are retained to get a clear picture of the actual wave conditions prevailing in the region of study. A weighted averaging method of smoothing (Ou, 1977) is applied here to obtain 33 bands with 16 degrees of freedom, without the low/ high frequency cut off, for comparison with the theoretical models and for graphical presentation.

3.6.3. Wave-by-Wave Analysis

In wave-by-wave analysis the zero-crossing method is generally accepted as a standard procedure. In this method, the MWL fixed by the eye, is drawn for the selected length of the record. The individual wave heights and periods can be measured by following two procedures, zero-up-crossing or zero-down-crossing methods. In the zero-up-crossing method, the points where the wave record crosses the MWL in an upward direction is marked and a wave is defined between two successive zero-up-crossings. The height of the wave is the

difference in elevation between the highest crest and the lowest trough between the two up-crossings and its period is the time interval between these two crossings. Similarly, in the zero-down-crossing method a wave is defined as the one between the two successive zero-down-crossings. The height and period of the wave is defined as in zero-up-crossing method. Individual wave heights and periods may differ in these two methods and hence the estimate of the maximum wave height in a record also may be different. However, in a comparative study of the two methods of analysis, no significant influence of the method is observed in the height statistics particularly H_{rms} and H_s and in the probability density distribution (Dattatri, 1985).

In the present investigation, the zero-up-crossing method of analysis is carried out for the study of the distributions of wave heights and periods. The heights and periods of individual waves are derived from the digitized data using a computer algorithm (Varkey and Gopinathan, 1984). This programme identifies the individual wave by the zero-up-crossings and measures the maxima and minima and the corresponding periods. The exact wave height is calculated from the interpolated crest and trough values using Stirling's formula (Scarborough, 1966). Necessary modifications are made in the above algorithm to incorporate

73

the correction for pressure attenuation as applicable to the location of study and the recording system employed.

In accordance with the frequency response of the recording system (Fig.3.6) waves with period less than 3 s are scanned out. The higher non-linear effect due to the exponential increase of the pressure attenuation correction factor (Eq.3.5) in the lower periods are also eliminated by this scanning. However, this removes the lower period tail of the probability density distributions. Since the density and energy in this range are not significant this does not affect the probabilistic characteristics. The different height and period parameters (H_{max}, H_{sw}, $\bar{H}$, T_c, T_z and T_s), spectral width (ϵ_w), steepness, individual and joint distributions of heights and periods are determined from the remaining individual waves.

CHAPTER 4

OBSERVED WAVE SPECTRAL AND STATISTICAL CHARACTERISTICS

The observed wave spectra, the spectrally obtained parameters and the statistical characteristics obtained from the wave-by-wave zero-up-crossing analysis are presented. Characteristics of the different parameters during rough and calm sea conditions are identified. Relations between the various parameters are also examined.

4.1. OBSERVED SPECTRA

Typical examples of the observed spectra are depicted in Fig.4.1. The spectra are generally multi-peaked. Out of the 317 spectra examined, 286 exhibited multi-peakedness. The peak period ($T_p = 1/f_m$, f_m being the frequency corresponding to the maximum energy density, known as the peak frequency) and the period corresponding to the major secondary peak are examined. The major secondary peak periods ranged from 2-16 s with energy density varying from 0.01-2.74 m^2s. The secondary peaks are generally on the lower period side of the main peak. When the average and standard deviation of peak periods are 11.2 and 2.5 s, those of the major secondary peak period are 6.4 and 3.1 s respectively.

Various reasons are put forward for the existence of multiple peaks in shallow waters. Multiple peaks can be due
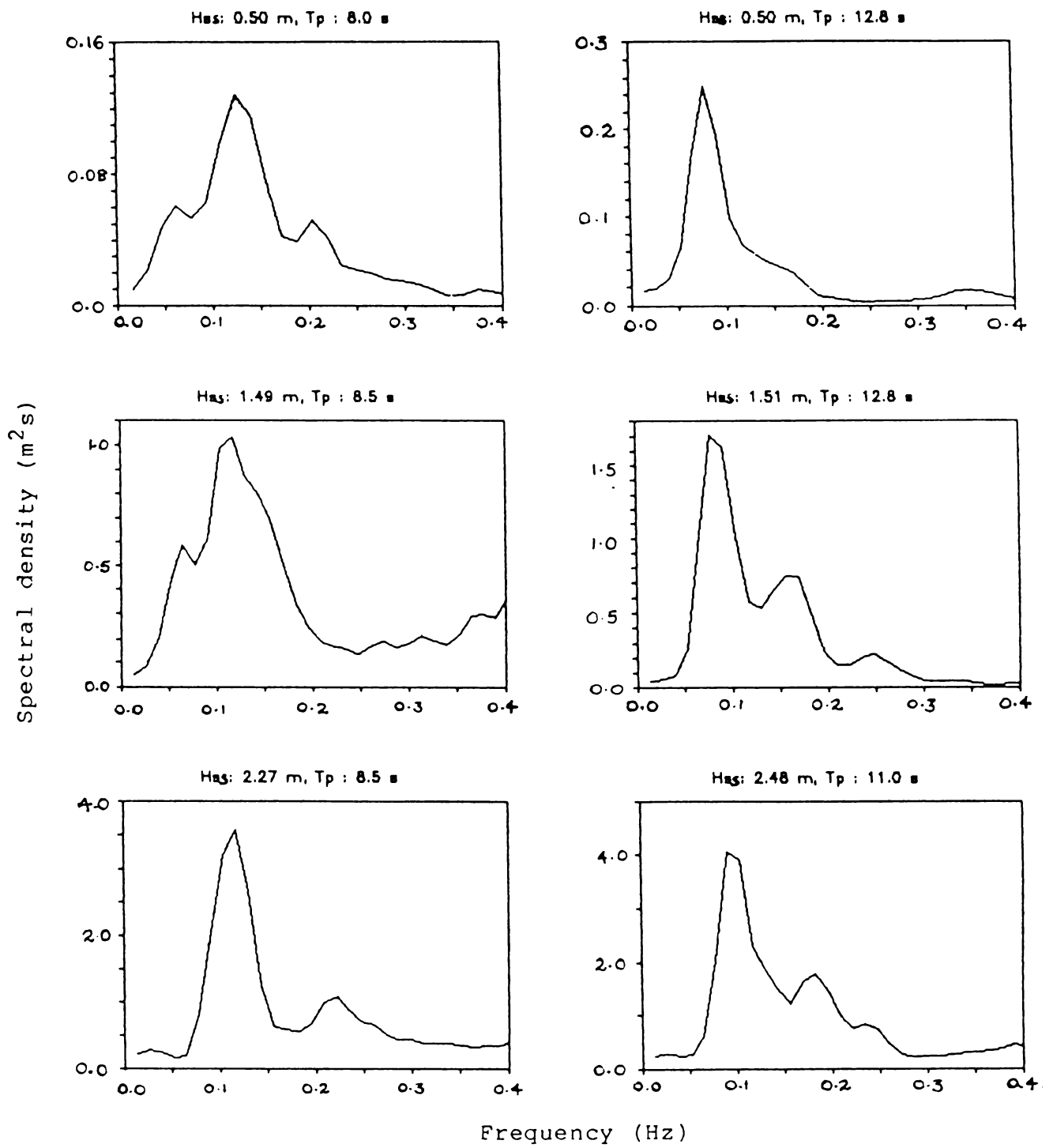
Fig.4.1 Typical examples of observed spectra.

to the co-existence of swells and wind waves. Peaks at higher harmonics of the peak frequency can occur due to the non-linear effects in the shallow waters. When a single-peaked spectrum propagates to the shallow waters, increasing fraction of the energy will be shifted to the higher harmonics of the dominant frequency (f_m) mainly due to wave breaking. As a result of this the spectral peak at twice the peak peak frequency ($2f_m$) can be higher than the peak at f_m (Sawaragi and Iwata, 1976; Dattatri, 1978). Another situation in which multiple peaks are generated is when the waves cross a submarine bar. When the crest level of the bar is close to the water level, much of the energy is shifted to the higher harmonics and multiple peaks with almost equal energies are developed (Thompson, 1974; Dattatri, 1987). This is a special case of the non-linear interaction of sea bottom on the passing waves.

In the present case, the secondary peaks are not generated by submarine bars since no such topographical features are present in the shallow waters off this coast (Kurian et al., 1985b). The secondary peak periods do not show any dependence on the peak periods. In the plot of the major secondary peak periods against T_p (Fig.4.2) wide scatter is observed. Very few values fall along the second harmonic of the peak frequency ($2f_m = 1/(T_p/2)$). Most of the values are lower than $T_p/2$ with a few in the range $T_p - T_p/2$

76
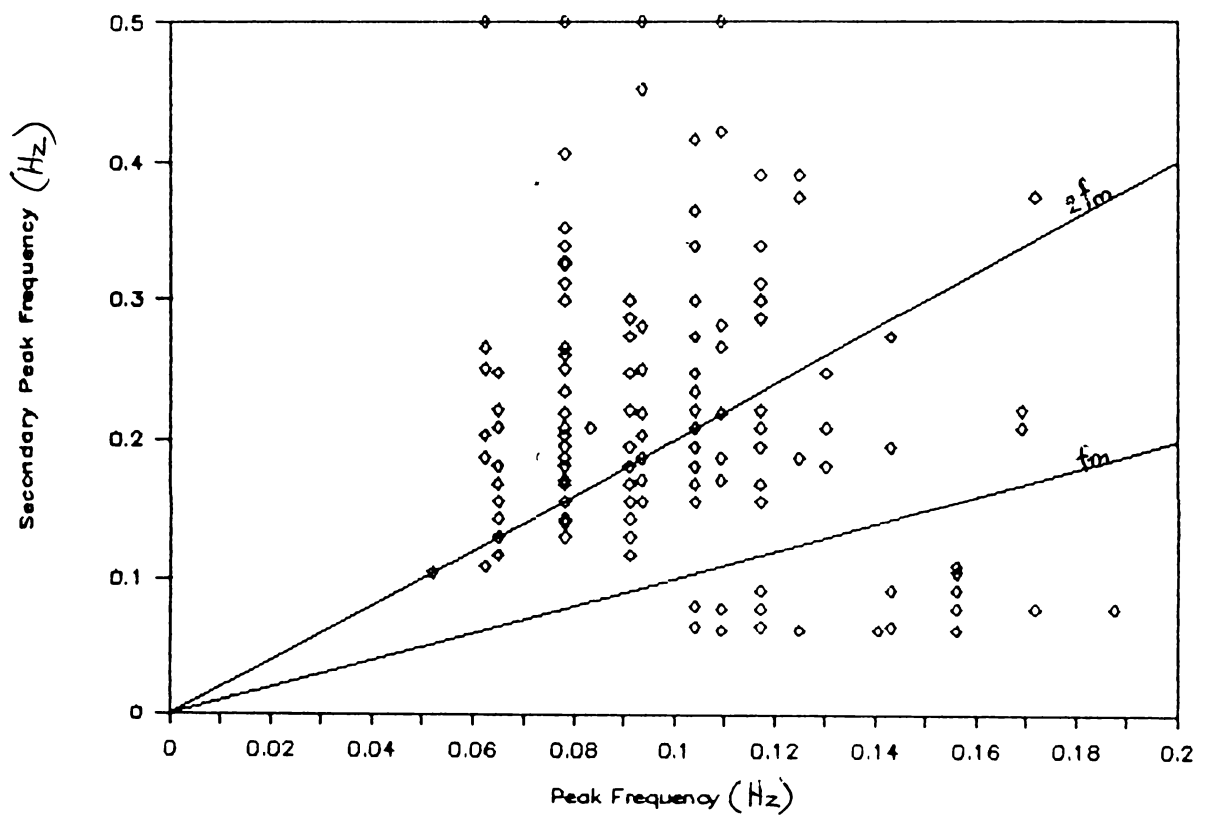
Fig.4.2 Plot of secondary peak frequency against
the dominant peak frequency.

and some even higher than T_p. The ratio of peak period to major secondary peak period ranged from 0.4 to 8 with an average of 2.1 and a standard deviation of 1 s. Among the 286 spectra with multiple peaks only 37 have the secondary peaks at the second harmonic of the peak frequency. The spectra for which secondary peaks are at $T_p/2$ are those having comparatively higher peak periods. The T_p in these cases range from 9.14-19.2 s with a mean of 12.46 and a standard deviation of 1.84 s. In the study of average spectra for US coastal waters, Thompson (1980) observed the major secondary peaks at $T_p/2$ for waves of peak periods higher than 10 s, especially for large wave heights. However, in the present case no dependence on wave height is observed (figure not presented). Hence, in most of the cases the secondary peaks observed may be due to the co-existence of swell and sea waves in this region.

4.2. OBSERVED SPECTRAL PARAMETERS

The different spectral parameters like significant wave height, peak period, slope of the high frequency side, spectral width parameters and spectral peakedness of the observed spectra are examined. The distribution of these parameters during the complete year as well as during periods of characteristic wave properties, like rough and fair wave conditions, are discussed in the following sections.

77

4.2.1. Significant Wave Heights

The significant wave heights (H_{ss}), computed with Eq.(3.9), ranged from 0.13-2.48 m during the period of study, with an average of 0.78 and a standard deviation of 0.52 m. However, it may be noted that the records representing very calm periods are not included in the analysis (see Sec.3.3), otherwise the minimum would have been much lower. From the temporal variation of H_{ss} (Fig.4.3) it can be seen that the wave height start to increase from the month of May and reaches the maximum value by mid-June. Then it decreases and attains lowest values by the first quarter of October. The low heights persist for the rest of the year. Intermittent calm periods are found to occur from the last quarter of June consequent to the formation of mudbanks.

As seen above, the higher waves occur during May-September. The maximum H_{ss} observed during this season is 2.48 m and the average for the season is 1.15 with a standard deviation of 0.52 m. The months of October-April is characterised by the low waves. The maximum H_{ss} observed during this season is only 0.97 m and the average is 0.44 m with a standard deviation of 0.18. Barring the calms during the mudbank periods, the lowest wave heights are observed during October-December.

The heights are distributed in two dominant ranges indicating two characteristic types of waves (Fig.4.4). They are 0.1-0.8 and 0.9-1.5 m contributing to 65 and 22% respectively. During May-September the maximum occurrence of H_{ss} is in the range 1-1.4 m which is 33.8% of the season and during October-April it is in the range 0.1-0.7, which contributes to 94%.

4.2.2. Peak Periods

The peak periods (T_p) ranged from 5.33-19.2 s with an average of 11.2 and a standard deviation of 2.5 s during the one year period. The highest value of 19.2 s occurred only once, otherwise the maximum T_p is only 15.6 s. The temporal distribution of T_p (Fig.4.5) shows that the periods are lower during the months of May-September. The values of T_p start to decrease from the middle of May, the lowest occurring during the period from the last quarter of May to mid-June. Again the long-period waves, along with the monsoonal ones appear from August. However, from October onwards the long-period swells start to dominate.

During May-September the dominant T_p is in the range 9-10 s which forms 29% of the season and 65.6% of the values are in the range 8-11 s. The long-period swells, with T_p in the range 12-13 s, appearing towards the end of this season

79
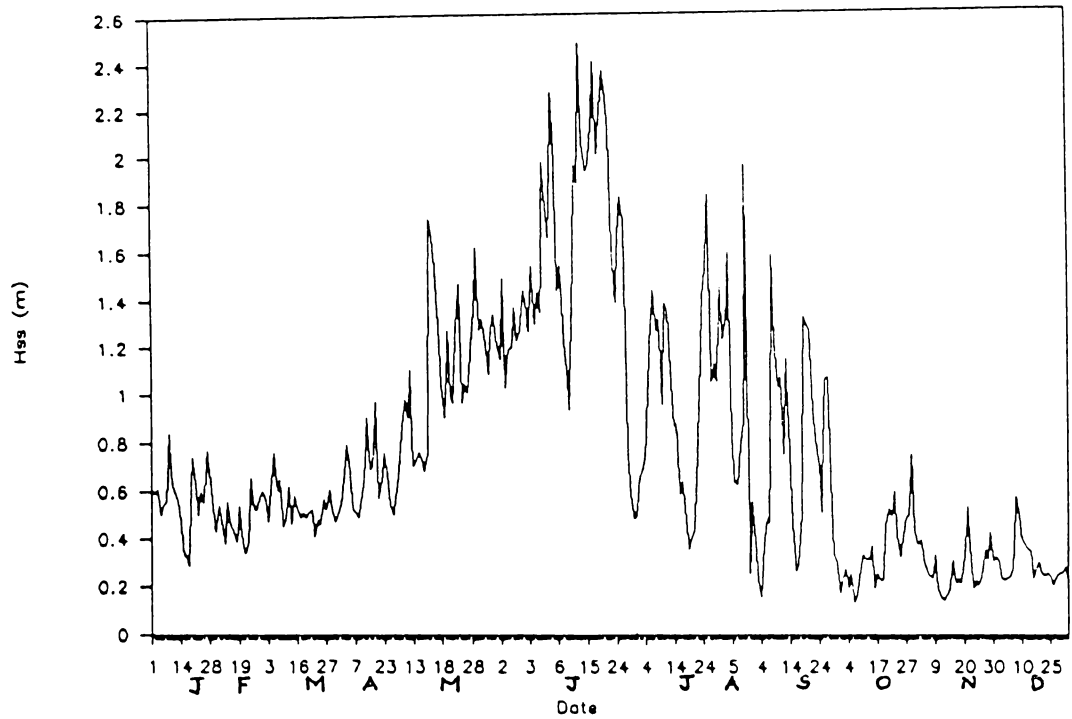
Fig.4.3 Temporal distribution of significant
wave height (H_{SS}).
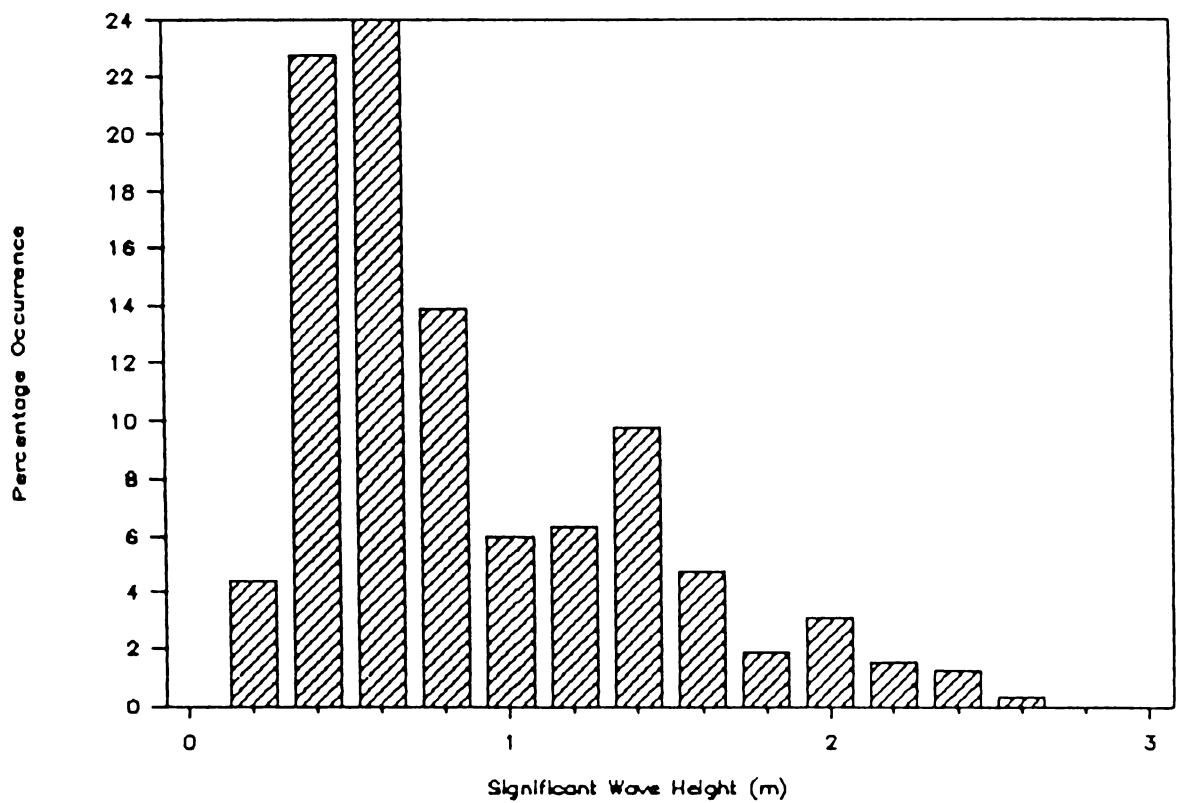
Fig.4.4 Frequency distribution of significant
wave height (H_{SS}).

contribute to 17.9% of the distribution. The average T_p during this season is 10.2 s with a standard deviation of 2.2.

During October-April the dominant T_p is in the range 12-13 s which contributes to 54.2% during this season. Waves with two other characteristic periods with T_p at 10-11 s and 15-16 s also exist during these months. They contribute to 16.3% and 14.5% respectively. The average T_p during this period is 12.1 with a standard deviation of 2.4 s.

The major secondary peak period values do not show any characteristic variation with season. They range from 2-16 s during both the seasons (May-September and October-April) with an average of 6.4 s. However, the variation is less during October-April, as indicated by the standard deviations (3.7 during May-September and 2.4 during October-April). These can be the contribution from the locally generated waves. The contribution of these waves to the total energy of the spectrum are very little when compared to that by the swells.

The frequency distribution of T_p (Fig.4.6) shows that waves with three different characteristic periods dominate in this region. Among these, T_p in the range 12-13 s dominate with 36.9% during the one year period followed by those in the range 9-11 s which contributes 33.4%. It can be noted from the figure that when the distribution is

80
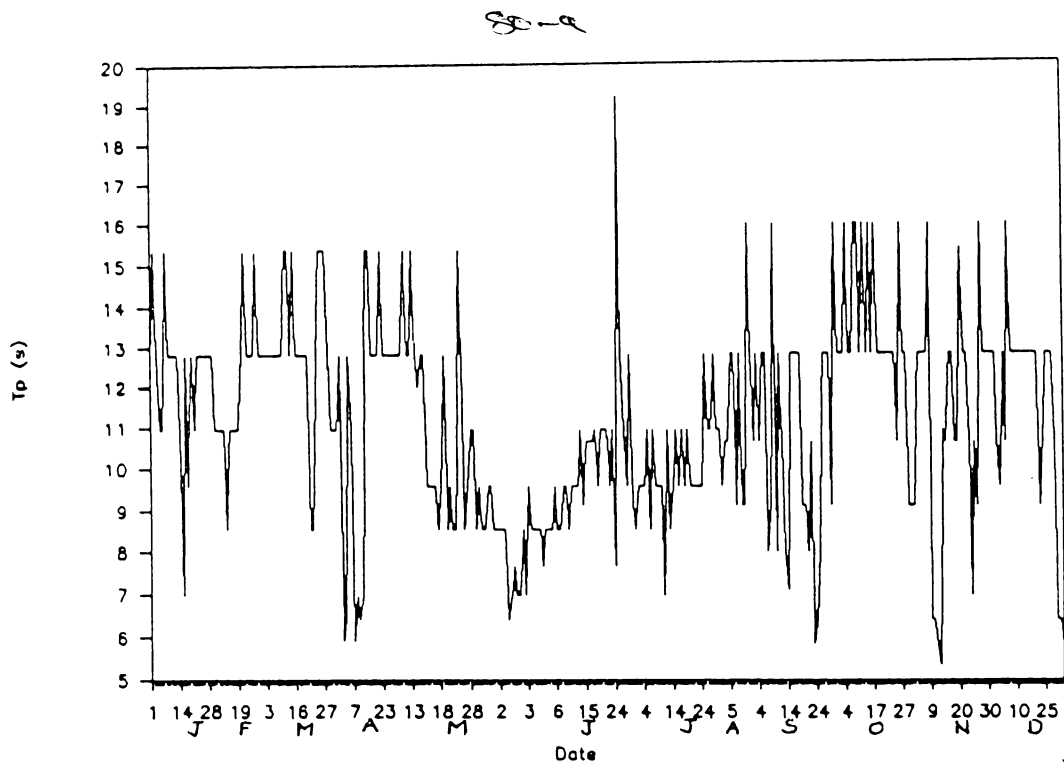
Fig.4.5 Temporal distribution of peak period (T_p).
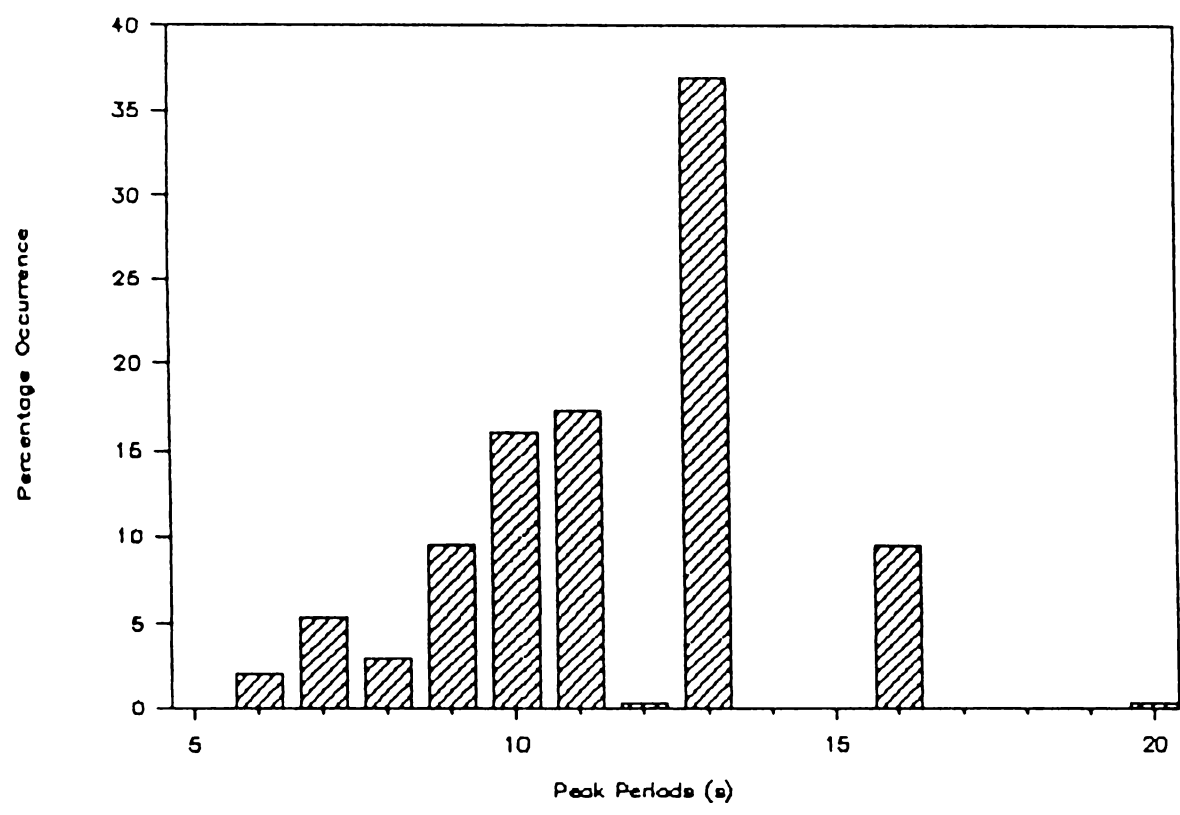
Fig.4.6 Frequency distribution of peak period (T_p).

continuous in the lower period ranges, it is discrete at narrow intervals at 12-13 s and 15-16 s. Dominance of the three typical T_p ranges (8-11, 12-13 and 15-16 s) is indicative of the arrival of waves of different characteristics from different generating areas. Following the discussion in Ch.3 (Sec.3.5) it may be inferred that during May-October the Arabian sea is the generating area for the waves arriving at this coast. During October-April the major contribution is from the long-travelled swells generated at two other far-off locations, one farther than the other.

4.2.3. Slope of the High Frequency Side of the Spectrum

The slope of the high frequency side of the spectrum calculated using Eq.(3.16) sometimes gives erroneous results due to the presence of secondary peaks within the range f_m-$1.8f_m$. The cases where the major secondary peaks fall in this range are excluded from the following discussion. However, other peaks, though not significant, may also affect the slope values. Since the number of observations without any peak in the range f_m-$1.8f_m$ are very few, the records with such minor peaks (in the above range) are not excluded. The slope values thus computed range from 0.22-4.76 with an average of 2.57 and a standard deviation of 0.97. There is considerable variation in slope during all the periods (Fig.4.7). However, a slight decrease in slope

81

is observed during May-September. The values start decreasing from May and the lowest are observed in June. It again increases with the retreat of this season. The average values for May-September and October-April are 2.32 and 2.72 with standard deviations of 0.85 and 1.01 respectively.

The values are almost normally distributed (Fig.4.8) with the peak in the range 2.1-2.2. However, when they are split into the two seasons, the peak is shifted to the lower values during May-September and to higher values during October-April (figures not presented). The maximum occurrences during May-September and October-April are in the ranges 2.00-2.25 and 3.00-3.25 respectively. Also, secondary peaks exist in the distributions in the ranges 2.50-2.75 and 3.50-3.75 during the above two seasons respectively.

It is to be noted that in shallow waters the slope of the high frequency side of the spectrum is always less compared to the equilibrium range value of wave spectral form in deep water conditions. In the shallow waters, the slope of the spectrum are reported to be lower by many researchers (see Sec.2.3) and values as low as 1.6 are reported.

In deep water, during the process of wave growth, non-linear wave-wave interaction/white-capping/breaking play an important role. Due to these processes some of the energy
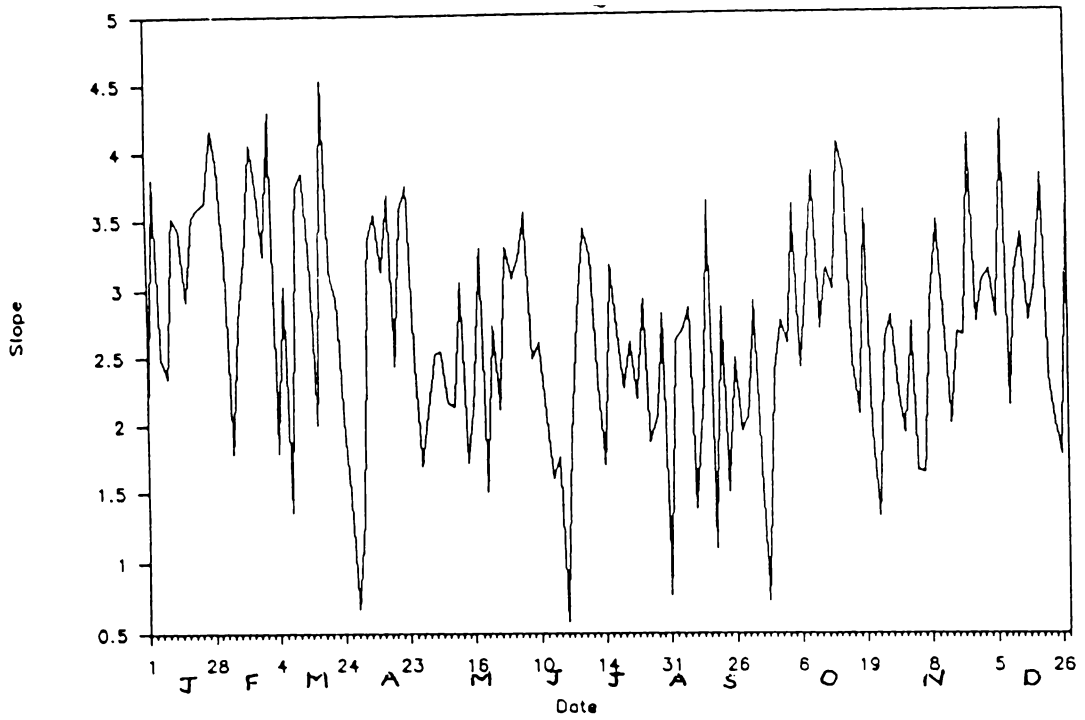
Fig.4.7 Temporal distribution of slope of the
high frequency side of the spectrum.
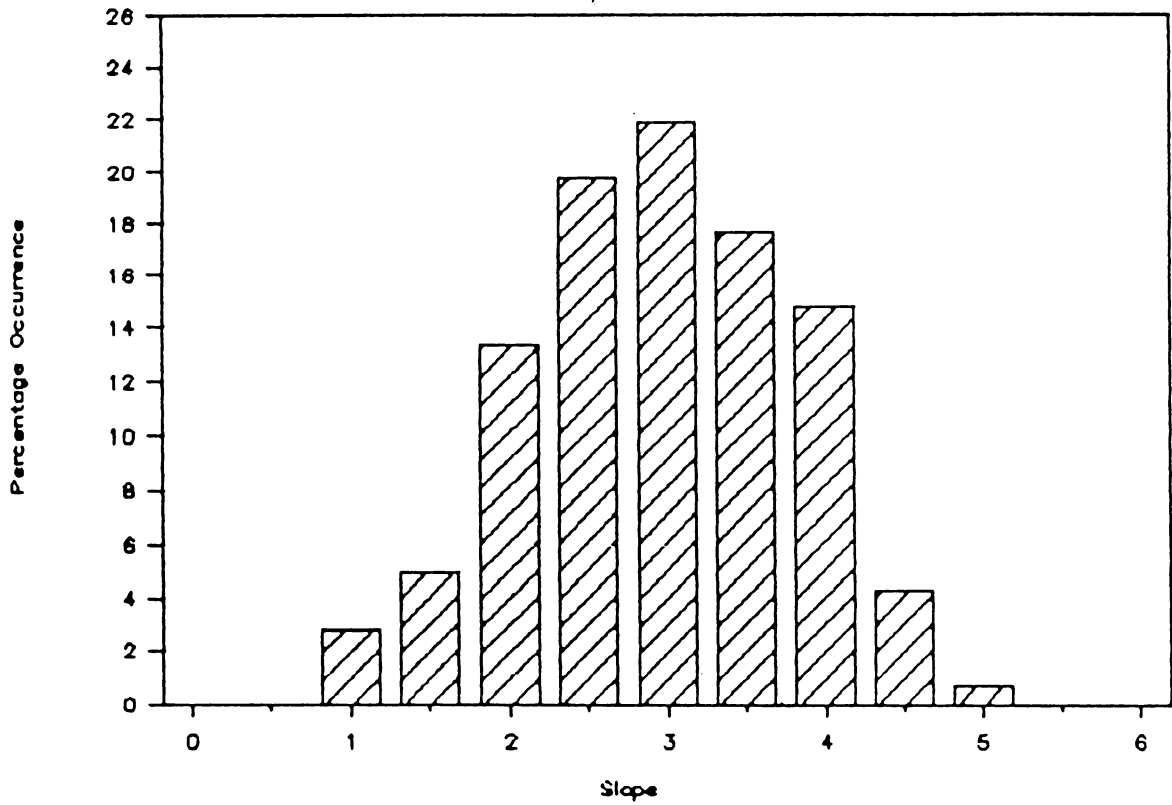
Fig.4.8 Frequency distribution of slope of the
high frequency side of the spectrum.

from the higher frequencies are transferred to the lower frequencies. Frequencies higher than f_m loses energy while f_m and frequencies lower than it gain energy as a result of the non-linear effects (Vincent, 1982). This results in an increase in the slope of the high frequency side of the spectrum. But, the shallow water waves are almost unrelated to the local wind conditions and hence the predominant waves observed in the shallow waters are generated elsewhere and propagated to the area of observation, after undergoing the different transformation processes like shoaling, refraction, diffraction, wave-wave/wave-current interactions, etc. The wave-wave interaction is comparatively insignificant during the propagation of waves outside the generating area unless it crosses over other fetches. It is the frictional attenuation that is important during the wave propagation in shallow waters and the energy loss will be more for waves with higher energies (Kurian, 1987). Consequently the slope of the high frequency side of the spectrum decreases significantly. It may be inferred from the above that the waves travelling over gently sloping bottom in shallow waters exhibit spectra with lesser slopes, when the local wave generation is not considered.

The still lesser slope observed during the monsoon periods may be due to the increased effect of frictional attenuation as the waves are of higher energy during this

season. However, most of the present data contain multiple peaks and hence the slope values computed with the present data cannot be used to check the dependence of the slope of the high frequency side of the spectrum on peak periods.

4.2.4. Spectral Width

The spectral width parameters presently in use are ε, ν and ν_1 (Eqs.3.13-3.15). The temporal distribution of these parameters computed from the wave spectrum are depicted in Fig.4.9 (a-c). Almost identical distributions are observed for these parameters. The values are comparatively lower during May-September. They start decreasing from May and reach the lowest value in June. With the withdrawal of this season, high values are once again observed. The highest values are observed in October. The range and average values of these parameters during both the seasons are presented in Table 4.1. This again shows that May-September is characterised by spectra with lower widths as evidenced by the low average values and the lesser scatter indicated by the standard deviation. The lower values observed during this season may be due to the predominance of waves generated by the monsoonal winds which have almost identical characteristics and the lesser significance of the low swells arriving from far-away locations. On the contrary, the higher values during October-April are the effect of the

84

presence of different wave trains of different characteristics. The larger range in values of spectral width parameters observed during the May-September, especially in July, may be due to the effect of the mudbanks which occur during this season. The waves are dampened in the mudbanks, the dampening being more on higher waves. Since the high monsoonal waves are attenuated, the locally generated waves become significant and this contribute to the increase in the width of the spectrum.

Table 4.1 Average Values of Spectral Width Parameters

	ϵ_s			ν			ν_1		
	1	2	3	1	2	3	1	2	3
Min.	0.63	0.64	0.63	0.34	0.37	0.34	0.32	0.35	0.32
Max.	0.89	0.89	0.89	0.82	0.70	0.82	0.63	0.57	0.63
Mean	0.76	0.73	0.79	0.52	0.48	0.56	0.46	0.43	0.49
S.D.	0.06	0.05	0.06	0.09	0.07	0.08	0.06	0.05	0.05

1: complete year; 2: May-September; 3: October-April

The value of ϵ is essentially 1 for sea waves and 0 for monochromatic waves. The values computed from a wave record sampled at a discrete interval can be lower due to the filtering out of high frequency components in the process of recording, digitization and analysis. The value of ϵ decreases with increase in sampling period due to the possible filtering out of the smaller waves (Goda, 1974). Since its

85

value is 1.0 for sea waves it cannot represent the shape or bandwidth of sea wave spectrum. However, in the shallow waters where the swells dominate this parameter can be useful in determining the sea state, since the sea waves contribute to an increase in its value.

The frequency distribution of ϵ_s (Fig.4.10a) shows that the maximum occurrence is in the range 0.75-0.8 (28.1%) followed by nearly equal frequency (25.2%) in the range immediately preceeding this, when the complete year is considered. When the data is divided into the above 2 seasons, it is seen that the lower values correspond to May-September and the higher to October-April. During May-September the maximum occurrence is in the range 0.7-0.75, which constitutes 35.8% of the season, and 93.4% are in the range 0.65-0.80. During October-April the maximum number of observations are in the range 0.80-0.85 with a 36.7% occurrence. However, 81.9% fall in the range 0.70-0.85.

The frequency distribution of ν shows two major maxima indicating the existence of two different characteristic waves (Fig.4.10b). The maximum occurrence is in the range 0.50-0.55 followed by 0.45-0.50, the former being 29% and the latter 28.4% during the year. The maximum occurrences with the above ranges correspond to the two seasons. During May-September the values in the range 0.45-0.50 constitutes
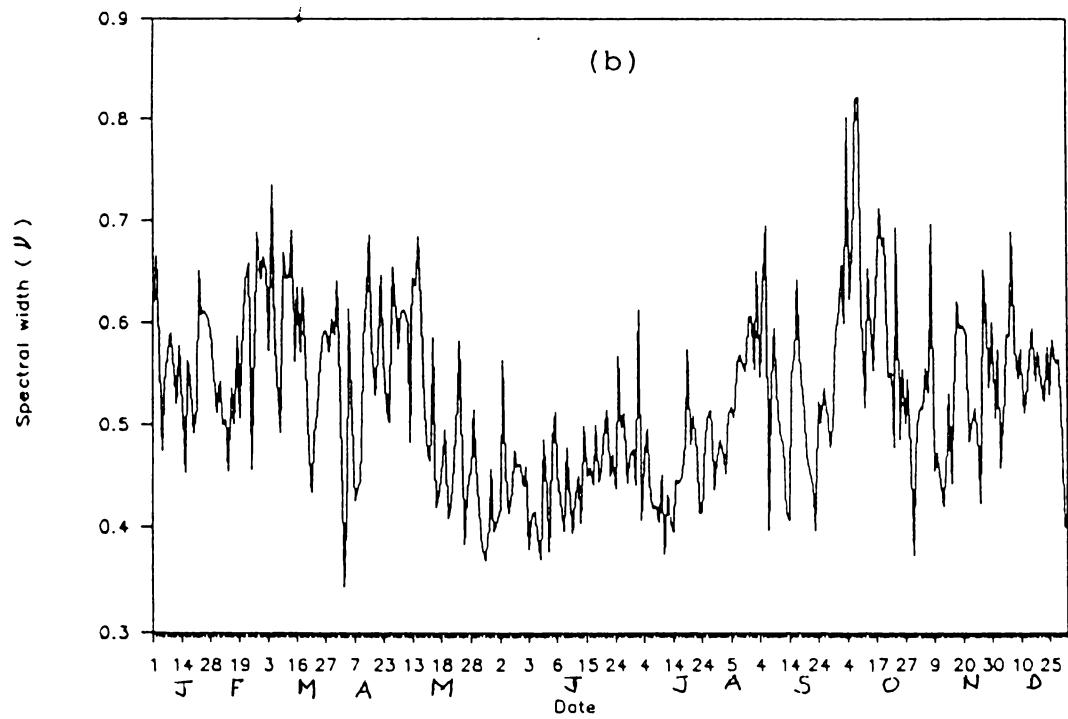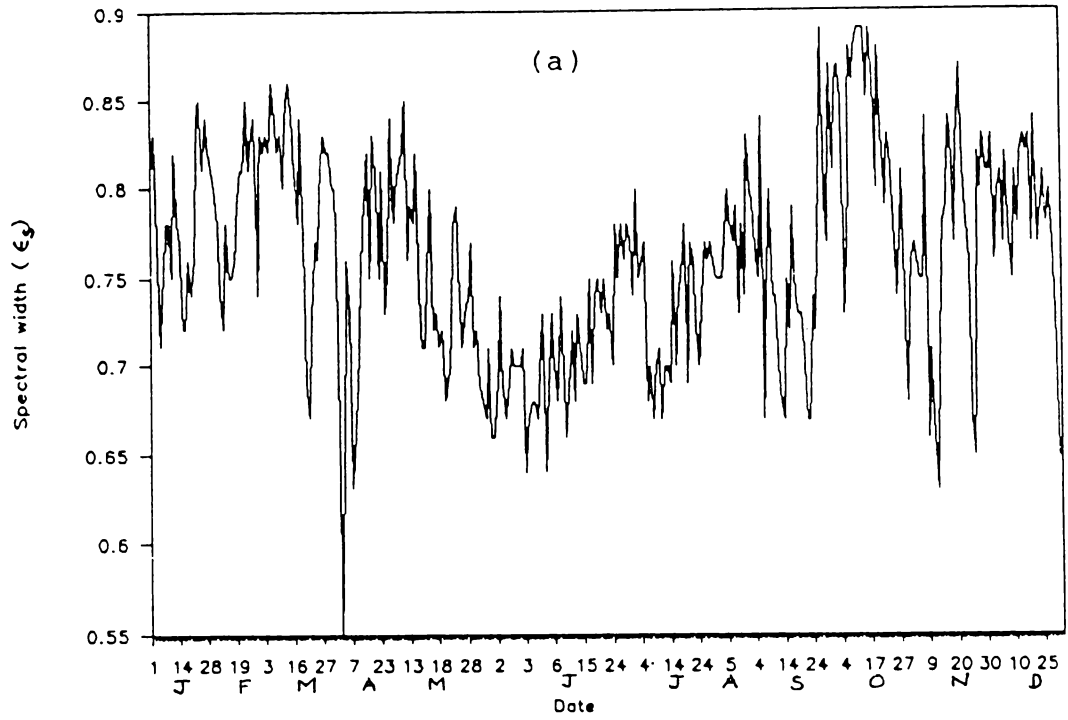
Fig.4.9 Temporal distribution of spectral width
parameters:(a) ϵ_s; (b) ν ; (c) ν_1 .

(c)

Spectral width ($\mathcal{U}$)

1 14 28 19 3 16 27 7 23 13 18 28 2 3 6 15 24 4 14 24 5 4 14 24 4 17 27 9 20 30 10 25
J   F   M   A   M   J   J   A   S   O   N   D

Date

Fig.4.9 continued.

(a)

Percentage Occurrence
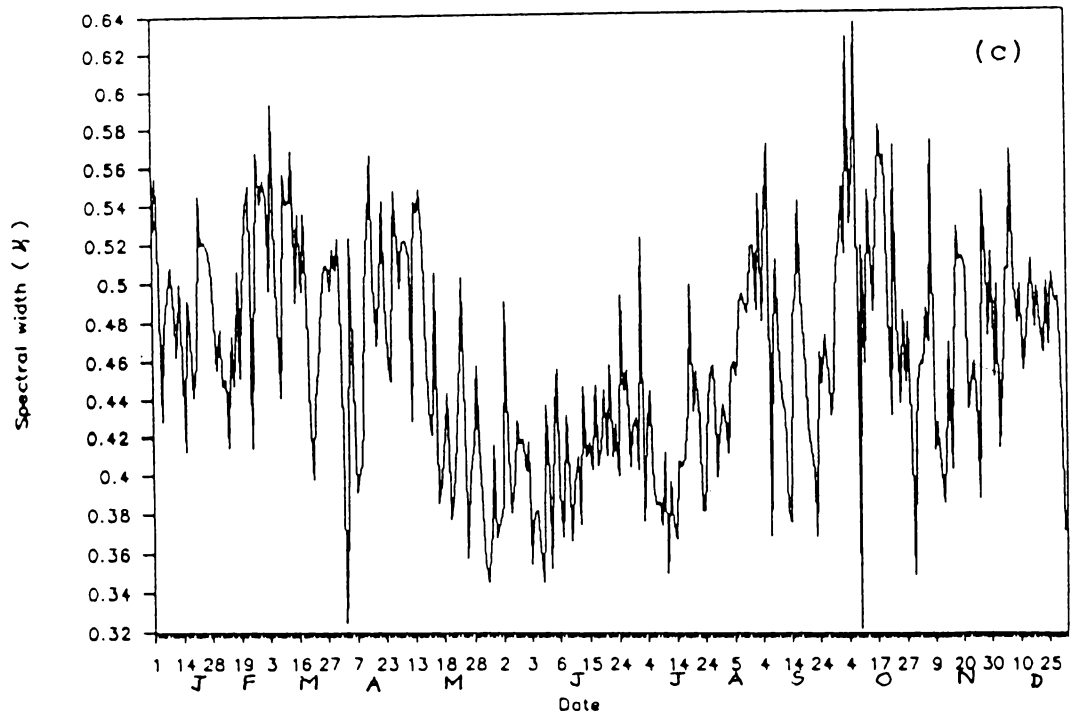
Spectral Width Parameter (ϵ)
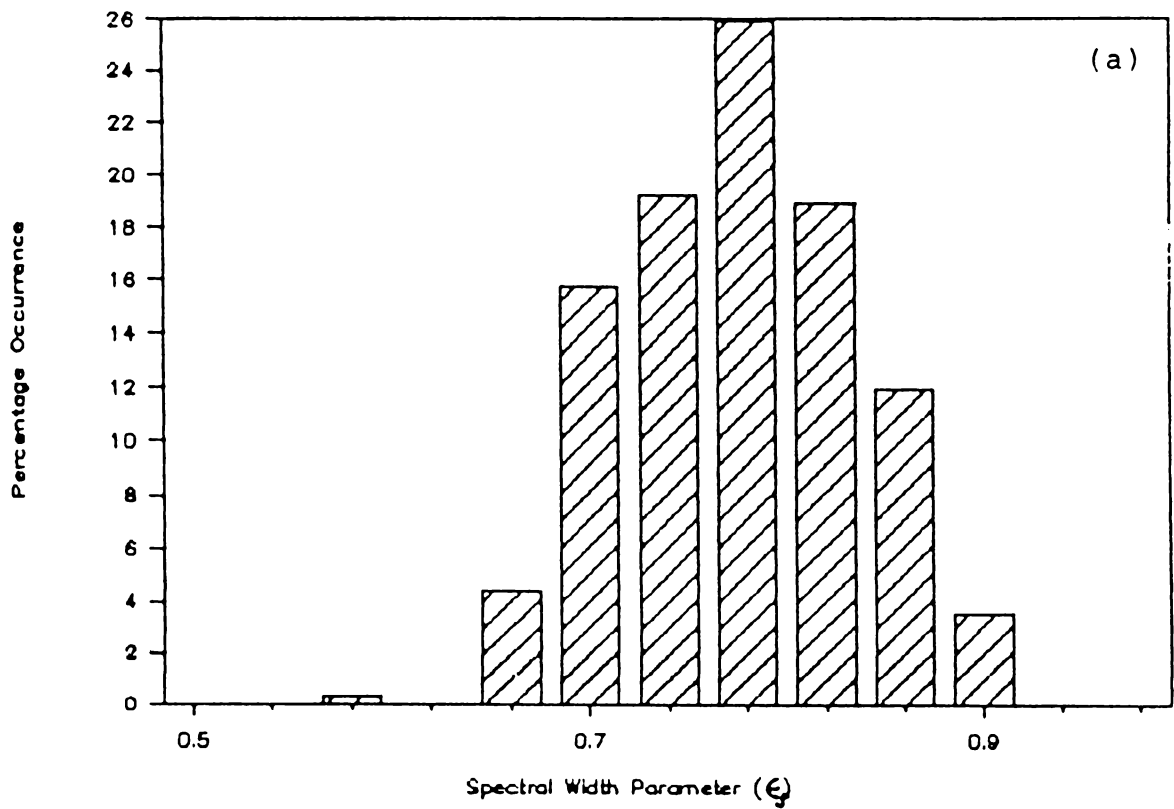
Fig.4.10 Frequency distribution of spectral width
parameters: (a) ϵ_s; (b) $\mathcal{V}$; (c) $\mathcal{V}_i$.

to about 41% of the season. During October-April the values are slightly higher and the maximum occurrence is in the range 0.50-0.55 followed by 0.55-0.60 which are 38% and 29% respectively of this season.

The distribution of ν_1 is similar to that of ν (Fig.4.10c). When the complete year is taken, the maximum number of values fall in the range 0.5-0.6 (38.8%) with a nearly equal frequency for the range immediately preceeding this (36.9%). As in the case of ν when the data is divided into the two seasons it is seen that the lower values belong to May-September and the higher values to October-April. The maximum occurrence during May-September is in the range 0.4-0.5 which is 58.3% of the season and that during October-April is in the range 0.5-0.6 which forms 52.4% of the values during the season.

4.2.5. Spectral Peakedness

The spectral peakedness parameter, Q_p (Eq.3.16) varied from values as low as 1.6 to as high as 11.4 with an average of 3.5 and a standard deviation of 1.5. No characteristic variation with month or season is observed in its temporal distribution (Fig.4.11). However, the occurrence of higher values are less during May-September. The seasonal averages for May-September and October-April are 3.2 and 3.9 with standard deviations of 1.2 and 1.6 respectively. The fre-

87

(b)

Percentage Occurrence

Spectral Width Parameter (ν)

(c)

Percentage Occurrence

Spectral Width Parameter (ν)
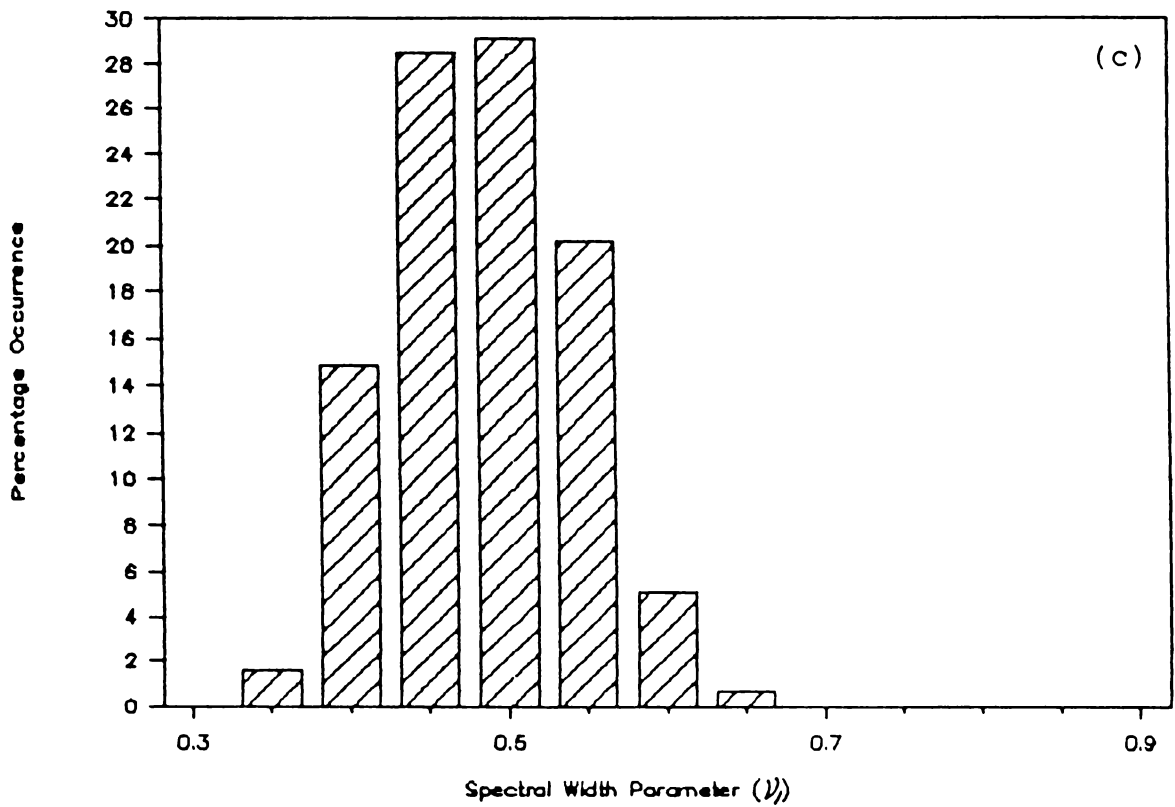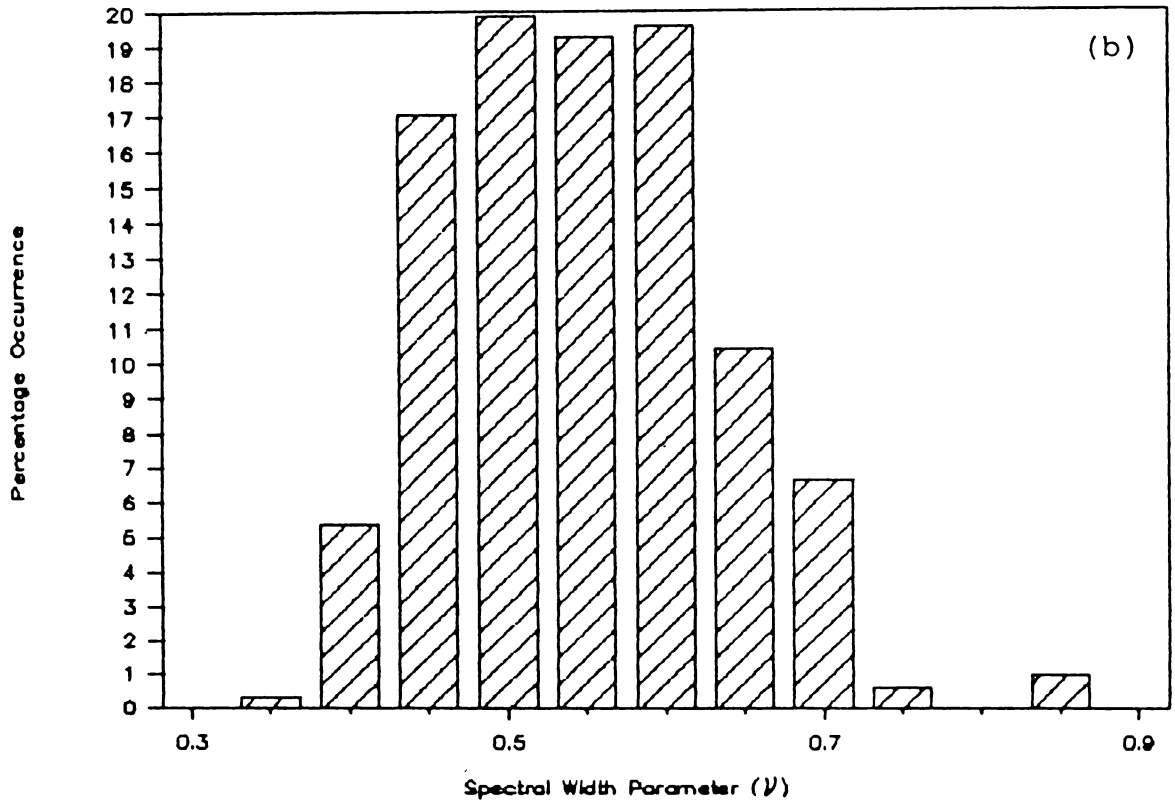
Fig.4.10 continued.

quency distribution (Fig.4.12) shows that the maximum number of occurrence is in the range 2.5-3.0 which constitutes 24.9% with 74.1% in the range 2.0-4.0. The season-wise distribution also shows that the maximum occurrence are in the range 2.5-3.0 during both the seasons, with 29.8% during May-September and 20.5% during October-April.· During May-September 84.8% are in the range 2.0-4.0 and during October-April 64.5% are in this range.

The values of spectral peakedness Q_p is dependent on the cut-off frequency, presence of secondary peaks and frequency resolution. Using the theoretical JONSWAP spectra Rye (1979) has shown that Q_p is little affected by the ratio of the Nyquist frequency to the peak frequency. But, the presence of relatively large secondary peaks causes to decrease the value of Q_p. With an increase in frequency resolution, which decreases the effective degrees of freedom (d.f.), the spectrum gets sharpened, as a result of which the value of Q_p is increased significantly. When the frequency resolution is increased from 0.0156 to 0.00098 Hz (decrease of effective d.f. from 84 to 4.6), the value of Q_p is raised from 2.7 to 8.4 (Goda, 1983). As a solution Rye (1982), based on his judgement of analysed data and simulation studies of wave profiles with JONSWAP spectrum, recommended the number of d.f. of about 16. Hence, a
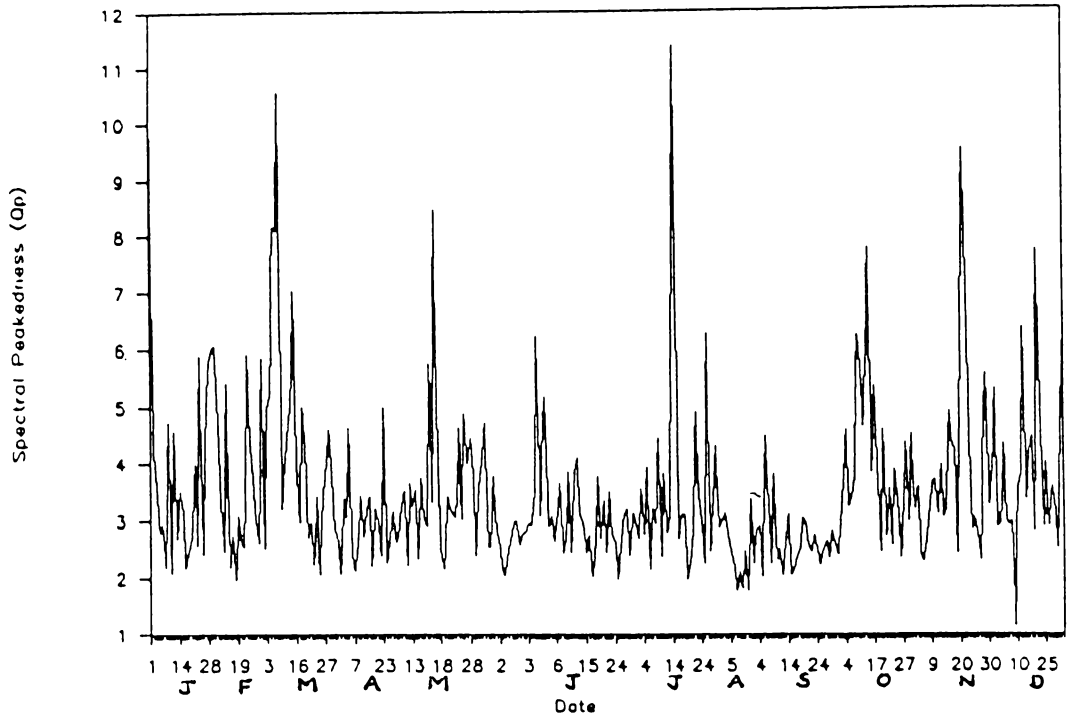
Fig.4.11 Temporal distribution of spectral peakedness parameter (Q_p).
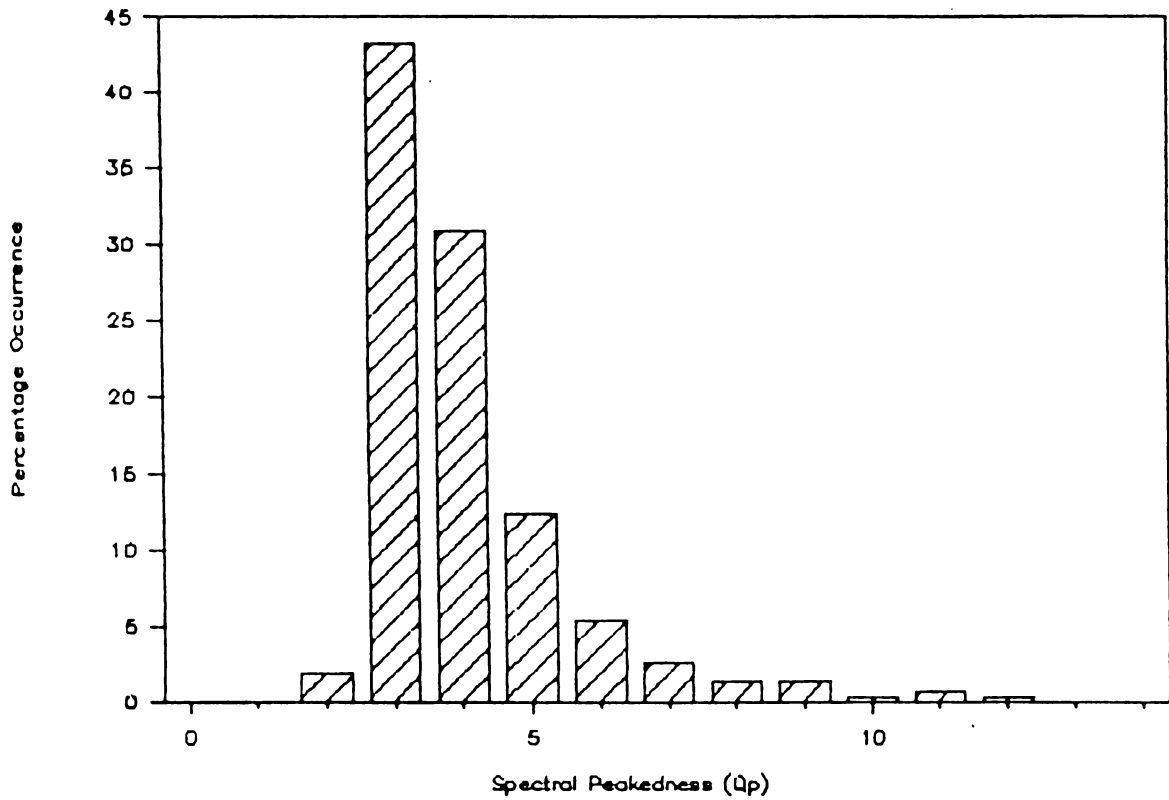
Fig.4.12 Frequency distribution of spectral peakedness parameter (Q_p).

recalculation of Q_p values is made using the smoothed
spectra with 16 d.f. When smoothed, the values are reduced
considerably. They range from 0.77-2.44 with an average and
a standard deviation of 1.39 and 0.30. These values do not
show any decrease during May-September, rather a slight
increase is observed during the peak monsoon months (June-
July). The values are slightly lower during August-October.
Hence the average values for the seasons do not show much
difference. The averages for the above seasons are 1.40 and
1.39 with standard deviations of 0.29 and 0.30 respectively.
This is contrary to the observation with higher frequency
resolution. From these results it may be inferred that Q_p
is not dependent on the seasonal properties of waves. A
plot of the Q_p values with and without smoothing (effective
d.f. 16 and 2) is given in Fig.4.13. No correlation is
observed between these values. This may be due to the
influence of secondary peaks. When higher resolution is
provided the secondary peaks can be strong at different
frequencies. When smoothing is done some of the secondary
peaks are suppressed considerably depending upon the
spectral estimates in the nearby frequencies. That is, Q_p
can be taken as a wave property only when secondary peaks
are negligible. Goda (1983) also observed that it is not
advisable to calculate the spectral peakedness parameter
based on spectra with large fluctuations. In the shallow
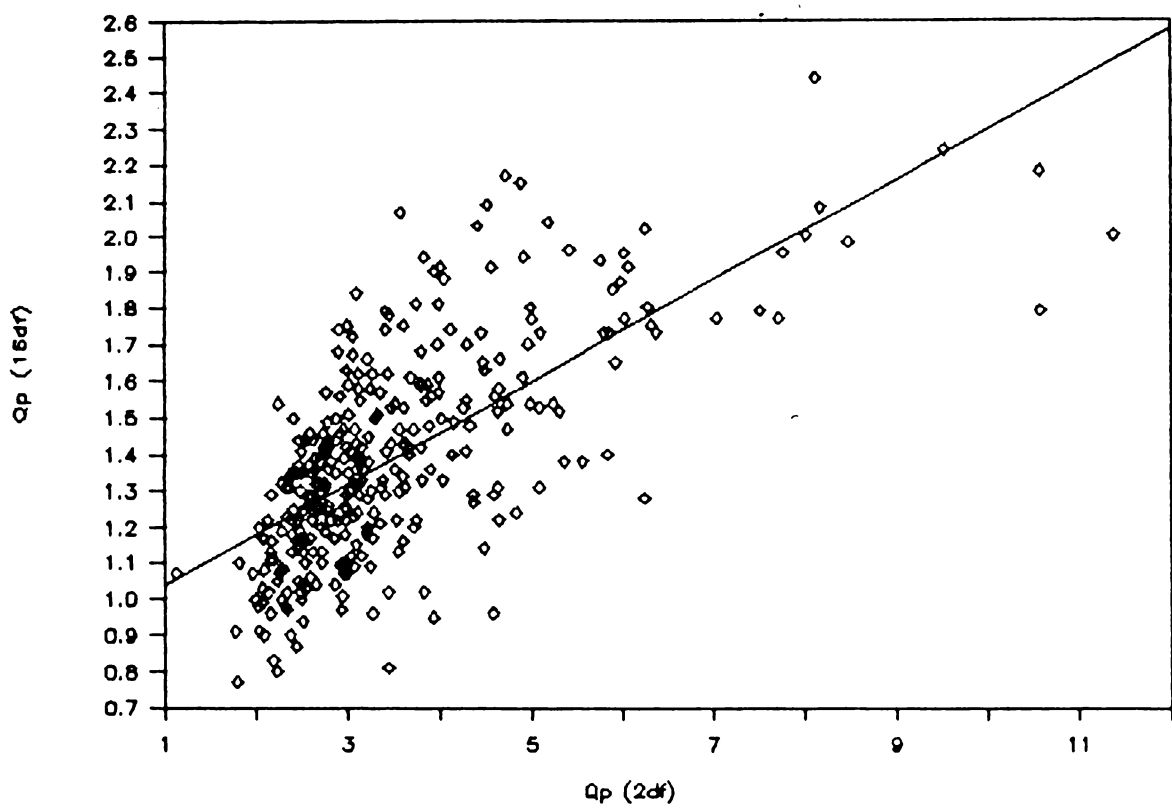
Fig.4.13 Scatter diagram of Q_p from spectra
computed with two different resolutions
(degrees of freedom 2 and 16).

water conditions multi-peakedness is a common phenomenon due to various reasons as discussed in Sec.4.1. In general, Q_p cannot be taken as a criterion for drawing conclusions regarding the characteristics of waves in shallow waters unless there is a single-peaked spectrum.

4.3. AVERAGE SPECTRA

Individual shallow water wave spectra may be quite irregular and change substantially with time. In order to identify typical spectra for a particular condition it is desirable to condense the individual spectra into a more concise form. Presently there is no satisfactory technique in use for isolating and summarising general characteristics of field spectra. One of the usual methods is to compute spectral statistics, which are based on the moments of the spectrum. Hoffman (1974) grouped the spectra according to H_{ss} and computed the mean and standard deviation of the spectral densities in each band. Some other researchers made the grouping according to H_{ss} and T_p values (Gospodnetic and Miles, 1974; Thompson, 1980; etc.). This approach seems to be more reliable since the average spectrum for a specific height-period range provides information on the various distinct characteristics of the particular wave condition. However, the averaging has to be done according to the specific purpose for which it is

required. For example, if the wave condition for a particular season is required it is desirable to compute the average spectrum for that season irrespective of the wave height/period values and compute the statistical parameters from it. On the other hand, for characterising the spectrum for its shape or to compare it with a theory, it is desirable to compute the average spectra according to some specified characteristics such as height or period. In this study the monthly average spectra is computed to explore information on the monthly average wave characteristics. Similarly, the average spectra for height and period intervals of 0.25 m and 1 s are computed to examine the spectral shape and to compare with different models.

4.3.1. Monthly Average Spectra

The monthly average spectra are presented in Fig.4.14. The spectra are predominantly single-peaked; no major secondary peaks are observed. However, secondary peaks with lesser energy generally occur during October-April. The secondary peak becomes most clear in April and from May onwards it starts to disappear. Again it makes its appearance in October and persists during the rest of the year. When the secondary peak energy is of considerable magnitude (about 25-35%), they are at twice the peak frequency. During the other occasions, they are around this
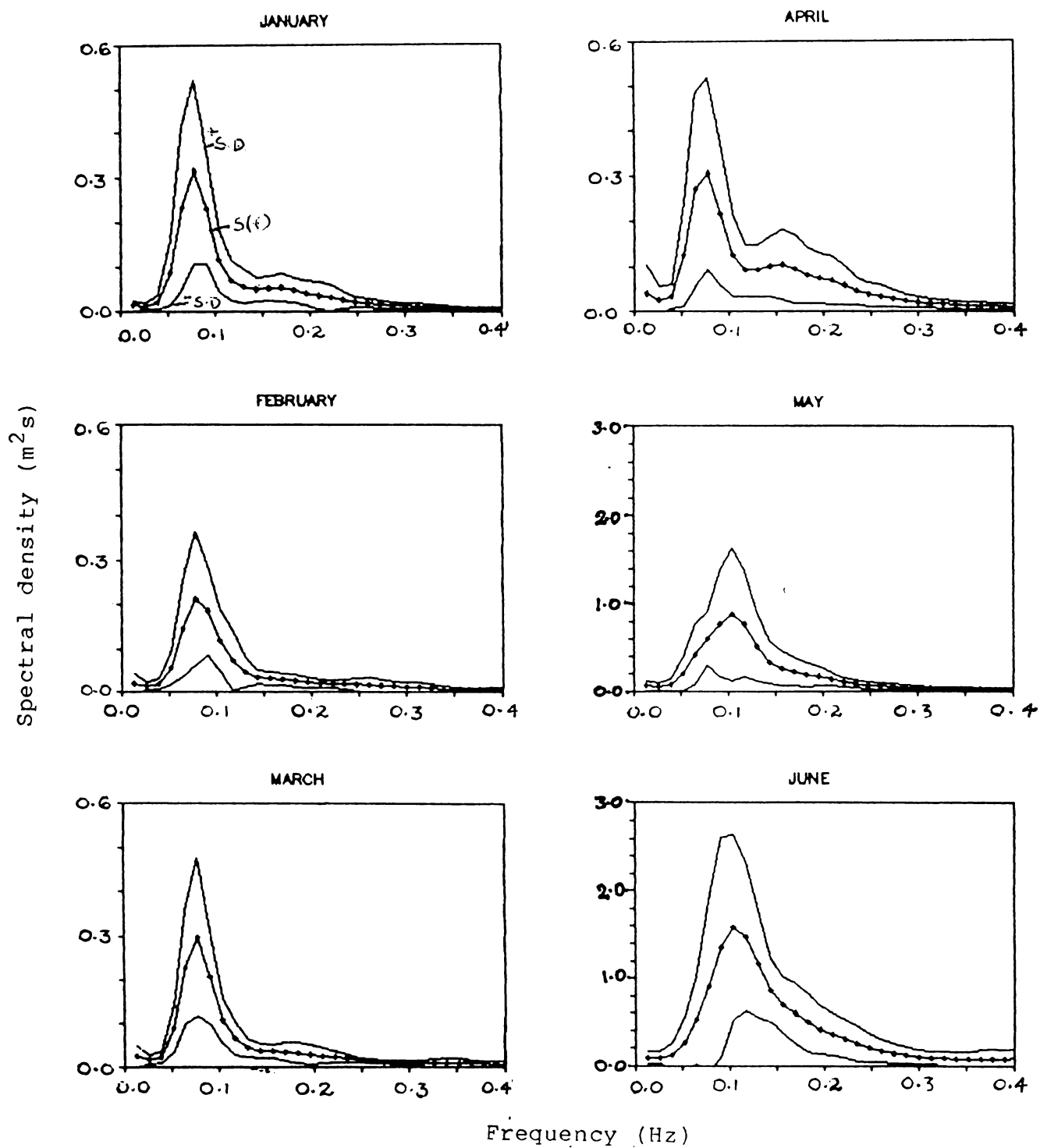
Fig.4.14 Monthly average spectra.
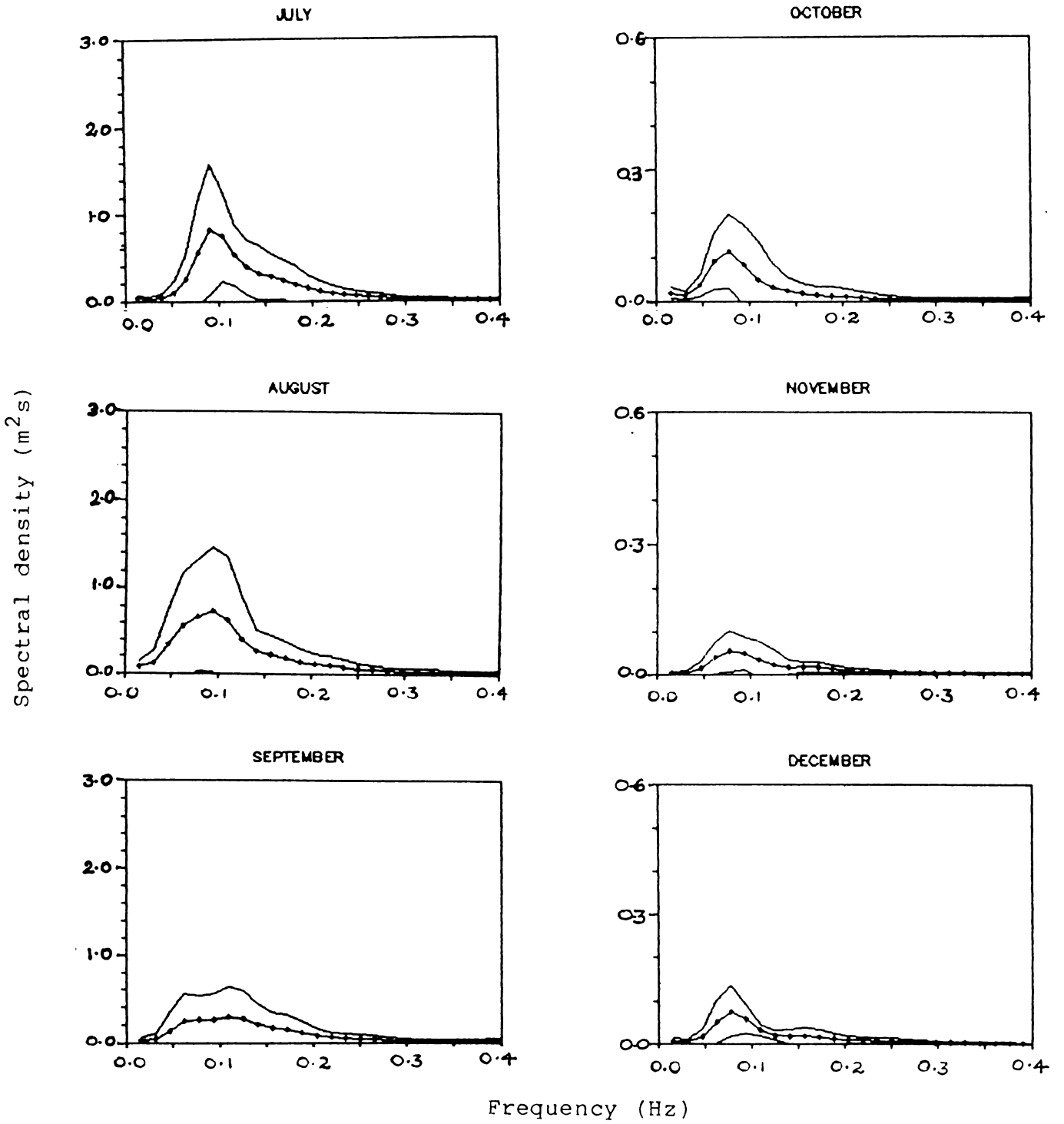
Fig.4.14 continued.

value, and are of lesser energy density, the maximum energy density of these being only 17% of the peak energy density.

The spectral parameters computed from the average spectra are presented in Table 4.2. The energy is high during May-September with the highest in June and the lowest in November. Among the lower energies present during October-April, the post-monsoon (October-December) is comparatively calmer. The average H_{ss} during May-September is 1.16 with a standard deviation of 0.26 m and that during October-April is 0.47 with a standard deviation of 0.14 m. These average values agree with the averages computed with the individual values for both the seasons (1.15 m during May-September and 0.44 m during October-April).

T_p values are lower during May-September, as observed in the distribution of individual values, and they vary from 9.1 to 11.0 s with an average of 10.0 and a standard deviation of 0.70 s. During October-April the peak period is constant at 12.8 s. The variation of spectral width parameters (ϵ_s, ν and ν_1) during both the seasons are identical to that discussed in the previous sections. Hence a detailed discussion is not presented here.

From the above discussions it can be seen that the waves during May-September and October-April exhibit characteristic properties of heights, periods and spectral

Table 4.2 Spectral Parameters from Monthly Average Spectra

Month	H_{ss}	T_p	$S(f_m)$	Q_p	Slope	ϵ_s	ν	ν_1
Jan	0.58	12.8	0.31	1.28	2.84	0.81	0.61	0.52
Feb	0.50	12.8	0.21	1.26	2.99	0.82	0.64	0.54
Mar	0.55	12.8	0.30	1.33	3.12	0.83	0.66	0.55
Apr	0.68	12.8	0.31	1.01	1.69	0.78	0.60	0.52
May	1.12	9.6	0.90	1.34	2.74	0.79	0.52	0.46
Jun	1.64	9.6	1.58	1.27	2.11	0.75	0.52	0.46
Jul	1.06	11.0	0.82	1.40	1.96	0.76	0.50	0.44
Aug	1.13	10.7	0.74	1.06	2.26	0.86	0.69	0.57
Sep	0.84	9.1	0.30	0.99	1.74	0.83	0.65	0.55
Oct	0.38	12.8	0.11	1.09	2.49	0.87	0.81	0.63
Nov	0.29	12.8	0.05	1.07	2.02	0.84	0.67	0.55
Dec	0.31	12.8	0.08	1.15	2.76	0.85	0.68	0.56
Max:	1.64	12.8	1.58	1.40	3.12	0.87	0.81	0.63
Min:	0.29	9.1	0.05	0.99	1.69	0.75	0.50	0.44
Avg:	0.76	11.6	0.48	1.19	2.39	0.82	0.63	0.53
S.D:	0.39	1.5	0.43	0.14	0.47	0.04	0.08	0.05

widths. May-September is characterised by high waves associated with comparatively shorter periods and spectral widths. During October-April low waves with comparatively higher periods and spectral widths persist at this location. Hence, the former may be classified as 'rough season' and the latter as 'fair season'.

4.3.2. Average Spectra at Height-Period Ranges

Mean spectra are computed for significant wave height and peak period intervals of 0.25 m and 1 s. Those spectra corresponding to the lower energy conditions and lower peak periods exhibit multiple peaks. The major secondary peaks observed in such cases are mainly in the range 15-16 s. The dominance of this period is an indication of the presence of long travelled swells in this region. However, as seen in the previous section, the presence of these waves are not noticeable at higher energy conditions, as the energy content of these waves are very low compared to the monsoonal ones. The presence of secondary peaks observed at the lower periods in the spectra having very low and very high energies may be due to the lesser number of records available for averaging. When the number of spectra available for averaging is more, the secondary peaks may be smoothed out.

The spectral parameters of these average spectra show wide variation compared to the average of the spectral parameters computed for the height ranges (see Sec.4.4). One of the reasons for this variability may be the lesser number of spectra available for averaging in certain ranges like the lower as well as the higher heights and periods. Hence the cases, where average could not be taken due to availability of only one spectrum in that particular range,

94

are not included for the following discussions. Another reason for the higher variability of the parameters may be the presence of multiple peaks in some ranges. The slope of the average spectra range from 1.58 to 3.43 with a mean of 2.41 and a standard deviation of 0.45. The Q_p values range from 1.02 to 1.57 with an average of 1.3 and a standard deviation of 0.14. Since slope and Q_p are more susceptible to errors with the presence of secondary peaks, the cases where major secondary peaks are present are also not considered for this calculation. Relations between the parameters derived from these average spectra are examined in the following section along with the discussion on the relation between the parameters derived from individual spectra and their averages at specified height intervals.

4.4. RELATION BETWEEN THE SPECTRAL PARAMETERS

The correlation between the spectral parameters are computed and the coefficients are presented in Table 4.3. On a comparison of the above parameters significant dependence is shown by the spectral width parameters only. The spectral width parameters ε_s, ν and ν_1 show good correlation between each other. A plot of ε_s and ν_1 against ν is presented in Fig.4.15. ν_1 exhibits very good positive linear dependence on ν and a correlation coefficient as high as 0.93 is observed (Table 4.3).

By definition ν and ν_l are functions of 0th, 1st and 2nd moments of the spectrum. From Eqs.(3.14) and (3.15) it can be seen that

$$\nu_l = \nu^2/(1+\nu^2) \qquad\qquad\qquad \dots\dots(4.1)$$

Hence a better correlation can always be expected. Moreover, either ν or ν_l can be used, since they are interchangeable through Eq.(4.1). As the properties and variations of these parameters are identical, only one of them need to be considered for practical applications.

Table 4.3 Correlation Between the Spectral Parameters

	H_{ss}	Slope	Q_p	ϵ_s	ν	ν_l	T_p
H_{ss}	1.00	-0.29	-0.10	-0.40	-0.46	-0.44	-0.32
Slope	-0.29	1.00	0.31	0.19	0.13	0.11	-0.06
Q_p	-0.10	0.31	1.00	0.33	0.08	0.04	0.14
ϵ_s	-0.40	0.19	0.33	1.00	0.77	0.76	0.73
ν	-0.46	0.13	0.08	0.77	1.00	0.93	0.91
ν_l	-0.44	0.11	0.04	0.76	0.93	1.00	0.69
T_p	-0.32	-0.06	0.14	0.73	0.71	0.69	1.00

ϵ_s also shows good positive correlation with ν (Fig.4.15) and a correlation coefficient of 0.77 is obtained. The linear regression fit of ϵ_s with ν is given by

$$\epsilon_s = 0.535\,\nu + 0.48 \qquad\qquad\qquad \dots\dots(4.2)$$

ε_s by definition is a function of 0th, 2nd and 4th moments of the spectrum. Hence it gives a different concept compared to ν and ν_l. However, the usefulness of these parameters is questioned by some researchers. Goda (1974) suggests that ε_s vary with sampling interval and hence it cannot be regarded as a good estimate of the spectral shape. He presents Q_p as an alternative to ε_s, ν and ν_l to determine the shape of the spectrum. Rye (1976) examined the variations of these parameters with the cut-off frequency. His results show that ε_s, ν and ν_l vary with the cut-off frequency, the maximum variation being in the values of ε_s, and Q_p is non-dependent on the cut-off frequency. Hence he also recommended Q_p to characterise the spectral shape instead of ε_s, ν or ν_l. However, Q_p is dependent on the frequency resolution (Goda, 1983). Also, the presence of secondary peaks, which is a characteristic feature of the shallow water wave spectra, affects its values. In the present study values of Q_p do not show any characteristic variation with the wave conditions (with heights, periods or seasons). However, ε_s, ν and ν_l exhibit such a characteristic dependence (Sec.4.2.4). Since the frequency resolution and digitization interval are kept constant in the present analysis, the values of Q_p are not affected by the frequency resolution and the variations in ε_s, ν and ν_l are independent of the sampling. Hence, the characteristics observed

97

in ϵ_s, ν and ν_l can be attributed to the wave characteristics. Thus, it is reasonable to conclude that Q_p cannot be regarded as a good shape parameter for shallow water wave spectra . On the other hand, though ϵ_s, ν or ν_l cannot be regarded as good estimators of the spectral shape, they can be considered for a qualitative determination of the presence of different sea and swell wave components.

The other parameters that show mutual dependence are the spectral width parameters and T_p. ϵ_s, ν and ν_l exhibit good correlation with T_p, with coefficients of the order of 0.69 and more. The values of these parameters are found to increase with T_p, eventhough with some scatter in their plots (Fig.4.16a-c). The best fit of these parameters obtained from linear regression analysis are

$$\epsilon_s = 0.175T_p + 0.564 \qquad \qquad \dots\dots(4.3)$$

$$\nu = 0.246T_p + 0.248 \qquad \qquad \dots\dots(4.4)$$

$$\nu_l = 0.016T_p + 0.278 \qquad \qquad \dots\dots(4.5)$$

As a result of the dependence of the spectral width parameters on T_p, the variation of T_p, ϵ_s, ν and ν_l with other parameters are almost identical. These parameters decrease with increase in energy. They decrease until H_{ss} takes a value of about 1.4 m and then onwards (for the higher wave
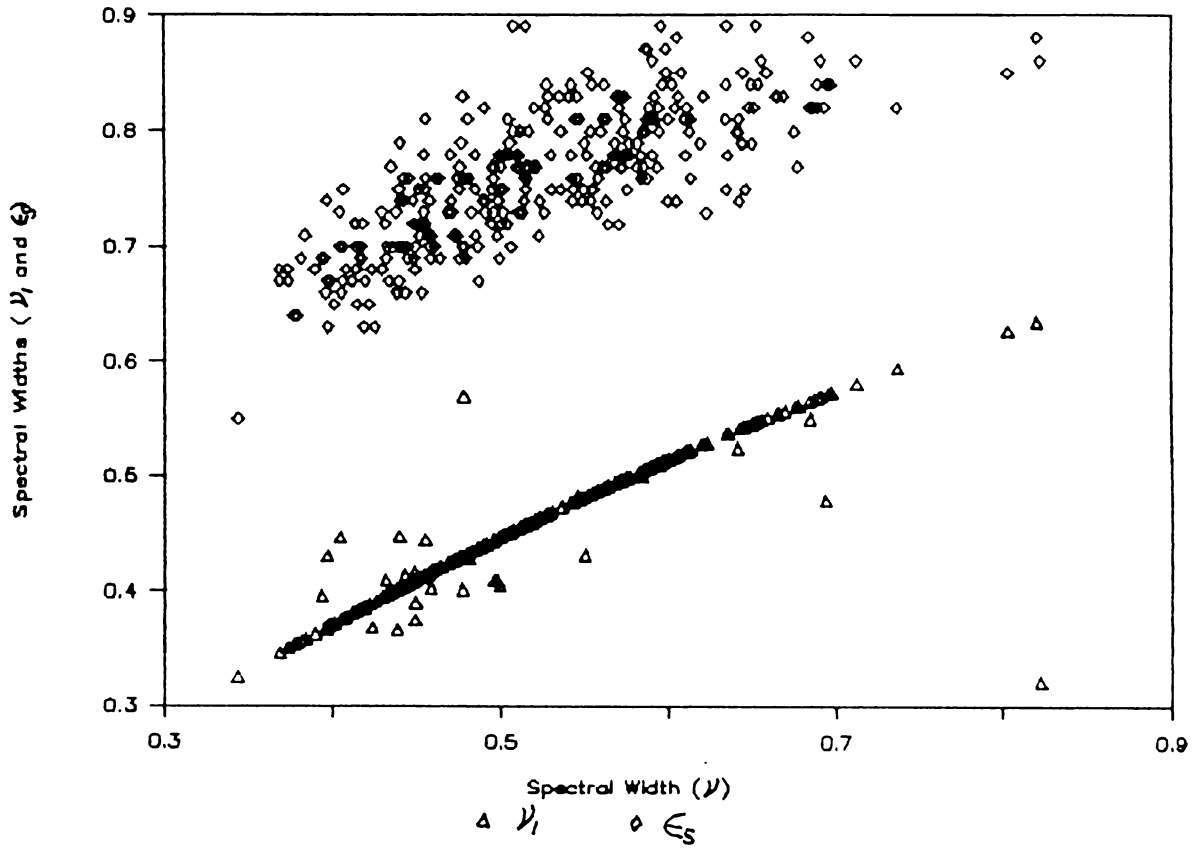
Fig.4.15 Relation between spectral width parameters.
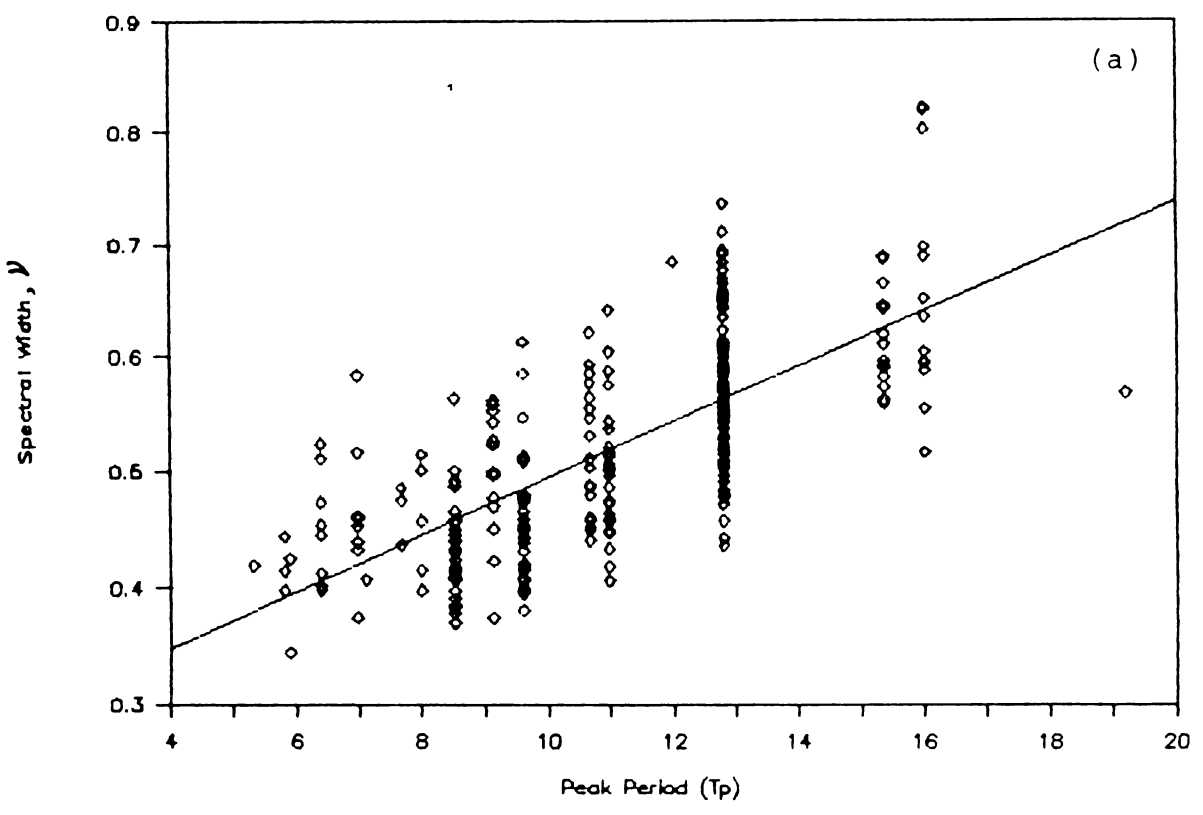
Fig.4.16 Relation between peak period and spectral width
parameters :(a) ν ; (b) ν_1 ; (c) ϵ_s.
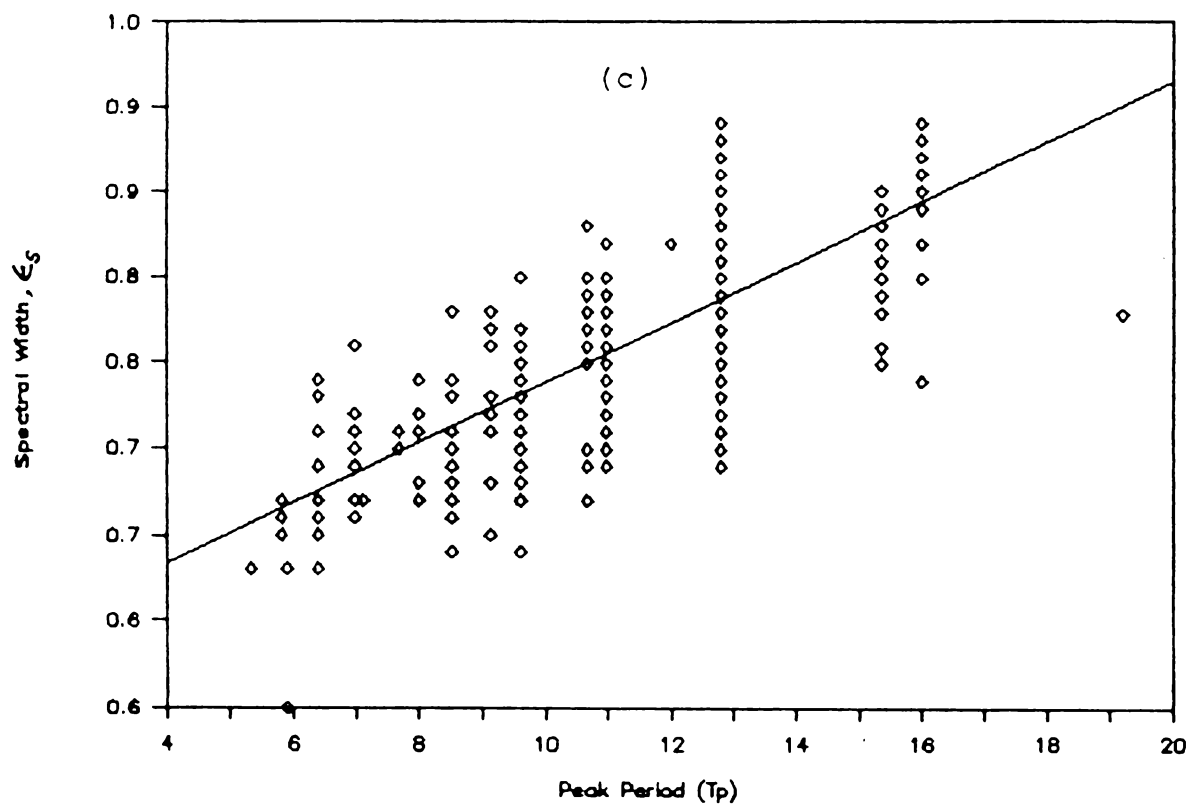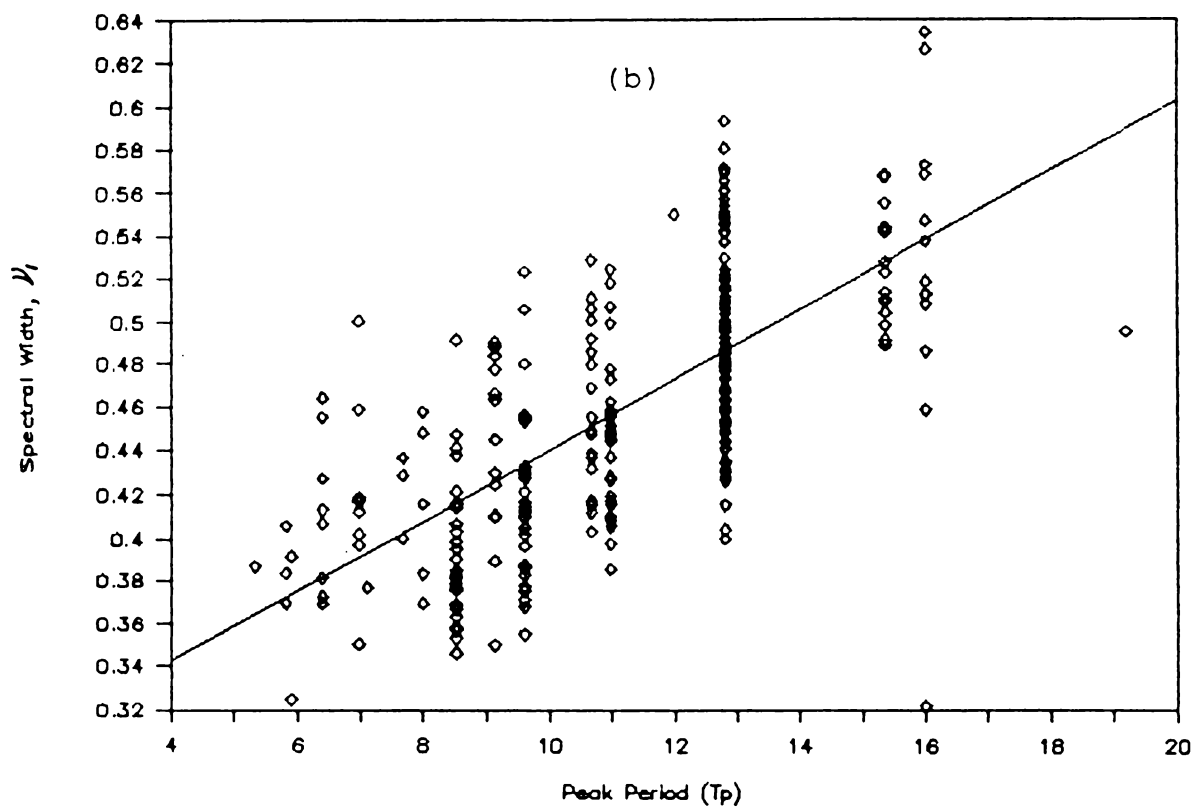
Fig.4.16 continued.

energy conditions) they remain almost stationary. The high energy waves occur during May-September and are the waves generated in the Arabian Sea due to the strong monsoonal winds (see Ch.3). They retain their characteristics (as seen in the previous sections) and hence the lower values of the above parameters prevail for the larger wave heights without appreciable change. Since the higher period waves are those generated at farther places compared to the monsoonal waves, it is quite possible that the shorter period waves generated at nearby places also arrive along with the higher period waves, resulting in higher width of the spectrum in the shallow water. But for the high energy monsoonal waves they have the generating area at comparatively nearer places and hence possibility of occurrence of other short period waves generated at still lesser distances are less resulting in narrower spectra with lower peak periods.

In addition to the examination of individual values of spectral parameters, their averages at height intervals of 0.25 m are also examined. The dependence of the various parameters discussed above are exhibited more clearly by the average values. An interesting result observed in this comparison is the correlation of the slope of the spectrum to the energy. The average slope values decrease systematically with increase in m_0 (Fig.4.17). The best fit is represented by the relation

- G4C33 -

$$\text{slope} = 2.651 - 4.14m_0 \qquad \dots(4.6)$$

Similarly, the relations obtained between the spectral width parameters and peak periods are also more clearly indicated with the average values. The plots of ε_s and ν_1 against ν are presented in Fig.4.18. The following relation is obtained against Eq.(4.2).

$$\varepsilon_s = 0.57\nu + 0.46 \qquad \dots(4.7)$$

Plots of the spectral width parameters against T_p are presented in Fig.4.19. The best fit lines corresponding to Eqs.(4.3-4.5) are obtained as

$$\varepsilon_s = 0.026T_p + 0.462 \qquad \dots(4.8)$$

$$\nu = 0.044T_p + 0.029 \qquad \dots(4.9)$$

$$\nu_1 = 0.029T_p + 0.133 \qquad \dots(4.10)$$

Whereas considerable scatter is observed when the individual values are considered, the average values exhibit very little scatter. Hence, the relations depicted from the average values can be considered as representative of the relationship between the parameters.

The relations observed above, between the average of the spectral parameters in specified height ranges, are found to follow qualitatively in the case of the spectral

100
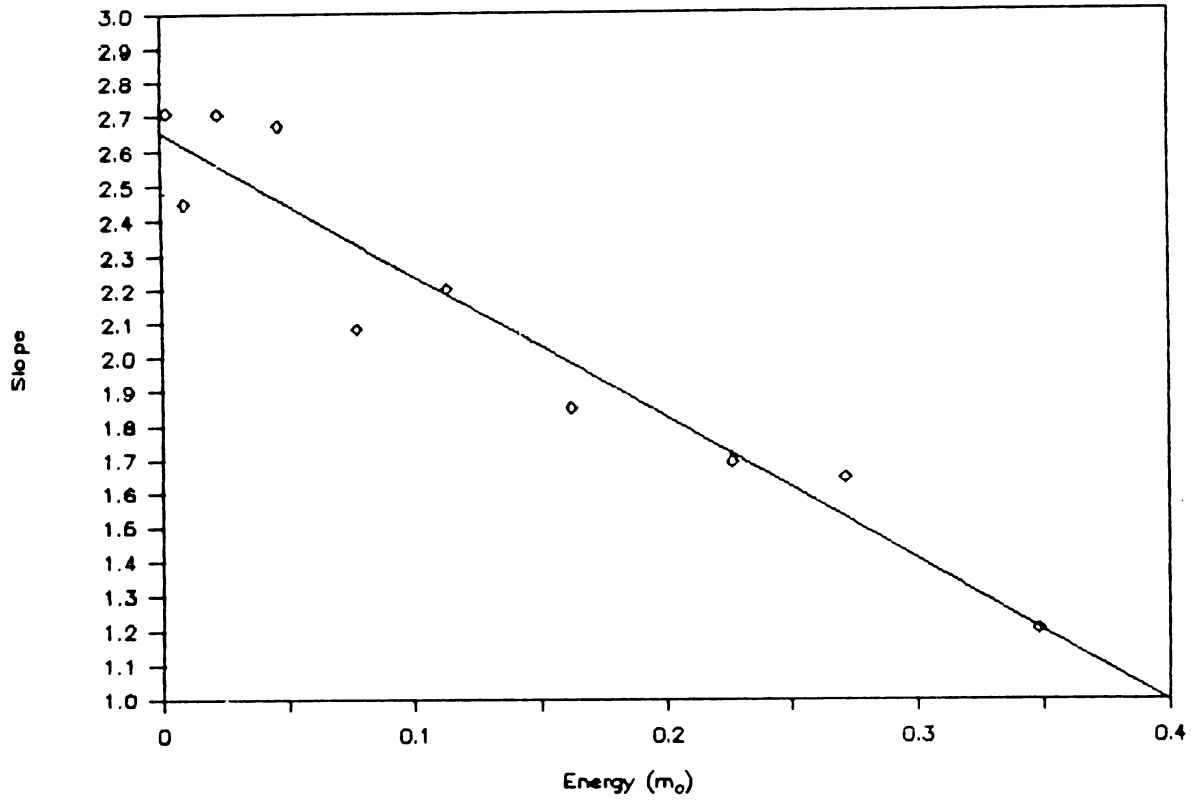
Fig.4.17 Relation between slope and energy
of the average spectra.
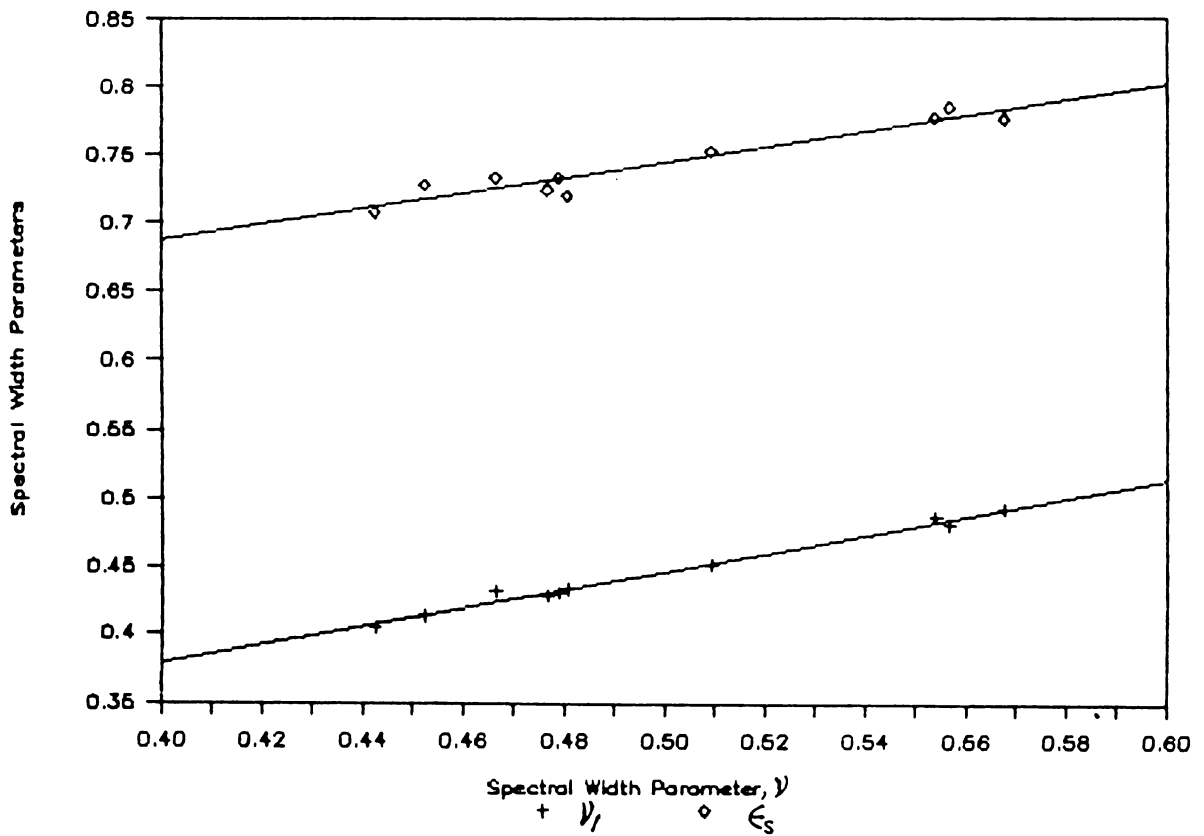
Fig.4.18 Relation between the average spectral width
parameters in specific height intervals.

parameters derived from the average spectra in the specified height-period ranges also. The regression equations obtained with these parameters are slightly different from the ones presented above. The standard errors of estimates are less in the case of Eqs.(4.6-4.10) and hence they may be used for all practical purposes.

4.5. STATISTICAL PARAMETERS FROM WAVE-BY-WAVE ANALYSIS

The distributions of the different statistical height and period parameters obtained from the wave-by-wave zero-up-crossing analysis are discussed in this section.

4.5.1 Heights

The ranges, averages and standard deviations of the maximum wave height (H_{max}), significant wave height (H_{sw}) and average wave height ($\bar{H}$) obtained from the wave-by-wave (zero-up-crossing) analysis are presented in Table 4.4. Since the temporal and frequency distributions of the significant wave height obtained from the spectral analysis (H_{ss}) are already presented in Sec.4.2, the above distributions of H_{sw} are not presented here. Similarly, as H_{max} and $\bar{H}$ are related to the significant wave height, and a comparison of these are to be made in Sec.4.6, the distributions of these parameters are also not presented here.

101

Table 4.4 Observed Height Parameters (Average)

	H_{max}			H_{sw}			$\bar{H}$		
	1	2	3	1	2	3	1	2	3
Min.	0.20	0.20	0.22	0.14	0.14	0.14	0.10	0.10	0.10
Max.	3.49	3.49	2.22	2.74	2.74	1.07	1.92	1.92	0.69
Mean	1.23	1.81	0.71	0.88	1.31	0.50	0.59·	0.88	0.34
S.D.	0.79	0.76	0.30	0.59	0.58	0.20	0.40	0.41	0.14

1: complete year; 2: May-September; 3: October-April

The ranges of H_{max}, H_{sw} and $\bar{H}$ for the year as a whole and that during the months May-September are found to be the same. The lower values during the months of intense wave activity is the result of calms prevailed amidst the monsoon due to the formation of mudbanks. However, the averages are in agreement with the observation made in Sec.4.2.

4.5.2. Periods

The different wave period parameters obtained by the wave-by-wave zero-up-crossing analysis are presented in Table 4.5. The average periods (T_z) are in the range 6.4-13.7 s. The mean of T_z is 9.3 with a standard deviation of 1.4 s during the year. The range of T_z during the rough and fair sea states are almost the same as that observed for the complete year. However, the range is slightly narrower during May-September. The mean of T_z during this season is

slightly lower at 8.6 s and that for October-April is slightly higher at 9.9 s, indicating the predominance of comparatively lower period waves during May-September and higher period ones during October-April. This is in accordance with the observation made in Ch.3.

The periods corresponding to the significant wave heights (T_s) are always higher than T_z, and the crest periods (T_c) are always lower, as expected. The values of T_s and T_c during May-September and October-April are distributed identical to T_z. Similar features are observed in Ch.3 with the 4 year's data also. The percentage occurrence of T_z, T_s and T_c are presented in Fig.4.20 (a-c). The dominant T_z during May-September is in the range 8-9 s which constitute about 38%, and 88% is in the range 7-10 s. During October-April the dominant T_z is in the range 9-10 s which constitute. to about 22% with nearly equal occurrence

Table 4.5 Observed Period Parameters (Average)

	T_z			T_s			T_c		
	1	2	3	1	2	3	1	2	3
Min.	6.4	6.5	6.4	7.1	7.4	7.1	4.8	4.8	4.8
Max.	13.7	12.4	13.7	15.7	14.4	15.7	11.8	9.5	11.8
Mean	9.3	8.6	9.9	10.7	9.8	11.5	7.1	6.7	7.5
S.D.	1.5	1.1	1.5	1.8	1.5	1.8	1.1	0.8	1.3

1: complete year; 2: May-September; 3: October-April
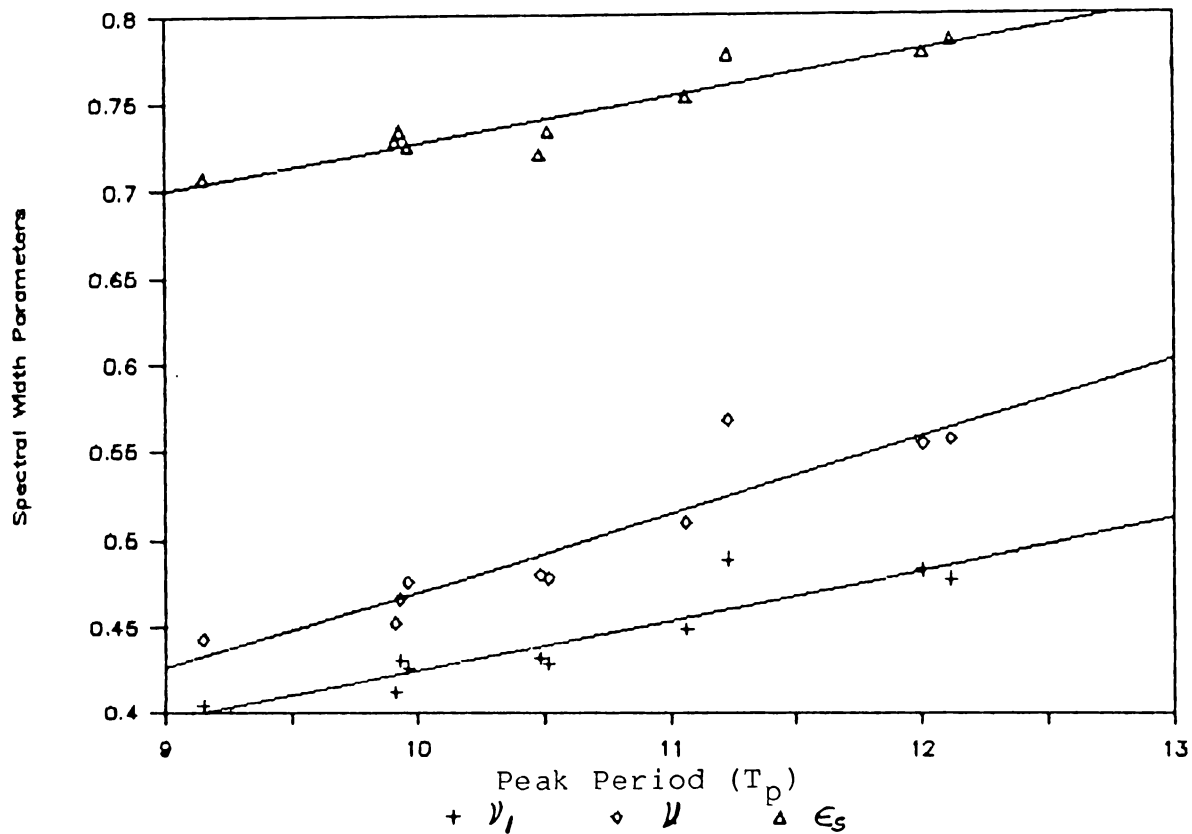
Fig.4.19 Relation between average peak period
and spectral width parameters in
specific height intervals.
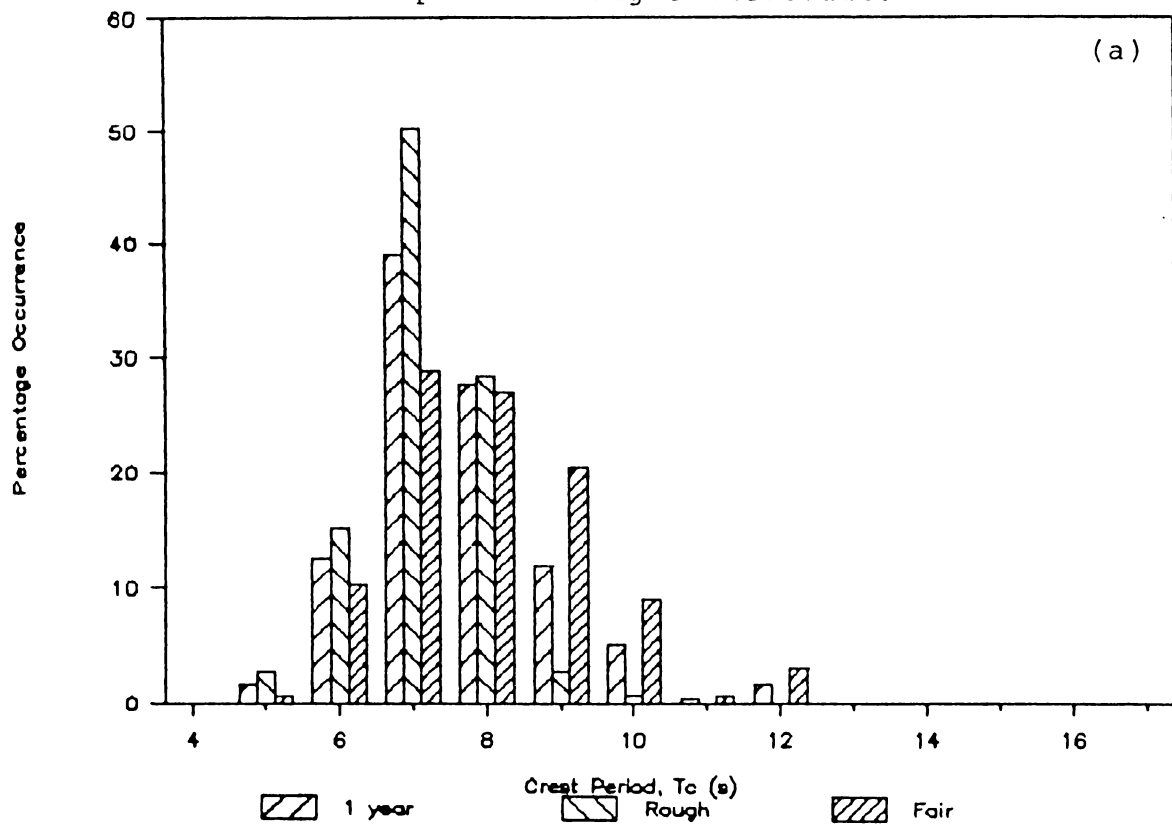
Fig.4.20 Frequency distribution of period parameters
for rough season, fair season and whole year :
(a) T_c; (b) T_z; (c) T_s.
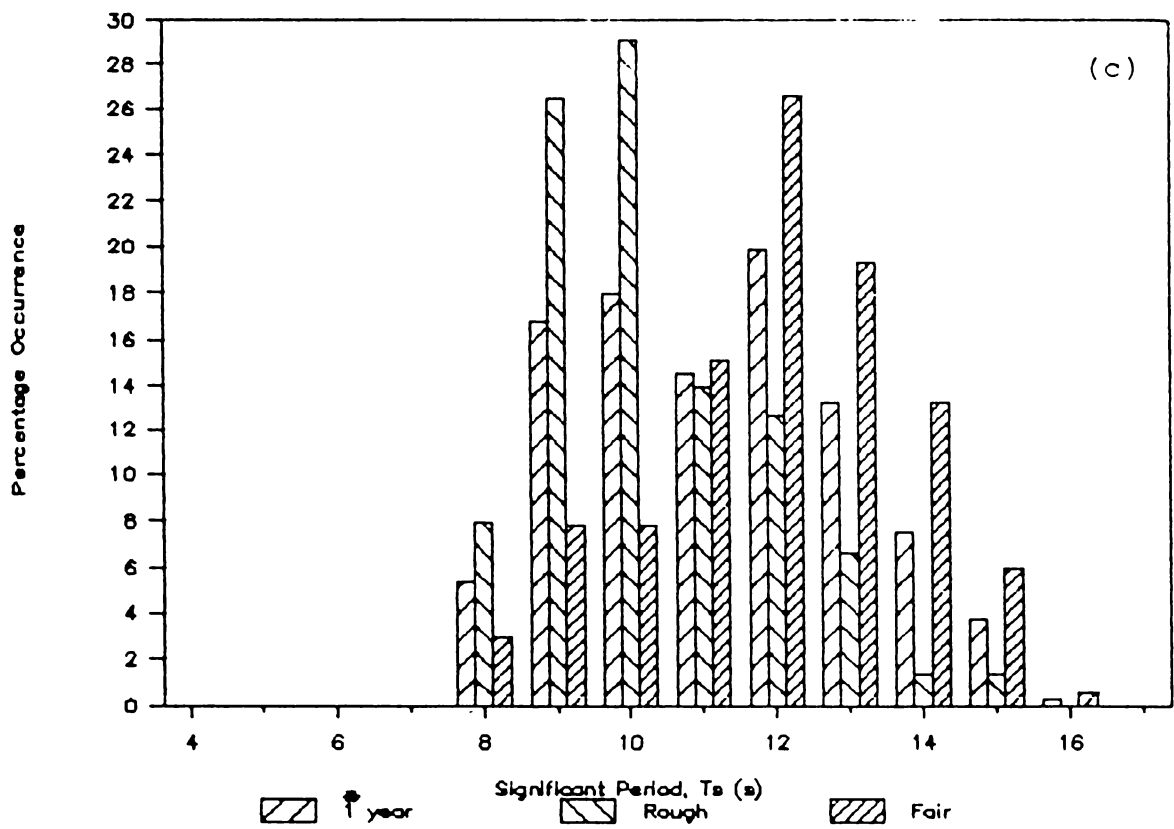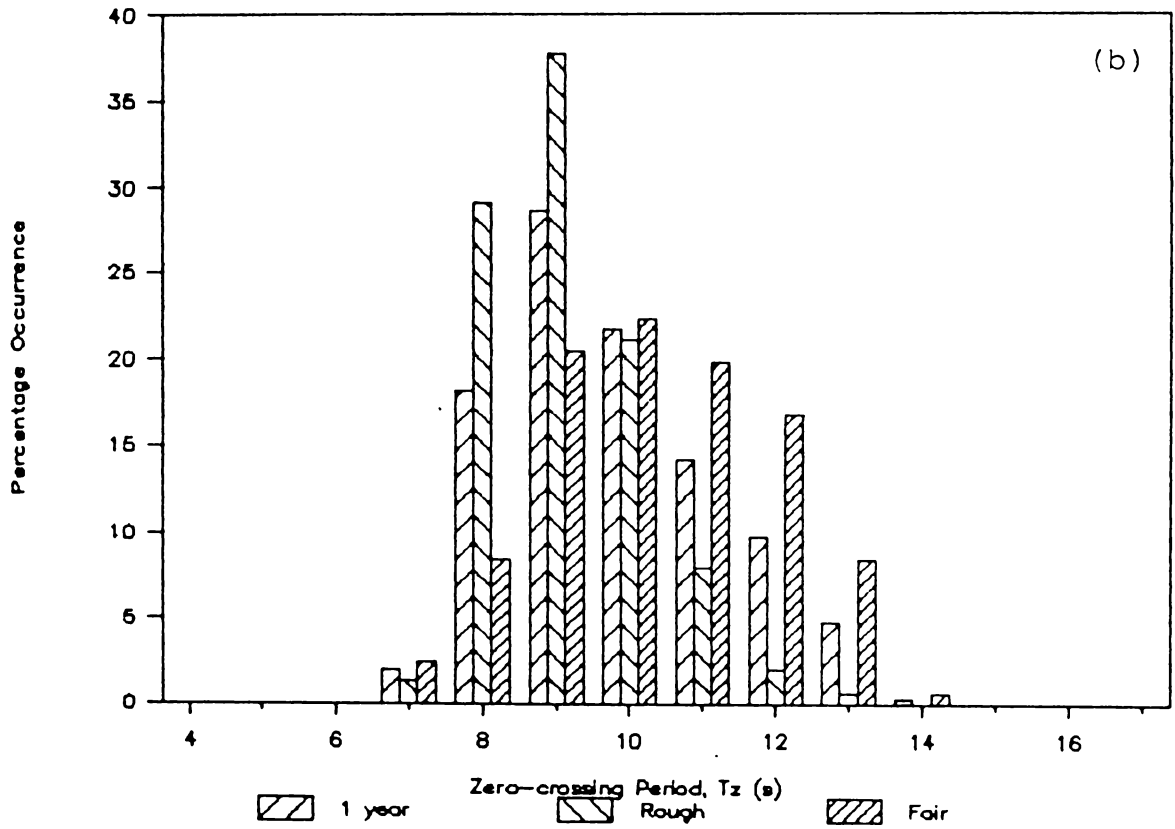
Fig.4.20 continued.

in the next lower and higher ranges. About 80% of T_z values during these months are in the range 8-12 s. The distribution of T_s and T_c are also identical to that of T_z. However, during each season the dominant T_s values are in distinctly separate ranges. During May-September the maximum number of T_s is in the range 8-10 s (56%) and during October-April it is in the range 10-13 s (61%). The temporal distribution of periods are found to be identical to that of T_p explained in Sec.4.2 and hence a discussion is not presented here.

4.5.3 Spectral Width

The spectral width parameter ϵ_w varied from 0.33-0.94 during the year with an average of 0.63 and a standard deviation of 0.1. The values are slightly lower during May-September and are confined to a comparatively narrower range. During this season it vary from 0.39-0.85 and during October-April it is in the range 0.33-0.94. The averages during May-September and October-April are 0.62 and 0.64 with standard deviations of 0.1 and 0.09, respectively. The percentage occurrence of ϵ_w during May-September, October-April and the complete year are presented in Fig.4.21. The dominant ϵ_w values during May-September and October-April are in the ranges 0.6-0.65 and 0.65-0.7, respectively, both constituting about 24% of the respective seasons. The above

104
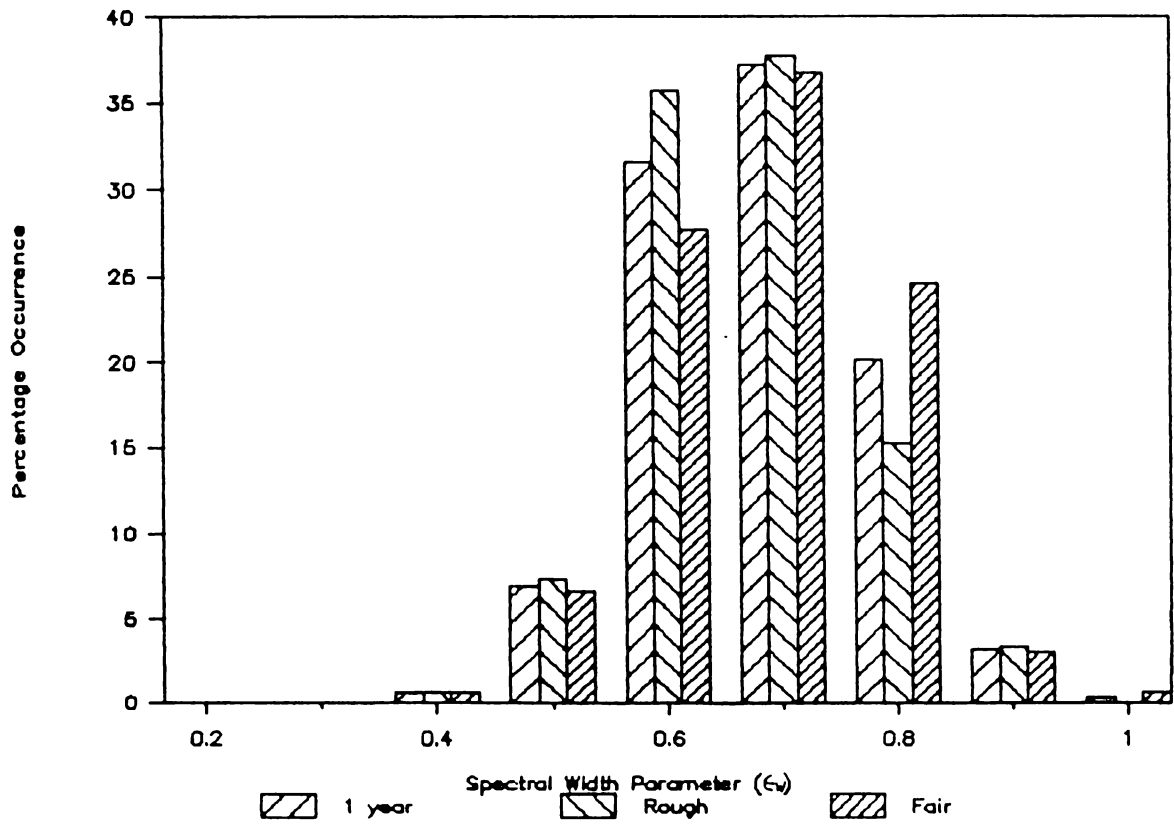
Fig.4.21 Frequency distribution of ε_w for rough
season, fair season and whole year.

observations are in agreement with the observations made in Ch.3 and Sec.4.2. The temporal variation of ϵ_w is similar to that observed for ϵ_s and since this aspect is dealt with in detail in Sec.4.2 a discussion on this is not presented here. However, a comparison of ϵ_s and ϵ_w will be made in the following section.

4.6. RELATION BETWEEN THE STATISTICAL PARAMETERS

The different methods of analysis usually provide different statistical parameters. Further, the same parameter derived from different methods may sometimes vary according to the method of analysis employed. For example, the significant wave height is derived in the zero-crossing analysis by considering the highest one-third of the waves present in the record, whereas it is derived from the total energy of the waves, thereby making use of all the component waves in the record, in the spectral analysis. Based on statistical interpretation of the distribution of waves, suitable coefficients are derived to correlate one parameter to the other. But, field evaluations show that these coefficients may vary depending upon the situation. For example, the significant wave height is 4 times the square-root of variance of the record, as per Rayleigh distribution. But it is often seen that the waves in the shallow waters deviate considerably from the Rayleighean and

hence it is possible that the constant may differ from 4 for shallow waters. Field and simulation studies also point to this direction. The same argument may hold good for other parameters also. Hence, a comparison of the identical parameters obtained from the zero-crossing and spectral analyses are made here to examine the relations between them. Also, a comparison between the different statistics of the same parameter obtained from the zero-crossing analysis, as done for the spectrally obtained parameters in Sec.4.2, is made to find their inter-relations.

4.6.1. Wave Height

The height parameters $\bar{H}$, H_{sw} and H_{max} are compared with each other and good positive correlations are obtained. H_{sw} and $\bar{H}$ exhibit better correlation with lesser scatter (Fig. 4.22a) compared to H_{sw} against H_{max} (Fig.4.22b). The variation of H_{max}, especially in the higher ranges, may be due to the selection of H_{max} from the finite length of the records. However, the agreement is rather good and the relations obtained may be useful for all practical purposes. From regression analysis the following relations are obtained.

$$\bar{H} = 0.675 \ H_{sw} \qquad \qquad \dots\dots(4.11)$$

$$\text{and} \ \ H_{max} = 1.374 \ H_{sw} \qquad \qquad \dots\dots(4.12)$$

The ratio of $H_{sw}/\bar{H}$ obtained here (1.48) is about 7% less

106
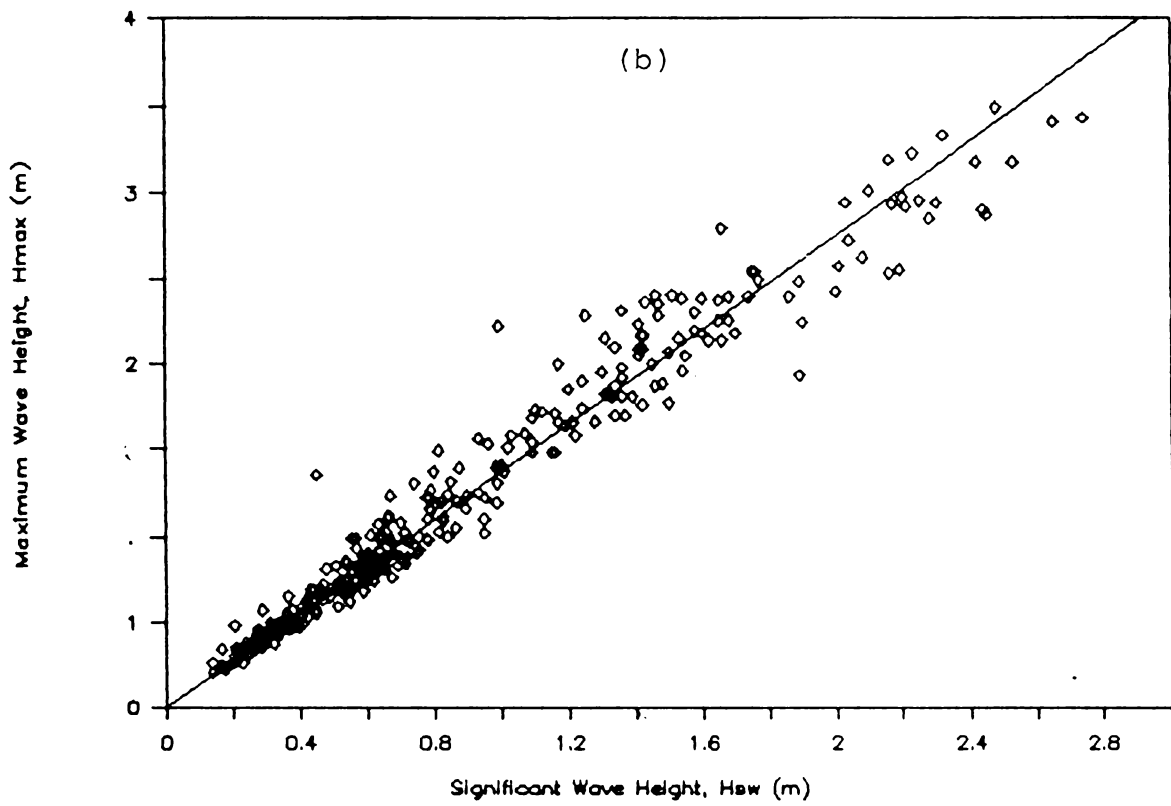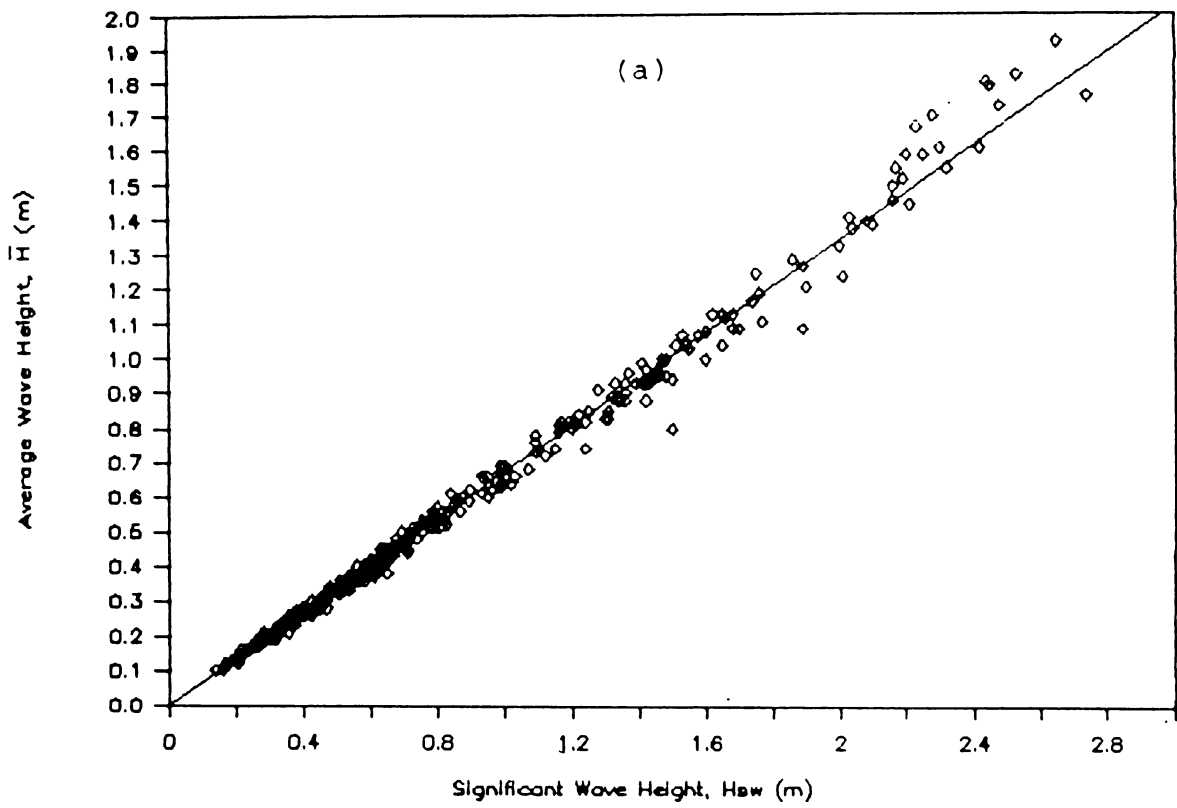
Fig.4.22 Relation between wave height parameters :
(a) H_{sw} and $\bar{H}$; (b) H_{sw} and H_{max}.

than the theoretical value of 1.6 based on Rayleigh distribution. This may be due to the deviation of the wave height distribution from the Rayleighean in the shallow waters.

4.6.2. Wave Periods

The different wave period parameters 'show varying correlations with each other. The zero-crossing periods T_z and the period of the significant wave (T_s) show better dependence with lesser scatter (Fig.4.23a). The crest period (T_c) also exhibit linear dependence, though with some scatter (Fig.4.23b). The plot of T_c against T_s (Fig.4.23c) show wider scatter. The average relation between these parameters are obtained as

$$T_s = 1.15 \; T_z \qquad\qquad .....(4.13)$$

$$T_c = 0.76 \; T_z \qquad\qquad .....(4.14)$$

The period parameters T_s, T_z and T_c show wider scatter with the period of maximum energy density (T_p) obtained from spectral analysis. On regression analysis the following relations are obtained between these parameters.

$$T_s = 0.936 \; T_p \qquad\qquad .....(4.15)$$

$$T_z = 0.81 \; T_p \qquad\qquad .....(4.16)$$

$$T_c = 0.61 \; T_p \qquad\qquad .....(4.17)$$
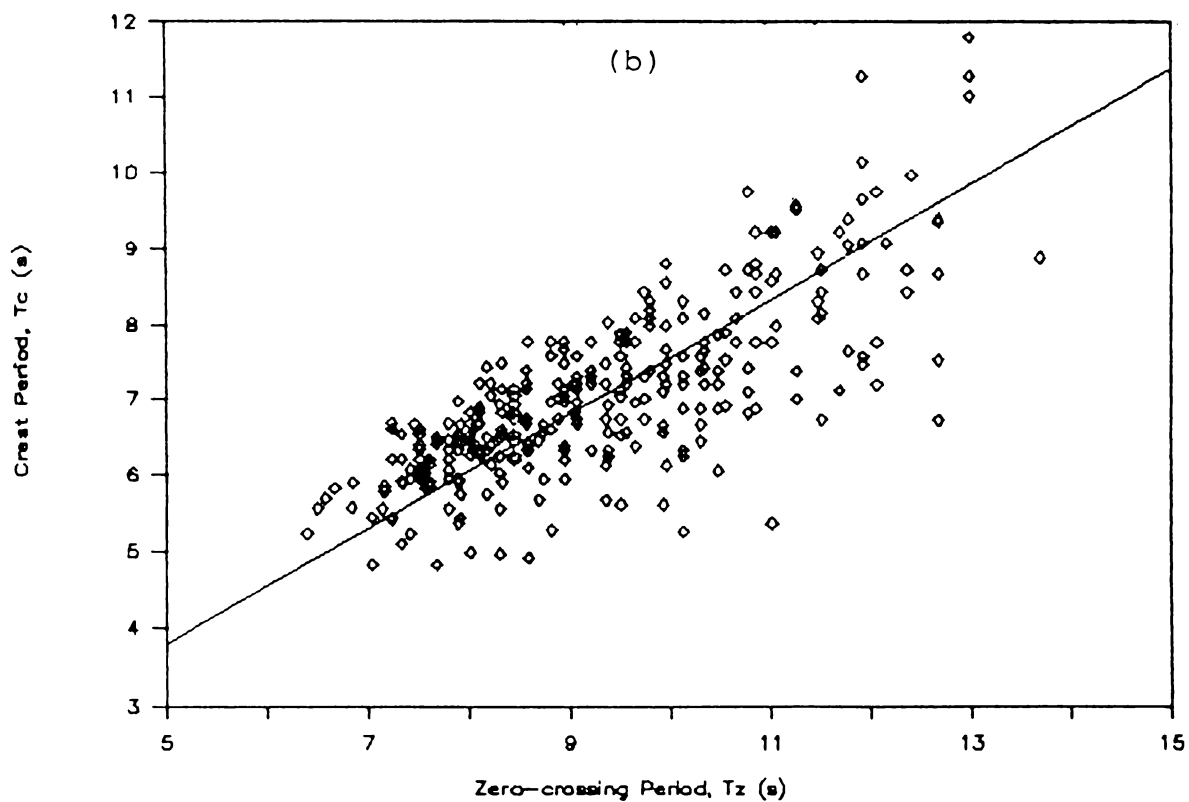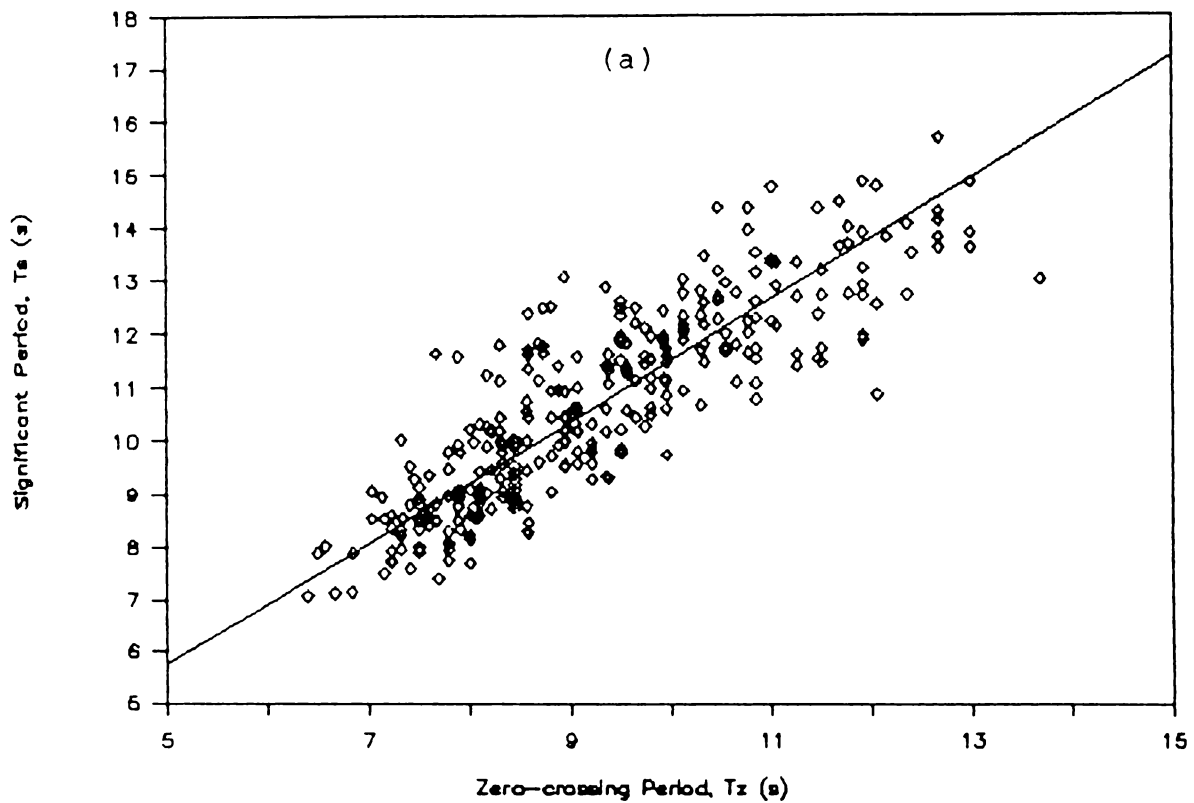
Fig.4.23 Relation between different period parameters :
(a) T_z and T_s; (b) T_z and T_c; (c) T_s and T_c.

The peak frequency ($f_m = 1/T_p$) which is an input parameter in all the spectral models and in almost all practical applications can be obtained from these equations. However, usually the significant wave height (H_s) and the period corresponding to these waves (T_s) are usually employed. Eq.(4.17) can be used to obtain f_m from T_s, and from the present data the relation

$$f_m = 1/1.07 \; T_s \qquad\qquad \ldots\ldots(4.18)$$

is obtained. Different values are suggested for the constant in Eq.(4.18) by various researchers. The value is suggested by Bretschneider (1977) as 1.057, by Mitsuyasu (1969) as 1.06, by Goda as 1.08 and by Ou (1977) as 1.13. The value obtained in the present study is closer to the values suggested by majority of the researchers and hence Eq.(4.18) can be applied to obtain f_m for this as well as for other coasts with similar characteristics.

4.6.3. Spectral Width

A comparison between the spectral width parameters obtained from the spectral analysis is already presented in Sec.4.4. A comparison of these parameters with that obtained from zero-crossing analysis (ϵ_w) is presented here. ϵ_s and ϵ_w do not show much dependence between each other by showing large scatter (Fig.4.24a). However, ν and ν_1 are

103
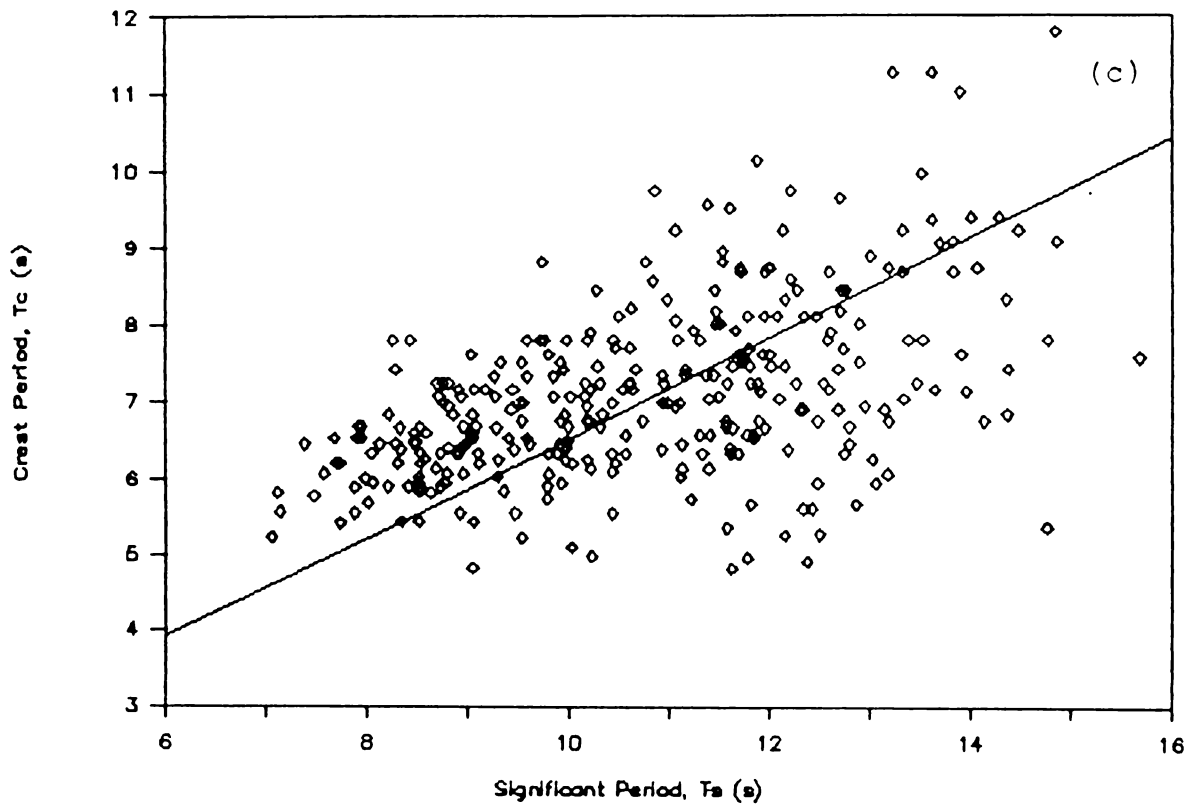
Fig.4.23 continued.
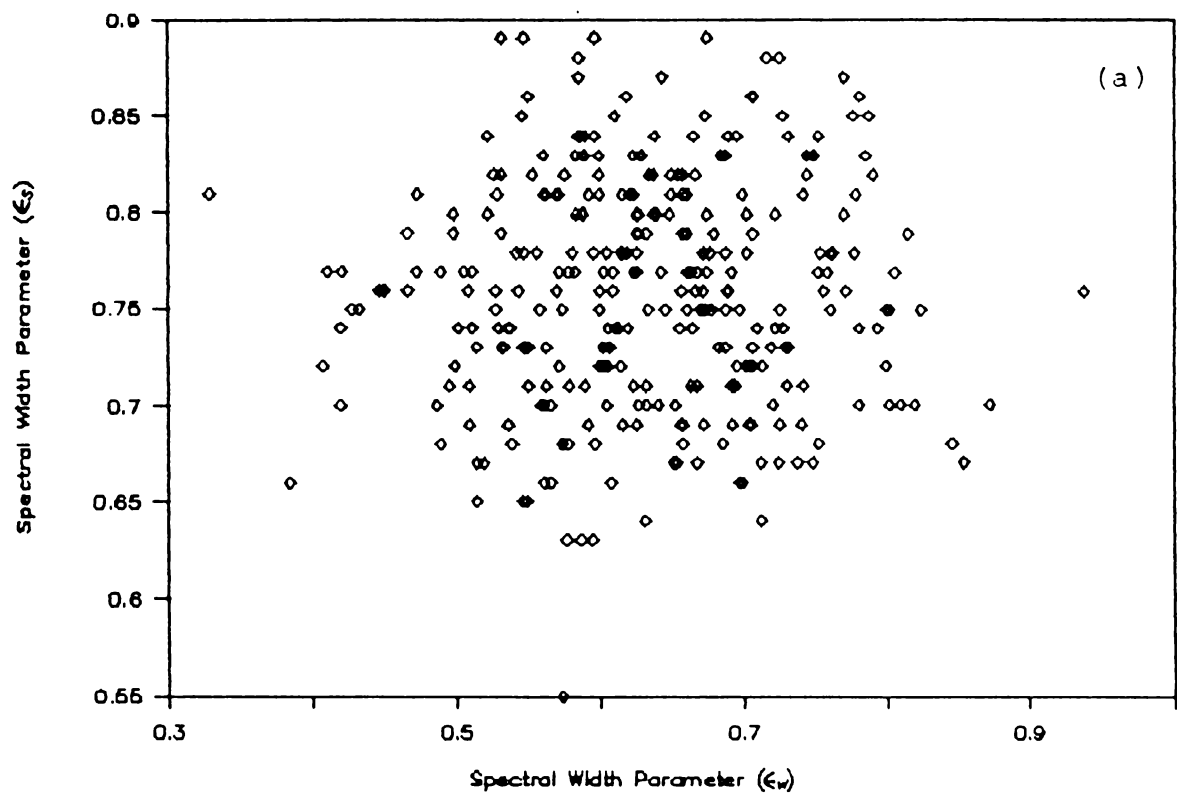
Fig.4.24 Relation between spectral width parameters :
(a) ε_w and ε_s; (b) ε_w and ν ; (c) ε_w and ν_1 .

found to be better correlated to ε_w (Fig.4.24b-c) though with some scatter. The regression relations obtained for these parameters are

$$\nu = 0.82 \ \varepsilon_w \qquad\qquad \ldots\ldots(4.19)$$

$$\nu_1 = 0.72 \ \varepsilon_w \qquad\qquad \ldots\ldots(4.20)$$

The poor dependence of ε_s and ε_w may be attributed to the analysis procedures used to derive them. In the zero-crossing analysis, the lowest waves, which do not cross the MWL, are filtered off while they *are* retained in the spectral analysis. Hence, depending on the characteristics of the wave records (time series), the values computed with each method may differ by varying extents. This applies to the parameters ν and ν_1 also. But, ε_s is a function of the higher moments, thus is more influenced by the frequencies, unlike ν or ν_1 which are functions of the lower moments. This may be the reason for the comparatively better dependence obtained for ν and ν_1 with ε_w.

4.7. CONCLUSIONS

The multi-peakedness observed in more than 90% of the spectra obtained from this location is mainly due to the co-existence of different wave trains arriving this coast from different generating areas. The waves occurring during the months of May-September exhibit distinct characteristics.
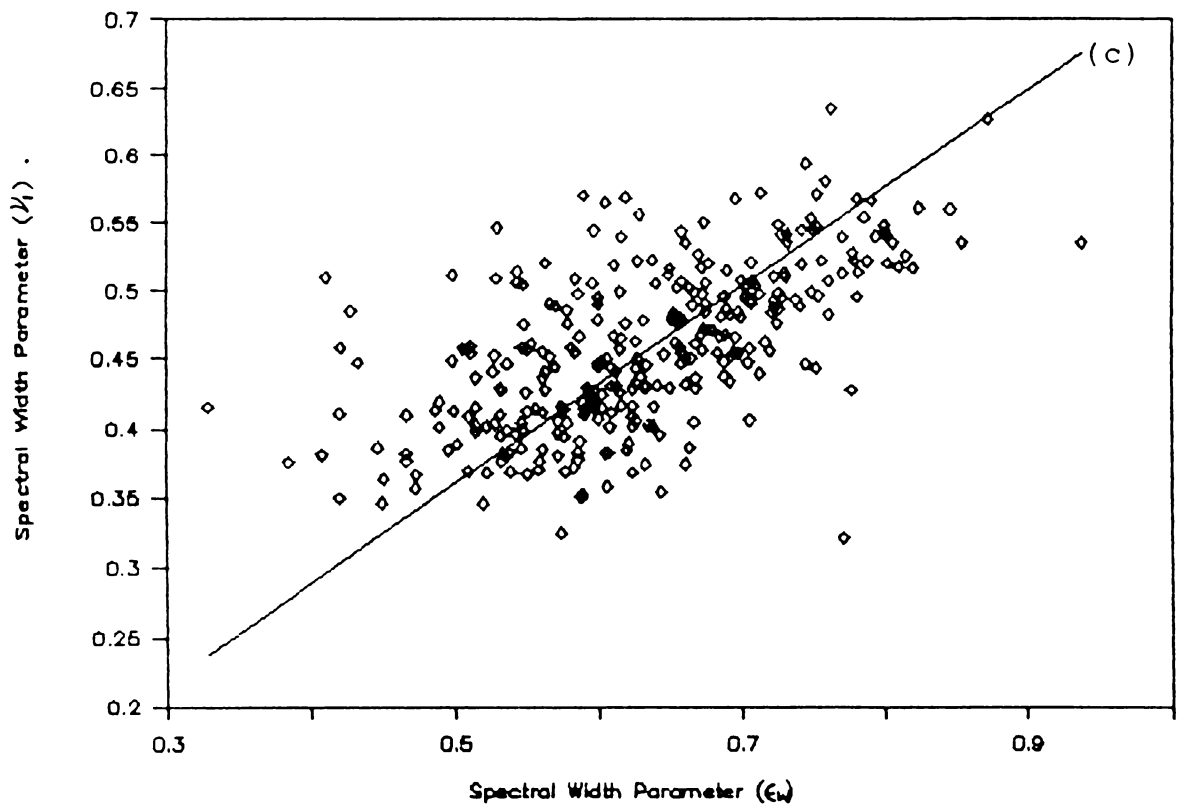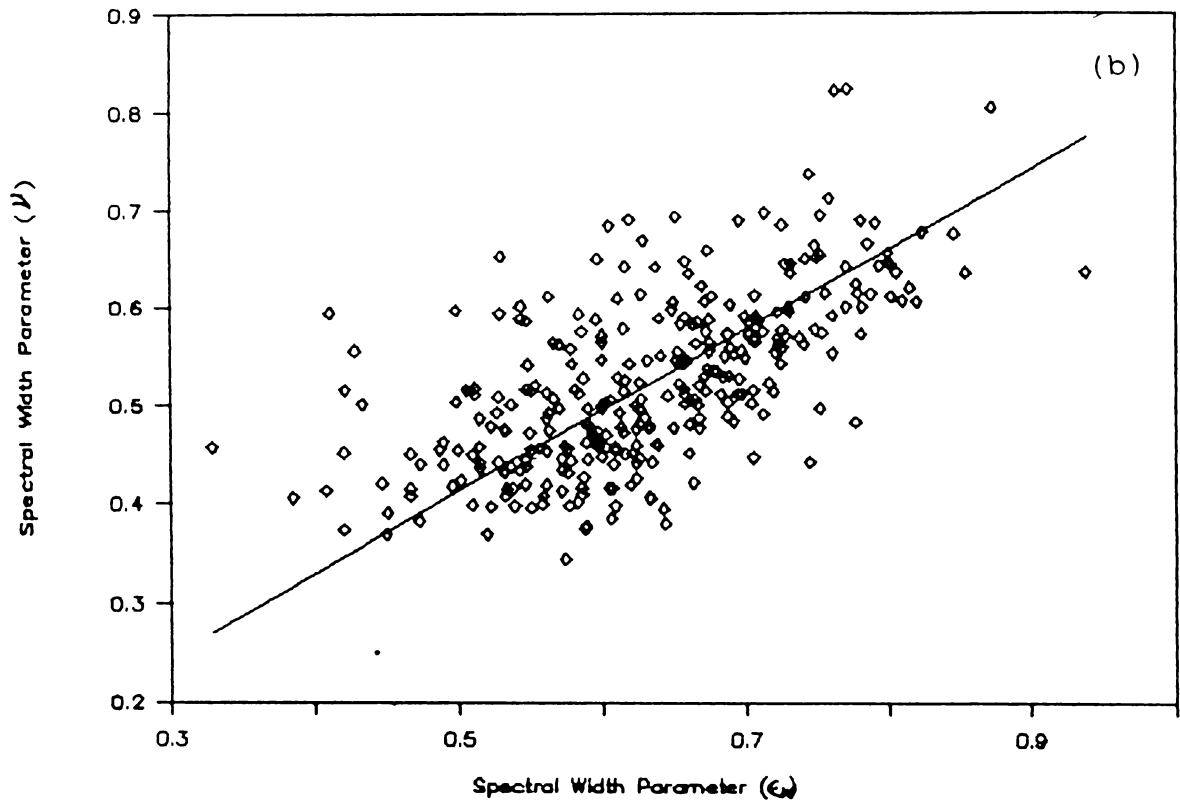
Fig.4.24 continued.

During these months the waves are generally high associated with comparatively lower periods and spectral widths. During October-April the waves are of lower heights associated with comparatively higher periods and spectral widths. Hence, May-September may be classified as the rough season and October-April may be classified as the fair season (of wave climate) for this location. During the rough season the waves generated in the Arabian Sea, and during the fair season those generated at two different and far-away locations constitute the wave climate in this area. A detailed study involving generation, propagation and directional spreading is required to identify these generating areas.

The spectral peakedness parameter Q_p cannot be taken as a measure of the width of the spectrum in shallow waters due to the presence of multiple-peaks in most of the shallow water spectra. The spectral width parameters ϵ_s, ν and ν_1 exhibit characteristic properties during the rough as well as the fair seasons. These parameters can be useful in estimating the sea state in shallow waters where swells are dominant.

The parameters computed from the average spectra agree well with the average of the spectral parameters sampled at 1 per day. Decrease in slope of the high frequency side of the spectrum with increasing energy is observed with the

monthly average spectra. The relation between slope and energy of the spectrum can be determined from Eq.(4.6). The spectral width parameters are dependent mutually as well as to the peak period through Eqs.(4.7-4.10).

The statistical height parameters show very high correlation between each other, which can be represented by Eqs.(4.11-4.12). The ratio $H_{sw}/\bar{H}$ is about 7% less than the theoretical value based on Rayleigh distribution of wave heights. The different statistics of periods exhibit varying degrees of correlation, among which T_z and T_s are better correlated. The relation between the period parameters can be represented by Eqs.(4.13-4.14). The period parameters are also related to the peak period/frequency through Eqs.(4.15-4.17). The peak frequency, which is usually employed in almost all the applications, can be computed from the significant wave period using Eq.(4.18).

The spectral width parameters derived from spectral and zero-crosssing analyses deviate from each other, owing to the differences/limitations of the methods. As the spectrally obtained parameters ν and ν_1 are statistically more stable, and are better correlated to ϵ_w, they may be used for practical purposes. However, only one of them need be considered, since they are related through Eq.(4.2) by definition.

CHAPTER 5

WAVE SPECTRAL MODELS

The individual wave spectra computed from the recorded data are compared with different spectral models suggested for shallow water conditions. A new empirical model is derived for shallow water applications and is verified with the measured spectra. The other theoretical shallow water spectral models selected for this study are the Kitaigorodskii et al. spectrum, the TMA spectrum in its original form and with certain modifications, the Wallops spectrum and the GLERL spectrum. Since the Scott spectrum and its modified form (Scott-Weigel spectrum), though originally derived for deep water conditons, has found its application in many shallow water conditions also (Ch.2), these models are also selected.

5.1. DERIVATION OF A SHALLOW WATER SPECTRAL MODEL

Most of the shallow water spectral models are derived from some deep water models by applying a shallow water dispersion relatioship. For example, Kitaigorodskii et al. (1975) applied a dispersion relationship to Phillips' spectral model to arrive at a new shallow water model and Bouws et al. (1985) applied the relationship derived by Kitaigorodskii et al. on the JONSWAP model to derive the TMA spectral model. The JONSWAP spectrum which is in fact the

112

modification of the P-M spectrum for the conditions of growing seas may be suitable for similar conditons in the shallow water when the appropriate dispersion relationship is applied. The shallow water spectra, generally, are not related to the local wind conditions. That is, the shallow water wave spectra result from the waves generated at some other locations and propagated towards the coast and are thus swell dominated. In such a case, a better model suitable for transformation to shallow water conditions will be one which is able to predict the deep water saturated sea state successfully. The P-M spectrum is one such model supported by various field and laboratory data for its ability to simulate the spectra of deep water saturated sea conditions. The functional form of this model is given as

$$S(f) = \alpha\, g^2 (2\pi)^{-4}\, f^{-5}\, \exp\,[-(5/4)(f/f_m)^{-4}] \quad \ldots\ldots(2.13)$$

By incorporating the finite depth dispersion parameter proposed by Kitaigorodskii et al. (1975) in the P-M spectrum, the shallow water model, which may be called Pierson-Moskowitz-Kitaigorodskii (PMK) spectrum, can be obtained as

$$S(f) = \alpha\, g^2 (2\pi)^{-4} f^{-5} \exp\,[-(5/4)(f/f_m)^{-4}]\Phi(\omega_h)\ldots(5.1)$$

The function $\Phi(\omega_h)$ is dimensionless and varies monotonously from 1 in deep water to 0 in depth h=0. It is expressed as

$$\Phi(\omega_h) = \Phi(2\pi f\,(h/g)^{1/2}) \qquad\qquad \ldots\ldots(2.26)$$

113

For shallow waters $\Phi(\omega_h)$ is less than 1 and in such cases the function is well approximated by

$$\Phi(\omega_h) = 1/2 \ (\omega_h)^2 \qquad \qquad \ldots\ldots(2.27)$$

By applying this approximation, Eq.(5.1) becomes

$$S(f) = 0.5\alpha \ g^2(2\pi)^{-2}f^{-3} \ \exp \ [-(5/4)(f/f_m)^{-4}]\ldots\ldots(5.2)$$

If the dispersion relationship of Kitaigorodskii et al. is valid, the PMK spectrum (Eq.5.2) must be able to predict the swell dominated shallow water wave spectra. Validation of this model is carried out alongwith the other models.

5.2. COMPARISON OF MEASURED SPECTRA WITH MODELS

Typical examples of spectra predicted by different models corresponding to an observed spectrum are given in Fig.5.1. There is no standard test, till date, to examine the fitness of a theoretical spectral model to the observed spectrum. The procedure followed in almost all the studies in the past is to make a visual comparison. This is possible when the number of observed spectra and the number of models to be tested are limited. As the number of data and models are large in the present study, the deviation index method suggested by Liu (1983) is adopted for testing the goodness of fit. The deviation index is given by

$$DI = \sum \ [(S(f_i)-S_T(f_i))*100/S(f_i)] \ [S(f_i) \ \Delta f/E]\ldots.(5.3)$$
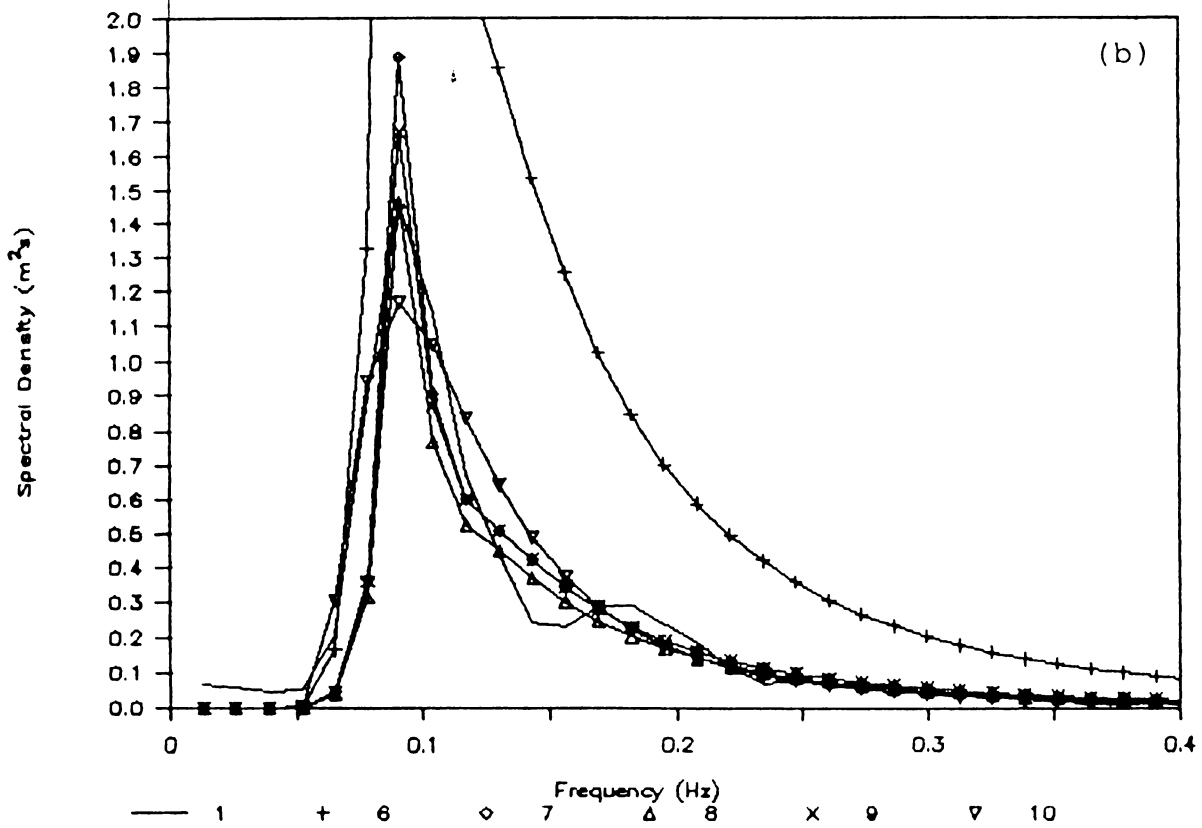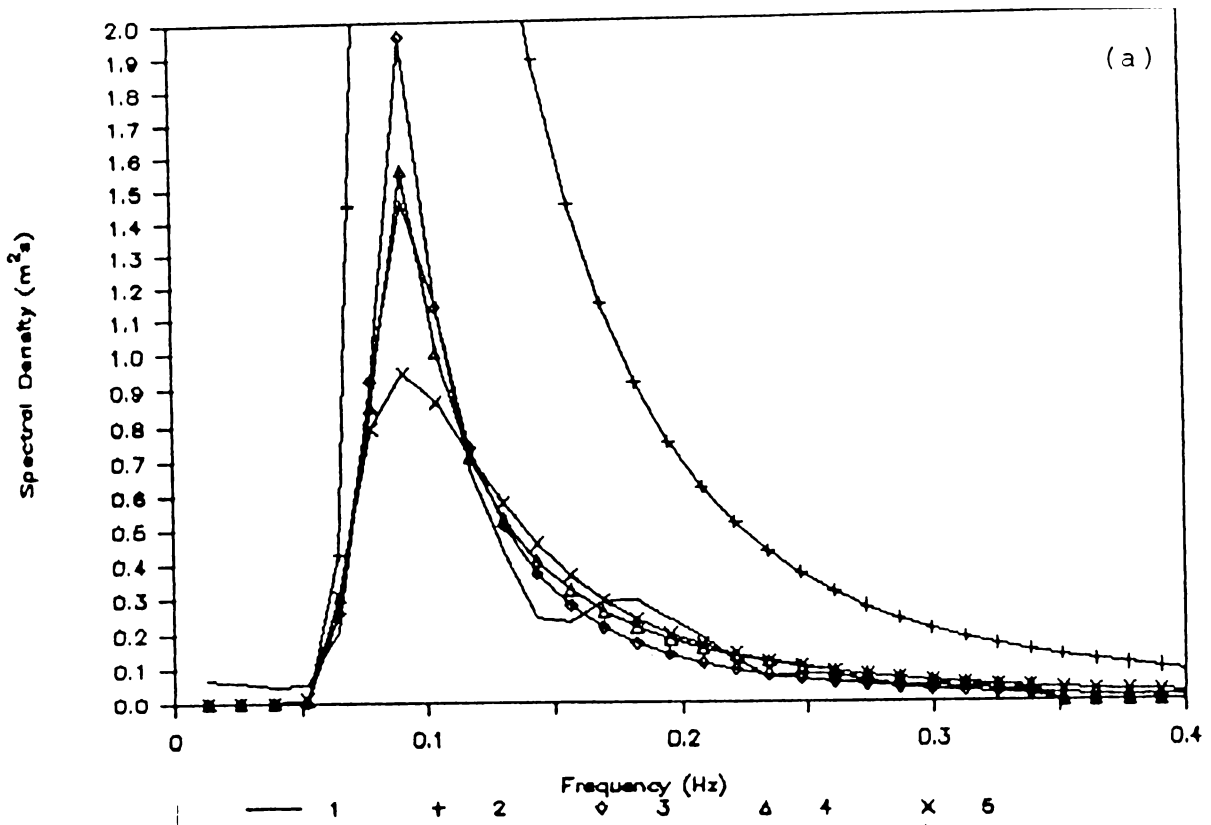
1: observed, 2: Jensen's, 3: Scott, 4: Scott-Weigel,
5: PMK, 6: TMA with average JONSWAP parameters,
7: TMA with α_v and JONSWAP parameters, 8: TMA (original),
9: TMA with computed γ and α_v, and 10: Wallops spectrum.

Fig.5.1 Typical examples of spectra predicted by different
models corresponding to an observed spectrum.

where $S(f_i)$ and $S_T(f_i)$ are the measured and theoretical spectral densities at frequency f_i. E is the total energy of the observed spectrum and Δf is the frequency interval used in calculating the spectrum. This deviation index is actually the sum of percentage deviations of the theoretical spectral densities from the observed ones weighted by the relative magnitude of the observed spectral density. A perfect representation will yield a zero DI and hence a smaller DI implies a better fit. No criterion is established for the acceptance/rejection of a model based on the value of DI. Hence a criterion for the acceptance or rejection of a model is fixed based on the placement of the theoretical spectrum with respect to the confidence limits. The upper and lower confidence limits of the observed spectra are calculated at the 0.05 level of significance. A model is considered to fit the measured spectrum when the DI value of the model is less than the DI value of lower confidence limit (DI_{LC}) with respect to the observed spectrum.

In addition to the application of the 'Deviation Index' to examine the fitness of models, total energy, peak frequency and peak energy density derived from the models are also compared with the observed values to determine the applicability of the different models.

5.2.1. Jensen's Model

The spectral model suggested by Kitaigorodskii et al. (1975) depicts the high frequency side of the spectrum only. Hence the slope of the high frequency side is the only parameter that can be compared. Jensen (1984) modified this model by adding the low frequency face (Eq.2.31) assuming the original form for the high frequency tail.

The DI values for this model range from 37 to very high values like 70,000. The higher values correspond to the low wave heights. This model is found to fit the data in only 4 cases, which is only 1.26% of the total records used for the study. Those 4 cases which fit the observed spectra correspond to the high energy conditions (H_s > 1.8 m) associated with lower wave periods (T_p < 11 s). The cases with T_p higher than 10 s fit in when H_s is about 2.5 m. In this model, the energy density is a function of the peak frequency and hence as the peak period increases, the energy also increases in the order of T_p^3 (Eq.2.31). The fitting of this model to the higher waves is indicative of the validity of the power law of T_p in the high energy conditions. The total energy and peak energy density predicted by this model are depicted in Fig.5.2 (a-b). The energies are over-estimated in most of the cases, the average ratio being > 50. From these figures also it can be

116

seen that the energy and $S(f_m)$ predicted by this model become closer to the observed values only when the energy of the observed waves are high ($H_{ss} \simeq 2.5$ m).

5.2.2. TMA Spectrum with Phillip's Constant α and Average JONSWAP Parameters

The TMA spectrum in its original form requires the 5 free parameters to be derived from the observed spectrum. If some useful averages are available for the scale and shape parameters, α_J, γ, δ_a and δ_b, the number of free parameters is reduced to f_m and hence the application of this model becomes easier. So the TMA spectrum with Phillips' constant as the scale parameter and average JONSWAP values of shape parameters ($\gamma = 3.3$, $\delta_a = 0.07$ and $\delta_b = 0.09$) is tried.

The DI values are found to be very high in most of the cases. They range from 33 to more than 89,000. As in the case of Jensen's spectrum, the higher values correspond to the lower wave heights. This model fits only in 6 cases, out of which 4 are the same as that fits the Jensen's spectrum. The total energy and $S(f_m)$ predicted by this model are depicted in Fig.5.3 (a-b). The values are overestimated many times. Here also the energy densities are functions of f_m and the model resembles with Jensen's.

117

5.2.3. TMA Spectrum with Scale Factor α_V and Average JONSWAP Parameters

The TMA spectral model assumes the scale parameter α_J as a function of the observed spectral density. Vincent (1984) in his study showed that this coefficient is a function of the steepness (Eq.2.36). Considering this observation, Phillips' constant in the form tried in the above section is replaced with α_V and the spectrum corresponding to each observed ones are computed. The values of α_V range from 0.000015 to 0.013. Large variation in the values around the mean 0.0016, as shown by the standard deviation of 0.0023, with a mean of 0.0016.

This form presents a better fit with the data. The DI values for this model are found to be considerably lower (29-114) compared to that obtained with the Phillip's constant as scale parameter. This observation is in confirmation to the observation of Vincent (1984) that the scale parameter is proportional to the steepness rather than being a constant. The DI values are always lesser than the DIs corresponding to the upper confidence limit spectra. They are less than DI_{LC} in 58 cases which contribute 18.3% of the total. This is found to have the best fit to spectra with lower peak periods. However, at low T_p this gives better fit in the lower height ranges also. The total energy

predicted by this model is closest (> 99%) to the observed values (Fig.5.4a). But, the peak energy densities are over-predicted in most of the cases (Fig.5.4b). This may be due to the choice of the peak enhancement factor (γ = 3.3).

5.2.4. TMA Spectrum with Derived γ and α_J (Original Form)

In the Sec.2.5.3 it is seen that the peak energy densities are over-predicted due to the choice of peak enhancement factor. The value of 3.3 is suggested for the JONSWAP conditions. This may not be suitable to other locations with different environmental conditions. Hence, the peak enhancement factor is calculated for each observed spectrum. They range from 0.77 to 14.93 with average 3.42. Though this value is closer to the JONSWAP average, the individual values show wide variation as indicated by the high value of standard deviation (2.23). Also, the scale parameter α_J is computed for each case. The values of α_J range from 7.39×10^{-6} to 1.21×10^{-2}. The values show wide range around the mean 0.0014 with a standard deviation of 0.00215. These values are nearer to the α_V values obtained from the relation suggested by Vincent (1984). The use of average JONSWAP values of the two shape parameters δ_a and δ_b yields an error of 15% only at 80 d.f. (Arunavachapun, 1987). Since the sampling errors being at the same magnitude as the statistical variability for the shape parameters
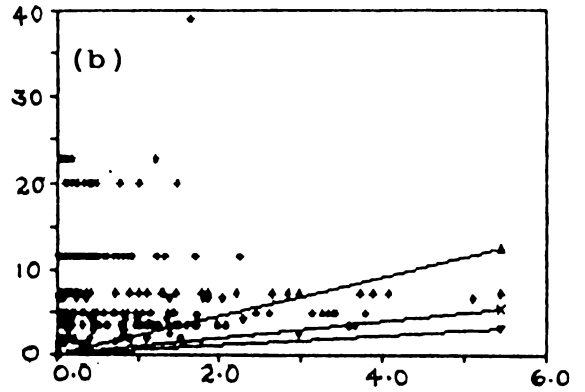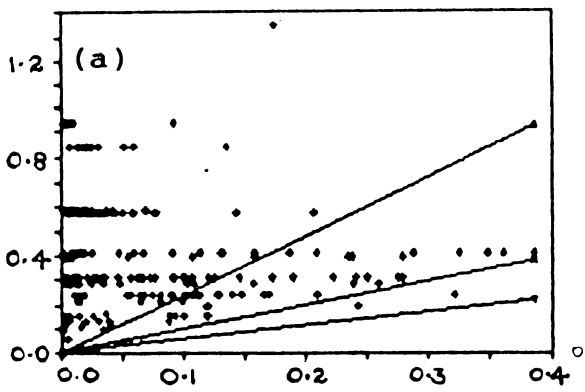
Fig.5.2 Plot of computed (a) energy and (b) peak energy
density against measured: Jensen's model.
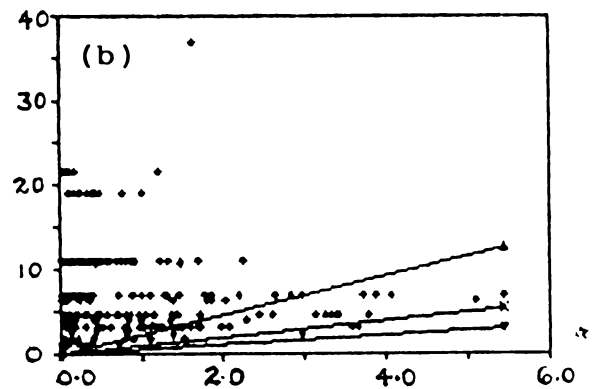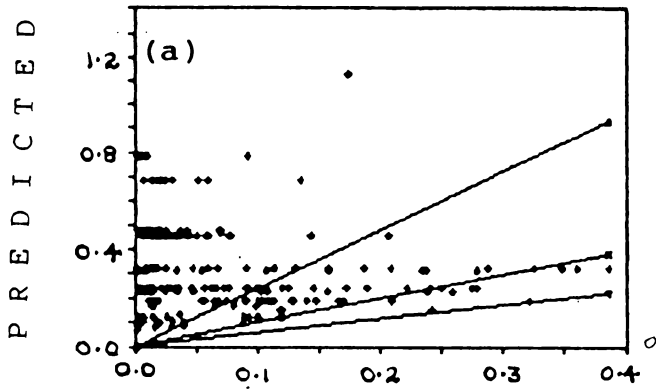
Fig.5.3 Plot of computed (a) energy and (b) peak energy density
against measured: TMA model with α and average
JONSWAP parameters.

OBSERVED
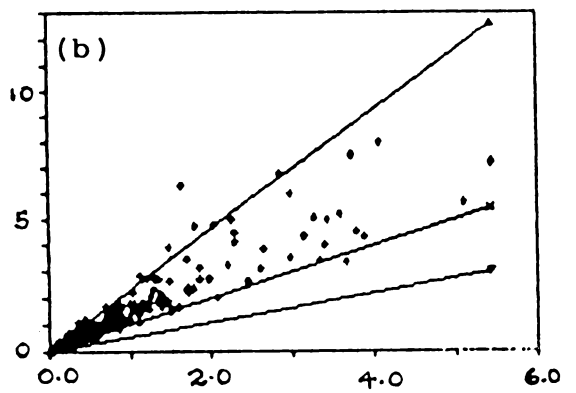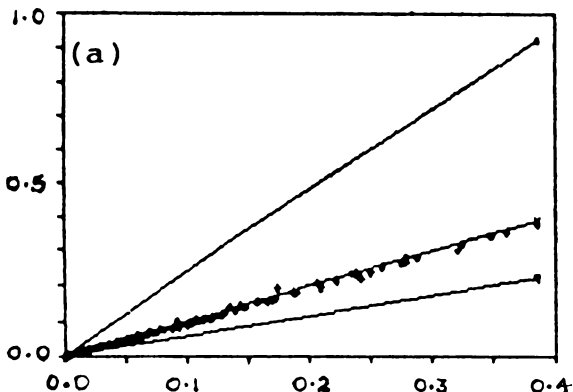
Fig.5.4 Plot of computed (a) energy and (b) peak energy dendity
against measured: TMA model with α_v and average
JONSWAP parameters.

(✻———✻1:1 correspondence; ▲———▲ upper confidence limit
and ▽———▽ lower confidence limit)

(Arunavachapun, 1987), the average JONSWAP values of the two shape parameters δ_a and δ_b (0.07 and 0.09 respectively) are used in the computation of spectra using this model.

The DI values obtained with this form vary between 20 and 94 only, indicating a better fit to the observed spectra in most of the cases. In 169 cases (53.3%), the DI values are less than DI_{LC}. In the higher energy conditions ($H_{ss} >$ 1.4 m) it gives DIs lesser than the DI_{LC}. In the lower energy conditions the fitness is not as good as the cases of high energy conditions. The lesser fit in this range may be due to the existence of major secondary peaks in the lower energy cases, which make the squared deviation larger. The total energy is underestimated by about 30% by this model (Fig.5.5a). However, the peak energy density is simulated correctly (Fig.5.5b). This indicates that it is the shape parameter that requires modification to obtain a better estimate of the total energy. But as the peak energy density is estimated correctly the choice of peak enhancement factor γ is in order. The average value of γ for the cases where the DI values are lower than DI_{LC} is 3.0. Then it is the shape parameter δ_a and δ_b that causes underestimation of energy densities at the tails of the spectrum. That is, f_m, α_J, γ, δ_a and δ_b have to be defined from the observed spectrum. In other words, the spectrum has to be fully defined apriori.

120

5.2.5. TMA Spectrum with α_V and Derived γ

For the computation of all the controlling parameters that define the TMA spectrum, the original spectrum in full is required. For practical purposes this may not be available in all the cases. Hence some average parameters are required. The spectral parameters usually available are the total energy of the spectrum and the peak frequency. The spectral scale parameter α_V can be obtained from these parameters. Hence, it will reduce the number of parameters by 1, if the use of this coefficient in the TMA specktrum simulates the observed ones correctly. The scale parameter α_J is replaced by α_V in Eq.2.35 and the spectra are recalculated to compare with the observed ones. The results are not very encouraging. The DI values have a wide range (24-175). Also, the number of cases where the DIs fall below DI_{LC} is only 120 (37.9%) against the 169 cases with α_J. Moreover, the cases where the lower DIs are observed are mostly the cases which give an equal or still lesser DI value when α_J is used. Here also, the total energy is underestimated in most of the cases (Fig.5.6a). But, they are more closer to the observed values, especially in the low energy conditions. The $S(f_m)$ values are mostly overestimated (Fig.5.6b). However, the overestimation is lesser than that for the case with average JONSWAP shape parameters and scale parameter α_V.

121

5.2.6. Wallops Spectrum

The Wallops spectrum redefines the scale parameter β as an internal parameter from the total energy of the spectrum as is done in Vincent (1984). Also, it defines a variable exponent, m, of the frequency, as a function of the total energy, instead of a fixed value assumed in other models. Hence the number of parameters is limited to 2 as against 5 in the TMA spectrum. The values of β range from 4.57×10^{-6} to 6.24×10^{-3}. The value of m vary from 1.0 to 14.5, the average being 5.6. The variations observed in the values of β and m are large. Since β and m are functions of the energy, variation in accordance with the variation of the energy can be expected.

This model fits the observed data well in a large number of cases. The values of DI range from 17 to 278. The average DI is 56 but there is wide variation in the values as indicated by the standard deviation of 25. In 120 cases the DI values are lower than DI_{LC}. As observed from the DI values, this model gives better fit where H_s is above 0.75 m. In this range (H_{ss} is ≥ 0.75 m), the DI values are lower than DI_{LC} in 81 cases (67%) of the total of 121 cases. The total energy is estimated almost correctly but are overestimated in a few cases where T_p is high (Fig. 5.7a). The large deviations found in the high energy cases

122

are those with T_p higher than 10 s. But, the total energy estimated is nearer to the observed values, even in the high energy conditions (where $H_{ss} \geq 2.0$ m), where $T_p < 10$ s. Similarly, the peak energy density is predicted correctly, but are underestimated in the higher energy conditions where the T_p values are higher (Fig.5.7b). This indicates that the width of the spectrum may be more in the high energy cases. Q_p computed with this model is found to decrease systematically with increase in H_{ss}. This can be expected as the negative exponent of the frequencies (m) in Eq.(2.38) is a function of the total energy of the spectrum (Eqs.2.41 and 2.43). Since m is the parameter that determines the slope of the spectrum, the spectral peakedness parameter Q_p also becomes dependant on the total energy.

5.2.7. Scott Spectrum

The semi-empirical Scott spectrum (Eq.2.21) simulates the observed spectra in a large number of cases. The DI values range from 21 to 110 with an average of 54. The variation of DIs are not as high as that for the other models, as indicated by the standard deviation of 19. The values are found to be equal to or less than DI_{LC} in 129 cases, which is 41.1% of the total. The total energy predicted by this model is proportional to the observed values, but are slightly overestimated (Fig.5.8a). The

123
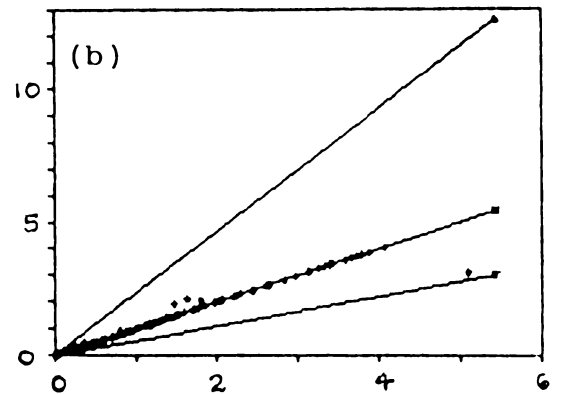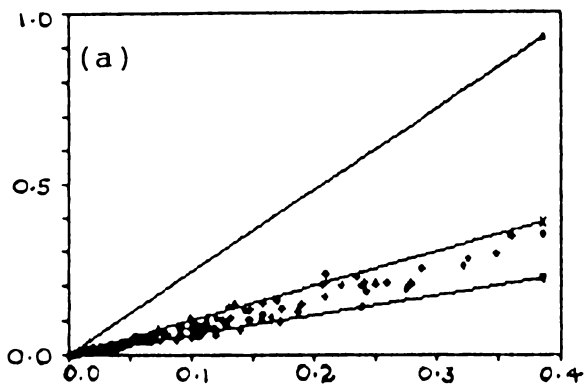
Fig.5.5 Plot of computed (a) energy and (b) peak energy density
against measured: TMA model (original form).
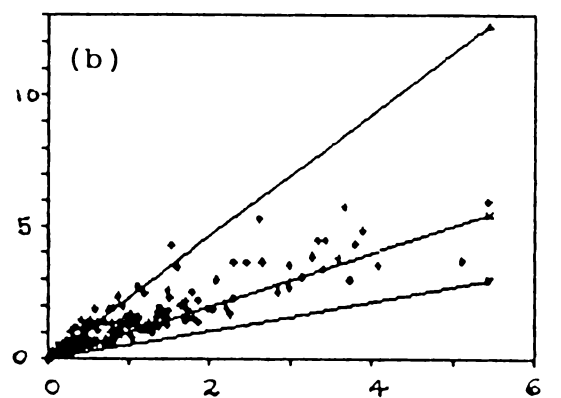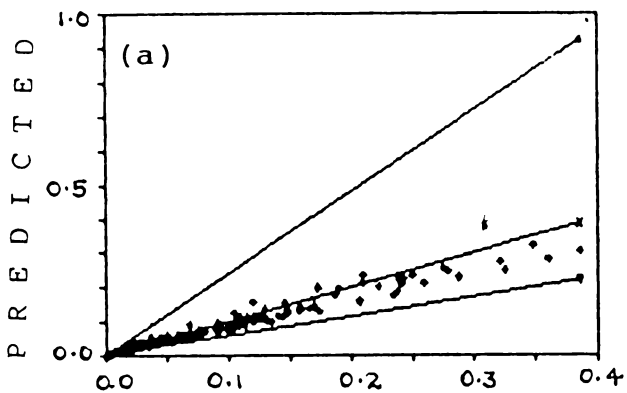
Fig.5.6 Plot of computed (a) energy and (b) peak energy density
against measured: TMA model with α_v and derived
peak enhancement factor.
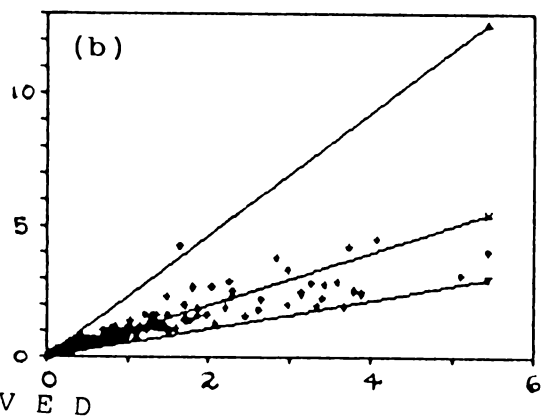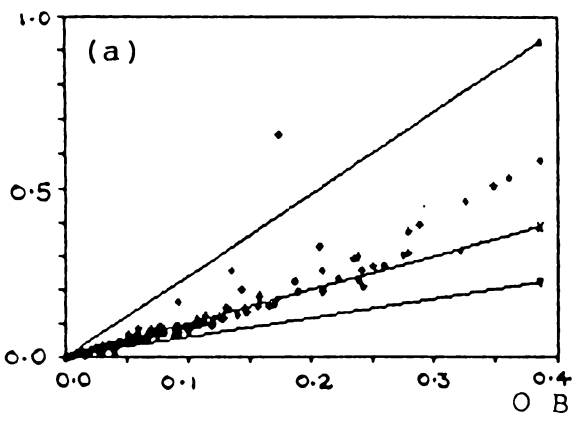
Fig.5.7 Plot of computed (a) energy and (b) peak energy density
against measured: WALLOPS model.

(►————◄ 1:1 correspondence; ▲————▲ upper confidence limit
and ▼————▼ lower confidence limit)

$S(f_m)$ values, on the other hand, are overestimated by about 78% (Fig.5.8b). This may be due to the higher peakedness of this model due to the higher negative exponent (-5) of the frequency assumed in its derivation.

5.2.8. Scott-Weigel Spectrum

The Scott-Weigel spectral model (Eq.2.22) with the variable coefficients (A and B), which are functions of the total energy of the spectrum, is also found to simulate the spectra better than the Scott spectrum. The DI values range, in this case, from 20 to 99 with an average of 53 and a standard deviation of 18. The values are slightly lower than the corresponding values for Scott spectrum, indicating a better fit than the Scott spectrum. However, the number of cases in which the DI values are lower than DI_{LC} is only one less than that for the Scott spectrum. Simulation by this model is found to be better in the high energy conditions compared to the Scott spectrum. This is made possible by the choice of the values for A and B according to the energy of the spectrum. This choice also makes the predicted total energy closer to the observed (Fig.5.9a). Here also, the values of $S(f_m)$ are over-predicted in most cases (Fig.5.9b). But the rate of over-prediction is less compared to the Scott spectral model, especially in the high energy conditions. In the cases where the energy is very
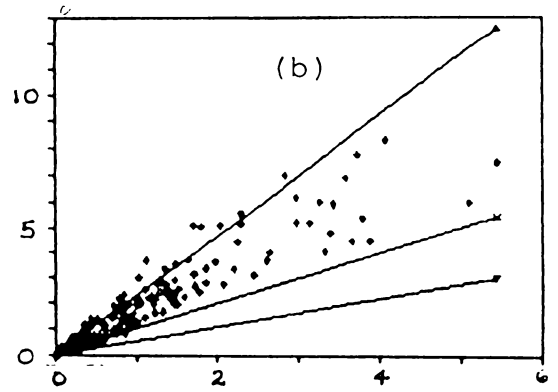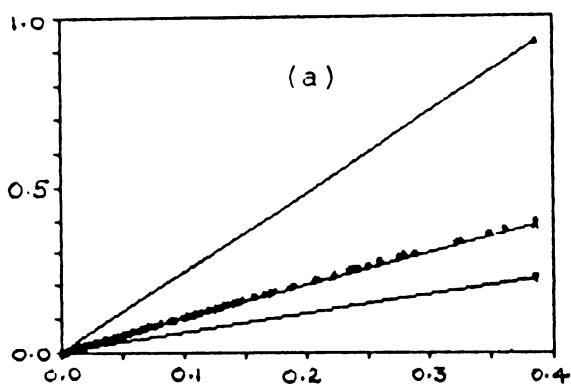
Fig.5.8 Plot of computed (a) energy and (b) peak energy density,
against measured: Scott's model.
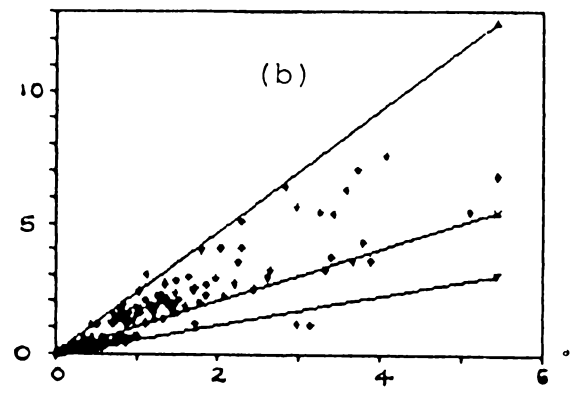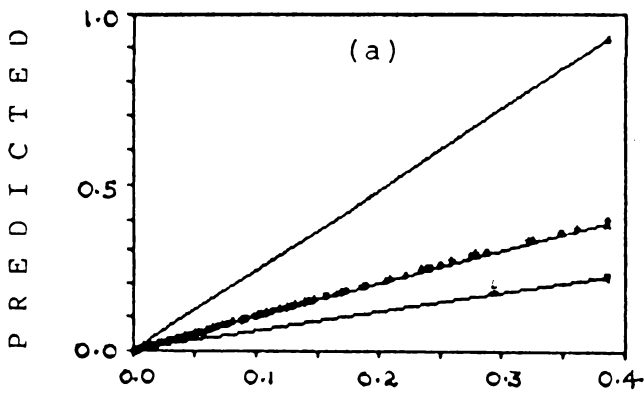
Fig.5.9 Plot of computed (a) energy and (b) peak energy density
against measured: Scott-Wiegel model.
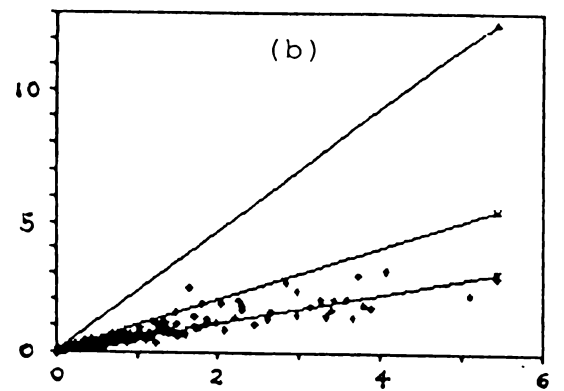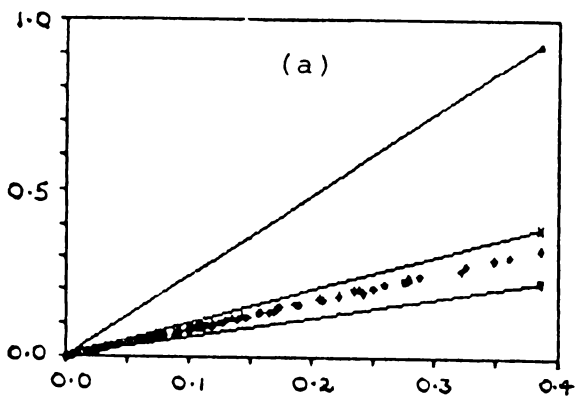
OBSERVED

Fig.5.10 Plot of computed (a) energy and (b) peak energy density
against measured: PMK (new) model.

(×——× 1:1 correspondence; ▲——▲ upper confidence limit
and ▼——▼ lower confidence limit)

low the values are predicted almost correctly. The correct simulation of total energy and lesser over-prediction of $S(f_m)$ indicate that the peakedness is higher, as discussed in the Sec.5.2.7, but it is seen that the values are considerably modified from the Scott model.

5.2.9. PMK Spectrum

The PMK spectrum (Eq.5.2) with Phillips' constant as the scale parameter simulated the observed spectra correctly in the high energy conditions only. The DI values range from 27 to more than 46,000. The energy densities are over-estimated in the low energy conditions. DI values $\leq DI_{LC}$ is obtained in 11 cases only, which correspond to Hs > 1.9 m. When the scale factor α is replaced by α_V better fit is obtained in a large number of cases, as shown by the DI values which range from 23 to 98 only. The average DI is 54 with a standard deviation of 16. This shows a fit better than the Scott spectrum. The DI values are lower than DI_{LC} in 114 cases. The total energy is proportional to the measured, but are underestimated (Fig.5.10a). The peak energy density is also underestimated (Fig.5.10b). This indicates that the scale factor may be low and requires modification.

The peak frequencies estimated by this model is found to be shifted to the higher frequencies. The variation is linear and is estimated to be about 7%. This is the influence of the dimensionless function $\Phi(\omega_h)$ which acts more strongly on lower frequencies than on higher frequencies, As a result, the spectral density estimated by the PM spectrum is reduced more on the lower frequencies and the reduction is less on succeeding frequencies. Consequently maximum density is attributed to a frequency higher than the actual f_m which is an input to the model. This can be compensated by applying a peak enhancement factor, as done in the case of JONSWAP spectrum. If the peak enhancement factor of the JONSWAP model is adopted here in this model, this becomes the TMA spectrum modified with α_v (Sec.5.2.6). It is already seen that this modified form does not fit well with the data, it underestimates the total energy and over-estimates the maximum energy density. Another way to compensate for the shift in f_m is to apply a factor to the coefficient of the exponent, so that the estimated energy densities will be higher. This will enable the enhancement of the underestimated total energies and the peak energy densities. It is seen that the factor -3/4 (in place of -5/4 in the PM spectrum) can simulate f_m correctly. The PMK spectral model is modified in this line and the simulated spectra are compared with the average spectra computed for

the different height and period ranges. The results of comparison of this model alongwith other models are given in the following section.

5.2.10. GLERL Model

The GLERL spectral model (Eq.2.49) is based on many empirical constants, the determination of which is cumbersome. A few cases were computed and it is found that the determination of these constants by repetetive iteration takes much time in an IBM PC/XT computer. Moreover, the fitness of this model with the data is very poor in the few cases tested. Hence, a detailed analysis is not attempted.

5.3. COMPARISON OF AVERAGE SPECTRA WITH MODELS

The average spectra at H_{ss} intervals of 0.25 m and T_p intervals of 1 s also show characteristics similar to that observed with the individual spectra (Sec.5.2), in the comparison with models. The DI values obtained with these average spectra are lower than those obtained in the case of individual spectra. The values obtained for the different models are presented in Table 5.1. The TMA spectrum gives the lowest range of DI values and the variation is also the least, as shown by the standard deviation, for this model. This is followed by the PMK spectrum with the modified coefficient for exponent (here after will be referred as PMK

Table 5.1 DI Values of Spectral Models for H_{ss}-T_p Range Spectra

No[†]	UC	LC	PMK	SCOT	SCT-W	JENS	TMAJ	TMAJV	TMA	TMAV	WLP[*]
1	133.3	45.0	78.6	87.9	82.7	4718.5	3579.8	74.0	62.9	112.2	66.9
2	132.5	44.8	68.4	99.5	88.6	3965.4	3041.7	81.3	63.0	94.6	81.1
3	132.3	44.7	27.7	51.5	33.5	8718.0	6796.4	41.0	36.0	35.8	69.0
4	133.2	45.0	32.1	48.8	38.3	14183.5	11137.3	49.6	41.9	44.2	72.3
5	133.7	45.2	33.5	42.0	44.1	18081.5	14367.7	53.7	42.8	49.2	67.5
6	134.3	45.4	38.4	37.9	59.0	28476.8	23081.3	65.1	47.1	58.2	56.4
7	132.0	44.6	55.9	78.0	70.1	1443.4	1100.9	66.4	49.6	69.9	65.2
8	132.6	44.8	34.3	57.6	47.2	1672.7	1292.1	52.4	41.9	44.8	60.2
9	132.4	44.7	30.6	42.0	41.0	2870.5	2228.1	45.1	37.8	42.0	50.2
10	132.3	44.7	26.8	49.1	33.6	3401.7	2657.0	45.7	36.8	36.5	63.0
11	133.2	45.0	30.7	36.8	44.4	5756.9	4561.8	47.4	40.1	45.5	54.5
12	133.5	45.1	32.8	37.7	33.2	10474.2	8481.7	55.6	37.6	42.4	61.1
13	132.0	44.6	38.3	68.0	48.3	402.0	294.9	44.5	43.0	42.1	72.6
14	132.8	44.9	60.8	92.1	78.3	558.3	428.0	71.3	59.2	75.1	71.7
15	132.8	44.9	64.3	67.2	69.1	1233.1	950.5	71.7	54.4	73.2	62.1
16	132.6	44.8	40.5	47.9	47.8	926.2	707.6	50.9	36.4	47.8	43.7
17	132.5	44.8	22.7	44.2	30.5	1786.5	1385.9	38.7	33.4	32.3	51.3
18	132.8	44.9	34.5	39.0	41.6	2296.1	1810.5	49.1	43.6	53.3	46.2
19	132.7	44.8	27.4	33.6	39.1	3513.8	2833.2	49.2	35.4	38.7	44.1
20	132.0	44.6	68.4	91.2	83.3	226.5	178.8	76.7	61.2	90.9	74.0
21	131.9	44.6	50.0	55.8	46.0	259.7	185.4	51.9	52.6	61.0	31.6
22	136.7	46.2	76.4	79.8	81.0	421.8	322.6	81.1	67.9	129.8	50.4
23	132.4	44.7	32.5	54.5	42.0	356.8	263.2	51.5	42.6	43.2	38.3
24	132.4	44.7	25.6	40.8	33.6	473.0	354.6	37.6	29.1	32.7	32.0
25	131.9	44.6	50.5	36.7	25.1	669.9	506.6	29.0	22.4	21.3	27.0
26	132.6	44.8	29.2	32.2	43.2	1175.9 \	924.3	44.7	37.0	43.5	33.1
27	133.1	45.0	32.7	32.7	38.6	1378.9	1102.4	54.9	37.7	45.5	53.4
28	133.0	45.0	60.6	76.6	72.4	127.3	102.0	68.4	52.3	70.7	49.1
29	132.0	44.6	50.1	47.9	47.1	233.0	176.4	53.7	41.3	54.9	34.9
30	132.4	44.7	27.0	42.3	34.5	314.8	237.6	43.9	34.5	35.9	28.0
31	132.4	44.7	21.2	25.7	17.4	446.7	332.9	29.7	21.9	24.0	19.0
32	132.3	44.7	21.8	26.2	21.9	686.0	532.9	41.2	27.8	29.5	33.2
33	132.0	44.6	37.0	45.2	32.8	831.6	659.6	61.4	38.7	38.8	80.5
34	132.4	44.7	57.6	72.1	65.8	87.7	74.9	63.1	49.2	73.0	49.0
35	132.4	44.7	44.5	65.1	57.4	110.8	86.8	55.5	39.5	53.1	40.2
36	132.5	44.8	35.9	43.8	38.1	130.6	97.3	43.1	36.5	41.7	26.4
37	132.3	44.7	17.3	45.8	32.4	201.5	147.0	36.8	26.7	27.5	24.3
38	132.2	44.7	22.6	34.3	25.2	256.1	188.9	37.3	28.8	28.8	24.3
39	132.9	44.9	53.6	69.9	57.0	510.7	396.3	65.0	43.3	43.8	99.8
40	132.3	44.7	30.8	43.1	34.5	75.4	55.8	40.7	36.4	37.3	21.2
41	132.7	44.8	45.4	44.1	40.9	108.4	86.8	48.0	38.1	52.4	41.1
42	132.8	44.9	36.1	43.0	36.7	168.9	127.6	49.4	38.4	43.7	45.7
43	132.0	44.6	26.6	45.0	33.8	300.8	222.0	42.9	30.5	30.0	48.2
44	132.6	44.8	60.1	64.5	49.3	663.9	540.8	78.2	42.8	42.9	284.1
45	132.9	44.9	48.9	68.1	59.4	49.5	47.0	54.7	45.9	55.0	51.3
46	132.7	44.8	48.7	32.5	29.9	36.1	37.1	36.9	33.7	45.2	45.2
47	132.2	44.7	37.2	43.6	37.9	60.0	49.7	45.2	34.6	40.4	40.1
48	132.1	44.6	18.0	46.2	30.5	92.0	63.5	38.1	23.9	23.8	36.5
49	132.8	44.9	28.5	48.2	34.8	187.5	137.0	50.8	33.0	33.7	69.0
50	132.3	44.7	25.3	48.3	42.3	40.9	36.6	38.2	32.4	32.2	28.6
51	132.3	44.7	20.9	44.6	38.0	67.5	51.6	41.4	27.9	28.7	50.5
52	133.2	45.0	41.5	70.4	65.0	47.6	51.1	53.4	45.4	46.6	42.4
53	132.5	44.8	19.3	46.4	39.9	42.3	35.9	37.9	25.5	25.4	53.3
Max:	136.7	46.2	78.6	99.5	88.6	28476.8	23081.3	81.3	67.9	129.8	284.1
Min:	131.9	44.6	17.3	25.7	17.4	36.1	35.9	29.0	21.9	21.3	19.0
Avg:	132.7	44.8	38.5	52.1	46.0	2364.5	1870.7	51.6	40.0	48.4	54.0
S.D:	0.7	0.2	14.8	17.6	16.9	5056.0	4058.1	13.0	10.5	21.5	36.3

† For corresponding H_{ss} and T_p ranges see Table 6.1.
* For expansion of abbreviations, see overleaf.

Expansion of Abbreviations in Table 5.1

UC	:	Upper confidence limit spectrum
LC	:	Lower confidence limit spectrum
PMK	:	PMK spectral model
SCOT	:	Scott's spectral model
SCT-W	:	Scott - Weigel spectral model
JENS	:	Jensen's modification of the Kitaigorodskii et al. spectrum
TMAJ	:	TMA spectral model with average JONSWAP scale and shape parameters
TMAJV	:	TMA spectral model with Vincent's scale parameter and average JONSWAP shape parameters
TMA	:	TMA spectral model in original form
TMAV	:	TMA spectral model with Vincent's scale parameter
WLP	:	Wallops spectral model

spectrum). TMA spectral model with computed γ and α_V and the Wallops model show the widest range of DI values.

As seen in Sec.5.2 the TMA spectrum in its original form has the DI values lower than the DI_{LC} in maximum number of cases (75%). This is followed by the PMK model with 69% of cases having DI values lower than DI_{LC}. The Scott-Weigel in 62%, TMA with α_V in 58% and Scott and Wallops in 40% each of the cases tested have DI values lower than DI_{LC}. The TMA model with the average JONSWAP parameters and α_V as the scale parameter fits the data in a very few cases only. In 36% of the cases the DI values are lower than DI_{LC}.

The total energy estimated by the models is presented in Fig.5.11 (a-g). The energy is estimated close to the observed values by a few models. The Scott-Weigel model estimated the values ranging from 0-19% over the observed values. On an average the values are overestimated by 2% only. This model is followed by the Scott model which predicted the values in a range varying from 29-156% of the observed values with the average 4% higher. The TMA model with average JONSWAP shape parameters and α_V as scale parameter estimated the values in the range 84-111% with the average 4% less than the observed. The PMK model estimated the values in the range 84-101% of the observed with average underestimated by about 5%. The original TMA model under-
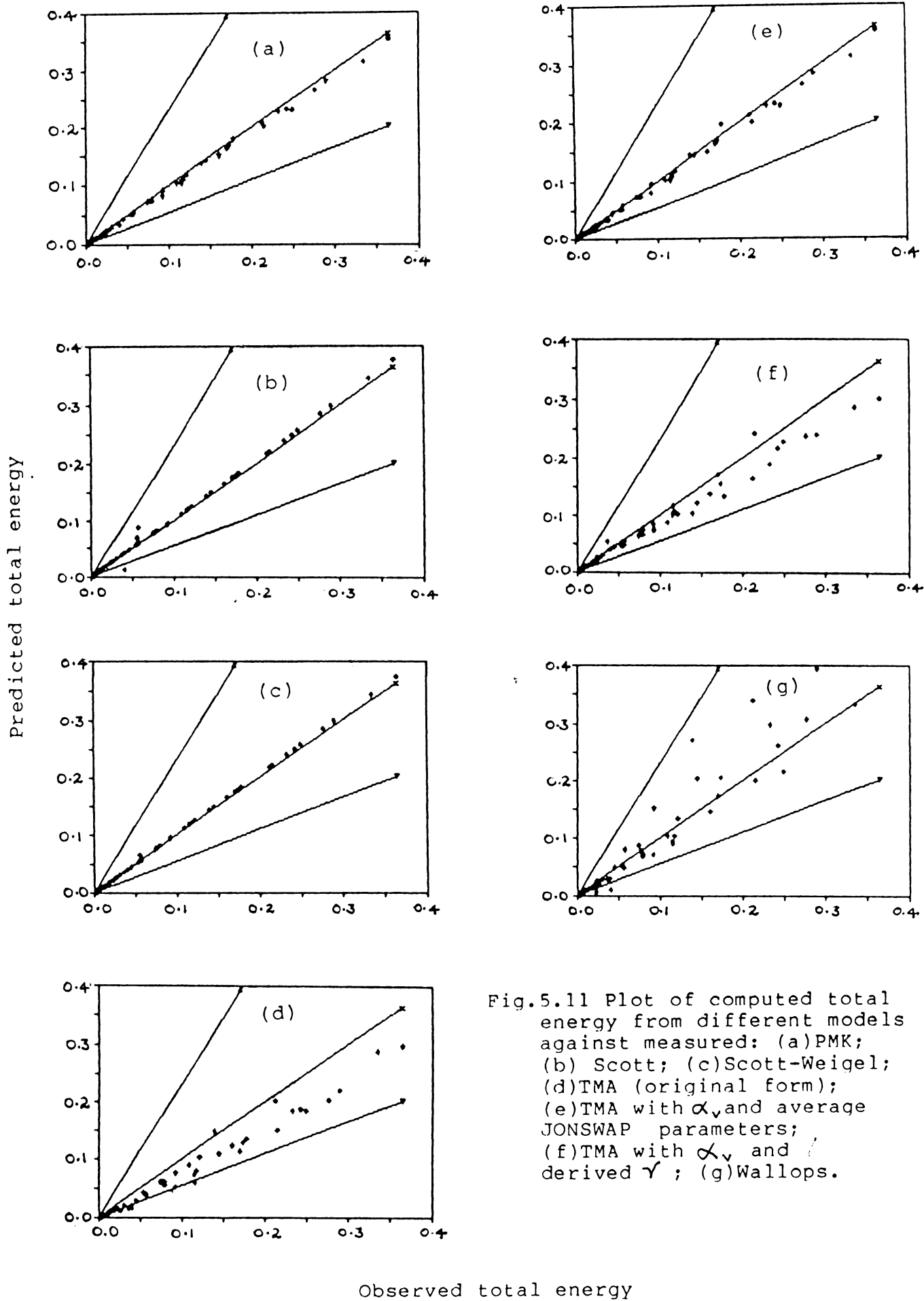
Fig.5.11 Plot of computed total
energy from different models
against measured: (a)PMK;
(b) Scott; (c)Scott-Weigel;
(d)TMA (original form);
(e)TMA with α_v and average
JONSWAP parameters;
(f)TMA with α_v and
derived γ ; (g)Wallops.

Predicted total energy

Observed total energy

estimated the energy by about 31%. This model with the scale factor α_v estimated the values in a range varying from 75-148% of the observed with the average about 8% lower than the observed. The energy predicted by the Wallops model show wide variability (26-380%). The values are found to be overestimated at high energy conditions. The Jensen's form of the Kitaigorodskii et al. spectrum and the TMA model with average JONSWAP parameters highly overestimated the energy in most of the cases.

The peak energy densities predicted by the different models are plotted against the observed values in Figs.5.12 (a-g). The TMA model is found to estimate the values correctly. The Wallops model also simulated the peak well, but with scatter. The values are found to be slightly overestimated in those cases with lower peak energy densities and underestimated in the high peak energy density cases. This model predicted the values in the range 37-265% of the measured values with the average overestimated by about 18%. The PMK model underestimated the values, at 47-195% of the measured, with the average about 14% lower than the measured. All the other models overestimated the peak energy densities by about 40% or more.

129
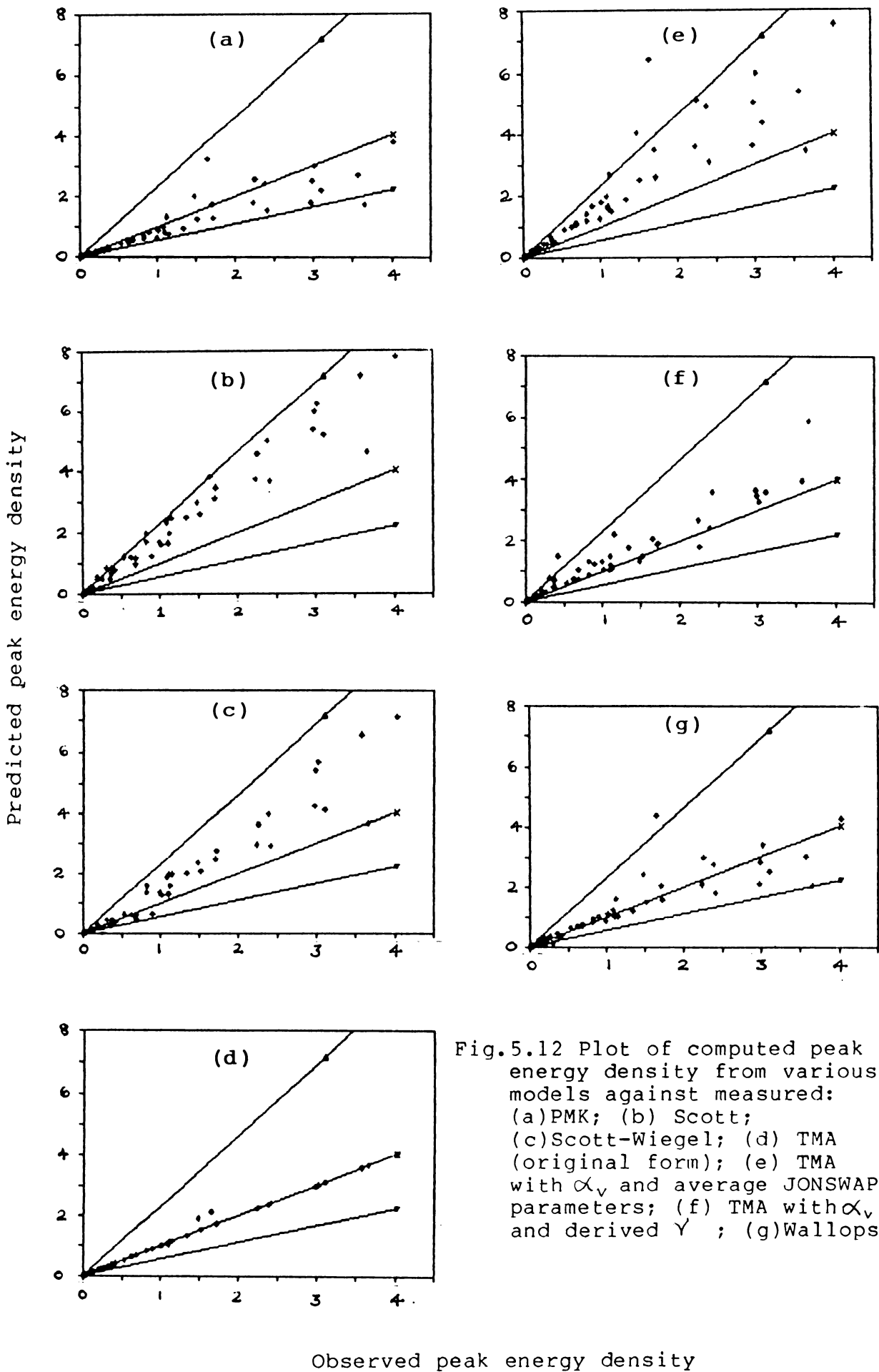
Fig.5.12 Plot of computed peak
energy density from various
models against measured:
(a)PMK; (b) Scott;
(c)Scott-Wiegel; (d) TMA
(original form); (e) TMA
with α_v and average JONSWAP
parameters; (f) TMA with α_v
and derived γ ; (g)Wallops.

Predicted peak energy density

Observed peak energy density

5.4. A DISCUSSION ON THE SCALE FACTOR

In order to define the spectrum, different models adopt different scale parameters. In Kitaigorodskii et al. and Jensen's forms the Phillip's constant (α) is used as the scale factor. The TMA model assumes the scale factor of the JONSWAP type (α_J) obtained by fitting the measured spectrum to the P-M spectrum in the frequency range $1.35f_m < f < 2f_m$, through the equation,

$$\alpha_J = (2\pi)^4 f^5 g^{-2} \exp [(5/4)(f_m/f)^4]S(f)df \quad \dots\dots(5.4)$$

Vincent (1984) suggested a modification to this relation and put forward a relation as a function of the total energy and the peak frequency. Wallops spectrum defines its own scale factor β as another function of the total energy and the peak frequency. The Scott and Scott-Weigel spectral forms use the total energy scaled by another constant as the scale factor for their empirical models.

On an examination of the relation between the different scale factors mentioned above, the parameter used in TMA (α_J) and the modification suggested by Vincent (α_V) are found to be related to each other (Fig.5.13). They may be represented by the regression equation

$$\alpha_V = 1.023 \ \alpha_J \qquad\qquad \dots\dots(5.5)$$
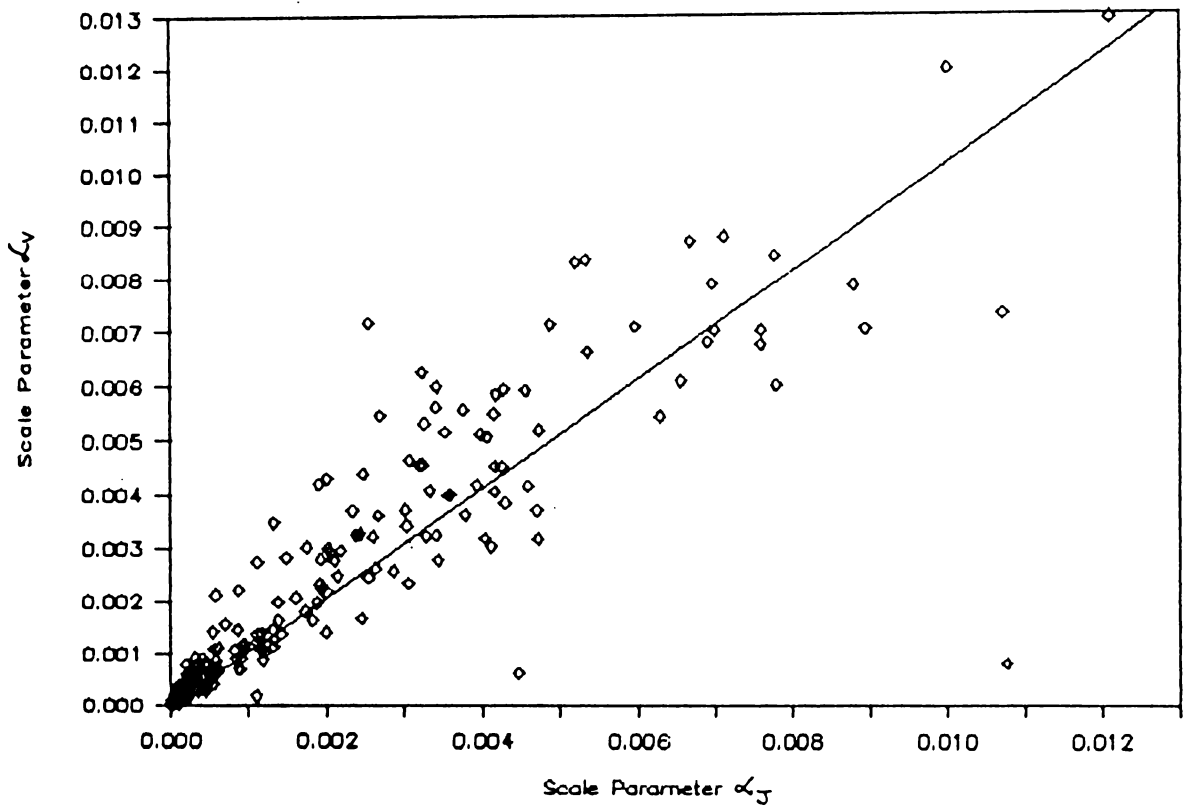
Fig.5.13 Relation between α_J and α_V.

The α_V values are found to be slightly higher. The deviation is more at the lower energy cases and less at the higher energy conditions. In the lower energy cases the ratio of α_V/α_J range from 1 to 4 and in the higher energy cases it is very close to 1. As indicated above, α_J is derived from the spectral densities in the high frequency range and $\dot{\alpha}_V$ is derived from the total energy of the measured spectrum. When the values are comparable at the high energy conditions, higher values of α_V at low energy conditions can be possible due to two reasons - energy in the low frequency range of the spectrum being not proportional to that in the high frequency range, based on which α_J is computed, and/or the peak frequency being higher in the lower energy conditions. In the present data lower as well as higher peak frequencies are present in both the conditions, though the number of occurrences are few. Hence, the higher values of $\dot{\alpha}_V$ observed at lower energy conditions may be due to the first reason. But, it appears to be proportional at the high energy conditions. The shape parameter β of the Wallops spectrum is not related to α_J or α_V. Further, these parameters are not found dependent on other spectral parameters.

5.5. CONCLUSIONS

The models which depend entirely on the peak frequency do not show satisfactory representation of the data. Thus, the Jensen's modification to the Kitaigorodskii et al. model which is entirely a function of frequency, fit in a very few cases only and the total energy and peak energy density are highly overestimated by this model. On the other hand, the models with total energy as one of the defining parameters exhibit better performance. Even the deep water Scott model and its modification by Weigel give better representation than the Jensen's model. However, the dispersion relationship proposed by Kitaigorodskii et al. is found to be a stepping stone to derive shallow water spectral models. Some of the models derived based on this relation give satisfactory results.

The TMA model gives better results and follow the observed spectra in a large number of cases. This model is particularly useful for high energy conditions where H_s is of the order of 1.4 m and above. On the average, the total energy is overestimated, especially in the low energy cases. However, the peak energy density is estimated correctly by this model. This model is defined with 5 free parameters, and the derivation of these parameters requires the full spectrum as input. But, in most practical cases, it is not

132

possible to define the full spectrum apriori to calibrate this model. Hence, a model with lesser number of free parameters would be useful. If the average JONSWAP scale and shape parameters along with Phillip's constant are used in the TMA model, the number of free parameters can be reduced to 1. But, in that case the fit is very poor. The total energy as well as the peak energy density are over-estimated. The application of the coefficient suggested by Vincent (1984) improves the performance of this form, but not to a level satisfactory for applications. This modifi-cation makes the total energy to be predicted correct to 99%, but the peak energy density is overestimated. This form is capable of simulating the shallow water spectra correctly for low energy and low peak period cases. Further, if the peak enhancement factor is made free, ie., to be estimated from the measured spectrum, its application can be extended to all T_p ranges for the low energy conditions. The total energy is slightly underestimated and the peak energy density is overestimated by this form, especially in the high energy cases. The Wallops spectral model finds its application in the cases with H_s > 0.75 m with $T_p \leq 10$ s, to simulate the shallow water wave spectra. At higher T_p ranges ($T_p \geq 10$ s), the total energy is over-estimated and the peak energy density is underestimated by this model. Hence, care should be taken while applying this

133

model to the cases with large peak periods, especially with high energy. The Scott model and its modification by Weigel estimate the total energy comparable to the observed. However, the peak energy density is overestimated by these models, especially at high energy cases. The modification by Weigel improves the model slightly, but the coefficients A and B need further modification to simulate the shallow water spectra correctly for all conditions.

A new shallow water spectral model derived from the P-M spectrum with the application of the dispersion relationship proposed by Kitaigorodskii et al. (called PMK spectrum) presents a better fit to the data. Though this comes second to the TMA model (which has 5 free parameters), the former requires only the 2 commonly available spectral parameters (m_0 and f_m) to define the spectrum. Hence, when the full spectrum is not available to calibrate the 5-parameter TMA model, the 2-parameter PMK or Scott-Weigel spectral models can be used for practical applications.

CHAPTER 6

WAVE HEIGHT AND PERIOD DISTRIBUTION MODELS

The probability distribution of wave heights, periods and their joint distribution are computed from the data and their characteristics are discussed. The observed distributions are compared with different theoretical/ empirical models and the ranges of applicability of these models are examined.

6.1. DISTRIBUTION OF ZERO-CROSSING WAVE HEIGHTS

The distributions of individual zero-crossing wave heights are computed for each record at height intervals of 0.2 m, typical examples of which are presented in Fig.6.1. The observed distributions exhibit multiple modes in some of the cases, especially in the high energy conditions. This may be due to the finite length of records considered for the analysis. If samples consisting of sufficiently large number of waves are considered, the insignificant modes may be got eliminated. The short-term height distributions derived from the data are compared with different theoretical/empirical models. The records corresponding to 10 ranges of H_{sw} at an interval of 0.25 m and 8 ranges of T_p at an interval of 1 s are combined and the resultant height distributions are also computed. The distributions thus obtained are also compared with the models and the results are presented in section 6.1.2.
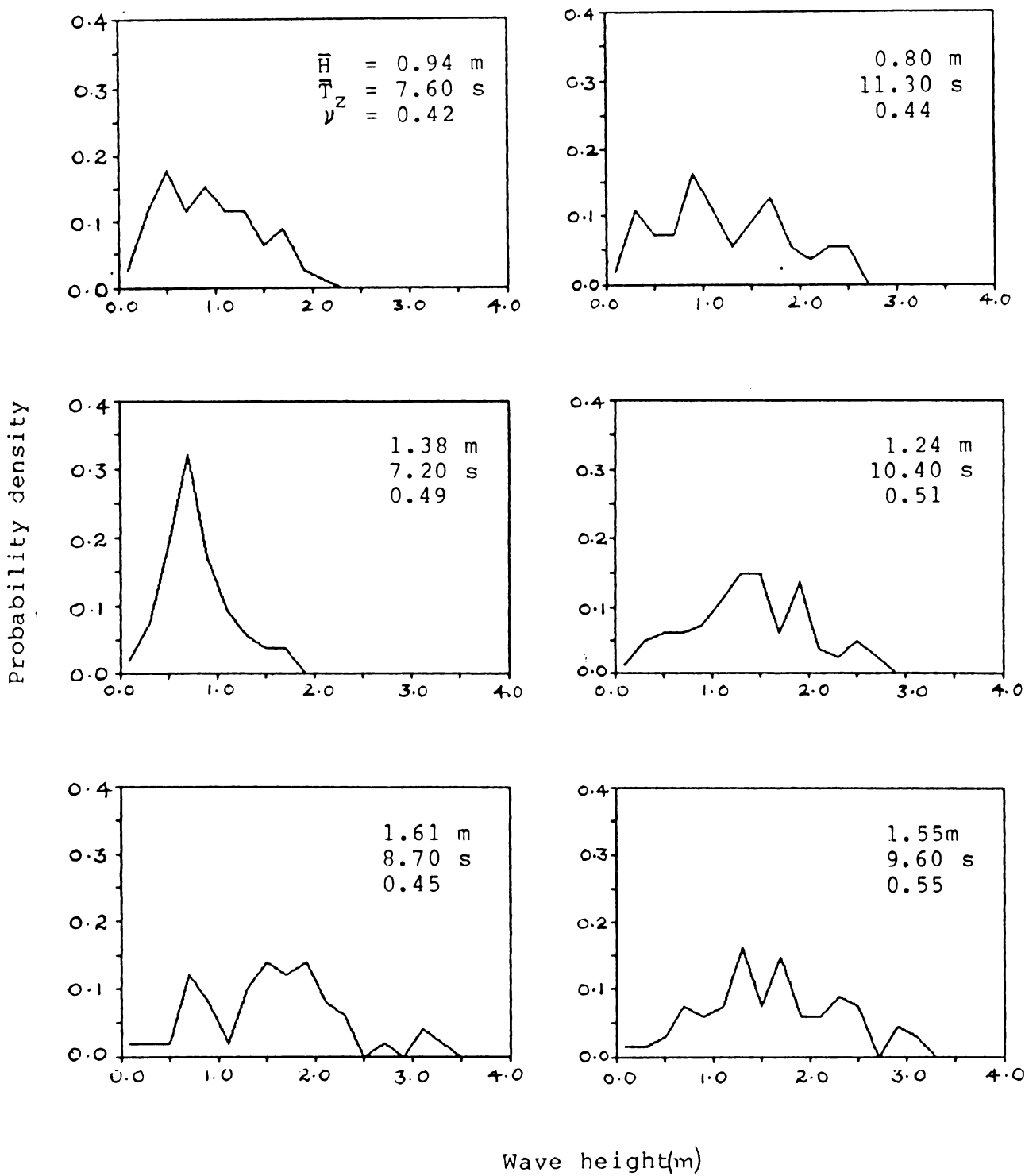
Fig.6.1 Typical examples of observed height distribution.

6.1.1 Comparison of Short-Term Distributions with Models

The distribution of zero-crossing wave heights computed from each record are compared with the different theoretical/empirical models in this section. The usual practice is to make visual comparisons to examine the fit of a theory with the data. Typical examples of the distributions predicted by the different models are presented in Fig.6.2. A visual comparison is very difficult when the number of records and models considered are large, as in the present case. An alternative is to apply statistical tests of goodness of fit. A valid test that can be applied here is the χ^2 goodness of fit test. Hence, the fitness of each model to the data is evaluated using the χ^2 test at 0.05 level of significance. The cases where the different models fit the data are presented in Appendix-A. In order to apply this test, the data has to be grouped into bins of frequencies not less than 5. Hence, the tail of the distribution has to be truncated by adding it to the nearest class to make the frequency $\geq$ 5. In some cases, like the very low height conditions, this may give unrealistic fits with very few number of classes (like 2 or even 1 sometimes). In such cases, visual comparison is made to evaluate the fitness. In addition to the application of the χ^2 test, the cumulative probability densities of the statistical height parameters, $\bar{H}$, H_{sw} and H_{max} predicted by

136
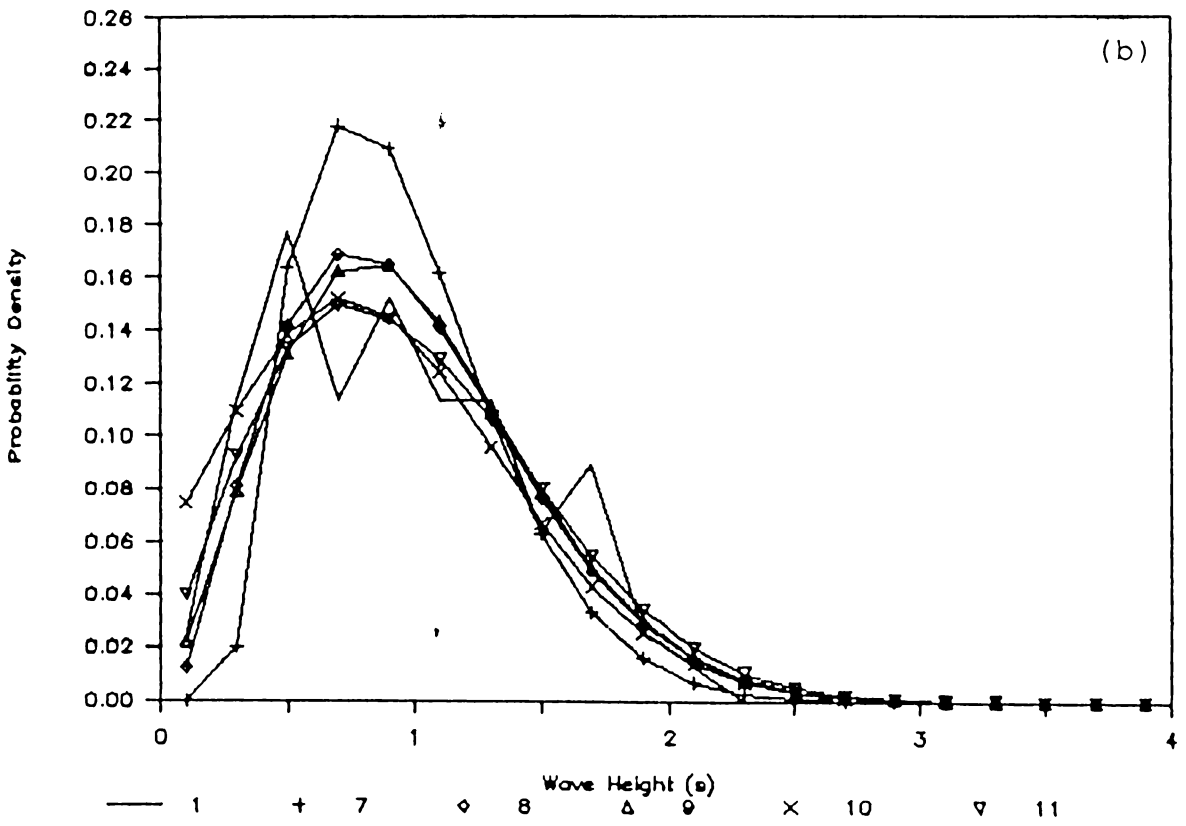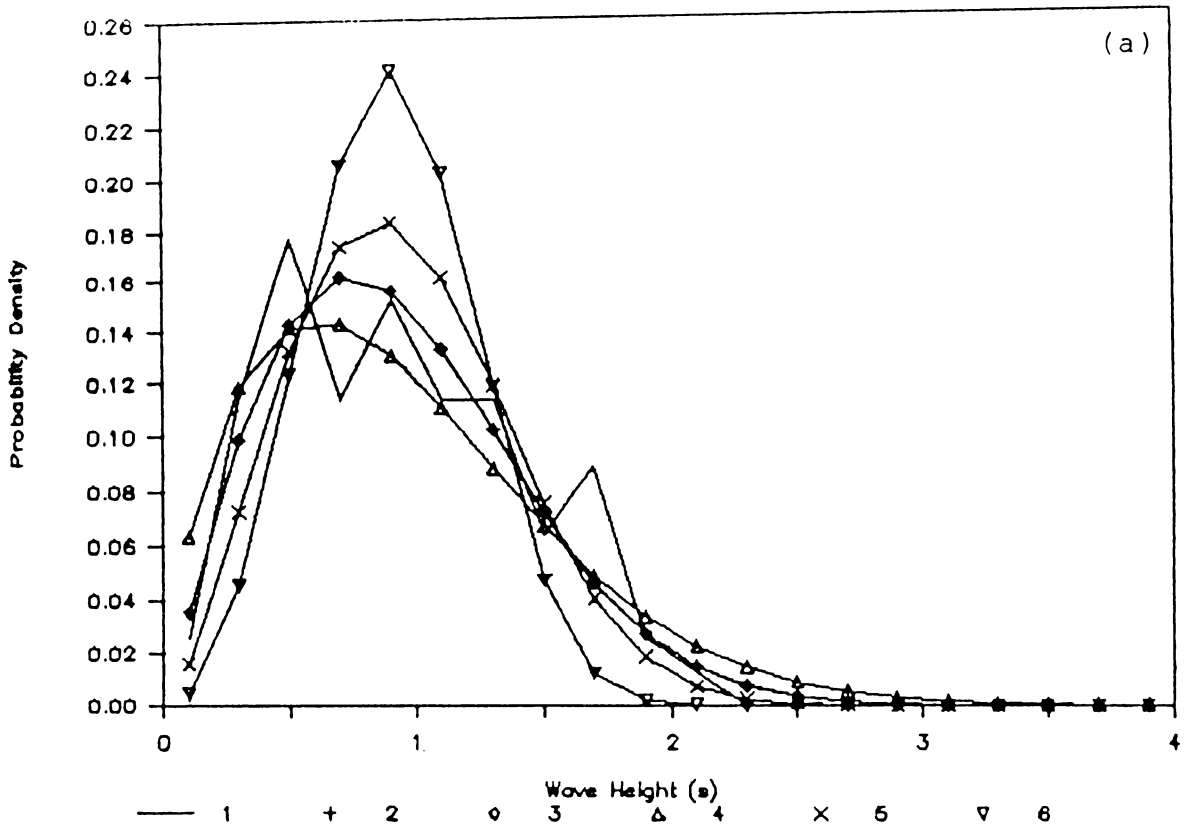
1: Observed, 2: Rayleigh, 3: Goda's, 4: Weibull,
5: Gluhovskii's, 6: Ibrageemov's, 7: Tayfun's,
8: Longuet-Higgins'(1975), 9: Longuet-Higgins'(1983),
10: CNEXO and 11: CNEXO (modified) distributions.

Fig.6.2 Typical examples of height distribution
predicted by different models corres-
ponding to an observed distribution.

the models are also compared with the corresponding values obtained from the data. The results are discussed in sub-sections 6.1.1.1 through 6.1.1.8.

6.1.1.1. Rayleigh distribution

The Rayleigh model for the distribution.of individual wave heights (Eq.2.64) is found to fit the observed data in 277 cases constituting 87.7% of the data set. The fit is found to be equally good during the rough as well as the fair seasons. During the rough season this model is found to fit in 86.7% of the cases and during the fair season fit is obtained in 88.6% of the cases. Also, the fit is found to be independant of H_{sw} and steepness (corresponding to the significant wave height and average zero-crossing period). Fit is obtained at all H_{sw} and steepness ranges. However, it may be noted that values of steepness above 0.4 is very few in the data and the model is found not to fit in those cases.

The cumulative probability densities of $\bar{H}$, H_{sw} and H_{max} predicted by this model are presented against the observed values in Fig.6.3 (a-c). The probability densities of $\bar{H}$ are overestimated in most of the cases and the predicted values are almost constant with lesser variations. On the average, the densities are higher by about 5%. The probability

densities of H_{sw} and H_{max} are closer to the observed, but are slightly underestimated, the rate of which is about 2%, on the average.

The basic assumption in applying the Rayleigh distribution to wave heights is the narrow bandedness of the spectrum. In the present case the spectral width parameters ranged widely indicating broad band spectra in a large number of cases. and the Rayleigh model is found to fit in the entire range. Applicability of Rayleigh distribution beyond the narrow band assumption has been observed by many other researchers (Longuet-Higgins, 1975; Chakraborty and Snider, 1974; Dattatri et al., 1979).

6.1.1.2. Goda's model

The truncated Rayleigh distribution suggested by Goda (Eq.2.69) is found to fit in 227 cases, which constitutes 71.8%. This model is found to have better representation of the rough weather data. During the rough season fit is obtained in 78.7% and during the fair season it fits in 65.7% of the cases. This model also is found to be independent of the H_{sw}, T_p, spectral width and steepness values like the Rayleigh distribution.

The probability density of $\bar{H}$ is overestimated by this model also (Fig.6.4a). The deviations are larger than that

observed with Rayleigh. The average rate of overestimation is about 13%. As the statistical height parameter becomes larger, the ratio of predicted to the observed probability becomes lower and lower. When the $P(\bar{\bar{H}})$ values are highly overestimated, the values of $P(H_{sw})$ are closer to the observed (Fig.6.4b) and are higher by about 2% only. In the case of $P(H_{max})$ the values are very much comparable to the observed values (Fig.6.4c). In fact, they are underestimated slightly, but the rate is much less than 1% only.

This model is a modification of the Rayleigh form to incorporate the breaking and broken components of waves present in the shallow waters. Thus, this model is expected to have a better representation of the shallow water height distribution than the Rayleigh model. Since this is not achieved, the applicability of the 'breaker index' (this determines the shape of the distribution) to different environmental conditions has to be examined. As this model fits more of the rough weather data than the fair weather ones, it appears that the breaker index with the recommended constants (Eqs.2.71 and 2.72) wrongly estimates some of the non-breaking cases as breaking. Hence, modification of these constants and validation of the breaker index is necessary for applications at different locations.

139
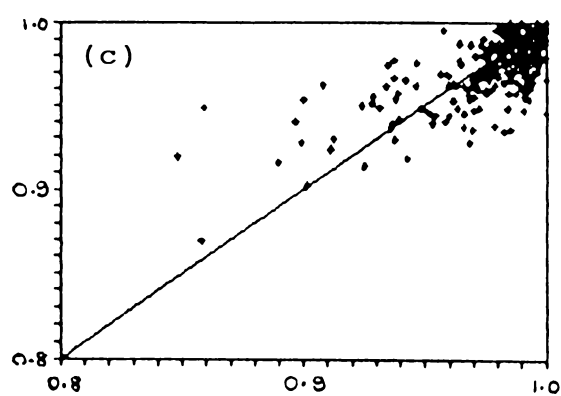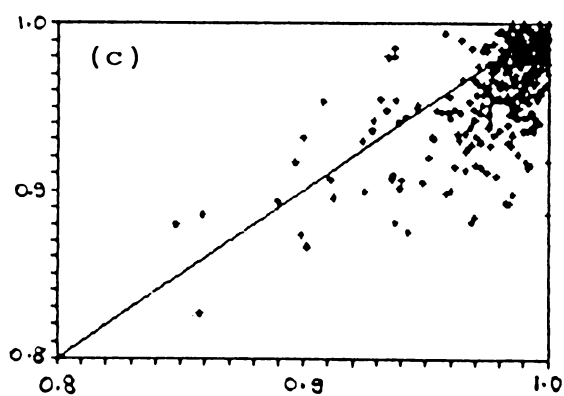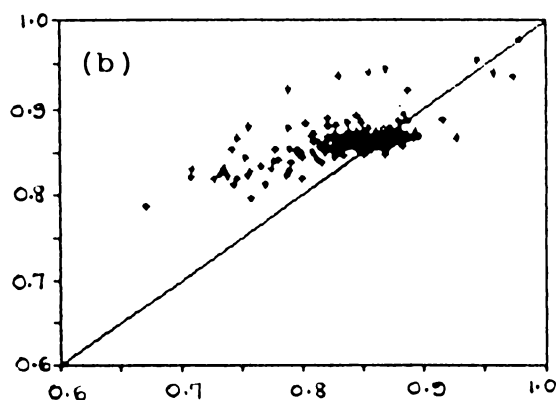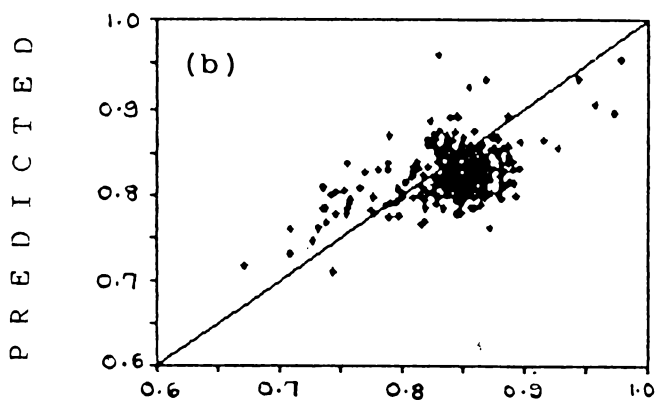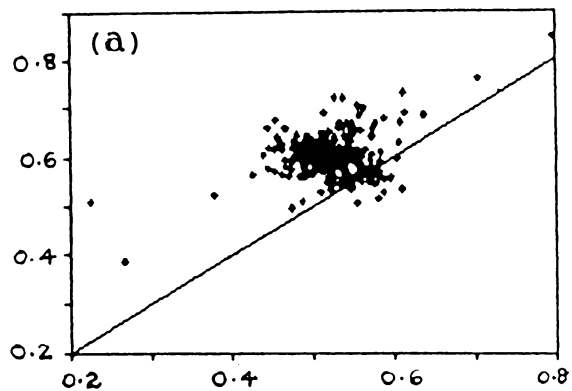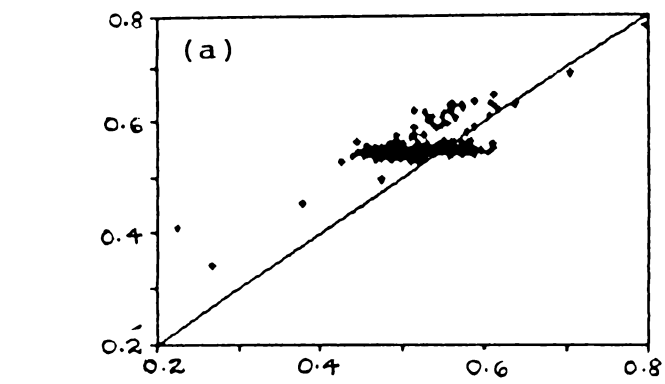
Fig.6.3 Plot of cumulative probability densities of height distribution predicted by Rayleigh model against observed:(a) $\bar{H}$; (b) H_{sw} ; (c) H_{max}.

Fig.6.4 Plot of cumulative probability densities of height distribution predicted by Goda's model against observed:(a) $\bar{H}$; (b) H_{sw} ; (c) H_{max}.

6.1.1.3. Weibull distribution

The Weibull disribution (Eq.2.73) is found to follow the data in 252 cases (77.7%). The fit is found to be better during the fair season with 86.7% of the data following this model. During the rough season it fits in 72% of the cases. Fit is observed in all the ranges of H_{sw}, T_p, steepness and spectral width ranges present in the data.

The probability densities of $\bar{H}$ are slightly over-estimated in this case also (Fig.6.5a). On the average, $P(\bar{H})$ is higher than the observed by about 3%. The predicted probabilities of H_{sw} and H_{max} are lower than the observed in most of the cases (Fig.6.5b-c). The average rate of under-estimation is about 4% for $P(H_{sw})$ and 3% for $P(H_{max})$.

Forristall (1978) obtained good fit with this model for the data from storms in the Gulf of Mexico. The present data is found to deviate from this model more than the Rayleigh distribution. When Rayleigh is a function of 0th moment of the spectrum, Weibull is a function of the higher moments. That is, the frequency (or period) has more influence on this model compared to Rayleigh. The deviation of the present data set from this model may be an indication that the influence of period is less on the distribution of shallow water waves, where the effect of refraction, shoaling, bottom friction, etc. are more due to the gently sloping bottom.

6.1.1.4. Gluhovskii's model

The Gluhovskii function (Eq.2.65) is found to simulate the observed height distribution in 296 cases which constitute to 93.7% the total observations. The fit is equally good for both the seasons with a fit in 95.3% of the cases during the rough season and 92.2% during the fair season. Fit to the data is obtained with this model in all the observed ranges of H_{sw}, T_p, steepness and spectral width in the data.

When predicted $P(H_{sw})$ and $P(H_{max})$ values are very close to the observed, $P(\bar{H})$ values are slightly overestimated by this model also (Fig.6.6a-c). On the average $P(\bar{H})$ values are higher by about 2%. The ratio of predicted $P(H_{sw})$ to the observed is 1, on the average, the deviation being less than 0.1%. $P(H_{max})$ values predicted are lower by about 1%, on the average.

Gluhovskii distribution is reported to follow the observed height distributions closely for other parts of this coast (Saji, 1987). Unlike the other models, this model is depth dependent. From the close fit observed in the maximum number of cases, it may be inferred that the distribution of wave heights in the shallow water is depth dependent.

141

P R E D I C T E D
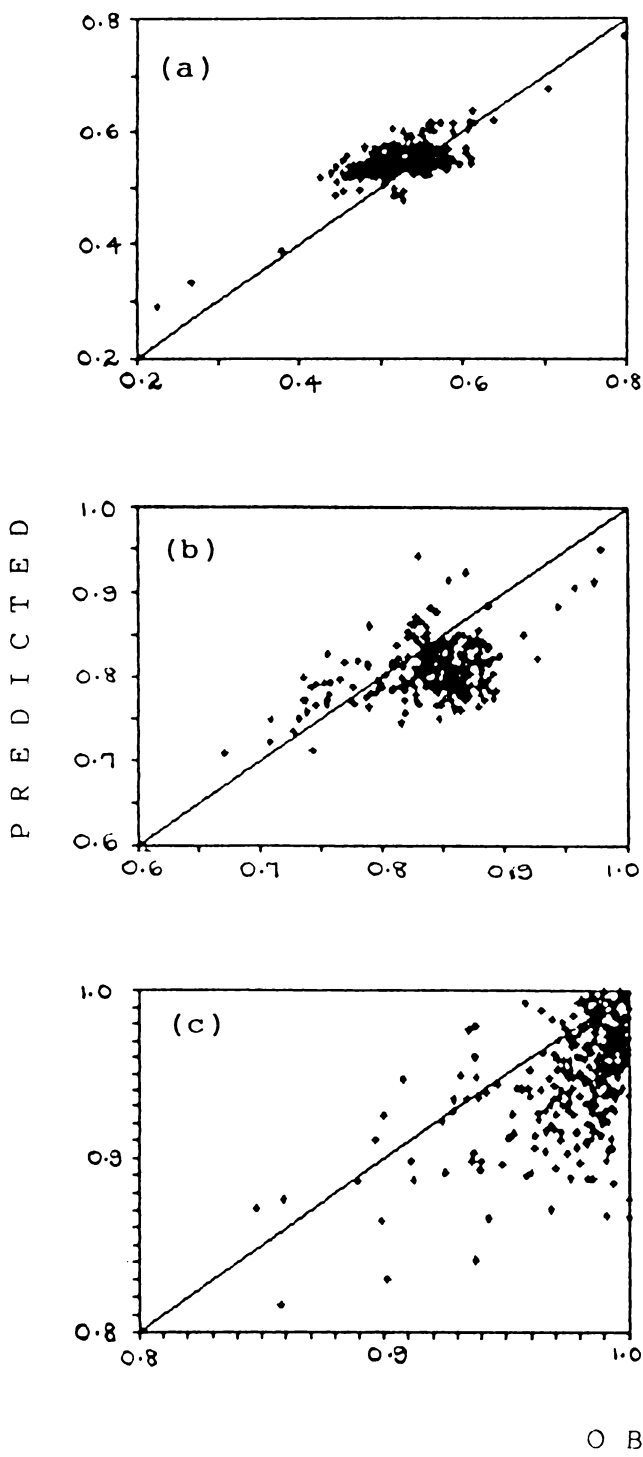
O B S E R V E D

Fig.6.5 Plot of cumulative probability densities of height distribution predicted by Weibull model against observed:(a) $\bar{H}$; (b) H_{sw} ; (c) H_{max}.
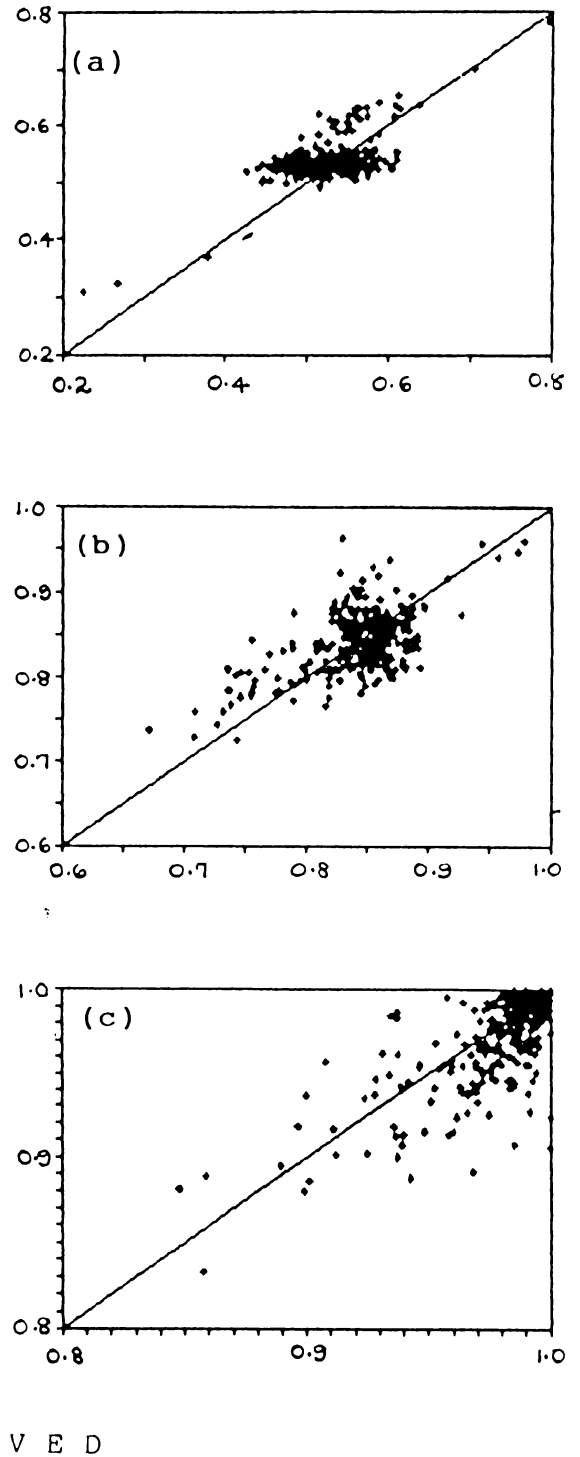
Fig.6.6 Plot of cumulative probability densities of height distribution predicted by Gluhovskii's model against observed : (a) $\bar{H}$;(b) H_{sw} ;(c) H_{max}.

6.1.1.5. Ibrageemov's model

This model (Eq.2.67) is found to have very poor representation of the observed height distribution. Fit is obtained only in 65 cases which constitute to 20.6% of the data set. The representation by this model is nearly the same during both the seasons. Fit is obtained in 22.7% and 18.7% of the cases during the rough and fair seasons, respectively. Although the applicability of this model is poor, the cases where it fits the data fall in all ranges of H_{sw}, T_z, steepness and spectral width, indicating that this model is not dependant on these parameteres, eventhough wave period is one of parameters used in defining this model.

The probability densities of $\bar{H}$, H_{sw}, and H_{max} predicted by this model are plotted against the observed values in Fig.6.7 (a-c). The probabilities of $\bar{H}$, H_{sw} and H_{max} are overestimated in majority of the cases. $P(\bar{H})$ values are higher, on the average, by about 4% and $P(H_{sw})$ values are higher by about 11%. The predicted $P(H_{max})$ are at the maximum of the cumulative probability curve in most of the cases.

This model is a modification of the Gluhovskii's by incorporating period as an additional parameter. However, it fails to simulate the observed height distribution in most of the cases, where the Gluhovskii's function estimates

142

the values more closely with the observed. This indicates again that the period is not a controlling parameter for the distribution of wave heights in shallow waters, when compared to the depth. Reports of validation of this model elsewhere is not seen in the literature.

6.1.1.6. Tayfun's model

The Tayfun's function for wave heights (Eq.2.77) is also found to be very poor in simulating the shallow water distribution of individual wave heights. With the present data it fits only in 57 cases (18%). However, this model is more suitable for the rough sea conditions. The cases where this model fits the data are the cases of the rough weather conditions. During May-September this model is found to follow the data in 36.7% of the cases and the fit is found to be better for the higher ranges of H_{sw}, steepness and spectral width and for the lower ranges of T_z. That is, this model may be applicable to the conditions of high, steep waves, such as that occur during the peak monsoon.

The probability densities of $\bar{H}$, H_{sw} and H_{max} predicted by this model is presented in Fig.6.8 (a-c). The probabilities of $\bar{H}$ are estimated in a large range, most of which are lower than the observed. It does not show any correlation with the observed, except in a few cases.

143

P R E D I C T E D
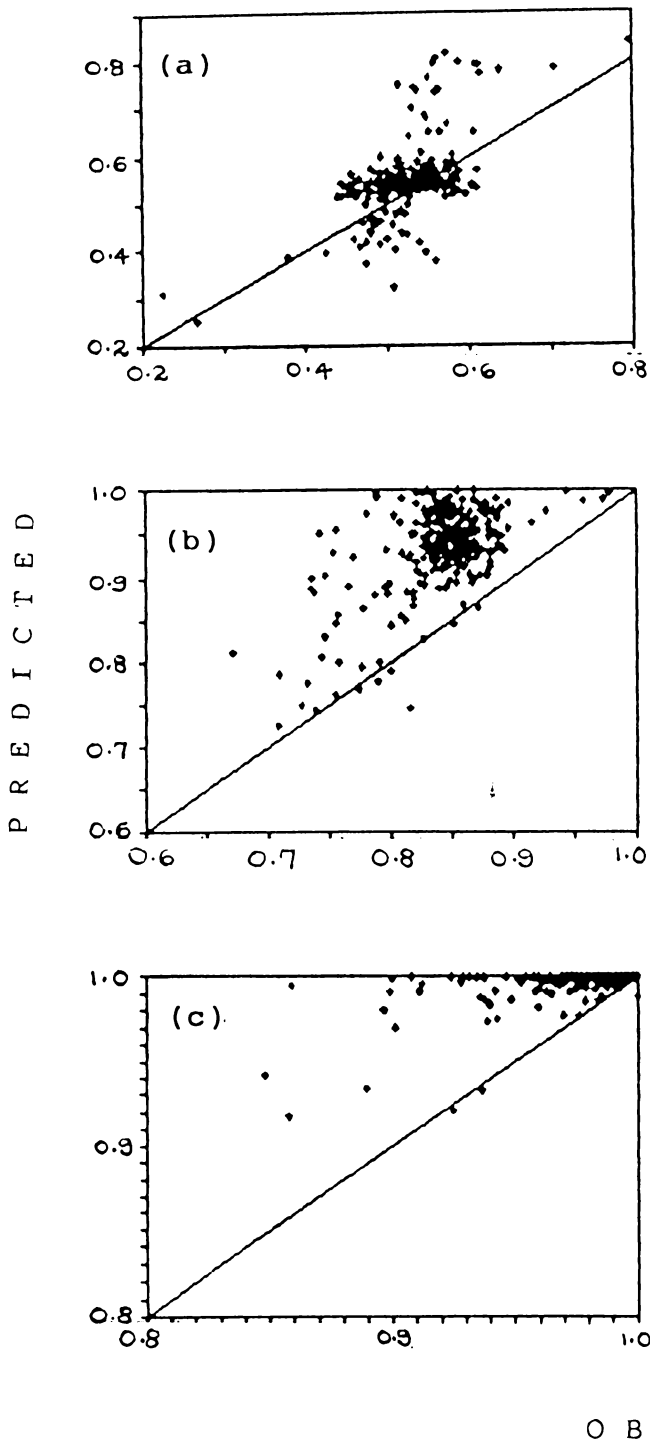
O B S E R V E D

Fig.6.7 Plot of cumulative probability densities of height distribution predicted by Ibrageemov's model against observed : (a) $\bar{H}$;(b) H_{sw} ;(c) H_{max}.
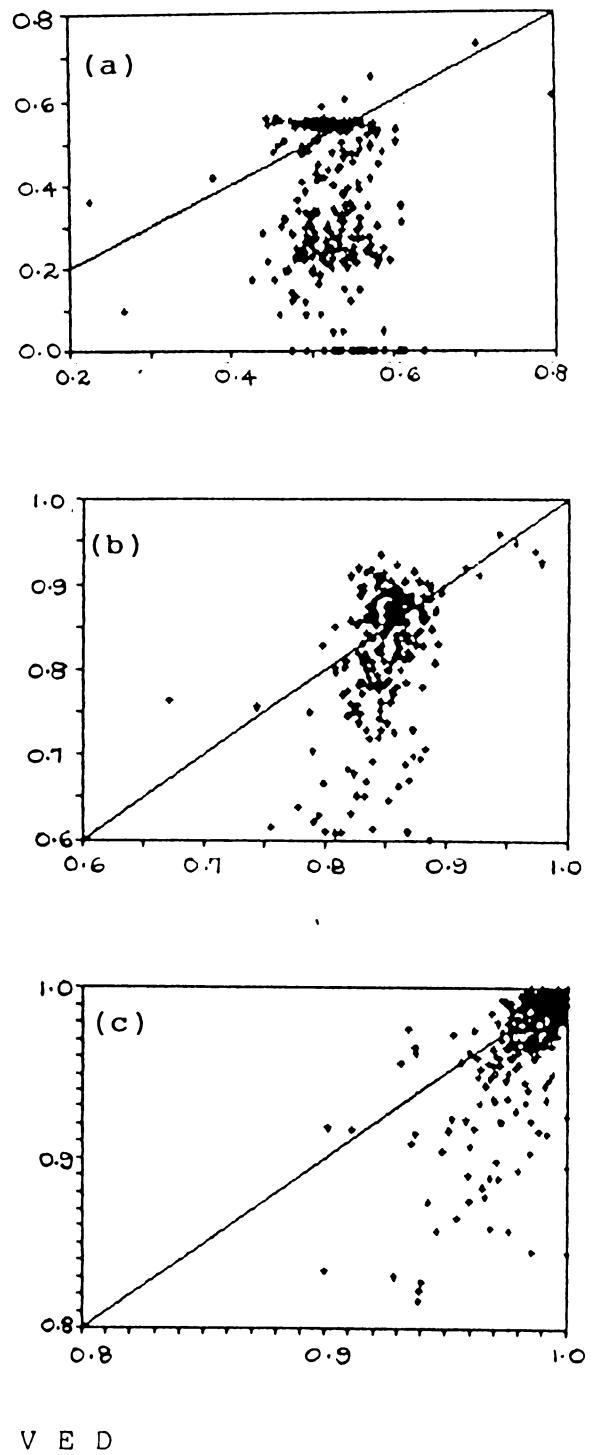
Fig.6.8 Plot of cumulative probability densities of height distribution predicted by Tayfun's model against observed:(a) $\bar{H}$; (b) H_{sw} ; (c) H_{max}.

$P(H_{sw})$ and $P(H_{max})$ estimated by this model are closer to the observed in most of the cases. But the range is wider and a few values are very low compared to the observed. On the average, the values are lower by about 10% in the case of $P(H_{sw})$ and 3% in the case of $P(H_{max})$.

The Tayfun's distribution function is developed with the observation that the crests and troughs of the ocean waves do not occur at the same time and the envelope of the waves will change during the half wave period, if the spectrum is narrow (Tayfun, 1983b). If the wave is high, it is likely that when the crest is near an extreme of the envelope the associated trough will have a smaller amplitude, so that the wave height will be less than twice the amplitude (Forristall, 1984). In such cases, it is hypothesised that it is the wave envelope that follow the Rayleigh distribution rather than the waves themselves. In the present case this model is found to simulate the observed distributions corresponding to the rough weather conditions. During the rough season the waves observed here are of higher energy associated with comparatively lower periods and spectral widths (Ch.3 & 4). Thus the hypothesis of wave envelope following the Rayleigh distribution (rather than the wave heights) appears to be true when the waves are high and the spectrum is narrow. However, the failure of this model in the cases of spectrum with lower energy and larger width,

where the wave heights are found to follow the Rayleigh distribution, indicates that the envelope approach is not valid to such cases. Hence, it is suggested that this model my be used to simulate the wave height distribution in shallow waters during high wave activity or storm conditions.

6.1.1.7. Longuest-Higgins' models

The distribution of heights and periods suggested by Longuet-Higgins in 1957 was recapitulated in 1975. By integrating the joint probability density function given in Eq.(2.90), the function for the distribution of heights is obtained as Rayleighean. This was modified by him later (Eq.2.91) to incorporate the effects of non-linearity and finite band width (Longuet-Higgins, 1980 and 1983). The probability density function of heights obtained from the above 2 models (Longuet-Higgins, 1975 and 1983), by integrating the joint probability functions with respect to period, are compared with the observed height distributions. An examination of the performance of these models may throw more light into the quantum of the effects of non-linearities on the distribution of wave heights in the shallow water conditions.

The first model (Longuet-Higgins, 1975) fit in 288 cases which constitute to 91.1%. The modified form

(Longuet-Higgins, 1983) fits almost equally well, but less by a few number of cases. It fits in 280 cases which is 88.6%. During the rough as well as the fair seasons both the models fit nearly equally, the modified form showing slightly better fit during the rough season. During the rough season both the forms fit in 90.7% of the cases each and during the fair season the first form fits in 91.6% and the modified form fits in 86.7%. In all the ranges of H_{sw}, T_p, steepness and spectral width present in the data, both the forms are found to fit almost equally.

The probability densities of $\bar{H}$ predicted by both the models are found to be closer to the observed values, but are slightly underestimated by the first form and overestimated by the modified form (Fig.6.9a-b). On the average, when $P(\bar{H})$ values are underestimated by about 6% by the first form, it is overestimated by about 5% by the modified form. The values of $P(H_{sw})$ are also estimated in a similar manner by both the forms, the modified form being in better agreement with the observed (Fig.6.9c-d). On the average, the first form underestimates the values by about 5% and the values predicted by the modified form deviates by less than 0.1% only. Also, the scatter is minimum in the case of the modified form. The values of $P(H_{max})$ are underestimated by both the forms, but the deviations are

146

less with the modified form (Fig.6.9e-f). The predicted values, on the average, are lower by 13% in the case of the first and about 1% in the case of the modified forms. That is, the probability density of the lower ranges of heights are simulated equally correctly by both the forms and heights of the order of H_{sw} and more, where the effects of non-linearities are more pronounced, are simulated more correctly by the modified form. As the probability densities of the larger height ranges are of importance in practical applications, the modified form of the distribution function may be more suitable.

6.1.1.8. CNEXO models

Intergrating the joint probability distribution function for heights and periods suggested by the group of CNEXO (Eq.2.93) with respect to period, the distribution function for heights is obtained. The probability density function for individual wave heights thus derived is nearly the Rayleighean when spectral width is not large. Goda (1978) observed that the rank correlation $r(H,T)$ would be a better parameter rather than ϵ_w in this model. The relation is thus modified by substituting $r(H,T)$ in place of ϵ_w. The probability distributions of heights computed using these functions (original and modified forms) are compared with the observed height distributions.

147
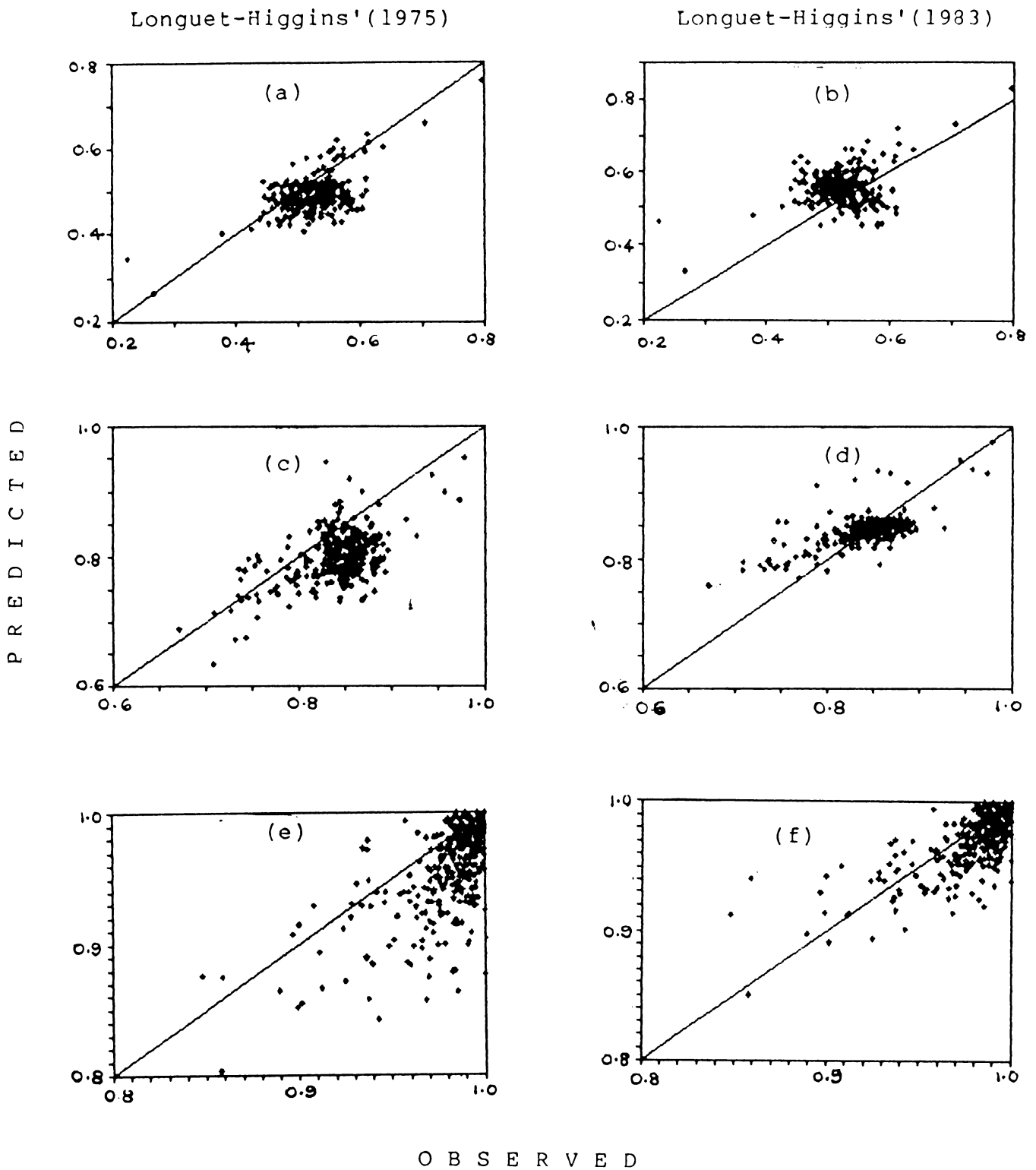
Fig.6.9 Plot of cumulative probability densities of height
distribution predicted by Longuet-Higgins 1975 and
1983 models against measured respectively:
(a) & (b) $\bar{H}$; (c) & (d) H_{sw} ; (e) & (f) H_{max}.

On comparison of the distributions predicted by the above 2 forms, it is found that both the forms do not give satisfactory results. They fit in very few cases only. However, the performance of the modified form is better than the original. When the original form fits in 116 cases which contribute to 36.7% of the data, the modified form fits in 178 cases (56.3%). On a closer examination, the fit is found to be better during the rough season for both the forms. The original form fits in 43.3% of the cases during this season and 30.7% during the fair season. The fit by the modified form during the rough and fair seasons are 60 and 53% respectively.

Both the forms give fit in all the ranges of H_{sw}, T_p, spectral width and steepness. However, the fit is found to be better at higher steepness ranges by the original form. The modified form give better representation at the lower steepness as well.

The probability densities of $\bar{H}$ predicted by both the forms are higher than the observed in all the cases, except in a very few ones (Fig.6.10a-b). On the average, the values are overestimated by about 22% by the original form and about 18% by the modified form. The P(H_{sw}) values are also overestimated by these models, but are comparatively more closer to the observed (Fig.6.10c-d). On the average,

148

$P(H_{sw})$ values are higher by about 4% in the case of the original form and about 3% in the case of the modified form. However, the values of $P(H_{max})$ are predicted more correctly by these models (Fig.6.10e-f). The average deviation from the observed, in both the cases are much less than 1% only. That is, though the modification of the model with $r(H,T)$ in place of ϵ_w improves the model slightly, it does not bring it to the desired level for applications in shallow waters.

6.1.2. Comparison of Observed Distributions in the $H_{sw}-T_p$ Ranges with Models

The different models considered above for comparison with the distribution of wave heights in individual records are also compared with the distribution of heights obtained by grouping the different records in H_{sw} intervals of 0.25 m and period intervals of 1 s. Upon grouping 13 classes do not follow any of the models, due to the presence of multiple modes in the distribution. Hence, these cases are not considered for the comparison. A few cases with multiple modes are not excluded, since one or the other of the models fit in those cases.

The observed distributions are generally positively skewed and the coefficient of skewness are predominantly in the range 0.1-0.8 with an average around 0.4. The dominant kurtosis values are in the range 2-4 with the average

149
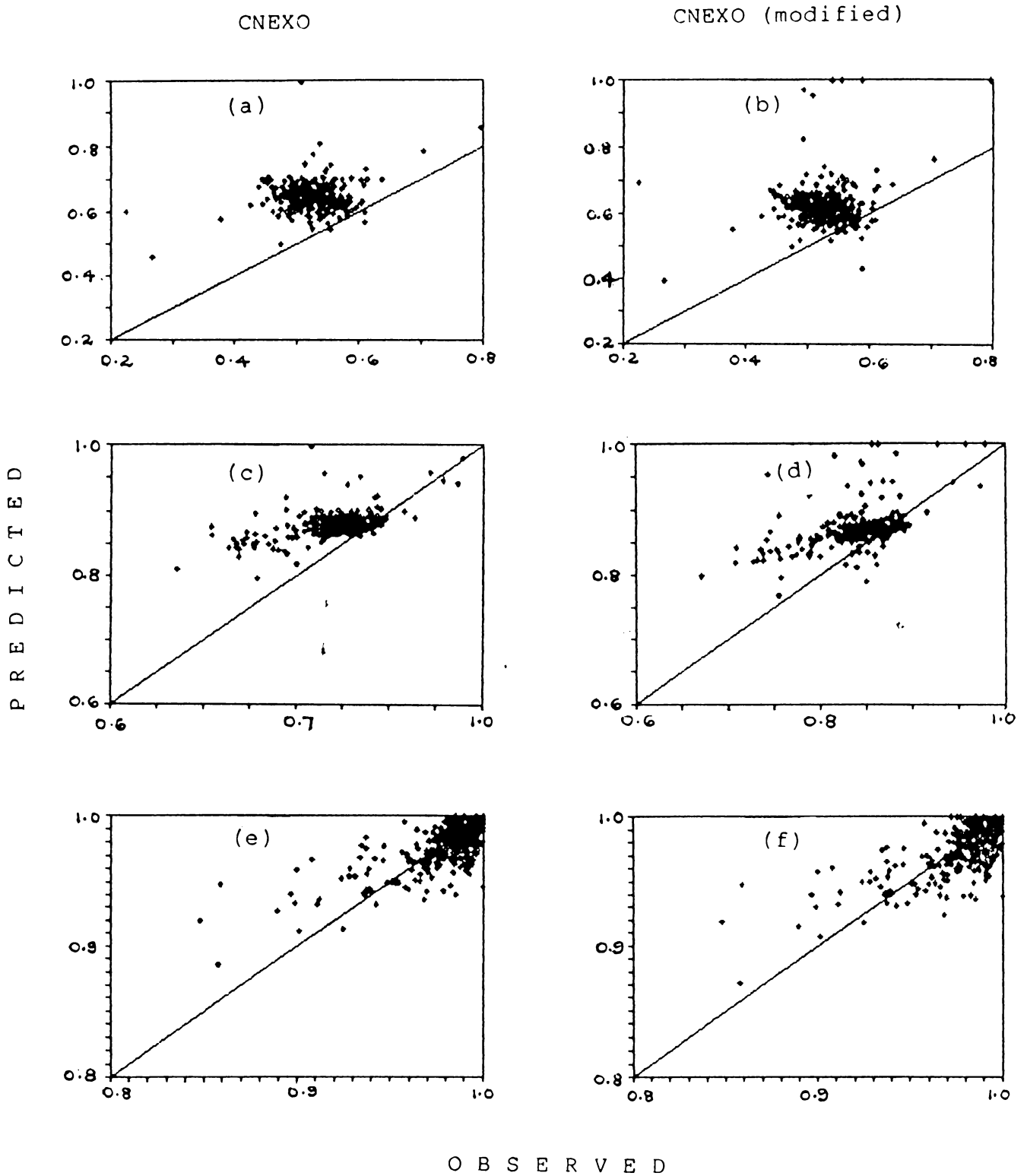
Fig.6.10 Plot of cumulative probability densities of height
distribution predicted by CNEXO models (original
and modified) against measured respectively:
(a) & (b) $\overline{H}$; (c) & (d) H_{sw} ; (e) & (f) H_{max}.

slightly less than 3, which is the value for a normal distribution. This marked skewness and the lower values of kurtosis indicate the degree of deviation of the distribution from the normal. However, the fit or non-fit of models are not found to be dependent on values of skewness or kurtosis.

The average skewness and kurtosis of the Gluhovskii's distribution is in good agreement with that obtained from the data. All other models show higher skewness and kurtosis, except Ibrageemov's, which has values lower than the data. Gluhovskii's model fit in all ranges of skewness and kurtosis present in the data. The Longuet-Higgins' 1975 model and Goda's model show a fit in the lower ranges of skewness only. They do not fit in any case corresponding to the higher values of kurtosis also. All the other models has a few cases of their fit in the lower ranges of skewness and kurtosis, with the modified form of CNEXO fitting in the very low ranges only.

The cases where the different models fit the data are presented in Table 6.1. Gluhovskii's and modified Longuet-Higgins models give better fit with the data. They follow the data in about 80.5% of the cases. Rayleigh and Weibull funtions follow the data almost identically and they fit in 46.3% each. Fit by Tayfun's model in 34.1%, Goda's in 31.7%,

150

Table 6.1 Fit of Different Height Distribution Models to Data in H_{ss}-T_p Ranges

No	H_{ss}(m)	T_p(s)	Avg	Gl	L1	L2	Rl	Gd	Wb	Ib	Ty	C1	C2
1	0.00-0.25	5 - 6	3										
2	0.00-0.25	6 - 7	3	x				x		x			
3	0.00-0.25	9 -10	3	x				x		x			
4	0.00-0.25	10 -11	11							x			
5	0.00-0.25	12 -13	16							x			
6	0.00-0.25	15 -16	4		x	x							
7	0.25-0.50	6 - 7	4	x	x	x	x	x	x				x
8	0.25-0.50	8 - 9	4	x	x	x	x	x	x				
9	0.25-0.50	9 -10	8	x	x	x							
10	0.25-0.50	10 -11	13			x							
11	0.25-0.50	12 -13	42										
12	0.25-0.50	15 -16	12	x		x	x		x				
13	0.50-0.75	5 - 6	2	x	x	x	x						
14	0.50-0.75	6 - 7	3										
15	0.50-0.75	8 - 9	2										
16	0.50-0.75	9 -10	2	x		x							
17	0.50-0.75	10 -11	8	x		x							
18	0.50-0.75	12 -13	41										
19	0.50-0.75	15 -16	10	x		x							
20	0.75-1.00	5 - 6	1	x	x	x	x	x	x				x
21	0.75-1.00	6 - 7	1	x							x	x	
22	0.75-1.00	7 - 8	1	x	x	x	x	x		x			
23	0.75-1.00	8 - 9	2										
24	0.75-1.00	9 -10	5	x	x	x							
25	0.75-1.00	10 -11	3	x	x	x							
26	0.75-1.00	12 -13	12	x		x							
27	0.75-1.00	15 -16	2										
28	1.00-1.25	6 - 7	3										
29	1.00-1.25	8 - 9	6			x							
30	1.00-1.25	9 -10	6	x	x	x							
31	1.00-1.25	10 -11	3	x	x	x	x	x					
32	1.00-1.25	12 -13	5	x	x	x	x	x					
33	1.00-1.25	15 -16	1	x	x	x	x	x	x			x	x
34	1.25-1.50	6 - 7	3	x		x							
35	1.25-1.50	7 - 8	3										
36	1.25-1.50	8 - 9	12	x									
37	1.25-1.50	9 -10	9	x	x	x							
38	1.25-1.50	10 -11	5	x									
39	1.25-1.50	15 -16	1	x	x	x	x	x	x	x	x		x
40	1.50-1.75	8 - 9	4	x	x	x	x		x				
41	1.50-1.75	9 -10	4										
42	1.50-1.75	10 -11	3										
43	1.50-1.75	12 -13	1	x	x	x	x		x	x	x		
44	1.50-1.75	19 -20	1	x	x	x	x	x	x		x	x	x
45	1.75-2.00	7 - 8	1	x	x	x	x	x	x				
46	1.75-2.00	8 - 9	1	x	x	x	x	x	x	x	x	x	
47	1.75-2.00	9 -10	4	x	x	x	x		x		x		
48	1.75-2.00	10 -11	3	x	x	x			x		x		
49	1.75-2.00	12 -13	1	x		x	x		x				
50	2.00-2.25	8 - 9	1		x	x	x	x	x				x
51	2.00-2.25	9 -10	3	x	x	x	x	x	x		x		
52	2.25-2.50	8 - 9	2										
53	2.25-2.50	10 -11	4	x					x		x		

Avg: Number of records used for averaging
Gl: Gluhovskii, L1, L2: Longuet-Higgins 1975 and 1983
Rl: Rayleigh, Gd: Goda, Wb: Weibull, Ib: Ibrageemov
Ty: Tayfun, C1, C2: CNEXO original and modified

Ibrageemov's and modified CNEXO in 11.6% each and original CNEXO in 7.3% of the cases are obtained.

In the lower height range of 0-0.25 m the fit is very poor for most of the models (Table 6.1). Tayfun's function gives the best representation in this range followed by Longuet-Higgins' 1975 model. Weibull distribution and Longuet-Higgins' modified form are found to fit in a very few cases. In other ranges, Gluhovskii's and Longuet-Higgins' modified forms follow the observed distribution in a large number of cases. They fit the data in all the ranges of H_{sw} equally well, except the lowest (0-0.25 m). Weibull and Tayfun's models represent the data better in the higher ranges of H_{sw}. Ibrageemov's and the CNEXO models fail to fit the data in the lower as well as the higher H_{sw} ranges. Rayleigh and Goda functions represent all the height ranges, except in the lowest (0-0.25 m), though not as good as Gluhovskii's and modified Longuet-Higgins' models.

When the fit is examined in relation to the T_p values, almost all the models fit equally in all the ranges of T_p. Gluhovskii's model give the best fit, followed by the modified Longuet-Higgins'. This is followed by the 1975-form of Longuet-Higgins . All these 3 models show better representation in the T_p range 9-10 s. Rayleigh and Goda's functions show best representation in the lower T_p ranges of 7-8 s.

151

The probability densities of the different height parametes predicted by the models are identical to that observed in Sec.6.1. Gluhovskii's model predicts the values nearest to the observed. The maximum deviation is less than 2% only. $P(\bar{H})$ and $P(H_{sw})$ values are overestimated by about 1% and 1.5% and $P(H_{max})$ is predicted correctly by this model. The modified form of Longuet-Higgins also predicts the probability densities close to the observed values. The maximum deviation is in the case of $P(\bar{H})$ and are on the average overestimated by about 3%. $P(H_{sw})$ is overestimated by about 1% and $P(H_{max})$ is overestimated by less than 1% by this model. The deviations of the predicted values of these height parameters from the observed are found to be more with the other models. The $P(\bar{H})$ values are overestimated by about 4, 5 and 6% respectively by Weibull, Rayleigh's and Ibrageemov's functions. Goda's and the two forms of CNEXO's models highly overestimate the values, in the range 12-20%, whereas Tayfun function underestimates them by about 33%.

$P(H_{sw})$ values simulated by Rayleigh is in good agreement with the observed. When Goda's and CNEXO's models overestimate the values by 4-6%, Weibull and Longuet-Higgins' first form underestimate them by about 2-3%. The $P(H_{sw})$ values predicted by Ibrageemov's and Tayfun's models show maximum deviation, Ibrageemov's overestimating them by

152

about 13% and Tayfun's underestimating by about 11%. However, $P(H_{max})$ values are predicted closely with the observed by all the models. When the values estimated by Goda's and both the CNEXO models are in close agreement with the observed, Rayleigh model underestimate them by about 1% and Weibull, Tayfun's and Longuet-Higgins' first form estimate the values lower by about 2% and Ibrageemov's model overestimates them at this rate.

On a closer examination of the different probability densities predicted by the models, it can be seen that $P(\bar{H})$ is predicted most correctly by Gluhovskii's model with minimum scatter. $P(H_{sw})$ is predicted closest to the observed by Rayleigh followed by Longuet-Higgins' modified form and Gluhovskii's model. Weibull and Longuet-Higgins' first form also predict the values comparable to the observed, but are slightly underestimated. $P(H_{max})$ values are estimated nearer to the observed by all the models, except Ibrageemov's which always overestimates the values. The values predicted by Gluhovskii's model is found to be closest to the observed with minimum scatter followed by the modified form of Longuet-Higgins'.

The depth controlled function of Gluhovskii simulates the probability densities of all the statistical height parameters, whereas the other models overestimate them in

153

the lower height ranges. This indicates also that the distribution of wave heights in shallow waters is always depth dependant.

6.2. DISTRIBUTION OF ZERO-CROSSING WAVE PERIODS

The distributions of individual zero-crossing wave periods are computed from each record at 1 s interval. Typical examples of the observed short-term period distributions are presented in Fig.6.11. Multi-moded distributions are observed in a large number of cases. The reason for this may be the same as in the case of height distributions. The observed distributions are compared with the different theoretical/ empirical models. The period distributions are also computed from the records grouped according to H_{sw} and T_p ranges, as done in the case of height distribution (section 6.1.2). They are also compared with the different models and the observations are presented in sub-section 6.2.2.

6.2.1. Comparison of Short-Term Distributions with Models

The distribution of zero-crossing periods obtained from each record are compared with the different models in this section. Typical examples of the period distributions predicted by the models are presented in Fig.6.12. In this case also, it is practically very difficult to do visual compari-

154
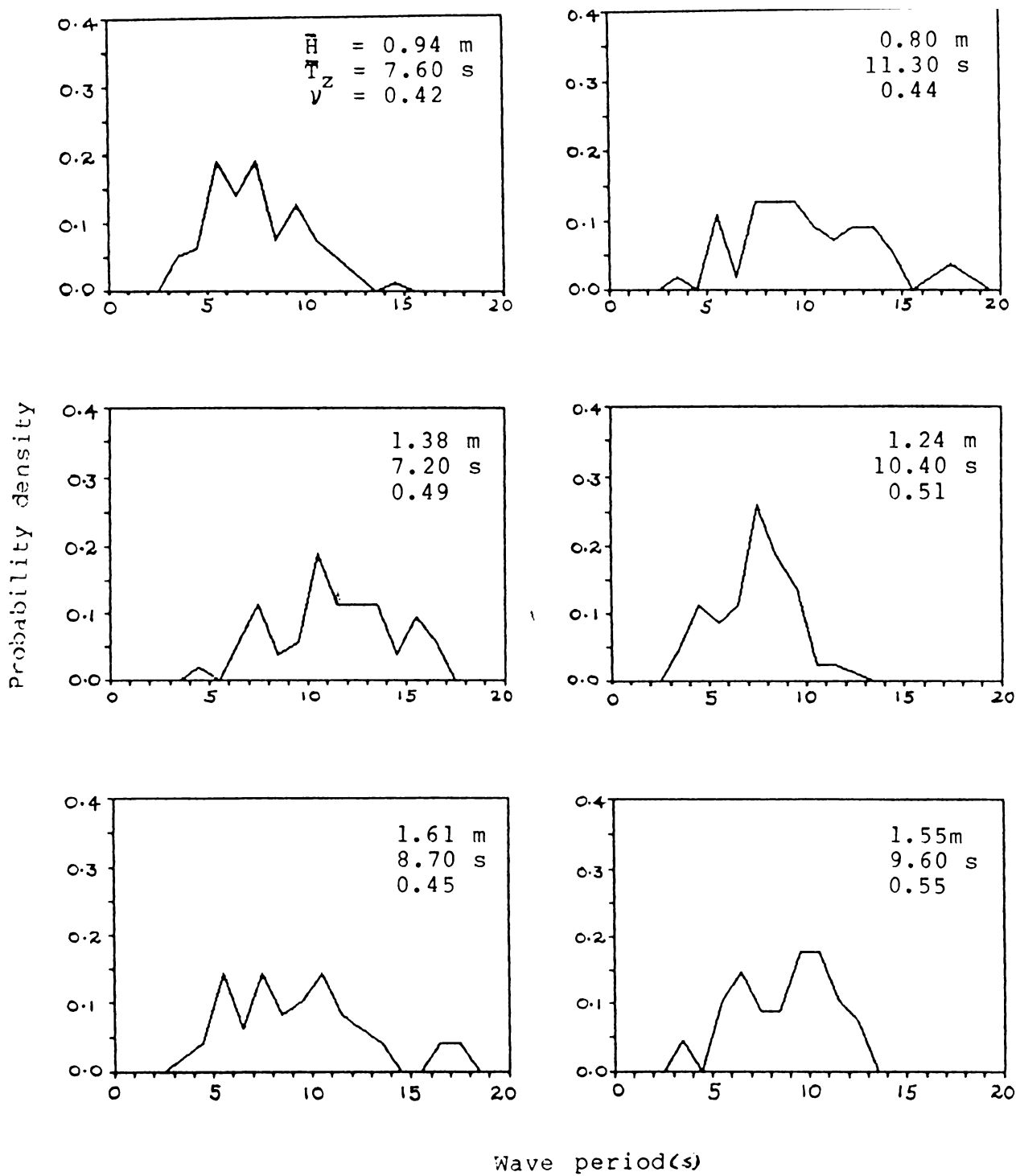
Fig.6.11 Typical examples of observed period distribution.

son of the observed distribution with the models, since the number of observed distribution as well as the number of models considered are large. The only satisfactory test that can be applied in this case is again the χ^2 goodness of fit test. Hence, the fitness of the different models is evaluated using the χ^2 test at the 0.05 level of significance. The cases where the models fit the data are presented in Appendix-A. In addition, the cumulative probability densities of T_c, T_z and T_s in the observed distributions are also compared with the corresponding values predicted by the different models. The results are discussed in sub-sections 6.2.1.1 through 6.2.1.5.

6.2.1.1. Rayleigh models

The Rayleigh distribution for wave periods suggested by Bretschneider (Eq.2.69) is found to fit the data in 171 cases constituting 54.1% of the cases. This model fits more cases during the rough season than the fair season. During the rough season it follows the data in 62.7% and during the fair season it follows in 46.4% of the cases. However, this model is found to fit equally in all ranges of H_{sw}, T_z, steepness and spectral width.

The cumulative probability densities of T_c, T_z and T_s predicted by this model are closer to the observed values (Fig.6.13a-c). The range of values are maximum for $P(T_z)$ and

155
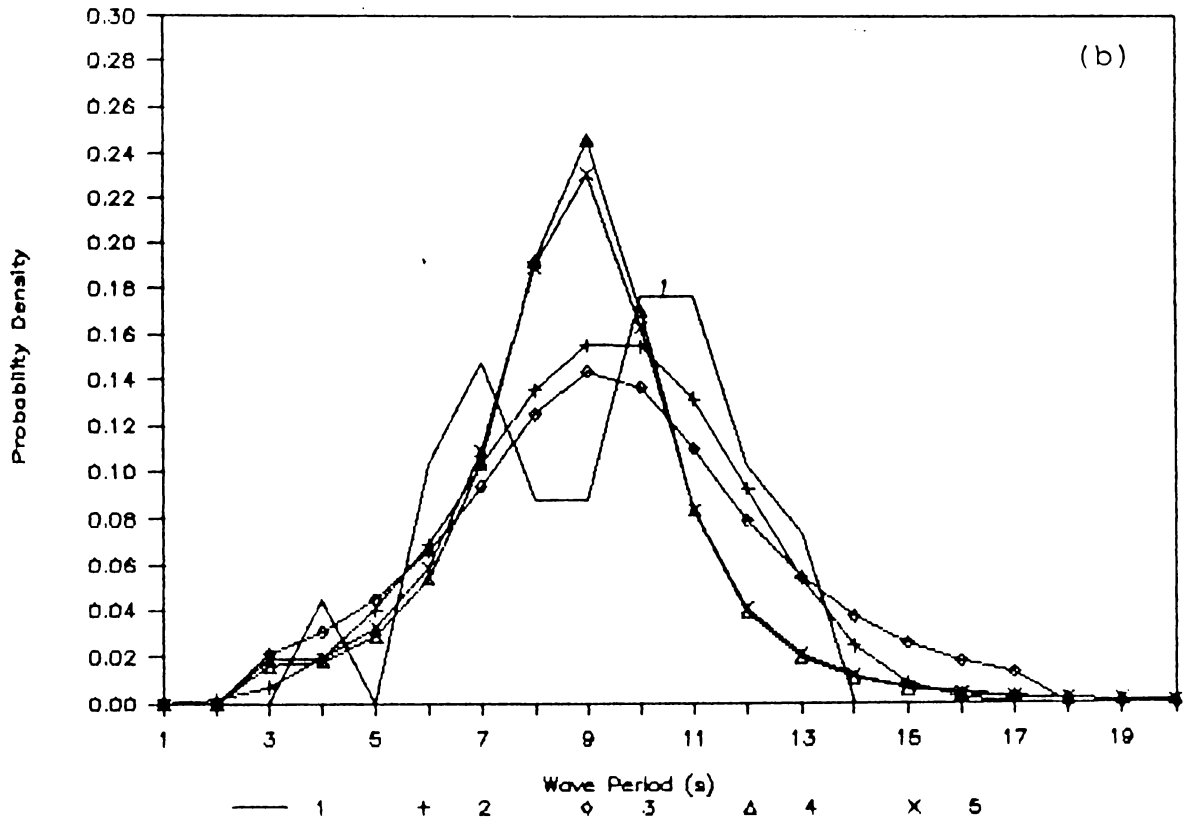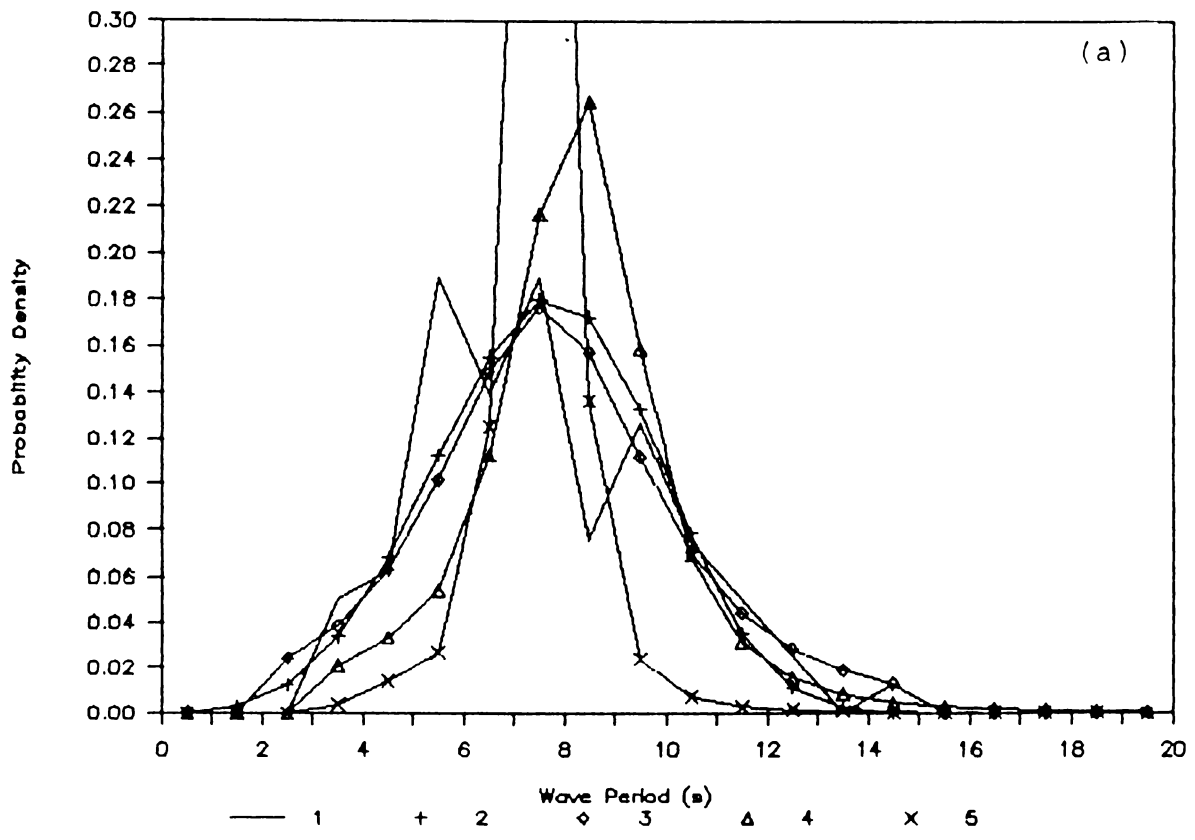
1: Observed, 2: Rayleigh, 3: Tayfun's, 4: CNEXO
and 5: CNEXO (modified) distributions.

Fig.6.12 Typical examples of period distributions
         predicted by different models corresponding
         to an observed distribution.

least for $P(T_c)$. The $P(T_c)$ values are almost constant in a very narrow range and on the average are lower by about 4% than the observed. The predicted values of $P(T_z)$ are also nearly constant, but with a wider range. On the average $P(T_z)$ predicted by this model is lower than the observed by 5%. The values of $P(T_s)$ are in good agreement with the observed, but with some scatter. On the average, the predicted values are higher by about 2%. That is, the forward phase of the probability distribution of periods (the lower period ranges) are more flattened by this model, but can be used to estimate the cumulative probabilities of the higher periods ($> T_z$).

The Rayleigh model is adopted to represent the short-term distribution of wave periods by Longuet-Higgins, Gluhovskii and Tayfun while deriving their equations for the joint distribution of wave heights and periods. The period distributions obtained from Eqs.(2.89-2.91) are Rayleighean. The distribution of periods obtained from Gluhovskii's and Longuet-Higgins's models are the same as the Rayleigh distribution discussed above, with identical fit with the data. So, a discussion of the distributions obtained from these models are not presented here. However, Tayfun's model is a modification of the Rayleigh form by normalising the relation to have a unit area over the restricted

156

interval $(-1/\nu$, $+1/\nu$) of the normalised period. The distribution of periods predicted by the Tayfun's model is discussed in the following section.

6.2.1.2. Tayfun's model

Tayfun's model for the distribution of individual wave periods, derived from his model for the joint distribution of heights and periods (Eq.2.98), is found to fit in a large number of cases. Fit is obtained in 219 cases which constitute to 69.3% of the data. The fit is found to be better during the months of monsoonal wave climate. During May-September fit is obtained in 80.7% of the cases and during October-April, when fair weather conditions prevail, this model fits the data in 59% of the cases. The model is found to fit the data in all the ranges of H_{sw}, T_z, steepness and spectral width ranges. However, the fit in the case of lowest steepness values are not as good as in the other ranges.

The probability densities of T_c, T_z, and T_s predicted by this model also show characteristics almost similar to that observed in the case of Rayleigh and Gluhovskii models (Fig.6.14a-c). Though the ranges of values are comparatively more with this model they are distributed around the observed values almost equally on the higher and lower sides. On the average, the values are in agreement with the

157
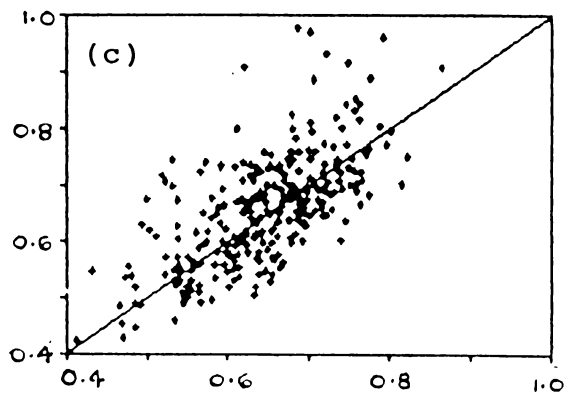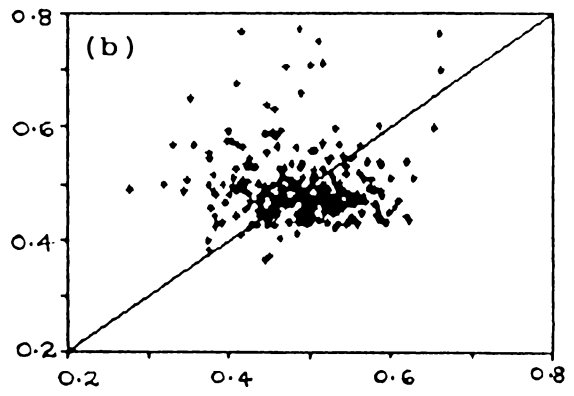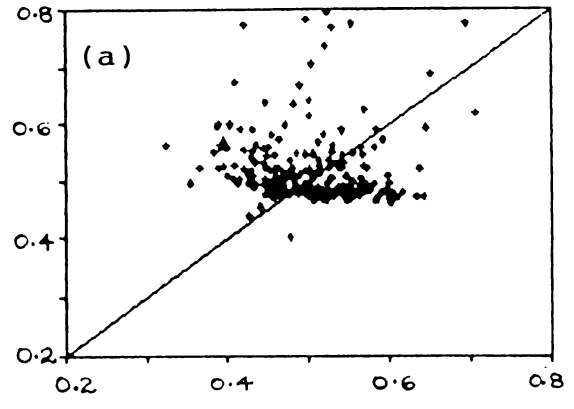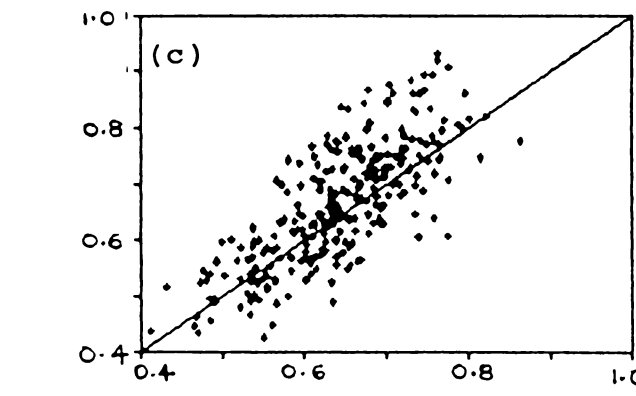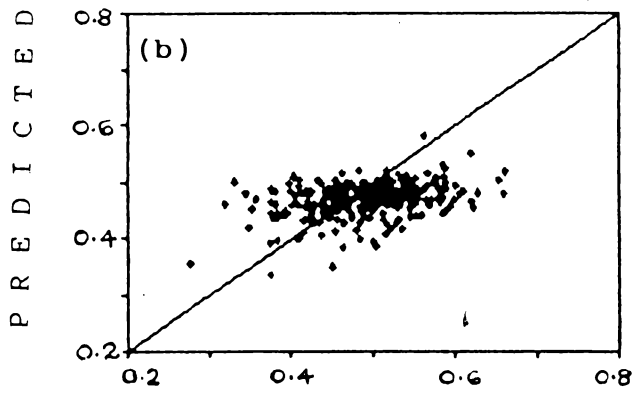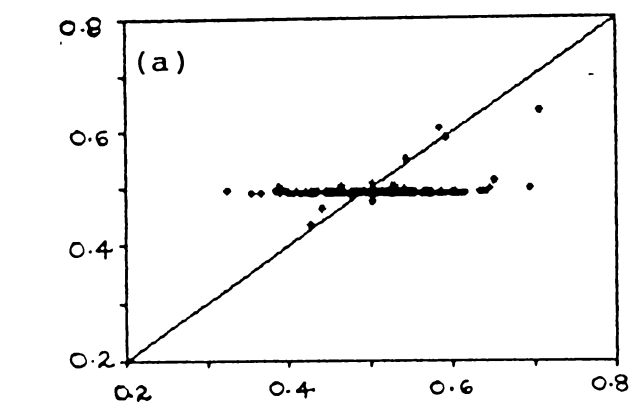
P R E D I C T E D

O B S E R V E D

Fig.6.13 Plot of cumulative
    probability densities of
    period distribution pre-
    dicted by Rayleigh model:
    (a) T_c; (b) T_z; (c)T_s.

Fig.6.14 Plot of cumulative
    probability densities of
    period distribution pre-
    dicted by Tayfun's model:
    (a) T_c; (b) T_z; (c)T_s.

observed as shown by the regression analysis. The predicted values of $P(T_c)$, $P(T_z)$ and $P(T_s)$ deviate from the observed by less than 1% only. The underestimation of the lower period statistics by the Gaussian normal models and the equally good fit obtained for all the statistical periods with this model shows that the shallow water wave periods are not distributed Gaussian normal.

6.2.1.3. CNEXO models

The CNEXO disributions for periods are obtained by integrating Eq.2.94 and the equation obtained by modifying this equation by replacing the spectral width parameter with $r(H,T)$, with respect to height. The original form and its modification are found to be very poor in representing the shallow water wave period distribution. Altogether, the original model fit in 92 cases and the modified form in only 8 cases constituting to 29.1% and 2.5% respectively. Among the cases where fits are obtained, the original form follows the rough season waves and the modified form follows the fair season ones. The original form fit in 35.3% of the cases during the rough season and 23.5% during the fair season. The modified form fit in less than 1% during the rough season and 4.2% during the fair season. The cases where the original form fit, fall in all ranges of H_{sw}, T_z, steepness and spectral width. However, sufficiently large

158

number of cases which fit the data are not available to assess the fit at different height, period or spectral width ranges. The very few cases where the modified form fit the data are in the low height and steepness ranges with higher period and spectral width.

The probability densities of T_c, T_z, and T_s are highly overestimated by both forms (Fig.6.15a-f). The rate of overestimation is more for lower period parameters and lesser for higher period parameters. The average rate of overestimation of $P(T_c)$ and $P(T_z)$ by the original form are 21% each and that by the modified form are 15% and 10% respectively. Similarly the values of $P(T_s)$ are overestimated by about 8% and 9% respectively by the original and modified forms.

6.2.2. Comparis/on of Short-Term Distributions in $H_{sw}-T_p$ Ranges with Models

The distribution of periods are computed with the data grouped into different H_{sw} and T_p ranges, as done for the distribution of heights. The multiple modes observed in the period distribution computed from individual records are more pronounced now, and almost all show major secondary modes. As a result, the χ^2 values become very high and practically no fit is obtained with any of the models in

159

Fig.6.15 Plot of cumulative probability densities of period distribution predicted by CNEXO models (original and modified respectively: (a) & (b) T_c; (c)&(d) T_z; (e)&(f) T_s.

number of cases which fit the data are not available to assess the fit at different height, period or spectral width ranges. The very few cases where the modified form fit the data are in the low height and steepness ranges with higher period and spectral width.

The probability densities of T_c, T_z, and T_s are highly overestimated by both forms (Fig.6.15a-f). The rate of overestimation is more for lower period parameters and lesser for higher period parameters. The average rate of overestimation of $P(T_c)$ and $P(T_z)$ by the original form are 21% each and that by the modified form are 15% and 10% respectively. Similarly the values of $P(T_s)$ are overestimated by about 8% and 9% respectively by the original and modified forms.

6.2.2. Comparision of Short-Term Distributions in $H_{sw}-T_p$ Ranges with Models

The distribution of periods are computed with the data grouped into different H_{sw} and T_p ranges, as done for the distribution of heights. The multiple modes observed in the period distribution computed from individual records are more pronounced now, and almost all show major secondary modes. As a result, the χ^2 values become very high and practically no fit is obtained with any of the models in

159

Fig.6.15 Plot of cumulative probability densities
of period distribution predicted by CNEXO
models (original and modified respectively:
(a) & (b) T_c; (c)&(d) T_z; (e)&(f) T_s.

most of the cases. Hence a discussion on the fit based on this multi-moded distributions is irrelevant and hence not attempted here.

6.3. JOINT DISTRIBUTION OF HEIGHTS AND PERIODS

The joint distribution of zero-crossing heights and periods are computed for each record, at height intervals of 0.2 m and period intervals of 1 s. Typical examples are presented in Fig.6.16. The observed distributions show different shapes depending upon the characteristics of the waves present in each record. In general, they are deviated from symmetry and are skewed positive. The observed distributions are compared with the different theoretical/empirical models in the following sub-sections.

6.3.1. Comparison of Short-Term Joint Distributions with Models

In order to examine the fitness of a model with the observed joint distributions there is no standard test, as seen in the case of wave spectrum. The procedure usually adopted is to make visual comparisons of the contours drawn for the observed and model distributions. Typical examples of the distributions predicted by the different models is presented in Fig.6.17. When there are a large number of observations and models, it is difficult to make visual

160
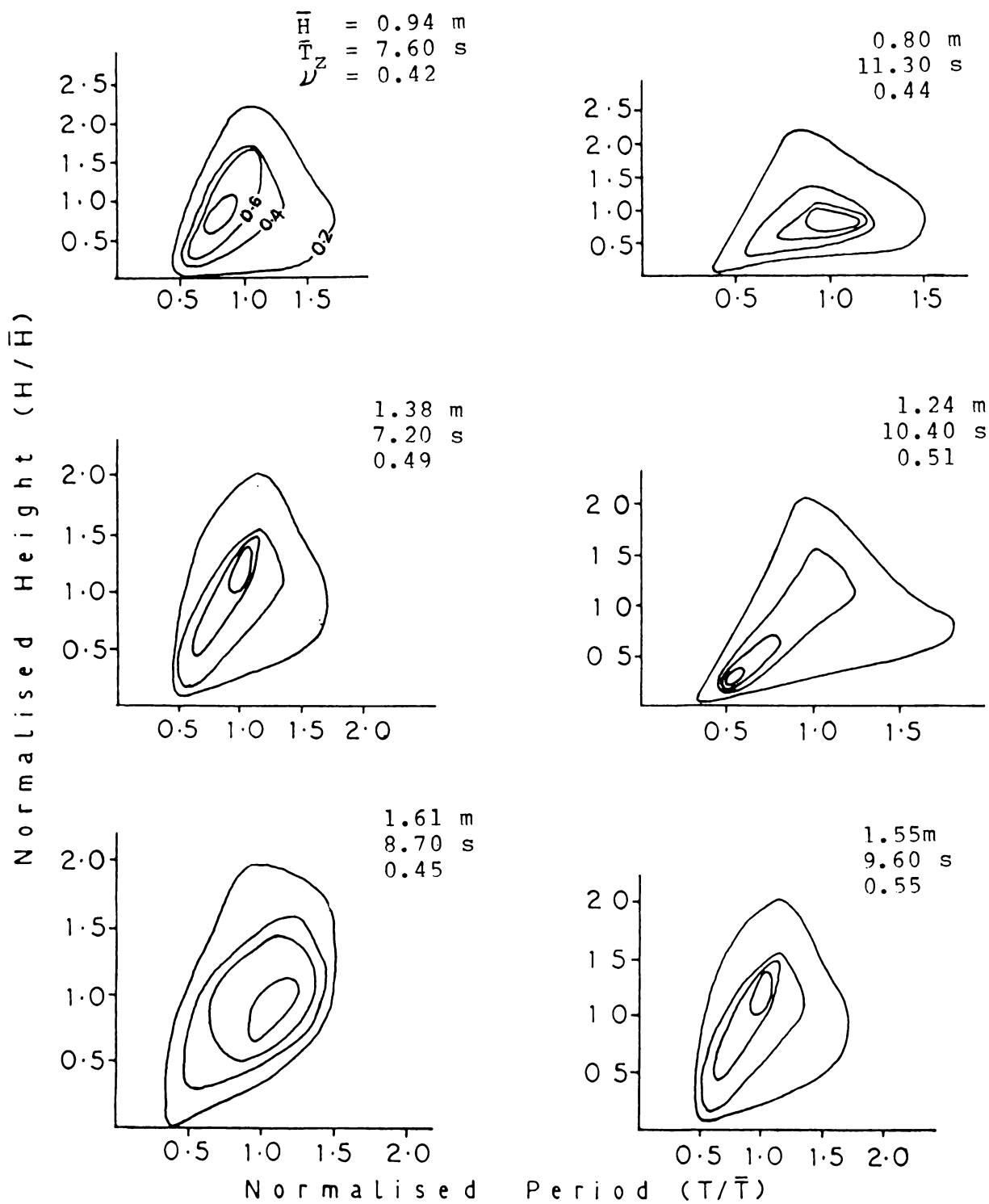
Fig.6.16 Typical examples of observed joint
distribution of heights and peiods.

comparisons. Moreover, each model exhibits characteristic shape of the distribution. A valid statistical test in such cases is the X^2 test. In order to use this test, the data has to be grouped so as to get number of frequencies $\geq$ 5 in each bin (also see Sec.6.3.1). But, such a grouping will eliminate the tail of the distribution, which are the most interesting portion of the height-period distribution for practical applications. Since no other altrnative is left, the X^2 values are computed without grouping the low frequencies in the tail of the distribution. Now, the goodness of fit cannot be made based on the values of standard X^2 distribution with different degrees of freedom. Hence, in order to find the suitability of models a different approach is made. For each record a comparison between the values obtained for the different models is made and the model which give the lowest value of X^2 is selected. The model that gives the lowest X^2 values in maximum number of cases is considered as the best among the various models. The X^2 values obtained for different models is presented in Appendix-B and the results are discussed in sub-sections 6.3.1.1 through 6.3.1.5.

6.3.1.1. Rayleigh model

The X^2 values obtained for Rayleigh (Eq.2.87) range from 26 to 529 with an average around 130 (Appendix-B). This

RAYLEIGH

GLUHOVSKII

TAYFUN

LONGUET-HIGGINS
(1975)

LONGUET-HIGGINS
(1983)

CNEXO

CNEXO (modified)

Height (H/H̄)

Normalised

Normalised Period (T/T̄)
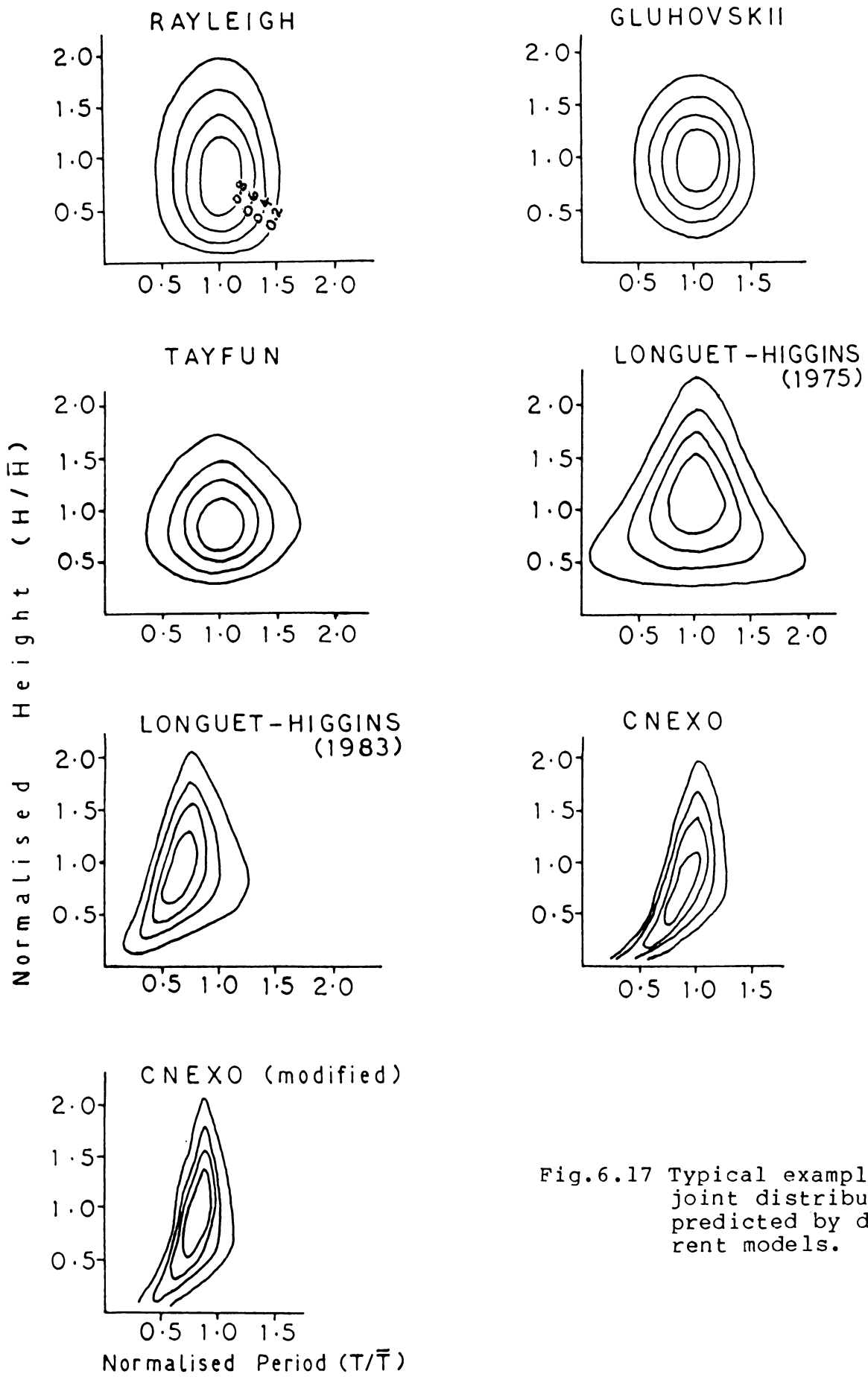
Fig.6.17 Typical examples of
joint distribution
predicted by diffe-
rent models.

model has the lowest χ^2 values in only 4 cases constituting about 1% only. When examined according to H_{sw}, T_z and spectral width ranges, it is found that the very few cases where the χ^2 is the least, correspond to lower as well as higher ranges of H_{sw}, middle ranges of T_z (8-11 s) and higher ranges of ϵ_s. However, since the number of cases of best fit are very few, specific conclusions cannot be drawn from these observations.

The modes are incorrectly placed by this model. They are at larger heights and periods when the observed ones are nearer to the origin. But, when the observed modes are at larger heights and periods, this models place them nearer to the origin.

The very poor performance of this model may be due to the positive correlation present between heights and periods, as against the assumption in developing this model. The observed heights and periods show significant correlation in most of the cases, the coefficient ranging from -0.06 to +0.77 with an average of 0.41 and a standard deviation of 0.16.

6.3.1.2 Gluhovskii's model

Gluhovskii's model (Eq.2.89) is also not found to follow the observed distribution in most of the cases. The

χ^2 values range from 12 to 427 with an average of 128. The values are the lowest in 18 cases which is about 6% of the cases examined. The few cases of best fit obtained represent all the ranges of H_{sw}, T_z and spectral width present in the data set. However, the fit is comparatively better in the higher ranges of H_{sw} and lower ranges of T_z (Appendix-B). The mode of the predicted distribution deviate from the observed in many cases, as seen with the Rayleigh model. However, the deviations are less in this case. On the average, the modes are close to the observed height values but are shifted slightly to the higher periods.

6.3.1.3. Tayfun's model

Tayfun's model (Eq.2.98) fit the data in maximum number of cases (Appendix-B). Generally, the values are lower with this model. They range from 15 to 276 with an average of 73. The χ^2 values obtained with this model are the lowest in 226 cases which is 72% of the data. This model is found to have representation in all the ranges of H_{sw}, but is not very good in the cases of very low and very high H_{sw} values. When the data is grouped in 0.25 m H_{sw} interval, the χ^2 values are the lowest in more than 60% for all the groups in the H_{sw} range 0.25-1.75 m. Similar fit is obtained in all the T_z and ε_w ranges present in the data

set. When the modes are examined, some deviation is observed, but are closer to the observed ones.

The better fit obtained in period and joint distributions with this model indicate the conspicuous deviation of these distributions from the normal. Since the distribution of heights are not simulated correctly by this model, it may be the period distribution concept of Tayfun that contribute to the success of this model over the others. Since the present location is a typical example of shallow water effects due to gently sloping bottom, where the transformation processes, especially the bottom friction, is more pronounced (Kurian, 1987), it is reasonable to conclude that Tayfun's model is suitable for simulating the joint distribution of shallow water waves.

6.3.1.4. CNEXO models

The original as well as the modified forms of the distribution suggested by the group of CNEXO (Eq.2.94 and its modification) are found not to perform satisfactorily. The χ^2 values range from 12 to 673 in the case of the original form and from 11 to 835 in the case of the modified form (Appendix-B). The average χ^2 values for these models are 148 and 153 respectively. Eventhough the range and average are more for the modified form, it has more number of cases with lowest χ^2 values compared to the original

form. When the values are the lowest in 15 cases (5%) for the original form it is the lowest in 32 cases (10%) for the modified form. Both the forms are found to follow the data better at the cases of high H_{SW} values, but deviate in the cases where T_Z values are very low or very high. The modified form has its best fit at the highest H_{SW} ranges, where the Tayfun's model fails. Both the CNEXO models have their best representation in the T_Z ranges between 8 and 12 s. As regard to spectral width, the original form has its lowest χ^2 values in the range of ε_w from 0.7 to 0.85 only. The modified form represents all the ranges present in the data set, but show better performance in the lowest ranges.

The modes predicted by the first form are found to be shifted considerably to the origin. The modified form predict the modes at larger heights and periods in the cases for which the observed modes are nearer to the origin. On the other hand, when the observed modes are at larger heights and periods, the predicted modes are found to be shifted towards the origin. In general, both the forms predict the modes shifted to the lower heights and periods, the deviation being large with the original form and lesser with the modified form. The modes are incorrectly placed by this model in cases of lower width of spectrum also (Srokosz, 1988). The observation that the modified form fits

165

the data in more cases compared to the original indicates that it is the rank correlation between heights and periods that is preferable to e_w in determining the joint distribution with the CNEXO model, as suggested by Goda (1978).

6.3.1.5. Longuet-Higgins' models

The models suggested by Longuet-Higgins (Eqs.2.90 and 2.91) simulate the joint distribution in a few cases only. The χ^2 values range from 13 to 385 for the first form and 26 to 498 for the modified form (Appendix-B). The averages for these models are 118 and 157 respectively. The χ^2 values are the lowest in 16 cases (5%) with the 1975-form and in only 5 cases (2%) with the modified form. The cases where these forms has the best fit are only those with low H_{sw} values (but not in all cases of low H_{sw} values). The few cases of best fit also correspond to the lower ranges of periods. The first form is found to represent T_z in the range 6-11 s with better representation in the lower periods. The modified form represents the T_z range of 7-9 s only. With regard to spectral width, a similar picture is obtained. Though the first form represents the full range of spectral width present in the data, better performance of the model is found in the lower ranges. The modified form is found to represent the e_w in the range 0.65-0.75 only, the performance being better at the higher vlues.

The first form predicts the modes at much larger heights and lower periods than the observed. But, when the observed modes are very close to the origin, the predicted modes are at higher periods. The modes predicted by the modified form are at larger heights when the observed are near the origin and at lower heights when it is at larger heights. The periods corresponding to the predicted modes are generally lower in most of the cases. However, specific conclusions cannot be drawn in this case also, due to the fewer number of cases available for comparison. Longuet-Higgins distributions are based on narrow band assumption and are functions of the spectral width parameter. Hence, there is no surprise in the poor fit obtained for these models with the present data having dominant wide band spectra.

6.4. CONCLUSIONS

Among the different models available for the computation of short-term distribution of wave heights in shallow waters, the one suggested by Gluhovskii is capable of simulating the observed distribution in shallow waters satisfactorily. The cumulative probability densities of H, H_{sw} and H_{max} predicted by this model are in agreement with the data. The modified Longuet-Higgins' form performs better than the original and represents the rough sea conditions

167

more accurately. Though the Rayleigh model does not represent the data in as many cases as Gluhovskii's or Longuet-Higgins' modified forms, it fits in a large number of cases and can be considered as a good approximation for all conditions, owing to its simplicity as a single-parameter model. Weibull and Goda's models fit in more· cases during the rough sea conditions. When $P(\bar{H})$ is overestimated by most of the models, the values of $P(H_{max})$ are predicted more or less closer to the data, except by Ibrageemov's (which overestimates the probabilities of all the above statistical parameters). Very poor fit is obtained with the models of Tayfun, Ibrageemov and CNEXO. The Tayfun's model simulates the distribution closely with the observed for cases with higher energy and spectral width and lower T_z. The substitution of $r(H,T)$ in place of spectral width in the CNEXO model is found to improve the performance of the model, but not to the level required for practical applications. The better fit obtained with the modified form of Longuet-Higgins', though basically Rayleighean, indicates that the effects of non-linearities and spectral width affect the shallow water wave height distributions. The best fit obtained in the maximum number of cases with the depth-controlled Gluhovskii's function indicates that the distribution of wave height in the shallow waters are depth-dependant. The effects of non-linearities are accounted by

168

the depth factor in this model. The failure of the frequency/period dependant Ibrageemov's and Weibull distributions, compared to the depth controlled models, is indicative of the lesser influence of the wave period in the height distribution.

Among the various models tried, Tayfun's only can simulate the distribution of zero-crossing wave periods, that too for the high energy, shorter period monsoonal waves. The probability densities of T_c, T_z and T_s predicted by this model are closest to the observed. The CNEXO models always overestimate the probability densities. The Rayleighean models always underestimate the probability densities of T_z and lower periods. But, $P(T_s)$ values predicted by these models are closer to the observed with a variation within 2%. The substitution of $r(H,T)$ in the CNEXO model improves it but not to the level satisfactory for practical applications (as seen in the case of height distributions). The inclusion of the effects of non-linearities and spectral width in the Longuet-Higgins' modified equation make the period distribution to deviate more from the observed. This indicates that the distribution of period in the shallow waters are not affected by the non-linearities and width of the spectrum as it does in the case of height distribution.

The joint distribution of heights and periods are predicted closest to the observed by the Tayfun's model. Best results are obtained with this model in the height range 0.25 < H_{sw} < 1.75 m. The CNEXO models fail to simulate the observed joint distribution satisfactorily. However, the parameter r(H,T) in place of spectral width improves the model. At high energy cases, where the Tayfun's model does not perform satisfactorily, the modified CNEXO model finds its application. Better performance of this model is acheived at high energy cases with lower periods (T_z in the range 8-12 s). When the modes predicted by the Tayfun's model are in agreement with the observed ones, those predicted by the CNEXO models are generally at lower heights and periods. The Rayleigh and Longuet-Higgins's models exhibit very poor performance. The modifications made in Longuet-Higgins' (1983) equations is not found to have improved the model to any degree. The X^2 values obtained with the modified form is in fact larger in most of the cases.

CHAPTER 7

SUMMARY, CONCLUSIONS AND RECOMMENDATIONS

A brief summary along with the conclusions drawn is presented in this Chapter. On the basis of the observations made in the different Chapters recommendations for further research are given.

7.1. SUMMARY AND CONCLUSIONS

Detailed studies on the spectral and statistical characteristics along the Indian Coasts are limited. As far as the south-west coast is concerned, practically no systematic study on the wave characteristics are made. With a view to fill this lacuna, a comprehensive study on the wave climate, spectral and statistical characteristics of the shoaling waves off Alleppey, which is a typical location along this coast, is undertaken.

A review of the available literature on the wave spectral and statistical properties reveals that studies on shallow water wave spectrum and the short-term distribution of wave heights are abundant, but that on the distribution of individual wave periods and its joint distribution with heights are sparse. Even for the spectrum and the height distribution, a generalised model with universal applicability is yet to be developed. Different models are

suggested for different environmental conditions and the constants and coefficients vary from model to model. Field evaluation/calibration of these models is required to identify their validity at different locations.

The wave spectral models derived for deep water conditions generally fail in shallow waters.￼ However, the empirical Scott and Scott-Weigel models simulate the shallow water spectrum in some cases. Most of the shallow water models are the modification of one or other of the deep water models with another transformation model. The finite depth dispersion relationship formulated by Kitaigorodskii et al. (1975) serves as a foundation for the development of shallow water spectral models.

Most of the shallow water wave height distribution models are modifications of the theoretically sound Rayleigh model. Owing to the simplicity as a single-parameter model, the Rayleigh form is extensively used even in shallow waters as a first approximation. The depth-controlled forms appears to be promising. The envelope approach also offers scope for further developments. Models for the prediction of short-term distribution of wave periods are very few and the literature indicates that they are not capable of simulating the period distributions satisfactorily. The number of models available for the prediction of the joint

172

distribution of heights and periods are also few. Majority of them assume total independence of height and period distributions. Significant correlation between heights and periods are reported by many researchers and efforts are being made to incorporate the asymmetry of the joint distribution in the models. This may throw more light into the characteristics of the joint distribution of heights and periods in the shallow waters.

The present study is conducted with wave records collected systematically from a shallow water location along the Alleppey Coast. Waves are recorded at 3 hourly intervals using a pressure type recorder. The transducer is installed at 3.5 m below the MWL at a station having a depth of about 5.5 m. Data collected during a 4-year period (1980-84) is utilised to determine the wave climate at this location. From the analysis of these records the yearly variation in wave climate is found to be not significant. Hence the data covering a complete year is selected for the detailed study of the spectral and statistical characteristics of the shoaling waves. The wave spectra are computed using the FFT algorithm and the height, period and their joint distributions are derived using the zero-up-crossing method of analysis.

The wave climate at this location is influenced by the south-west monsoonal winds. During May-September the waves are characterised by larger heights associated with comparatively shorter periods and narrow spectrum. Low waves with comparatively larger periods with broad spectrum prevail during October-April. The period May-September and October-April may be classified as 'rough' and 'fair' seasons for this coast. Whereas the Arabian sea is the generating area for the waves during the rough season, waves from 2 different and far-away locations - one farther than the other - constitute to the wave climate at this coast during the fair season.

Multi-peakedness observed in almost all the spectra at this shallow water location is due to the co-existence of wave trains of different characteristics. Hence the secondary peaks are not at the higher harmonics of the peak frequency, as observed in some other shallow water locations. The spectral peakedness parameter Q_p does not show any characteristic properties with the wave climate, which may be attributed to the prevalence of secondary peaks in the spectra of the shallow water regions. But, the spectral width parameters ε_s, ν and ν_1 do exhibit such properties. Hence, these parameters can be used for a qualitative assessment of the swell dominated wave climate in shallow waters. They are dependent on each other and on

174

the peak periods. The parameters ν or ν_1 can be used in practical applications in preference to ε_s, as they are statistically more stable. The average spectra for different energy ranges show dependence of slope of the high frequency side of the spectrum on energy.

A new spectral model (PMK spectrum) is developed for the prediction of shallow water waves following the theories of Pierson-Moskowitz (1964) and Kitaigorodskii et al. (1975), and is calibrated with the observed spectra. The observed spectra are also compared with Kitaigorodskii et al.'s model with Jensen's modification, the TMA model in its original form and with a few modifications, the Wallops model and the GLERL model (Liu, 1983). The Scott's model and its modification by Weigel (1980), though originally developed for deep water conditions, are also attempted, considering their reported applicability at some shallow water locations along the Indian Coasts.

The shallow water dispersion relationship of Kitaigorodskii et al. (1975) is a useful tool to transform the deep water spectral models to the shallow waters. The models derived using this relationship are able to predict the shallow water spectrum correctly when suitable scale parameters are used. Those which are functions of the total energy are found to be good scale parameters.

175

The models which depend entirely on the peak frequency simulate the spectrum correctly at high energy cases ($H_s \geq$ 2.5 m) only. The TMA model in its original form (with 5 free parameters) simulate the shallow water spectra in a large number of cases. This model is particularly useful for high energy cases where H_s is of the order of 1.4 m and above. The peak energy density is predicted correctly by this model, but the total energy is overestimated, especially in the low energy cases. The average JONSWAP values of the scale and shape parameters are not useful for this location. Average value of the peak enhancement factor γ for the cases which fit this model is found to be equal to 3.0. The application of α_v in place of α_J, make the model to predict the total energy correctly, but the peak energy density is overestimated. With this modification, the TMA model can be used to simulate the shallow water wave spectrum correctly for low energy cases. These are multi-parameter forms and all the required parameters may not be readily available in all cases. In such cases, the new 2-parameter PMK model can be used for all practical applications. The Scott-Weigel model, though basically deep water one, is capable of simulating shallow water wave spectra, especially in the low energy cases. The total energy predicted by this model is comparable to the observed, but the peak energy density is overestimated,

especially at higher energy cases. The coefficients A and B need further modification for application of this model for all conditions. The Wallops model finds its application for the cases with H_s > 0.75 and T_p ≤ 10 s. In the cases of higher T_p values the total energy is overestimated and the peak energy density is underestimated by this model. Care should be taken while applying this model to cases with large peak periods.

The short-term distributions of wave heights computed from the data are compared with the distribution functions of Rayleigh, Goda, Weibull, Gluhovskii, Ibrageemov, Tayfun, Longuet-Higgins (1975 and 1983 models) and CNEXO in the original form and with the modification suggested by Vincent (1984). The depth-dependent models simulate the observed distributions better than the others. Gluhovskii's model is capable of simulating the observed height distributions satisfactorily at all conditions. Longuet-Higgins' 1983 form also simulates the distribution in a large number of cases, but is more suitable for high energy monsoonal/storm conditions. Weibull and Goda's models are also suitable for these high energy conditions, but are not as good as the Gluhovskii's or Longuet-Higgins' models. Tayfun's model simulates the distribution correctly in the cases with higher energy, spectral width and lower periods. Ibrageemov's and CNEXO models fail in most of the cases.

The substitution of $r(H,T)$ in place of ε_s in the CNEXO model improves its performance, but not to a level satisfactory for practical applications. The single parameter models based on Rayleigh distribution are good approximations for all wave conditions.

When most of the models overestimate the cumulative probability density of $\bar{H}$, Gluhovskii's function estimates the values correctly. It also estimates $P(H_s)$ and $P(H_{max})$ values close to the observed. $P(H_{max})$ values are predicted almost correctly by the other models also, except Ibrageemov's, which overestimates the probabilities of all the height parameters. This clearly indicates that the distribution of individual wave heights in the shallow waters is depth dependent and is independent of wave periods.

There is no satisfactory model, at present, to predict the shallow water wave period distributions for all conditions. Among the presently available ones, Tayfun's model is the only one capable of simulating it satisfactorily in a large number of cases. This model is particularly useful for the monsoonal waves with higher energy and lower periods. It also predicts $P(T_c)$, $P(T_z)$ and $P(T_s)$ close to the observed. The Rayleighean models predict $P(T_s)$ values within 2%, but always underestimate $P(T_z)$ and other lower period statistics. The CNEXO models overestimate the cumula-

tive probabilities of these parameters. The modification of Longuet-Higgins (1983) to incorporate the effects of non-linearities and spectral band width make the period distribution predicted by that model to deviate more from the observed, indicating that the period distribution in shallow waters is independent of the non-linearities and width of the spectrum.

The joint distribution of zero-crossing wave heights and periods deviate from symmetry. Though the shape of the distribution resembles with CNEXO and Longuet-Higgins' modified forms, the modes are incorrectly placed by these models. The Rayleighean models fail to simulate the joint distribution in most of the cases. Tayfun's model predicts the modes of the distribution close to the observed. Best results are obtained with this model in the H_s range of 0.25-1.75 m. The CNEXO model modified with r(H,T) improves the model and makes it capable of simulating the joint distribution correctly for those cases with higher energy and lower periods. For higher energy cases, where the Tayfun's model fails, this modified form of CNEXO can be used, if T_z is in the range 8-12 s, which is the case with the monsoonal/storm waves. That is, the Tayfun's model can be used for the low fair weather waves and the modified CNEXO model can be used for the high energy monsoonal waves, to determine the joint distribution.

179

7.2. RECOMMENDATIONS FOR FURTHER RESEARCH

The wave climate at this location during the rough season is found to be controlled by the monsoonal waves generated in the Arabian Sea. During the fair season waves from 2 distinct and far-away locations contribute to the wave climate here. Similar observations have been made for some other locations along the west coast of India . A comprehensive study involving wave generation and propagation with directional spreading is required to identify these generating areas. This will enable to predict the wave climate and their characteristics from the meteorological parameters which are now readily available, thanks to the remote sensing satellite.

The function used to compensate the attenuation of wave pressure with depth for the computation of the surface wave height and spectrum is derived from the linear wave theory. Deviations from this theory is identified by many researchers and a scale factor (usually called 'instrument factor') is recommended. Different values ranging from 1 to 1.5 are proposed for this factor. Moreover, some studies indicate that this factor is not a constant, but is a function of frequencies. In order to solve this problem and to arrive at a more correct expression to compensate the

pressure attenuation with depth further research is warranted. Also, it has to be examined whether the scale factor is also a function of wave heights and periods and will it be sufficient to modify the scale factor to accurately compute the surface wave heights and spectrum.

The new PMK spectral model proposed in this study could be tested only for waves with significant height $\leq$ 2.5 m with peak periods in the middle range. Verification of this model at other locations with different environmental conditions, especially with different bottom slopes and wider range of wave heights, periods and spectral widths has to be carried out.

Almost all the spectral models assume constant value of slope for the high frequency side of the spectrum for all energy conditions. In the analysis of the average spectra computed for different intervals of energies, it is observed that the slope is proportional to the energy. Further studies are required to understand the intricacies in the spectral slope-energy dependence.

The waves in shallow waters may contain both breaking and broken components. The short-term distribution of wave heights is influenced by these components. Goda (1970) proposed a 'breaker index' to determine these waves. The suggested constants and coefficients appear to vary for

different locations. Calibration of this model and modification, if necessary, have to be carried out for different environmental conditions. This will help to determine the distribution of heights and their joint distribution with periods in shallow waters more accurately.

REFERENCES

REFERENCES

Aranuvachapun,S. (1987). Parameters of JONSWAP spectral model for surface gravity waves-I. Monte Carlo simulation study. Ocean Engng., Vol.14, pp.89-100.

Arhan,M. and Ezraty,R. (1975). Saisie et analyse de Donnees des courants particulaires au voisinage du fond dans La Houla litttorale proche du deferlement., La Houille blanche No.7/8, pp.484-496.

Baba,M. (1983). Wave climate at selected locations along the southwest coast of India, Paper presented in the 19th General Assembly of IUGG, Hamburg.

Baba,M. (1985). Long-term wave monitoring along the Kerala Coast - some results. Proc. Nat. Conf. Dock and Harbour Engng., Bombay, pp.E-49-67.

Baba,M., Kurian,N.P., Hameed,T.S.S., Thomas,K.V. and Harish,C.M. (1987). Temporal and spatial variations in wave climate off Kerala, southwest coast of India. Indian J. Mar. Sci., Vol.16, pp.5-8.

Baba,M. and Harish,C.M. (1985). Wave height and period distribution off the southwest coast of India, Indian J. Mar. Sci., Vol.14, pp.1-8.

Baba,M. and Harish,C.M. (1986). Wave energy spectra for the southwest coast of India, Indian J. Mar. Sci., Vol.15, pp.144-152.

Baba,M., Harish,C.M. and Kurian,N.P. (1986). Influence of record length and sampling interval on ocean wave spectral estimates. Mahasagar - Bull. Nat. Inst. Oceanogr., Vol.19, pp.79-85.

Battjes,J.A. (1974). Surf similarity. Proc. 14th Coastal Engng. Conf., ASCE, Vol.1, pp.466-480.

Battjes,J.A. (1977). Probabilistic aspects of ocean waves, Communications on hydraulics, Department of Civil Engineerig, Delft University, Tech. Rep. No.77-2, 52pp.

Battjes,J.A., Zitman,T.J. and Holthuijsen,L.H. (1987). A reanalysis of the spectra observed in JONSWAP. J. Phys. Oceanogr., Vol.17, pp.1288-1295.

183

Bergan,A.O., Torum,A. and Traetteberg,A. (1968). Wave measurements by a pressure type wave gauge. Proc. 11th Coastal Engng. Conf., ASCE, Vol.1, pp.19-29.

Bhat,S.S. (1986). Short-term analysis of wave parameters - A case study, M.Tech. Thesis, Mangalore University.

Black,K.P. (1978). Wave transformation over shallow reef (Field measurement and data analysis), Tech. Rep. No.78-42, J.K.K. Look Laboratory of Oceanographic Engineering, University of Hawai.

Blackman,R.B. and Tukey,J.W. (1958). The measurement of power spectra. Dover Publications, New York.

Boisvert,W.E. (1966). Ocean currents in the Arabian Sea and North Indian Ocean. US Naval Oceanographic Office, Washington, D.C.

Bona,J.L., Pritchard,W.G. and Scott,L.R. (1981). An evaluation of a model equation for water waves, Phil. Trans. Royal Society, A 302, pp.457-510.

Bouws,E., Gunther,H. Rosenthal,W. and Vincent,C.L. (1985). Similarity of the wind wave spectrum in finite depth water - I: spectral form, Jounal of Geophysical Research, Vol.90 (C1), pp.975-986.

Bretschneider,C.L. (1959). Wave variability and wave spectra for wind-generated gravity waves, U.S. Army Corps of Engineers, Beach Erosion Board, Tech. Memo No.118, 192pp.

Bretschneider,C.L. (1963). A one-dimensional gravity wave spectrum, In: Ocean Wave Spectra, Prentice-Hall Inc., N.J., pp.41-56.

Bretschneider,C.L. (1977). On the determination of design wave spectrum. Bull. Look Laboratory, Honolulu, Vol.7, pp.1-23.

Burling,R.W. (1963). Discussion on 'The one-dimensional wave spectrum in the Atlantic Ocean and in coastal waters, In: Ocean Wave Spectra, Prentice-Hall Inc., N.J., pp.31-32.

Cartwright,D.E. and Longuet-Higgins,M.S. (1956). The statistical distribution of the maxima of a random function, Proc. Royal Society, Ser.A-237, pp.212-232.

184

Chakraborti,S.K. (1986). Unification of two-parameter energy spectrum models, J. Wat. Port, Coastal and Ocean Engng., Vol.112(1), pp.173-176.

Chakraborti,S.K. and Cooley,R.P. (1977). Statistical distributions of periods and heights of ocean waves, J. Geophys. Res., Vol.82 (9), pp.1363-1368.

Chakraborti,S.K. and Snider,R.N. (1974). Wave statistics for March 1968 North Atlantic storm. J. Geophys. Res., Vol.79 (24), pp.3449-3458.

Cizlak,A. and Kawalski,T. (1969).Wave pressure attenuation. Proc. 22nd International navigation Congress, Paris.

Cooley,J.W. and Tukey, J.W. (1965). An algorithm for the machine calculation of complex Fourier series. math. Comput., Vol.19, pp.297-30l

Darbyshire,J. (1952). The generation of waves by wind. Proc. Royal Society, Ser.A-215, pp.299-328.

Darbyshire,J. (1959). A further investigation of wind generated waves. Deut. Hydrogr. Zeit, Vol.12(1), pp.7-13.

Darbyshire,J. (1963). The one-dimensional wave spectrum in the Atlantic Ocean and in coastal waters. In: Ocean Wave Spectra, Prentice Hall Inc. N.J., pp.27-31.

Darlington,C.R. (1954). The distribution wave heights and periods in ocean waves. Quar. J. Royal Soc.,Vol.80, pp.27-31.

Dattatri,J. (1973). Waves off Mangalore Harbour-West Coast of India. J.Wat. Harbour Div., ASCE, Vol.99, pp.39-58.

Dattatri,J. (1978). Analysis of regular and irregular waves and perfomance characteristics of submerged breakwaters, Ph.D thesis, IIT, Madras.

Dattatri,J. (1985). Comparative study of zero up-crossing and zero down-crossing methods of wave record analysis. Proc. 1st Nat. Conf. Dock Harbour Engng., IIT, Bombay, pp.E81-86.

Dattatri,J. (1987). Ocean wave spectra with multiple peaks - an analysis. Proc. Symposium on short-term variability of phys. oceanogr. features in the Indian waters. NPOL, Cochin, pp.187-189.

Dattatri,J., Jothisankar,N., and Raman,H. (1977). Comparison of Scott spectra with ocean wave spectra. J. Wat. Port Costal and Ocean Engng., ASCE, Vol.103, pp.375-378.

Dattatri,J., Jothisankar,N., and Raman,H. (1979). Height and Period distributions of waves off Mangalore harbour - West coast of India. J. Geophys. Res., Vol.84, pp.3767-3772.

Deo,M.C. (1979). Probabilistic analysis ocean waves- a study. M.Tech thesis, IIT, Madras.

Deo,M.C. and Narsimhan,S. (1979). Probablistic analysis of ocean waves-a study. Report Indian Inst. Tech.,Bombay.

Draper,L. (1967). The analysis and presentation of wave data - a plea for uniformity. Proc. 10th Conf. Coastal Engng., ASCE, Vol.1, pp.1-11.

Ezraty,R., Laurent,M., and Arhan,M. (1977). Comparison with observation at sea of period on height dependent sea state parameters from a theoretical model. OTC 2744, 9th offshore Tech. conf., Houston, pp.149-154.

Forristall,G.Z. (1978). On the statistical distribution of wave heights in a storm. J. Geophys. Res., Vol.83, pp.2353-2358.

Forristall,G.Z. (1981). Measurements of a saturated range in ocean wave spectra. J. Geophys. Res., Vol.83, pp.8075-8084.

Forristall,G.Z. (1984). The distribution of measured and simulated wave heights as a function of spectral shape. J. Geophys. Res., Vol.89, pp.10547-10552.

Gluhovskii,B.H. (1968). Distribution characteristics of wave parameters and changes in wave action with depth (in Russian). Rep. St. Inst. Oceanology, Moscow, Vol.93, pp.98-111.

Goda,Y. (1970). A synthesis of breaker indices. Trans. Japan Soc. Civil Engineers, Vol.2, part 2, pp.227-230.

Goda,Y. (1974). Estimation of wave statstics from spectral information. Proc. Int. Symp. Wave Measurement and analysis, ASCE, Vol.1., pp.320-337.

Goda,Y. (1975). Irregular wave deformation in the surf zone. Coastal Engng. in Japan, Vol.18, pp.13-26.

Goda,Y. (1978). The observed joint distribution of the periods and heights of sea waves. Proc. 16th Int. Conf. Costal Engng., Hamburg, Vol.I, pp.227-246.

Goda,Y. (1979). A review on statistical interpretation of wave data. Rep. of the Port and Harbour Research Institute, Vol.18(1), pp5-32.

Goda,Y. (1983). Analysis of wave grouping and spectra of long-travelled swell. Rep. Port Harbour Research Institute. Vol.22(1), pp.3-11.   .

Goodknight,R.C., and Russel,T.L. (1963). Investigation of the statistics of wave heights. J. Wat. Harbour Div.(ASCE), Vol89, pp.29-54.

Gospodnetic,D. and Miles,M.D. (1974). Some aspects of the average shape of wave spectra at station 'India' ($50^\circ N$, $19^\circ W$). Proc. International Symp. Dynamics Marine Vehicles and Structures in Waves (IMECHE '74), Inst. Mech. Engineers, pp.19-32.

Grace,R.A. (1978). Surface wave heights from pressure records. Coastal Engng., Vol.2, pp.55-67.

Harish,C.M., and Baba,M. (1986). On spectral and statisical characteristics of shallow water waves. Ocean Engng., Vol.13(3)., pp.239-248.

Harris,D.L. (1972). Characteristics of wave records in coastalzone. In: Waveson beaches and resulting sediment transport, Academic press, Inc., pp.1-47.

Harris,D.L. (1974). Finite spectrum analysis of wave records. Proc. International Conf. Ocean Wave Measurements and Analysis, ASCE, pp.107-124.

Hasselmann,K, Barnett,T.P., Bouws,E., Carlson,H., Cartwright,D.C., Enke,K., Ewing,J. Gienapp,H., Hasselman,D.E., Richter,K., Sell,W. and Walden,H. (1973). Measurement of wind-wave grouth and swell decay the Joint North Sea wave Project (JONSWAP). Deutsches Hydrographisches Zeit, Suppl. A, Vol.8(12), 95pp.

Hasselmann,K., Ross,D.B., Miller,P. and Sell,W. (1976). A parametrical wave prediction model. J. Phys. Oceanogr., Vol.6, pp.201-228.

Hoffman,D. (1974). Analysis of measured and calculated spectra. Proc. Int. Symp. Dynamics Mar. Vehicles Structures Waves (IMECHE '74), pp.8-18.

Homma,M., Horikawa,K. and Komari,S. (1966). Response characteristics of underwater wave gauge. Proc. 10th Coastal Engng. Conf., ASCE, Vol.1,pp.99-114.

Houmb,O.G. and Overik,T. (1976). Parameterization of wave spectra and long term joint distribution of wave height and period. Proc. Behaviour Offshore Structures (BOSS '76), Trondheim, Norway, Vol.1, pp.144-169.

Huang,N.E., and Long,S.R. (1980). An experimental study of the surface deviation probability distribution and statistics of wind generated waves. J. Fluid Mech., Vol.101, pp.179-200

Huang,N.E., Long,S.R., Tung,C.C., and Bliven,L.F. (1981). A unified two-parameter wave spectral model for general sea state. J. Fluid Mech. Vol.112, pp.203-224.

Huang,N.E., Long,S.R., Tung,C.C., Yuan,Y. and Bliven,L.F. (1983a). A non-gaussian statistical model for surface elevation of nonlinear random wave fields. J. Geophys. Res., Vol.88, pp.7597-7606.

Huang,N.E., Long,S.R., Tung,C.C., Yuan,Y. and Bliven,L.F. (1983b). A study on the spectral models for waves in finite water depth. J. Geophys. Res., Vol.88, pp.9579-9587.

Ibrageemov,A.M. (1973). Investigation of the distribution functions of wave parameters during their transformation. Oceanology, Vol.13(4), pp.584-589.

Irie,I. (1975). Examinaion of wave deformation with field observation data. Coastal Engng. in Japan, Vol.18, pp.27-34.

Iwata,K. (1980). Wave spectrum changes due to shoaling and breaking: I, Minus-three-power-law on frequency spectrum. Osaka Univ., Tech. Rep. Vol.30, pp.269-278.

Jensen,R.E. (1984). Shallow-water spectral wave modelling. Proc. 19th Int. Conf. Coastal Engng., ASCE, Houston, Texas, Vol.I, pp.547-560.

Joseph,P.S., Kawai,S., and Toba,Y. (1981). Ocean wave prediction by a hybrid model - combination of single-parameterized wind waves with spectrally treated swells. Sci. Rep. Tohoku Univ. Ser.5, Vol.28(1), pp.27-45.

Kahma,K.K. (1981). A study of the growth of the wave spectrum with fetch. J. Phys. Oceanogr., Vol.11, pp.816-827.

Kinsman,B. (1965). Wind waves, Prentice Hall Inc., N.J.,676pp.

Kitaigorodskii,S.A. (1962). Applications of the theory of similarity to the analysis of wind-generated wave motion as a stochastic process. Izv. Geophs. Ser. Acad. Sci. U.S.S.R. Vol.1, pp.105-117.

Kitaigorodskii,S.A. (1983). On the theory of Equilibrium range in the spectrum of wind-generated gravity waves. J. Phys. Oceanogr., Vol.13, pp.816-827.

Kitaigorodskii,S.A., Krasitskii,V.P., and Zaslavskii,M.M. (1975). On Phillips theory of equilibrium range in the spectra of wind generated waves. J. Phys. Oceanogr., Vol.5, pp.410-420.

Kowles,C.E. (1982). On the effects of finite depth in wind-wave spectra: 1. A comparison with deep-water equilibrium-range, slope and other spectral parameters. J. Phys. Oceanogr., Vol.12, pp.556-568.

Koele,L.A. and De Bruyn, P.A. (1964). Statistical distribution of wave heights in correlation with energy spectrum and water depth. Proc. 9th Costal Engng. Cof., pp.123-139.

Krilov,U.M. (1956). Rep. St. Inst. Oceanology, Moscow, Vol.33, pp.30

Kuo,C.T. and Kuo,S.J. (1975). Effect of wave breaking on statistical distributions of wave heights. Proc. Civil Engineering in the Oceans-III, Delaware, pp.1211-1231.

Kurian,N.P. (1987). Wave height and spectral transformation in the shallow waters of Kerala Coast and their prediction. Ph.D. Thesis, Cochin Univ. Sci. Tech.

Kurian,N.P., Baba,M. and Hameed,T.S.S. (1985a). Prediction of nearshore wave heights using a refraction programme. Coastal Engng., Vol.9, pp.347-356.

Kurian,N.P., Hameed,T.S.S. and Baba,M. (1985b). A study of monsoonal beach processes around Alleppey, Kerala. Proc. Indian Acad. Sci. (Earth Planet. Sci.), Vol.94, pp.323-332.

Lee,T.T. and Black,K.P. (1978). Energy spectra of surf waves on a coral reef. Proc. 16th Coastal Engng. Conf. ASCE, Hamburg, Vol.1, pp.588-608.

Liu,P.C. (1983). A representation for the frequency spectrum of wind-generated waves. Ocean Engng. Vol.10, pp.429-441.

Liu,P.C. (1984). On a design wave spectrum. Proc. 19th Coastal Engng. Cof. Vol.I, pp.362-369.

Liu,P.C. (1985). Representing frequency spectra for shalllow water waves. Ocean Engng. Vol.12(2), pp.151-160.

Liu,P.C. (1987). Assessing wind wave spectrum representations in shallow lake. Ocean Engng. Vol.14, pp.39-50.

Longuet-Higgins,M.S. (1952). On the statistical distribution of the heights of sea waves. J. Mar. Res., Vol.11(3), pp.245-266.

Longuet-Higgins,M.S. (1957). The statistical analysis of a random moving surface. Phil. Trans. Royal Soc. London, Ser. A, Vol.249, pp.321-387.

Longuet-Higgins,M.S. (1963). The effect of non-linearities on statistical distributions in the theory of sea waves. J. Fluid Mech., Vol.17, pp.459-480.

Longuet-Higgins,M.S. (1975). On the joint distribution of the periods and amplitudes of sea waves. J. Geophys. Res., Vol.80(18), pp.2688-2694.

Longuet-Higgins,M.S. (1980). On the distribution of the heights of sea waves: some effects of nonlinearity and finite band width. J. Geophys. Res., Vol.85, pp.1519-1523.

Longuet-Higgins,M.S. (1983). On the joint distribution of wave periods and amplitudes in a random wave field. Proc. Royal Society, Vol.A389, pp.241-258.

Manohar,M., Mobarek,I.E, Marcos,A., and Rahul,H. (1974). Wave statistics along the northern coast of Egypt.

Mc Clain,C.R., Chen,D.T., and Hart,W.D (1982). On the use of laser profilometry for ocean wave studies. J. Geophys. Res., Vol.87, pp.9509-9515.

Mitsuyasu,H. (1969). On the growth of the spectrum of wind-generated waves (II). Rep. Res. Inst. Applied Mech., Kysusha University, Vol.17, pp.235-248.

Munk,W.H., and Arthur,R.S. (1951). Forecasting ocean waves, Compendium of meteorology, Amer. Met. Soc. pp.1082-1089.

Narasimhan,S. and Deo,M.C. (1979a). Spectral analysis of ocean waves - a study. Proc. Conf. Civil Engng. Oceans IV, ASCE, San Fransisco, Vol.2, pp.888-891.

Narasimhan,S. and Deo,M.C. (1979b). Spectral analysis of ocean waves - a study. Proc. Int. Conf. Computer applications in Civil engineering. Roorkee, pp.V7-V12.

Neumann,G. (1953). On ocean wave spectra and a new method of forecasting wind generated sea. Tech. memo 43, Beach Erosion Board, USA.

Ou,S.H. (1977). Pararmetric determination of wave statistics and wave spectrum of gravity waves. Nat. Cheng Kung University, Taiwan, Dissertation No.1-98pp.

Ou,S.H. (1980). The equlibrium range in the frequency spectra of the wind generated gravity waves, Proc. 4th Conf. on Ocean Engng. in the Rep. of China, Sept.1980.

Ou,S.H. and Tang,F.L.W (1974). Wave characteristics in the Taiwan Straits. Proc. Int. Conf. on Wave Measurements and Analysis, Vol.II, pp.139-158.

Phillips,O.M. (1958). The equilibrium range in the spectrum of wind generated gravity waves. J. Fluid Mech., Vol.4, pp.426-434.

Phillips,O.M. (1977). The dynamics of the upper Ocean. Cambridge University Press.

Pierson,W.J. and Marks,W. (1952). The power spectrum analysis of ocean-wave records. Trans. Amer. Geophys. Union, Vol.33, pp.834-844.

Pierson,W.J. and Moskowitz,L. (1964). A proposed spectral form for fully developed wind seas based on the similarity theory of S.A.Kitaigorodskii. J. Geophys. Res., Vol.69, pp.5181-5190.

Prasad,N.G. (1985). Analysis of waves off Karwar- West Coast of India. M.Tech. Thesis, Mangalore University.

Putz,R.R. (1952). Statistical Distributions of ocean waves. Trans. Amer. Geophys. Union, Vol.33, pp.685-692.

Rachel,C.E. (1987). Analysis of shallow water waves off Calicut: west coast of India. Dissertation, Mangalore University, Mangalore.

Rayleigh,J.W.S. (1880). On the resultant of a large number of vibrations of the same pitch and of arbitrary phase. Philosophical Magazine, Vol.10, pp.73-78, Reprinted in Scientific Papers, Dover, 1964.

Rice,S.O. (1944). Mathematical analysis of random noise, Part I-IV, The Bell System Tech. J., Vol.23, pp.282-332.

Rice,S.O. (1945). Mathematical analysis of random noise, Part I-IV, The Bell System Tech. J., Vol.24, pp.46-156.

Rudnick,P. (1951). Correlograms for Pacific Ocean Waves. Proc. Second Berkeley Symposium on Mathematical Statistics and Probability, pp.627-638.

Rye,H. (1976). 'Discussion on parameterization of wave spectra'. Proc. Behaviour Offshore Structures (BOSS '76), Trondheim, Norway.

Rye,H. (1979). Wave parameter studies and wave groups. Proc. International Conf. Sea Climatology, Paris, pp.89-112.

Rye,H. (1982). Ocean wave groups. Dept. Mar. Tech., Norwegian Inst. Tech., Rep. UR-82-18, 214pp.

Saji,A. (1987). Analysis of waves off Cochin: west coast of India. M.Tech. dissertation, Mangalore University.

Sawaragi,T. and Iwata,K. (1976). Wave spectrum of breaking wave. Proc. 15th Coastal Engng. Conf., ASCE, Vol.1, pp.580-594.

Scott,J.R. (1965). A sea spectrum for model tests and long-term ship prediction. J. Ship Res., Vol.9(3), pp.145-152.

Scarborough,J.B. (1966). Numerical mathematical analysis. Oxford and IBH Publishing Co., Calcutta.

Seiwell,H.R. (1948). Results of research on surface waves of the western North Atlantic, Paper Phys. Oceanogr. Met., Vol.10(4).

Shadrin,I.F. (1982). Deformed wave spectrum in the coastal zone. Oceanology, Vol.22, pp.694-696.

Shum,K.T. and Melville,W.K. (1984). Estmates of the joint statistics of amplitudes and periods of ocean waves using an integral transform technique. J.Geophys. Res., Vol.89, pp.6467-6476.

Silvester,R. (1974). Coastal Engineering, Vol.1 - Generation, propagation and influence of waves, Elsevier Publishing Company, 457pp.

Sivadas,T.K. (1981). A tide and wave telemetering system, Pro. 1st Indian Conf. Coastal Engng., Madras, Vol.1, pp.VII:57-60.

Srokosz,M.A. (1988). A note on the joint distribution of wave height and period during the growth phase of a storm. Ocean Engng., Vol.15, pp.379-387.

Srokosz,M.A. and Challenor, P.G. (1987). Joint distribution of wave height and period: a critical comparison. Ocean Engng., Vol.14, pp.295-311.

Sundar,V. (1986). Studies on analysis of ocean wave records off Madras. Proc. 3rd Indian Conf. Ocean Engng. Vol.I, pp.A191-A201.

Tang,F.L.W., Chen,Y.Y. and Lin,S.C (1985). Probability density function of surface elevation and wave height of random sea considering nonlinear effect. Proc. Int. Symp. Ocean Space Utilization '85, Tokyo, pp.165-172.

Tayfun,M.A. (1977). Linear random waves on water of nonuniform depth. Ocean Engng Rep. No.16, Part II, Dept. of Civil Engineering, University of Delaware, Newark, D.E (Ref. Coastal Engng. Conf. 1978 Proc.)

Tayfun,M.A. (1980). Narrow-band nonlinear sea waves. J.Geophys. Res. Vol.85, pp1548-1552.

Tayfun,M.A. (1981). Distribution of crest-to-trough wave heights. J. Wat. Port Coastal Ocean Div., ASCE, Vol.107, pp.149-158.

Tayfun,M.A. (1983a). Nonlinear effects on the distribution of crest-to-trough wave heights. Ocean Engng. Vol.10(2), pp.97-106.

Tayfun,M.A. (1983b). Effect of ‛spectrum bandwidth on the distribution of wave heights and periods. Ocean Engng., Vol.10(2), pp.107-118.

Thomas,K.V. and Baba,M. (1983). Wave climate off Valiathura, Trivandrum. Mahasagar - Bull. Nat. Inst. Oceanogr. Vol.16, pp.415-421.

Thompson,E.F. (1974). Results from the CERC wave measurement programme. Proc. Int. Symp. On Wave Measurements and Analysis, ASCE, pp.836-855.

Thompson,E.F. (1980). Energy spectra in shallow US Coastal waters. US Army, Corps of Engrs., Coastal Engng. Res. Centre, Tech. Paper No.80-2, 149pp.

Thompson,E.F. and Harris,D.L. (1972). A wave climatology for US Coastal waters. US Army, Corps of Engrs., Coastal Engng. Res. Centre, Reprint 1-72.

Thornton,E.B. (1977). Rederivation of the saturation ranges in the frequency spectrum of wind generated gravity waves. J. Phys. Oceanogr. Vol.7, pp.137-140.

Thornton,E.B. (1979). Energetics of breaking waves within the surf zone. J. Geophys. Res., Vol.84, pp.4931-4938.

Thornton,E.B. and Schaeffer,G. (1978). Probability density functions of breaking waves. Proc. Int. Conf. Coastal Engng., Vol.I, pp.507-519.

Thornton,E.B. and Guza, R.T. (1983). Transformation of wave height distribution. J. Geophys. Res., Vol.88, pp.5925-5938.

Toba,Y. (1973). Local balance in the air-sea boundary processes,3, On the Spectrum of wind waves. J. Oceanogr. Soc. Japan, Vol.29, pp209-220.

Varkey,M.J. and Gopinathan,C.S. (1984). Programs for spectral and zero-up-crossing analysis of wave records. National Inst. Oceanogr., Goa, Tech. Rep. No.5/84.

Vincent,C.L. (1981). A Method for estimating depth-limited wave energy. CERC,CETA NO.81-16.

Vincent,C.L. (1982a). Shallow water wave modelling. 1st Int. Conf. Meteorol. air-sea interaction coast zone, Am. Meteorol. Soc., Haugiee.

Vincent,C.L. (1982b). Depth limited significant wave height: A spectral approach. CERC, Tech. Rep. No. 82-3.

Vincent,C.L. (1984). Shallow water waves. A spectral approch. Proc. 19th Int. Conf. Coastal Engng. Housten, Texas, Vol.I, pp.370-382.

Vincent,C.L., Gosskopf,W.G. and Mc Tamany (1982). Transformation of Storm wave spectra in shallow water observed during the ARSLOE storm. Proc. OCEANS '82, pp.920-925.

Watters,J.K.A. (1953). Distribution of height in ocean waves. New Zealand J. Sci. Tech., B, Vol.34, pp.408-422.

Weigel,R.L. (1949). An analysis of data from wave recorders on the Pacific Coast of the United States. Trans. Amer. Geophys. Union, Vol.30, pp.700-704.

Weigel,R.L. (1980). Design wave. Short-term course on small harbour Engng. Vol.1, pp.4.1-4.55.

Wilson,B.W., Chakraborti,S.K. and Snider,R.H. (1974). Spectrum analysis of Ocean Wave Records. Proc. Int. Symp. Wave Measurements and Analysis, Vol.I, pp.87-106.

Yoshida,K., Kajiura,K. and Hidaka,K. (1953). Preliminary report of the observation of ocean waves at Hachijo Island. Rec. Oceanogr. Works Japan, Ser 1,pp.81-87.

APPENDICES

Appendix-A Fitness of the Models for Height and Period Distributions.

No	RecNo	Date	H_{sw}	T_z	R1	Ty	C1	C2	Gd	Wb	G1	Ib	L1	L2
1	20129	01-Jan-81	0.73	10.3	T				H	H	H		H	H
2	20132	02-Jan-81	0.63	10.1	T			T	H	H	H			H
3	20135	03-Jan-81	0.67	8.2	T						H		H	H
4	20138	05-Jan-81	0.56	7.5	T				H	H	H		H	H
5	20142	06-Jan-81	0.60	7.9						H			H	H
6	20146	07-Jan-81	0.63	9.4	T	T		T	H	H	H		H	H
7	20149	08-Jan-81	0.95	10.3	T	T					H		H	H
8	20152	09-Jan-81	0.69	9.0							H	H	H	
9	20155	12-Jan-81	0.64	11.1	H,T	T	T	T	H	H	H		H	H
10	20159	13-Jan-81	0.60	8.6	T		T	T	H	H	H		H	H
11	20162	14-Jan-81	0.54	9.1	H,T	T				H	H		H	H
12	20165	15-Jan-81	0.36	8.6								H	H	
13	20168	16-Jan-81	0.34	7.4	T					H	H	H	H	H
14	20171	17-Jan-81	0.32	8.5	T	T	T		H	H	H	H	H	H
15	20175	20-Jan-81	0.79	9.0	H,T	T				H	H	H	H	H
16	20179	21-Jan-81	0.64	9.0	T	T			H	H	H		H	H
17	20182	22-Jan-81	0.56	10.0	T			T	H	H	H		H	H
18	20185	23-Jan-81	0.63	10.7	T			T		H	H		H	H
19	20188	24-Jan-81	0.62	9.8	T	T			H	H	H		H	H
20	20192	27-Jan-81	0.95	11.1	H,T	T	T	T	H	H	H		H	H
21	20196	28-Jan-81	0.87	10.5	H,T	T	T	T	H	H	H			H
22	20199	29-Jan-81	0.59	10.0	T		T	T	H	H	H		H	H
23	20202	30-Jan-81	0.48	10.9	T	T	T					H		
24	20204	10-Feb-81	0.63	9.2	T	T				H	H	H	H	
25	20207	11-Feb-81	0.54	7.5	T		T	T	H	H	H		H	H
26	20210	12-Feb-81	0.42	9.2	H,T	T		T	H	H	H		H	H
27	20213	13-Feb-81	0.67	9.5	H,T	T	T	T	H	H	H		H	H
28	20216	16-Feb-81	0.49	8.5	T	T		T	H	H	H		H	H
29	20220	07-Feb-81	0.51	8.3	H,T	T	T	T	H	H	H		H	H
30	20223	18-Feb-81	0.45	9.0	H,T	T	T		H	H	H		H	H
31	20228	19-Feb-81	0.59	11.5	T	T	H,T	T	H	H	H		H	H
32	20232	20-Feb-81	0.45	10.9	H,T	T	T			H	H		H	H
33	20235	21-Feb-81	0.47	11.7	H,T	T	T	T	H	H	H			H
34	20238	23-Feb-81	0.51	12.7	H,T		H,T	T	H	H	H		H	H
35	20243	24-Feb-81	0.76	11.9	T	H,T		T			H	H		H
36	20247	25-Feb-81	0.61	10.9	H,T	T	T	T	H	H	H		H	H
37	20250	26-Feb-81	0.61	10.9	H,T	T	T	T	H	H	H		H	H
38	20253	27-Feb-81	0.70	9.4		T					H		H	H
39	20255	28-Feb-81	0.64	9.7	T	T		T	H	H	H		H	H
40	20258	02-Mar-81	0.57	9.5	T		T	T	H	H	H		H	H
41	20262	03-Mar-81	0.57	11.5	T	T	T	T	H	H	H		H	H
42	20265	04-Mar-81	0.67	9.0									H	
43	20267	05-Mar-81	0.98	11.5	T		T	T	H	H	H		H	H
44	20270	06-Mar-81	0.72	11.9	H,T	T	H,T	T	H	H	H		H	H
45	20273	07-Mar-81	0.75	11.9	H,T		H,T	T	H	H	H		H	H
46	20275	09-Mar-81	0.52	10.9	T		T	T	H	H	H		H	H
47	20279	10-Mar-81	0.58	11.9	T	T			H	H	H		H	H
48	20283	11-Mar-81	0.70	12.7									H	
49	20285	12-Mar-81	0.55	11.1	H,T	T	T	T	H	H	H		H	H
50	20287	13-Mar-81	0.66	12.2	H,T	T		T	H	H	H			H
51	20290	16-Mar-81	0.58	10.1	T	T		T	H	H	H		H	H
52	20294	17-Mar-81	0.56	9.5	T	T	T	T	H	H	H		H	H
53	20298	18-Mar-81	0.54	10.1	T		T	T	H	H	H		H	H
54	20301	19-Mar-81	0.55	9.8	T	T			H	H	H		H	H
55	20304	20-Mar-81	0.57	7.3	T		T	T	H	H	H		H	H

No	RecNo	Date	Hsw	Tz	R1	Ty	C1	C2	Gd	Wb	Gl	Ib	L1	L2
56	20307	21-Mar-81	0.53	7.8	T	T	T	T	H	H	H		H	H
57	20310	23-Mar-81	0.55	9.8	T	T		T	H	H	H		H	H
58	20315	24-Mar-81	0.52	10.0	H,T	T	T	T	H	H	H		H	H
59	20316	25-Mar-81	0.51	9.7	T	T				H	H		H	H
60	20318	26-Mar-81	0.64	10.1	H,T	T	T	T	H	H	H		H	H
61	20321	27-Mar-81	0.60	10.9	T	T		T	H	H	H		H	H
62	20324	28-Mar-81	0.65	10.9	H,T	T	T	T	H	H	H		H	H
63	20326	29-Mar-81	0.66	10.7	H,T	T	H,T	T	H	H	H		H	H
64	20328	30-Mar-81	0.55	10.3	T	T	T					H	H	
65	20332	31-Mar-81	0.54	9.1	T		T	T	H	H	H		H	H
66	20336	01-Apr-81	0.62	8.1	T		T	T	H	H	H		H	H
67	20338	02-Apr-81	0.66	6.4	T			T	H	H	H		H	H
68	20341	03-Apr-81	0.79	6.8		T				H	H	H		
69	20345	04-Apr-81	0.78	8.7	T				H	H	H		H	H
70	20347	06-Apr-81	0.67	9.1	T					H	H		H	H
71	20352	07-Apr-81	0.53	7.2	H,T	T	T	T	H	H	H		H	H
72	20356	09-Apr-81	0.55	7.5	T	T	T			H	H		H	H
73	20359	09-Apr-81	0.62	8.3	T			T	H	H	H		H	H
74	20362	10-Apr-81	0.72	8.7	T	T				H	H		H	H
75	20366	13-Apr-81	1.07	10.5										
76	20370	15-Apr-81	0.86	11.7	T	T			H	H	H		H	H
77	20373	18-Apr-81	0.99	9.2	T	T			H		H	H	H	H
78	20375	20-Apr-81	0.99	11.9	H,T	T	T	T	H		H		H	H
79	20379	21-Apr-81	0.66	10.1	T	T	.		H	H	H			H
80	20382	22-Apr-81	0.81	8.8	T			T	H	H	H		H	H
81	20386	23-Apr-81	0.90	10.1	T				H	H	H		H	H
82	20389	24-Apr-81	0.78	9.0	T	T				H	H		H	H
83	20392	25-Apr-81	0.65	10.0	T	T				H	H		H	H
84	20394	27-Apr-81	0.69	11.3	H,T	T		T	H	H	H		H	H
85	20400	28-Apr-81	0.67	9.1	T	T			H	H	H		H	H
86	20403	29-Apr-81	0.79	9.5	T		T	T	H	H	H		H	H
87	20405	07-May-81	1.02	10.3	T	T	T	T	H	H	H		H	H
88	20407	08-May-81	1.15	10.5	T		T		H	H	H		H	H
89	20410	11-May-81	0.99	10.9	H,T	T					H		H	H
90	20415	12-May-81	1.21	11.9	H,T	T	T	T	H	H	H		H	H
91	20422	13-May-81	0.82	7.9	T			T	H	H	H		H	H
92	20425	13-May-81	0.81	9.5	T				H	H	H		H	H
93	20430	14-May-81	0.83	9.5	T			T	H	H	H		H	H
94	20436	15-May-81	0.74	8.0	T			T	H	H	H		H	H
95	20440	16-May-81	0.74	7.3	T				H	H	H		H	H
96	20442	17-May-81	0.95	7.9	T	T		T	H		H		H	H
97	20444	18-May-81	2.03	9.4	H,T	T		T	H	H	H		H	H
98	20445	18-May-81	1.70	8.5	T	T	T	T						
99	20446	18-May-81	1.68	9.1	T	T	T	T	H	H	H		H	H
100	20447	18-May-81	1.37	8.5	H,T	T	T			H	H		H	H
101	20448	18-May-81	1.16	8.0	H,T	H,T			H		H		H	H
102	20452	19-May-81	1.10	7.8	H,T	T	T	T	H		H		H	H
103	20460	20-May-81	1.51	7.5	H,T	H,T	T	T	H	H	H	H	H	H
104	20458	21-May-81	1.09	7.9	H,T	H,T	T				H	H	H	H
105	20476	22-May-81	1.16	8.6	H,T	H,T	T				H	H	H	H
106	20484	23-May-81	1.58	9.5	T			T	H	H	H		H	H
107	20492	24-May-81	1.62	9.8	T	H,T		T	H	H	H	H	H	H
108	20500	25-May-81	1.01	9.1	T				H		H		H	H
109	20508	26-May-81	1.21	9.2	H,T	H,T	H,T	T	H		H		H	H
110	20516	27-May-81	1.30	9.0	H,T	T	T	T	H	H	H		H	H

No	RecNo	Date	Hsw	Tz	R1	Ty	C1	C2	Gd	Wb	Gl	Tb	L1	L2
111	20524	28-May-81	1.36	9.0	T	H,T					H		H	H
112	20532	29-May-81	1.41	9.0	H,T	H,T	T				H		H	H
113	20540	30-May-81	1.86	7.9	H,T	H,T			H	H	H		H	H
114	20548	31-May-81	1.41	7.9	H,T	T	T	T	H	H	H		H	H
115	20549	31-May-81	1.41	8.2	H,T	T	T	T	H	H	H		H	H
116	20552	31-May-81	1.42	8.1	H,T	T	H,T	T	H	H	H		H	H
117	20553	01-Jun-81	1.31	7.8	H,T	T	H,T	T	H	H	H		H	H
118	20554	01-Jun-81	1.55	7.9	H,T	H,T	T	T	H	H	H		H	H
119	20559	01-Jun-81	1.54	7.5	H,T	H,T	T	T	H	H	H	H	H	H
120	20562	02-Jun-81	1.31	7.2	H,T	T	T	T	H		H		H	H
121	20563	02-Jun-81	1.50	7.5	H,T	T	T	T	H	H	H		H	H
122	20564	02-Jun-81	1.47	8.1	T	T		T	H		H		H	H
123	20565	02-Jun-81	1.17	7.4	T	T					H		H	H
124	20566	02-Jun-81	1.32	7.2	H,T	T	T		H		H		H	H
125	20567	02-Jun-81	1.36	7.7	T	H,T	T	T	H		H		H	H
126	20568	02-Jun-81	1.53	7.3	H,T	H,T	T			H	H	H	H	H
127	20569	03-Jun-81	1.34	7.6	T				H		H		H	H
128	20570	03-Jun-81	1.47	7.6	T	H,T		T	H	H	H	H	H	H
129	20571	03-Jun-81	1.54	8.1	T	H,T	T	T	H	H	H	H	H	H
130	20572	03-Jun-81	1.42	7.5	T	H,T		T	H		H		H	H
131	20573	03-Jun-81	1.43	7.8	T		T	T	H	H	H		H	H
132	20574	03-Jun-81	1.76	7.4	H,T	H,T	T	T	H	H	H		H	H
133	20575	03-Jun-81	1.89	7.8	H,T	H,T	T			H	H		H	H
134	20576	03-Jun-81	1.58	7.3	H,T	H,T	T	T	H	H	H		H	H
135	20577	04-Jun-81	1.65	8.0	H,T	H,T	T	T	H	H	H	H	H	H
136	20578	04-Jun-81	2.04	7.2	H,T	T			H	H	H		H	H
137	20580	04-Jun-81	2.08	8.0	H,T	H,T	T		H	H	H	H	H	H
138	20581	04-Jun-81	1.89	8.0	H,T	H,T	T	T	H	H	H		H	H
139	20584	04-Jun-81	2.74	7.6	H,T	T	T	T	H	H			H	H
140	20586	05-Jun-81	2.23	7.9	T	T				H	H	H		
141	20596	06-Jun-81	1.66	8.0	T	H,T	T		H	H	H		H	H
142	20598	07-Jun-81	1.74	8.1	H,T	H,T	H,T	T	H	H	H		H	H
143	20605	08-Jun-81	1.39	8.8	T	T	H,T	T	H	H	H		H	H
144	20610	09-Jun-81	1.34	8.1	H,T	T	T	T	H	H	H		H	H
145	20616	10-Jun-81	1.12	7.5	T	T	T	T	H	H	H		H	H
146	20624	11-Jun-81	1.65	8.5	H,T	T	T	T	H	H	H		H	H
147	20632	12-Jun-81	2.25	8.5	H,T	H,T		T	H	H	H	H	H	H
148	20640	13-Jun-81	2.10	8.8	H,T	H,T	H,T		H	H	H		H	H
149	20648	14-Jun-81	2.65	8.1	T	H,T				H	H	H	H	
150	20658	15-Jun-81	2.28	8.3	T	H,T				H	H	H	H	
151	20659	15-Jun-81	2.30	8.1	H,T	T			H	H	H		H	H
152	20660	15-Jun-81	2.21	7.6	T	H,T	T	T	H	H	H		H	H
153	20664	16-Jun-81	2.44	9.4	T	H,T	T			H	H	H	H	
154	20670	17-Jun-81	2.53	8.7	T	T	T			H	H			
155	20678	18-Jun-81	2.16	9.1	H,T	H,T	T	T	H	H	H		H	H
156	20686	19-Jun-81	2.48	8.8						H	H		H	
157	20692	20-Jun-81	2.45	9.7	T	T				H	H	H		
158	20695	21-Jun-81	2.20	8.8	T	H,T	T			H	H	H		
159	20701	22-Jun-81	2.42	8.8	H,T	H,T	T	T	H	H	H		H	H
160	20709	25-Jun-81	2.16	9.2	T	T								
161	20717	24-Jun-81	1.66	8.5	T	T	T	T	H	H	H		H	H
162	20725	25-Jun-81	2.00	10.5	T	H,T	H,T	T	H	H	H		H	H
163	20733	26-Jun-81	2.19	10.5	H,T	T				H	H			H
164	20740	27-Jun-81	2.01	10.7	T	T	H,T	T	H	H		H		H
165	20747	28-Jun-81	0.93	9.8	H,T	T	T	T	H	H	H		H	H

No	RecNo	Date	Hsw	Tz	R1	Ty	C1	C2	Gd	Wb	Gl	Tb	L1	L2
166	20757	29-Jun-81	0.65	8.3	H,T	T	T	T	H	H	H		H	H
167	20764	30-Jun-81	0.48	8.9	T	T	T					H	H	H
168	20768	01-Jul-81	0.60	10.0	T	T	T				H		H	H
169	20776	02-Jul-81	0.67	10.0	H,T	T	T		H	H	H		H	H
170	20784	03-Jul-81	0.78	10.0	H,T			T	H	H	H		H	H
171	20792	04-Jul-81	0.85	9.4	H,T	T	T	T	H	H	H	H	H	H
172	20800	05-Jul-81	1.00	7.9	H,T	T			H		H		H	H
173	20808	06-Jul-81	1.34	7.2	H,T	T	T	T	H		H	H	H	H
174	20816	07-Jul-81	1.60	8.3	H,T	T	T	T	H	H	H		H	H
175	20824	08-Jul-81	1.46	7.9	H,T		T	T	H	H	H		H	H
176	20832	09-Jul-81	1.36	8.5	H,T	T	T	T	H	H	H		H	H
177	20840	10-Jul-81	1.20	8.3	H,T	T	T	T	H		H		H	H
178	20848	11-Jul-81	1.60	8.5	H,T	T	H,T	T	H	H	H		H	H
179	20855	12-Jul-81	1.48	8.3	H,T	T			H	H	H		H	H
180	20863	13-Jul-81	1.22	9.2	T	T					H		H	H
181	20871	14-Jul-81	1.03	8.6	H,T	T	H,T	T	H	H	H		H	H
182	20879	15-Jul-81	0.96	9.0	H,T	T	T	T	H	H	H		H	H
183	20887	16-Jul-81	0.67	7.6	H,T	T		T	H	H	H		H	H
184	20894	17-Jul-81	0.71	8.2	T	T			H	H	H		H	H
185	20902	18-Jul-81	0.58	9.2	H,T	T	T	T	H	H	H		H	H
186	20909	19-Jul-81	0.38	8.6		T					H	H	H	H
187	20916	20-Jul-81	0.44	7.2	H,T	T	T		H	H	H		H	H
188	20924	21-Jul-81	0.47	8.3	T	T			H	H	H		H	H
189	20931	22-Jul-81	0.80	9.0	T	T	T				H	H	H	H
190	20939	23-Jul-81	1.09	8.6	H,T	T	T	T	H		H		H	H
191	20947	24-Jul-81	1.48	8.1	H,T	T	T	T	H	H	H		H	H
192	20955	25-Jul-81	1.75	9.4	T	T				H	H	H	H	H
193	20963	26-Jul-81	2.17	10.3	H,T	T		T	H	H	H	H	H	H
194	20971	27-Jul-81	1.25	9.1	H,T	T	T	T	H		H		H	H
195	20975	29-Jul-81	1.50	11.3	H,T	H,T	T	T	H		H		H	H
196	20983	30-Jul-81	1.17	9.0	H,T	T	H,T	T	H		H		H	H
197	20991	31-Jul-81	1.68	9.5		H,T	T	T	H		H			
198	20995	01-Aug-81	1.33	9.5	H,T	H,T		T	H		H		H	H
199	21000	03-Aug-81	1.46	9.6	H,T	H,T			H		H			H
200	21008	04-Aug-81	1.77	10.6	T	H,T	T	T	H	H	H		H	H
201	21011	05-Aug-81	0.90	9.8	H,T	T	H,T	T	H	H	H		H	H
202	21019	06-Aug-81	0.71	8.6	T	T			H	H	H		H	H
203	21027	07-Aug-81	0.82	9.9	H,T	T	T	T	H	H	H		H	H
204	21035	08-Aug-81	0.88	9.4	T	T	T		H		H	H	H	H
205	21043	09-Aug-81	1.00	7.9	H,T	T	T		H		H		H	H
206	21051	10-Aug-81	2.32	9.8	H,T	H,T	H,T	T	H	H	H		H	H
207	21056	31-Aug-81	0.28	8.6	T	T				H	H		H	H
208	21060	01-Sep-81	0.64	11.5	H,T	T	T	T	H	H	H			H
209	21067	02-Sep-81	0.53	9.6	T	T	T	T	H	H	H		H	H
210	21074	03-Sep-81	0.24	8.3	H,T		T	T	H	H	H		H	H
211	21081	04-Sep-81	0.16	8.2										
212	21095	06-Sep-81	0.19	10.6	H,T		T	T	H	H	H		H	H
213	21101	07-Sep-81	0.61	7.9	T	T	T		H	H	H		H	H
214	21107	08-Sep-81	1.90	9.6	T	H,T	T	T	H	H	H		H	H
215	21115	09-Sep-81	1.24	8.7	T		T	T	H	H	H		H	H
216	21123	10-Sep-81	1.09	7.7	T		T	T	H	H	H		H	H
217	21131	11-Sep-81	1.24	9.4	T	H,T	H,T	T	H	H	H		H	H
218	21136	12-Sep-81	0.78	7.0	T	T		T	H	H	H		H	H
219	21144	13-Sep-81	1.28	8.2	H,T	H,T		T	H		H	H	H	H
220	21152	14-Sep-81	0.79	8.1	T	T			H		H	H	H	H

No	RecNo	Date	Hsw	Tz	R1	Ty	C1	C2	Gd	Wb	Gl	Ib	L1	L2
221	21159	15-Sep-81	0.56	7.9	T	T	H,T	Γ	H	H	H		H	H
222	21165	16-Sep-81	0.28	7.0	T	T				H	H	H	H	H
223	21173	17-Sep-81	0.28	8.3	T	T				H	H	H	H	
224	21181	18-Sep-81	0.56	7.8	T	T	T		H	H	H		H	H
225	21184	19-Sep-81	1.36	8.1	H,T	H,T	H,T	T	H	H	H		H	H
226	21192	20-Sep-81	1.45	8.1	H,T	H,T	H,Γ	Γ	H	H	H		H	H
227	21200	21-Sep-81	1.42	7.4	T	T	T							
228	21207	22-Sep-81	0.93	6.5		T				H	H	H	H	H
229	21215	23-Sep-81	0.84	6.9	H,T	T		Γ	H	H	H	H	H	H
230	21224	24-Sep-81	0.83	7.1	T				H	H	H		H	H
231	21231	25-Sep-81	0.52	7.2	T		H,T	Γ	H	H	H		H	H
232	21238	26-Sep-81	1.42	9.9	T	H,T	T	Γ	H		H	H	H	H
233	21246	27-Sep-81	1.19	10.4	T	H,T	T	Γ	H	H	H	H	H	H
234	21248	28-Sep-81	0.75	10.4	H,Γ	T	T		H	H	H		H	H
235	21256	29-Sep-81	0.44	9.1	T	T	T	Γ	H	H	H		H	H
236	21262	30-Sep-81	0.47	12.4	H,Γ		T	T	H	H	H			H
237	21270	01-Oct-81	0.36	12.7	T	T	H,T	Γ	H	H		H		H
238	21276	02-Oct-81	0.29	12.1	H,Γ			Γ	H	H	H		H	H
239	21284	03-Oct-81	0.36	12.4	H,T	T	H,Γ	Γ	H	H	H		H	H
240	21290	04-Oct-81	0.21	11.0	T									
241	21297	05-Oct-81	0.28	7.7	T				H	H	H		H	H
242	21305	06-Oct-81	0.17	9.9	T									
243	21320	08-Oct-81	0.20	12.1	H,T					H	H		H	H
244	21326	09-Oct-81	0.30	10.8	T		Γ	T	H	H	H		H	H
245	21334	10-Oct-81	0.40	12.7	H,T	T	Γ	T	H	H	H		H	H
246	21338	12-Oct-81	0.32	13.0	H,T	T	H,T	H,T	H	H	H	H	H	H
247	21350	14-Oct-81	0.43	13.0	H,T	T	H,T	H,T	H	H	H		H	H
248	21358	15-Oct-81	0.38	13.0	T			T	H	H	H		H	H
249	21366	16-Oct-81	0.24	13.7	H,T	T	Γ	Γ	H	H	H		H	H
250	21373	17-Oct-81	0.34		H,T				H	H	H		H	H
251	21381	18-Oct-81	0.29	11.8	H,T			T		H	H	H	H	H
252	21389	19-Oct-81	0.28	12.7	H,T		Γ			H	H	H	H	H
253	21397	20-Oct-81	0.51	11.8	T	T					H	H	H	H
254	21405	21-Oct-81	0.65	11.5	H,Γ	Γ	Γ	T	H		H	H	H	H
255	21413	22-Oct-81	0.69	11.8	H,T	T	T	Γ	H	H	H		H	H
256	21421	23-Oct-81	0.68	12.1	H,T		Γ		H	H	H	H	H	H
257	21429	24-Oct-81	0.59	11.5	H,T	T	T	T	H	H	H	H	H	H
258	21437	25-Oct-81	0.42	10.6	H,Γ	T	Γ	T	H	H	H		H	H
259	21444	26-Oct-81	0.47	9.8	T			T	H	H	H		H	H
260	21451	27-Oct-81	0.54	11.5	H,T	Γ	Γ	T	H	H	H		H	H
261	21456	28-Oct-81	0.58	10.4	H,T	T				H	H	H	H	H
262	21457	31-Oct-81	0.84	8.6	T	T	T				H	H		
263	21459	02-Nov-81	0.56	8.6	T	T	T	T	H	H	H		H	H
264	21466	03-Nov-81	0.43	8.5	H,T	T	H,Γ	T	H	H	H		H	H
265	21473	04-Nov-81	0.41	8.9	H,T	T	Γ	Γ	H	H	H		H	H
266	21476	05-Nov-81	0.32	9.4	T	T				H	H	H	H	H
267	21484	06-Nov-81	0.34	8.6	T		T	T	H	H	H	H	H	H
268	21492	07-Nov-81	0.26	8.5	T					H	H		H	
269	21500	08-Nov-81	0.27	10.4	T	T	Γ	Γ	H	H	H		H	H
270	21507	09-Nov-81	0.36	6.7	T		Γ	T	H	H	H	H	H	H
271	21514	10-Nov-81	0.22	7.7	T					H	H		H	
272	21522	11-Nov-81	0.17	9.5	T					H	H		H	
273	21530	12-Nov-81	0.14	7.5										
274	21537	13-Nov-81	0.18	7.6	T					H	H		H	
275	21545	14-Nov-81	0.21	10.1	T		T	T	H	H	H		H	H
276	21548	16-Nov-81	0.32	11.3	H,T	T	H,T	Γ	H	H	H	H	H	H

No	RecNo	Date	Hsw	Tz	Rl	Ty	C1	C2	Gd	Wb	Gl	Ib	L1	L2
276	21548	16-Nov-81	0.32	11.3	H,T	Г	H,Г	Г	H	H	H	H	H	H
277	21556	17-Nov-81	0.27	10.8	H,Г		Г	Г	H	H	H		H	H
278	21563	18-Nov-81	0.24	10.4	H,T	T	T	Г	H	H	H		H	
279	21571	19-Nov-81	0.21	8.2	T					H			H	H
280	21577	20-Nov-81	0.41	11.9	T					H	H		H	H
281	21581	21-Nov-81	0.60	12.4	T			T	H	H	H		H	H
282	21589	22-Nov-81	0.40	11.0	H,T	T				H	H		H	H
283	21597	23-Nov-81	0.22	9.8	H,T	T				H	H		H	
284	21605	24-Nov-81	0.26	8.5	H,T	T				H	H		H	H
285	21613	25-Nov-81	0.23	8.3	H,T			Г		H	H		H	H
286	21621	26-Nov-81	0.25	6.6	T					H	H		H	
287	21623	27-Nov-81	0.40	10.8	T	T		T	H	H	H		H	H
288	21627	28-Nov-81	0.34	9.6	T	T			H	H	H	H	H	H
289	21632	29-Nov-81	0.45	11.5	H,T	T	H,Г	T	H	H	H		H	H
290	21639	30-Nov-81	0.35	9.7	H,T	T			H	H	H	H	H	H
291	21646	01-Dec-81	0.37	10.6	H,T	T	H,Г	Г	H	H	H		H	H
292	21648	02-Dec-81	0.37	10.8	H,T	Г	Г	Г	H	H	H		H	H
293	21651	03-Dec-81	0.27	9.4	H,Г	T		Г		H	H		H	H
294	21657	04-Dec-81	0.25	9.8	H,T	T	Г			H	H		H	
295	21663	05-Dec-81	0.27	9.6	H,T					H	H		H	H
296	21670	06-Dec-81	0.28	8.2	T					H	H		H	H
297	21672	07-Dec-81	0.42	11.3	T	Г	T	Г	H	H	H		H	H
298	21680	08-Dec-81	0.71	10.1	T			T	H	H	H		H	H
299	21688	09-Dec-81	0.59	8.7	T	Г	Г	T	H	H	H		H	H
300	21696	10-Dec-81	0.46	9.4	H,T	T		T	H	H	H		H	H
301	21704	11-Dec-81	0.36	8.7	T				H	H	H		H	H
302	21712	12-Dec-81	0.36	9.9	H,T	T	Г	Г	H	H	H		H	H
303	21720	13-Dec-81	0.39	11.0	H,T	T				H	H		H	H
304	21728	14-Dec-81	0.29	10.8	H,T	T		T	H	H	H		H	H
305	21735	15-Dec-81	0.30	11.0	H,T	T	Г	T	H	H	H	H	H	H
306	21743	16-Dec-81	0.32	8.3	T				H	H	H	H	H	H
307	21751	17-Dec-81	0.27	9.6	H,T	T	Г	Г	H	H	H		H	H
308	21759	18-Dec-81	0.27	9.1	H,T	T	T			H	H	H	H	H
309	21767	24-Dec-81	0.33	9.9	T	Г	T	T	H	H	H	H	H	H
310	21774	25-Dec-81	0.25	8.9	T					H	H		H	H
311	21782	26-Dec-81	0.21	8.6	H,T		Г	T	H	H	H		H	H
312	21789	27-Dec-81	0.26	10.8	H,T	T				H	H		H	H
313	21795	28-Dec-81	0.29	8.6	T	T				H	H		H	H
314	21802	29-Dec-81	0.28	8.3	T					H	H		H	H
315	21804	30-Dec-81	0.31	7.8	T	Г	T	T	H	H	H	H	H	H
316	21810	31-Dec-81	0.23	7.9	T					H	H		H	

RecNo: Record identification number.
Models - Rl: Rayleigh; Ty: Tayfun's; C1,C2: CNEXO (original and modified);
Gd: Goda's; Wb: Weibull; Gl: Gluhovskii's; Ib: Ibrageemov's;
L1,L2: Longuet-Higgins' (1975 and 1983).

Appendix-B x^2 values obtained for joint distribution models.

No	Rec'No	H_{sw}	T_z	R1	L1	C1	G1	T_y	C2	L2
1	20129	0.73	10.3	150.8	118.3	228.5	149.5	55.1	115.9	220.3
2	20132	0.63	10.1	305.1	257.7	137.2	332.4	66.4	166.4	232.9
3	20135	0.67	8.2	173.5	142.1	343.5	163.7	61.4	220.7	152.0
4	20138	0.56	7.5	113.9	180.0	473.9	110.3	51.8	135.5	231.6
5	20142	0.60	7.9	168.9	110.2	541.4	180.2	52.0	159.9	93.6
6	20146	0.63	9.4	160.0	97.2	217.3	147.4	42.9	159.9	135.0
7	20149	0.95	10.3	244.3	112.3	115.9	192.6	74.8	187.7	267.5
8	20152	0.69	9.0	225.9	149.4	156.9	199.5	59.2	212.0	243.0
9	20155	0.64	11.1	90.5	86.6	67.0	72.0	35.6	61.1	113.5
10	20159	0.60	8.6	214.9	124.9	119.9	227.9	54.1	168.3	122.0
11	20162	0.54	9.1	63.4	61.8	165.2	63.6	34.9	203.3	129.3
12	20165	0.36	8.6	90.5	59.2	394.6	91.6	59.9	66.0	85.3
13	20168	0.34	7.4	201.1	118.5	460.3	184.9	70.3	205.6	153.9
14	20171	0.32	8.5	47.5	46.7	72.0	46.4	67.7	84.6	104.7
15	20175	0.79	9.0	99.8	90.0	111.0	95.7	29.9	120.5	118.6
16	20179	0.64	9.0	96.5	76.6	140.8	97.9	36.9	134.2	127.5
17	20182	0.56	10.0	212.4	129.5	75.9	243.2	46.4	125.0	104.2
18	20185	0.63	10.7	104.0	133.2	213.7	101.3	38.4	292.5	151.7
19	20188	0.62	9.8	219.9	126.2	115.7	226.7	48.0	141.9	142.0
20	20192	0.95	11.1	117.1	172.0	95.9	120.5	54.2	79.1	160.2
21	20196	0.87	10.5	127.1	218.5	73.6	154.2	53.5	74.0	202.6
22	20199	0.59	10.0	111.0	109.0	89.9	116.8	47.8	93.3	155.9
23	20202	0.48	10.9	70.7	87.1	59.7	67.9	39.7	74.5	127.4
24	20204	0.63	9.2	123.1	97.5	355.6	130.8	33.6	120.3	143.1
25	20207	0.54	7.5	155.1	184.2	158.1	154.9	58.3	296.6	140.7
26	20210	0.42	9.2	73.4	75.5	86.1	72.8	55.6	605.6	190.1
27	20213	0.67	9.5	68.7	72.3	127.7	73.6	53.0	93.1	84.3
28	20216	0.49	8.5	132.0	103.4	215.3	129.8	42.3	161.0	143.9
29	20220	0.51	8.3	105.6	86.8	89.3	165.5	43.9	93.8	92.6
30	20223	0.45	9.0	53.4	80.9	65.2	52.6	52.9	76.3	215.3
31	20228	0.59	11.5	120.7	97.5	77.3	132.3	51.3	283.9	139.1
32	20232	0.45	10.9	37.8	48.3	61.7	36.6	33.2	134.1	94.5
33	20235	0.47	11.7	127.1	107.8	93.2	141.8	64.9	105.3	149.5
34	20238	0.51	12.7	59.7	140.5	54.7	69.6	32.5	73.3	175.4
35	20243	0.76	11.9	99.2	112.4	141.7	104.6	32.0	85.9	106.4
36	20247	0.61	10.9	94.6	109.4	127.7	96.2	52.8	131.9	145.2
37	20250	0.61	10.9	238.8	149.8	95.7	251.5	42.0	67.6	149.2
38	20253	0.70	9.4	215.7	106.2	150.0	208.0	49.9	154.7	402.4
39	20255	0.64	9.7	164.5	135.3	109.7	191.5	62.3	232.2	165.6
40	20258	0.57	9.5	209.3	208.3	189.7	227.8	44.8	208.2	149.1
41	20262	0.57	11.5	207.1	126.5	97.6	240.2	86.3	163.8	97.0
42	20265	0.67	9.0	207.5	154.0	167.7	208.0	54.8	177.1	404.6
43	20267	0.98	11.5	130.4	208.7	125.5	124.1	92.8	76.7	197.6
44	20270	0.72	11.9	86.1	86.0	55.9	94.9	48.0	82.5	133.8
45	20273	0.75	11.9	89.3	172.2	96.9	90.8	42.5	109.4	199.2
46	20275	0.52	10.9	104.2	152.6	80.8	108.8	37.4	113.9	180.7
47	20279	0.58	11.9	271.0	149.7	155.5	272.1	37.4	301.4	212.3
48	20283	0.70	12.7	173.6	115.5	105.3	189.2	63.1	128.2	230.4
49	20285	0.55	11.1	69.1	94.4	74.2	56.1	34.4	68.3	142.9
50	20287	0.66	12.2	91.0	101.3	109.2	92.0	52.2	132.5	204.0
51	20290	0.58	10.1	136.7	130.1	118.1	139.8	46.7	133.1	204.6
52	20294	0.56	9.5	179.3	112.9	314.3	207.6	39.9	204.9	177.2
53	20298	0.54	10.1	310.6	163.1	111.9	334.6	50.7	193.0	157.9
54	20301	0.55	9.8	137.8	115.1	115.5	145.2	49.2	107.4	164.5
55	20304	0.57	7.3	151.4	146.3	627.7	146.1	69.0	237.9	220.5

No	RecNo	H_{sw}	T_z	R1	L1	C1	G1	Fy	C2	L2
56	20307	0.53	7.8	88.9	85.7	102.5	93.3	42.4	174.9	72.1
57	20310	0.55	9.8	74.7	59.5	11.7	73.7	34.3	154.7	189.3
58	20315	0.52	10.0	122.9	105.4	122.7	132.0	37.3	211.9	146.8
59	20316	0.51	9.7	125.8	86.8	78.1	130.7	32.2	195.1	195.4
60	20318	0.64	10.1	93.8	94.7	73.7	93.9	27.4	76.4	97.9
61	20321	0.60	10.9	118.7	90.3	95.6	124.3	27.4	215.4	133.5
62	20324	0.65	10.9	112.6	124.5	163.9	120.5	50.9	141.0	160.0
63	20326	0.66	10.7	125.8	152.7	64.9	144.6	31.9	171.4	155.5
64	20328	0.55	10.3	59.9	78.3	95.6	55.9	30.7	133.5	147.9
65	20332	0.54	9.1	165.6	108.6	297.4	219.5	40.0	120.6	137.9
66	20336	0.62	8.1	206.5	179.6	129.6	220.3	80.7	147.3	140.9
67	20338	0.66	6.4	117.5	94.9	472.0	127.1	60.3	271.2	85.3
68	20341	0.79	6.8	79.5	89.6	111.6	75.2	40.9	94.8	71.8
69	20345	0.78	8.7	274.5	149.9	330.9	249.9	50.5	190.0	243.6
70	20347	0.67	9.1	88.1	88.1	175.9	91.3	33.9	346.5	175.5
71	20352	0.53	7.2	73.1	72.0	249.6	74.4	39.6	135.9	147.5
72	20356	0.55	7.5	102.1	88.8	409.3	107.2	43.7	175.7	194.5
73	20359	0.62	8.3	61.6	75.6	81.7	61.4	42.9	93.3	90.4
74	20362	0.72	8.7	157.3	135.9	120.3	182.7	44.4	180.2	181.3
75	20366	1.07	10.5	206.7	129.7	175.8	253.7	62.8	144.0	221.9
76	20370	0.86	11.7	221.1	144.4	149.0	197.2	63.9	124.5	388.5
77	20373	0.99	9.2	113.3	106.3	232.1	112.4	37.0	50.4	190.7
78	20375	0.99	11.9	87.5	89.0	91.0	78.8	56.0	107.4	155.1
79	20379	0.66	10.1	211.0	157.5	212.6	220.2	45.9	105.4	130.1
80	20382	0.81	8.8	268.6	163.4	672.7	263.6	52.6	198.6	234.5
81	20386	0.90	10.1	131.6	166.7	156.5	131.9	71.3	158.3	208.3
82	20389	0.78	9.0	179.4	153.3	227.0	199.6	69.1	227.6	372.5
83	20392	0.65	10.0	145.2	120.1	302.4	164.9	44.9	143.9	199.7
84	20394	0.69	11.3	59.5	104.1	68.8	61.2	41.0	147.0	231.4
85	20400	0.67	9.1	217.7	150.7	229.0	210.4	79.8	250.6	168.0
86	20403	0.79	9.5	270.6	198.2	200.8	274.8	86.8	315.0	199.0
87	20405	1.02	10.3	116.3	384.5	119.8	55.2	316.4	181.1
88	20407	1.15	10.5	342.0	290.4	221.6	366.1	154.9	312.1	246.6
89	20410	0.99	10.9	187.1	126.7	114.1	186.2	79.6	181.7	173.3
90	20415	1.21	11.9	154.5	104.0	100.6	165.7	79.7	180.3	154.8
91	20422	0.82	7.9	229.3	150.1	358.9	213.8	73.1	145.5	170.2
92	20425	0.81	9.5	329.8	193.2	157.8	313.5	100.1	154.2	313.2
93	20430	0.83	9.5	279.8	260.7	152.8	250.2	95.2	179.8	216.0
94	20436	0.74	8.0	171.9	130.4	230.1	167.3	47.7	126.9	145.2
95	20440	0.74	7.3	249.6	194.1	198.9	246.6	56.3	210.4	133.9
96	20442	0.95	7.9	138.8	134.2	130.6	145.9	75.2	179.4	136.9
97	20444	2.03	9.4	171.6	255.0	189.6	147.9	172.3	190.7	318.2
98	20445	1.70	8.5	178.9	220.4	151.7	215.1	184.2	156.1	296.0
99	20446	1.68	9.1	203.4	203.1	111.5	267.4	107.4	156.6	194.1
100	20447	1.37	8.5	139.4	149.8	102.9	157.0	116.1	139.5	151.9
101	20448	1.16	8.0	114.8	103.0	144.3	110.2	97.3	246.1	164.9
102	20452	1.10	7.8	76.5	94.8	91.9	56.9	49.4	110.0	141.3
103	20460	1.51	7.5	112.0	106.9	131.2	114.8	96.9	123.5	167.4
104	20458	1.09	7.9	71.2	65.3	71.9	63.3	45.8	172.7	117.7
105	20476	1.16	8.6	82.2	96.7	113.2	77.6	79.4	95.5	104.3
106	20484	1.58	9.5	123.9	168.9	93.1	133.2	147.6	93.1	135.5
107	20492	1.62	9.8	175.3	189.3	185.4	159.6	135.8	225.3	272.0
108	20500	1.01	9.1	154.5	154.8	186.4	189.3	71.7	154.4	120.0
109	20508	1.21	9.2	97.7	81.8	84.5	101.8	55.1	120.6	120.4
110	20516	1.30	9.0	135.6	109.9	82.2	153.3	68.4	113.0	131.8

No	RecNo	H_{sw}	T_z	R1	L1	C1	G1	Ey	C2	L2
111	20524	1.36	9.0	113.7	121.8	175.5	99.1	116.5	201.1	229.1
112	20532	1.41	9.0	176.6	175.5	146.5	170.3	130.7	155.8	185.0
113	20540	1.86	7.9	200.4	191.7	147.9	223.1	195.4	212.6	178.1
114	20548	1.41	7.9	136.8	139.3	95.9	142.7	93.2	119.7	114.0
115	20549	1.41	8.2	106.3	89.6	120.0	82.0	66.3	109.1	138.6
116	20552	1.42	8.1	110.0	99.6	90.9	113.9	100.0	88.6	124.4
117	20553	1.31	7.8	189.9	12.7	229.3	148.1	98.0	142.4	151.1
118	20554	1.55	7.9	111.7	102.9	133.7	125.1	95.6	103.3	135.0
119	20559	1.54	7.5	104.8	115.5	140.1	93.4	95.6	194.6	148.7
120	20562	1.31	7.2	96.3	106.1	194.4	61.1	58.0	232.0	96.0
121	20563	1.50	7.5	129.3	115.1	250.0	135.1	116.4	311.7	121.3
122	20564	1.47	8.1	125.0	162.1	154.4	114.5	104.8	83.0	180.0
123	20565	1.17	7.4	178.1	129.4	172.5	90.8	68.9	72.6	196.1
124	20566	1.32	7.2	126.2	125.3	192.3	101.0	98.2	135.1	164.9
125	20567	1.36	7.7	143.0	106.1	129.3	133.0	98.0	58.6	134.0
126	20568	1.53	7.3	99.4	104.3	133.7	97.7	86.3	120.6	153.7
127	20569	1.34	7.6	170.0	118.3	139.5	169.9	86.7	60.6	145.6
128	20570	1.47	7.6	111.0	111.7	181.1	97.3	85.1	127.9	130.4
129	20571	1.54	8.1	153.9	144.1	123.9	154.3	99.7	133.2	132.8
130	20572	1.42	7.5	93.8	100.7	94.4	105.1	90.7	103.0	156.3
131	20573	1.43	7.8	162.0	144.8	178.7	150.6	127.8	93.1	155.9
132	20574	1.76	7.4	96.9	88.2	89.1	100.1	96.4	150.8	158.1
133	20575	1.89	7.8	103.5	109.4	112.4	91.5	95.3	77.3	134.8
134	20576	1.58	7.3	93.2	83.3	91.5	91.5	77.5	135.0	97.9
135	20577	1.65	8.0	114.3	102.6	200.9	113.8	103.9	66.3	139.8
136	20578	2.04	7.2	168.8	227.4	155.4	230.8	181.0	159.5	256.9
137	20580	2.08	8.0	131.5	146.3	113.3	131.3	126.3	78.7	209.5
138	20581	1.89	8.0	154.3	134.4	196.7	148.8	154.7	98.1	268.0
139	20584	2.74	7.6	191.8	211.1	125.1	177.6	251.3	89.7	321.0
140	20586	2.23	7.9	202.2	197.3	169.7	131.4	197.7	191.6	436.8
141	20596	1.66	8.0	157.5	137.7	132.7	159.5	125.4	106.5	186.9
142	20598	1.74	8.1	115.6	106.9	175.9	99.1	83.7	203.6	140.6
143	20605	1.39	8.8	155.2	158.3	130.9	177.9	111.7	188.6	192.0
144	20610	1.34	8.1	153.3	176.4	151.2	196.4	102.3	138.9	136.5
145	20616	1.12	7.5	165.8	241.1	183.0	201.5	114.4	215.5	145.3
146	20624	1.65	8.5	165.6	154.6	133.1	193.1	106.6	220.9	134.2
147	20632	2.25	8.5	159.5	155.7	214.2	161.5	154.4	252.5	205.8
148	20640	2.10	8.8	159.6	149.1	145.4	121.8	143.0	66.0	194.6
149	20648	2.65	8.1	226.6	231.5	219.0	195.2	209.6	297.9	472.8
150	20658	2.28	8.3	251.7	229.7	267.1	285.3	229.6	137.2	304.3
151	20659	2.30	8.1	167.0	185.1	185.4	211.6	193.3	177.4	221.2
152	20660	2.21	7.6	187.0	280.1	230.0	281.9	215.9	161.2	289.6
153	20664	2.44	9.4	182.8	196.3	171.6	140.2	174.1	66.6	307.6
154	20670	2.53	8.7	147.8	191.7	211.6	121.5	160.9	76.6	218.9
155	20678	2.16	9.1	190.7	182.2	141.9	203.8	196.4	92.2	308.3
156	20686	2.48	8.8	206.5	219.1	185.4	192.5	223.6	199.7	250.9
157	20692	2.45	9.7	164.7	188.5	188.5	110.2	167.5	170.7	224.9
158	20695	2.20	8.8	151.2	178.8	123.6	138.8	145.2	114.7	282.0
159	20701	2.42	8.8	177.5	184.8	186.5	176.2	181.3	169.1	254.9
160	20709	2.16	9.2	254.7	250.4	229.4	318.7	276.4	144.1	346.5
161	20717	1.66	8.5	173.5	166.2	170.5	178.9	142.4	268.1	186.8
162	20725	2.00	10.5	230.1	225.0	219.4	215.5	187.0	173.5	202.5
163	20733	2.19	10.5	209.2	237.2	303.3	200.2	203.4	290.9	220.9
164	20740	2.01	10.7	275.7	362.6	123.2	426.7	200.6	298.3	251.4
165	20747	0.93	9.8	132.3	173.6	92.0	132.5	80.5	138.1	152.2

No	RecNo	H_{sw}	T_z	R1	L1	C1	G1	Ty	C2	L2
166	20757	0.65	8.3	131.0	134.4	103.5	145.8	56.4	81.4	65.4
167	20764	0.48	8.9	80.0	72.4	173.2	80.4	44.3	143.0	79.4
168	20768	0.60	10.0	69.3	63.1	74.7	66.8	20.6	110.3	104.6
169	20776	0.67	10.0	112.0	101.7	178.6	110.6	35.7	340.9	210.7
170	20784	0.78	10.0	76.0	90.7	74.6	74.7	30.1	138.6	86.4
171	20792	0.85	9.4	75.8	94.3	70.5	64.4	42.7	98.7	136.7
172	20800	1.00	7.8	134.4	128.5	111.6	137.1	73.0	125.4	110.0
173	20808	1.34	7.2	125.8	107.4	134.0	12.0	84.0	142.2	142.7
174	20816	1.60	8.3	129.7	141.6	128.3	140.9	95.6	163.9	142.1
175	20824	1.46	7.9	123.9	110.2	145.6	107.5	94.6	195.3	162.5
176	20832	1.36	8.5	122.6	110.1	119.9	117.9	99.6	106.7	145.8
177	20840	1.20	8.3	87.9	91.9	96.8	97.2	64.2	75.0	164.3
178	20848	1.60	8.5	93.0	104.8	113.6	93.1	82.6	140.1	153.7
179	20855	1.48	8.3	223.7	211.1	364.5	236.0	131.9	403.4	191.3
180	20863	1.22	9.2	136.3	137.5	202.3	157.4	87.4	118.8	168.1
181	20871	1.03	8.6	90.5	90.7	103.3	98.3	76.5	280.3	121.2
182	20879	0.96	9.0	97.1	126.9	140.5	93.6	56.9	90.7	142.9
183	20887	0.67	7.6	116.5	107.9	336.4	127.1	33.4	427.0	99.5
184	20894	0.71	8.2	111.7	116.3	97.6	116.8	57.4	98.4	79.8
185	20902	0.58	8.2	119.0	113.8	106.8	130.2	67.8	291.5	145.3
186	20909	0.38	8.6	90.3	63.9	115.2	84.2	57.1	373.2	73.7
187	20916	0.44	7.2	46.7	49.9	43.5	47.1	55.2	112.1	104.2
188	20924	0.47	8.3	103.2	77.2	104.3	103.7	41.2	124.4	74.7
189	20931	0.80	9.0	72.2	94.6	102.3	73.1	40.6	241.2	125.6
190	20939	1.09	8.6	101.2	101.7	103.3	85.3	74.0	417.1	142.8
191	20947	1.48	8.1	138.0	131.3	131.6	137.1	107.1	286.7	172.8
192	20955	1.75	9.4	186.4	193.4	220.3	140.2	132.7	237.1	305.7
193	20963	2.17	10.3	191.5	214.5	219.0	143.8	187.6	165.8	403.5
194	20971	1.25	9.1	167.3	168.0	129.1	207.5	63.9	333.6	283.7
195	20975	1.50	11.3	100.0	103.7	142.9	105.0	74.9	97.8	129.6
196	20983	1.17	9.0	107.7	88.0	104.7	75.4	66.7	124.1	137.3
197	20991	1.68	9.5	362.4	270.7	85.6	127.7	100.2	104.0	136.8
198	20995	1.33	9.5	137.2	138.2	149.5	132.2	114.0	170.2	156.3
199	21000	1.46	9.6	216.0	223.3	168.6	283.4	149.5	163.1	149.8
200	21008	1.77	10.6	235.3	206.6	183.3	239.5	174.2	204.4	251.1
201	21011	0.90	9.8	80.8	153.1	84.0	79.9	53.9	146.2	120.1
202	21019	0.71	8.6	147.4	157.1	107.4	173.1	55.3	127.0	110.9
203	21027	0.82	9.9	99.6	137.1	97.1	83.9	64.9	93.5	162.2
204	21035	0.88	9.4	267.6	226.8	164.0	119.2	69.7	133.0	121.8
205	21043	1.00	7.9	99.7	117.6	203.8	122.4	115.5	94.4	201.0
206	21051	2.32	9.8	159.7	202.9	107.9	129.2	153.9	158.6	180.1
207	21056	0.28	8.6	171.6	95.6	93.3	158.3	52.0	173.1	497.9
208	21060	0.64	11.5	189.7	148.4	159.2	219.7	42.4	78.2	161.7
209	21067	0.53	9.6	240.1	156.0	124.7	256.8	48.5	152.0	145.8
210	21074	0.24	8.3	106.6	43.0	288.7	94.7	54.0	58.9	119.2
211	21081	0.16	8.2	41.9	23.8	180.4	40.3	56.9	47.1	26.2
212	21095	0.19	10.6	41.0	42.0	63.0	41.0	45.0	132.1	110.2
213	21101	0.61	7.9	87.6	103.5	76.6	97.7	86.5	80.7	105.5
214	21107	1.90	9.6	206.4	265.0	312.0	201.9	254.4	82.7	434.0
215	21115	1.24	8.7	529.1	103.1	125.9	134.8	150.9	156.8	242.4
216	21123	1.09	7.7	140.4	134.8	187.0	153.4	51.4	78.9	100.6
217	21131	1.24	9.4	132.9	115.8	143.0	109.0	73.3	135.4	144.2
218	21136	0.78	7.0	84.4	128.9	84.7	99.5	51.9	76.8	64.3
219	21144	1.28	8.2	90.1	96.6	222.1	83.6	100.0	86.9	94.2
220	21152	0.79	8.1	111.6	87.0	263.2	110.3	60.7	61.4	70.0

No	RecNo	H$_{sw}$	T$_z$	R1	L1	C1	G1	Ty	C2	L2
221	21159	0.56	7.9	74.1	92.1	103.3	77.5	33.7	222.9	129.5
222	21165	0.29	7.0	46.6	46.4	426.6	47.1	61.3	61.8	61.6
223	21173	0.28	8.3	142.1	96.1	65.3	141.0	55.2	124.0	119.0
224	21181	0.56	7.8	101.7	80.9	66.4	96.3	36.9	118.2	80.7
225	21184	1.36	8.1	95.3	141.7	123.8	100.9	82.2	52.4	209.3
226	21192	1.45	8.1	172.5	151.7	187.2	195.6	90.5	130.4	119.6
227	21200	1.42	7.4	211.9	105.6	144.1	121.7	86.6	98.3	151.6
228	21207	0.93	6.5	106.4	113.2	115.3	97.4	46.0	113.1	95.9
229	21215	0.84	6.9	81.4	90.5	101.2	76.2	43.4	297.0	125.5
230	21224	0.83	7.1	87.5	134.4	81.6	89.7	79.1	104.2	92.6
231	21231	0.52	7.2	73.3	96.8	197.7	79.2	42.4	91.5	65.5
232	21238	1.42	9.9	164.5	146.2	150.3	132.9	98.2	125.8	183.4
233	21246	1.19	10.4	153.2	109.0	174.4	131.0	99.8	163.3	127.6
234	21248	0.75	10.4	100.3	104.2	143.9	92.9	36.4	120.6	97.4
235	21256	0.44	9.1	100.1	69.4	71.1	100.9	41.4	123.4	59.6
236	21262	0.47	12.4	157.6	155.0	130.7	153.5	87.0	99.7	91.8
237	21270	0.36	12.7	145.3	80.7	103.6	157.6	32.4	52.6	160.1
238	21276	0.29	12.1	40.7	45.2	67.4	43.7	39.1	194.7	125.6
239	21284	0.36	12.4	59.9	63.0	139.5	59.7	45.5	49.4	97.5
240	21290	0.21	11.0	88.4	53.6	63.3	95.3	40.0	103.5	102.2
241	21297	0.28	7.7	363.8	137.7	87.8	331.4	56.2	159.9	245.4
242	21305	0.17	9.9	40.5	25.9	49.9	43.6	45.0	32.0	74.2
243	21320	0.20	12.1	34.9	27.6	46.2	37.0	38.0	39.9	118.7
244	21326	0.30	10.8	170.3	124.3	143.9	75.0	36.6	129.8	160.6
245	21334	0.40	12.7	70.6	51.8	80.5	71.2	29.2	52.2	95.7
246	21338	0.32	13.0	37.2	46.1	64.9	35.6	37.8	41.1	37.1
247	21350	0.43	13.0	73.2	74.1	46.9	78.1	31.2	57.3	134.6
248	21358	0.38	13.0	69.6	112.4	52.1	67.4	34.0	73.7	129.6
249	21366	0.24	13.7	59.2	36.2	85.7	60.5	36.0	34.8	99.2
250	21373	0.34		55.4	41.9	31.2	55.0	15.0	113.0	87.0
251	21381	0.29	11.8	42.3	56.4	41.3	41.7	39.8	34.2	162.4
252	21389	0.28	12.7	40.0	49.8	54.1	39.7	37.9	62.0	262.7
253	21397	0.51	11.8	70.3	77.5	136.4	67.6	26.1	118.8	117.7
254	21405	0.65	11.5	63.7	67.9	159.2	65.7	38.4	115.9	129.5
255	21413	0.69	11.8	125.0	104.3	101.8	138.3	44.9	207.4	155.9
256	21421	0.68	12.1	66.3	118.2	67.2	61.6	46.5	109.7	297.1
257	21429	0.59	11.5	90.7	80.0	92.7	91.0	37.9	83.3	158.8
258	21437	0.42	10.6	69.4	70.7	91.5	67.2	34.5	206.3	113.0
259	21444	0.47	9.8	215.7	103.0	266.3	200.9	36.6	424.5	175.5
260	21451	0.54	11.5	59.2	55.7	60.1	57.6	26.3	72.0	134.2
261	21456	0.58	10.4	97.6	107.6	125.4	94.2	45.6	123.3	173.3
262	21457	0.84	8.6	64.2	91.7	46.3	58.9	46.4	73.5	133.6
263	21459	0.56	8.6	52.7	57.7	34.4	50.8	29.9	26.4	76.4
264	21466	0.43	8.5	55.7	58.4	49.3	57.0	44.2	195.6	58.8
265	21473	0.41	8.9	91.5	93.2	116.2	92.5	44.8	111.1	90.3
266	21476	0.32	9.4	72.9	57.6	117.8	69.5	48.2	371.0	105.2
267	21484	0.34	8.6	144.2	123.0	113.8	141.5	50.5	117.2	171.8
268	21492	0.26	8.5	197.7	137.8	163.3	176.5	58.0	113.8	137.2
269	21500	0.27	10.4	100.4	45.3	54.7	95.2	45.0	123.1	70.7
270	21507	0.36	6.7	67.8	62.4	101.5	67.6	62.5	500.6	67.0
271	21514	0.22	7.7	109.8	50.1	493.4	105.1	65.0	235.4	37.1
272	21522	0.17	9.5	97.3	34.0	57.5	92.0	63.0	79.5	73.8
273	21530	0.14	7.5	87.5	51.5	187.1	83.2	66.0	353.1	81.0
274	21537	0.18	7.6	40.0	41.6	342.8	42.2	63.9	835.1	29.4
275	21545	0.21	10.1	78.7	38.9	483.8	73.2	49.0	54.1	48.6

No	RecNo	H_sw	T_z	R1	L1	C1	G1	Fy	C2	L2
276	21548	0.32	11.3	78.2	89.7	78.9	97.2	38.2	97.5	101.1
277	21556	0.27	10.8	62.7	58.1	68.7	61.7	41.3	83.6	103.0
278	21563	0.24	10.4	37.7	48.0	267.1	38.3	47.0	100.7	106.6
279	21571	0.21	8.2	84.0	48.3	63.6	82.3	58.4	44.5	105.5
280	21577	0.41	11.9	111.1	86.3	111.1	109.4	39.1	105.2	243.2
281	21581	0.60	12.4	99.6	104.0	104.2	103.0	35.8	82.7	144.9
282	21589	0.40	11.0	70.2	54.0	121.7	69.0	36.2	56.6	104.3
283	21597	0.22	9.8	28.0	34.7	73.5	28.8	51.0	306.3	151.0
284	21605	0.26	8.5	26.1	23.9	39.5	24.9	68.0	235.5	121.8
285	21613	0.23	8.3	29.2	35.3	147.7	28.8	56.0	65.5	120.7
286	21621	0.25	6.6	47.7	53.0	79.1	47.4	71.0	118.0	139.5
287	21623	0.40	10.8	162.1	66.5	110.1	158.0	36.4	317.9	93.9
288	21627	0.34	9.6	115.1	72.5	331.9	114.9	45.8	83.5	147.9
289	21632	0.45	11.5	52.9	49.7	55.1	52.8	28.2	749.6	70.4
290	21639	0.35	9.7	80.5	58.5	72.6	76.3	55.1	131.8	82.0
291	21646	0.37	10.6	42.1	47.4	54.5	42.3	40.5	55.9	58.7
292	21648	0.37	10.8	104.9	46.8	71.9	107.3	37.5	95.1	78.9
293	21651	0.27	9.4	46.6	59.7	103.4	44.8	51.9	73.2	112.0
294	21657	0.25	9.8	36.2	59.4	26.6	36.0	61.0	22.4	80.4
295	21663	0.27	9.6	54.7	58.3	59.4	53.8	49.0	69.6	172.9
296	21670	0.28	8.2	161.9	88.9	80.1	164.8	54.1	142.9	93.9
297	21672	0.42	11.3	98.1	70.0	144.9	96.7	50.3	11.0	194.7
298	21680	0.71	10.1	136.2	114.8	254.2	138.0	40.4	157.8	166.5
299	21688	0.59	8.7	171.0	96.7	149.2	173.9	46.5	154.4	110.0
300	21696	0.46	9.4	116.7	64.3	57.2	124.6	33.9	103.0	76.9
301	21704	0.36	8.7	73.2	71.3	90.1	72.4	47.7	104.2	101.2
302	21712	0.36	9.9	72.6	65.3	125.6	76.0	40.9	44.4	70.7
303	21720	0.39	11.0	81.2	69.0	62.4	82.4	30.5	69.8	99.4
304	21728	0.29	10.8	51.9	44.2	82.4	51.2	42.9	79.1	119.6
305	21735	0.30	11.0	61.2	60.8	84.8	59.2	44.8	84.0	97.9
306	21743	0.32	8.3	134.7	100.1	106.9	149.3	53.4	147.8	97.7
307	21751	0.27	9.6	33.2	50.1	72.4	33.2	48.2	62.1	63.2
308	21759	0.27	9.1	37.0	33.7	41.4	34.8	51.9	40.5	109.8
309	21767	0.33	9.9	89.0	52.9	160.3	92.3	43.8	60.9	162.4
310	21774	0.25	8.9	134.8	87.9	92.8	131.8	54.0	273.7	86.7
311	21782	0.21	8.6	33.5	53.3	46.4	33.4	57.0	35.9	42.6
312	21789	0.26	10.8	36.4	34.0	68.8	35.9	43.3	140.1	149.2
313	21795	0.29	8.6	89.2	71.2	81.0	86.0	94.9	79.0	125.1
314	21802	0.28	8.3	47.6	51.5	157.6	47.6	57.9	373.1	46.1
315	21804	0.31	7.8	75.5	87.3	55.2	73.9	58.2	381.7	83.2
316	21810	0.23	7.9	81.4	128.2	311.7	77.7	62.0	59.5	48.3
Maximum :		2.74	13.7	529.1	384.5	672.7	426.7	276.4	835.1	497.0
Minimum :		0.14	6.4	26.1	12.7	11.7	12.0	15.0	11.0	26.2
Average :		0.89	9.3	129.7	117.7	148.1	127.7	73.4	159.3	156.8
Std Dev :		0.59	1.5	67.6	57.6	95.5	67.6	46.3	155.3	74.9

Abbreviations same as in Appendix-A.

PUBLICATIONS OF THE AUTHOR IN THE RELATED FIELDS

1. Study of waves and their refraction in relation to beach erosion along the Kerala coast. Centre for Earth Science Studies, Tech. Rep. No. 29, 1983. (M. Baba, N.P. Kurian, K.V. Thomas, M. Prasannakumar, T.S. Shahul Hameed and C.M. Harish).

2. Study of waves and their refraction in relation to beach erosion along the Kerala coast. Centre for Earth Science Studies, Tech. Rep. No. 31, 1983. (M. Baba, P.S. Joseph, N.P. Kurian, K.V. Thomas, T.S. Shahul Hameed, M. Prasannakumar and C.M. Harish)

3. Beach dynamics in relation to wave climate at Alleppey during monsoon season. Centre for Earth Science Studies, Tech. Rep. No. 38, 1984. (N.P. Kurian, T.S. Shahul Hameed and M. Baba)

4. Prediction of nearshore wave heights using a refraction programme. Coastal Engng., Vol.9, pp.347-356, 1985. (N.P. Kurian, M. Baba and T.S. Shahul Hameed)

5. A study of monsoonal beach processes around Alleppey, Kerala. Proc. Indian Acad. Sci. (Earth. Planet. Sci.), Vol.94, pp.323-332, 1985. (N.P. Kurian, T.S. Shahul Hameed and M. Baba)

6. Wave climatology for the southwest coast of India. Paper presented at the Int. Symp. on Concepts and Techniques of Applied Climatology, Waltair, 1985. (M. Baba, T.S. Shahul Hameed, N.P. Kurian, K.V. Thomas, P.S. Joseph, C.M. Harish, M. Prasannakumar and K.K. Varghese)

7. Impact of a permeable structure on shoreline development. In: B.P. Radhakrishna and K.K. Ramachandran (Ed.), India's Environment, Geological Society of India, Bangalore, pp.275-288, 1986. (T.S. Shahul Hameed, N.P. Kurian and M. Baba)

8. Computation of longshore currents. Indian J. Mar. Sci., Vol.15, pp.92-95, 1986. (T.S. Shahul Hameed, M. Baba and K.V. Thomas)

9. Beach modification due to alongshore and offshore transport. Proc.(abstracts) 20th Int. Conf. on Coastal Engng., Taiwan, pp.322-323, 1986. (M. Baba, T.S. Shahul Hameed and K.V. Thomas)

10. Discussion on 'Mathematical prediction of long-term shoreline changes at Visakhapatnam'. J. Institution Engrs. (India), Civil Engng. Div., Vol.67, pp.68, 1986. (M. Baba and T.S. Shahul Hameed)

11. Temporal and spatial variations in wave climate off Kerala. Indian J. Mar. Sci., Vol.16, pp.5-8, 1987. (M. Baba, N.P. Kurian, T.S. Shahul Hameed, K.V. Thomas and C.M. Harish)

12. Monitoring of coastal environment for its management. Proc. Coastal Zone-87, WW Div., ASCE, Seattle, pp.4764-4777, 1987. (M. Baba, N.P. Kurian, K.V. Thomas, T.S. Shahul Hameed and C.M. Harish)

13. Prediction system for waves and related coastal processes. Paper presented in the 19th General Assembly, IUGG, Vancouver, Canada, 1987. (N.P. Kurian, P.S. Joseph, T.S. Shahul Hameed and K.V. Thomas)

14. Wave climate and power off Trivandrum. In: Project report on sea trial of a 150 kw wave energy device off Trivandrum coast. Published by IIT, Madras on behalf of Dept. of Ocean Development, Govt. of India, 1987. (M. Baba, K.V. Thomas, T.S. Shahul Hameed, N.P. Kurian, C.E. Rachel, Saji Abraham and Ramesh Kumar)

15. Prediction of sediment transport and beach evolution. In: Ocean Waves and Beach Processes (Ed. M.Baba and N.P. Kurian), Centre for Earth Science Studies, Trivandrum, pp.205-224, 1988. (M. Baba, T.S. Shahul Hameed and K.V. Thomas)